Studies on Tissue Protective Cytokines in Remyelination and Regenerative Medicine

Georgina Gyetvai

July 2016

A thesis submitted in partial fulfilment of the requirements of the University of Brighton and the University of Sussex for the degree of Doctor of Philosophy

Abstract

There is growing interest in the tissue-protective effects of some cytokines, including erythropoietin (EPO) and the IL-6 family cytokine leukaemia inhibitory factor (LIF); both have receptors, and exert their effects, on cells other than their primary targets. In the nervous system, these cytokines could aid in the treatment of demyelinating diseases, such as multiple sclerosis, by protecting myelin from damage and supporting remyelination after damage has occurred. Previous work has shown that EPO increases myelination in oligodendrocytes, the cells responsible for myelin deposition in the central nervous system. I aimed to determine if LIF shares the promyelinating effects of EPO and understand more about the mechanisms mediating tissue-protective cytokine-induced myelination.

A model of rat oligodendrocyte precursor cells was used and their myelinating capacity was measured as represented by myelin oligodendrocyte glycoprotein (Mog) expression. Initially I studied EPO and LIF's effects on these cells before defining the molecular mechanisms causing their effects using microarray gene expression analysis.

EPO increased myelination by eight-fold, a level that was sustained at concentrations up to and including 400ng/ml. After treatment with LIF at 0.2ng/ml Mog expression was increased by two-fold, but concentrations above 2ng/ml caused a reduced expression of Mog. Interestingly, when LIF and EPO were added simultaneously there was a significant reduction in EPO-induced Mog expression suggesting that LIF induced an inhibitory feedback that was responsible for blocking not only its own, but also EPO's effect. The inhibitory feedback was replicated when LIF was replaced by ciliary neurotrophic factor (CNTF) and oncostatin M (OSM), glycoprotein 130 (GP130) cytokines that use the same receptor as LIF.

The signalling mechanisms that may have caused the inhibition of EPO-induced Mog were then investigated. Socs3, a known inhibitory feedback of LIF and other IL-6 cytokines, negatively correlated with Mog expression, as the higher concentration of LIF and the simultaneous EPO and LIF treatment induced the greatest Socs3 expression.

Gene expression microarray analysis was performed to elucidate further mechanisms that may cause the inhibition of EPO-induced Mog. A variety of candidate genes were identified and their expression validated by qPCR. The roles of Tlr2/Myd88 and lipocalin 2 were investigated further and Tlr2 activation showed a functional effect on Mog expression.

The results showed that LIF and other GP130 cytokines inhibited EPO's positive effect on myelination and clarified some of the mechanisms that resulted in inhibition. The implications of my work could be an increase in efficacy of EPO treatment, as the work has elucidated mechanisms that could inhibit EPO's pro-myelinating effect. Increased efficacy of EPO would impact new therapies and therapeutic approaches using tissue protective cytokines in regenerative medicine.

Table of Contents

List of Figures **8**
List of Tables **13**
Table **13**
Title **13**
Page **13**
List of Abbreviations **14**
Acknowledgements **17**
Author's declaration **18**
Chapter 1. Introduction **19**
1.1 Tissue protective cytokines 19
1.1.1 EPO 19
1.1.1.1 Non-erythropoietic functions of EPO 24
1.1.1.2 Neuroprotection 24
1.1.1.3 Functions in other tissues 25
1.1.1.4 Non-haematopoietic, tissue-protective EPO derivatives 27
1.1.1.5 Therapeutic uses of EPO 29
1.1.1.6 EPO in regenerative medicine 30
1.1.2 Interleukin-6 family of cytokines 31
1.1.2.1 Leukaemia inhibitory factor 31
1.1.2.2 Other interleukin-6 cytokines and their neuroprotective properties 38
1.2 Mechanisms of repair 39
1.2.1 Myelination 40
1.2.1.1 Mechanisms that induce myelination 42
1.2.1.2 The causes of demyelination 43
1.2.1.3 Why remyelination fails 45
1.2.1.4 EPO in remyelination 48
1.2.1.5 LIF in remyelination 50
1.2.1.6 Studying remyelination in vitro 51
1.2.2 Wound healing 52
1.2.2.1 Normal wound healing process 52
1.2.2.2 EPO in wound healing 56
1.2.2.3 LIF in wound healing 58

1.2.3 Applications of this thesis 59
1.3 Aims 60
Chapter 2. Materials and Methods 61
2.1 Materials and Suppliers 61
2.2 Commonly used buffers and solutions 62
2.3 Cell lines 64
2.3.1 CG4 cell line 64
2.3.2 sEnd-1 cell line 68
2.3.3 HaCaT cell line 68
2.4 In vitro oligodendrocyte myelination model 68
2.4.1 Myelination and signalling investigations 68
2.4.1.1 RNA extraction 69
2.4.1.2 Reverse transcription 70
2.4.1.3 Quantitative polymerase chain reaction 70
2.4.1.4 Western Blot Analysis 74
2.4.1.5 Gene silencing by siRNA transfection 80
2.5 Gene expression microarrays 80
2.6 Scratch assay 83
2.7 Statistics 84
Chapter 3. The effect of LIF on CG4 cells 87
3.1 Introduction 87
3.2 LIF induced Mog expression via a bell-shaped concentration response curve 87
3.3 LIF inhibited the induction of Mog by EPO 90
3.4 The effects of EPO and LIF on Mog were consistent in other myelin genes ... 91
3.5 Other IL-6 cytokines had the same effect on Mog expression as LIF 95
3.6 Conclusions 98
Chapter 4. Signalling mechanisms 100
4.1 Introduction 100
4.2 The inhibitory mechanisms of LIF are induced immediately 100
4.3 Egr2 mRNA expression did not correlate with inhibition of Mog 101
4.4 ERK1/2 phosphorylation did not correlate with inhibition of Mog 104
4.5 Socs3 induction occurred early in LIF signalling 105
4.6 Induction of Socs3 correlated with decreased Mog induction 108

4.7 Inhibition of STAT3 phosphorylation occurred only after a high concentration of LIF 112
4.8 Socs3 was also induced by OSM and CNTF 114
4.9 Inhibition of Socs3 116
4.10 A known inducer of Socs3 also inhibited EPO-induced Mog 125
4.11 Conclusions 128
Chapter 5. Gene expression microarray analysis of EPO-regulated genes 130
5.1 Introduction 130
5.2 Confirmation of the effect of EPO and LIF on CG4 cells 131
..... 134
5.3 Transcripts that are altered by differentiation 135
5.4 Transcripts that are altered by differentiation and by EPO 142
5.5 Transcripts that are altered by the addition of EPO 145
..... 155
5.6 Conclusion 156
Chapter 6. Gene expression microarray analysis of inhibition of EPO-induced Mog by LIF 158
6.1 Introduction 158
6.2 Analysis of genes altered after cytokine treatment for 1 hour 160
6.2.1 Transcripts altered by EPO and by EPO+LIF treatment 160
6.2.2 Transcripts altered by treatment with EPO+LIF compared to EPO alone 162
..... 168
6.2.2.1 Transcripts unaltered by EPO but upregulated by EPO+LIF 169
..... 178
6.2.2.2 Transcripts upregulated by EPO but downregulated by EPO+LIF ... 179
6.3 Analysis of genes altered after cytokine treatment for 20 hours 185
6.3.1 Transcripts altered by EPO vs the control and EPO+LIF vs EPO 185
6.3.2 Transcripts altered by treatment with EPO+LIF compared to EPO alone 197
6.3.2.1 Transcripts upregulated by EPO+LIF 200
6.3.3 Biological functionality of Tlr2 209
6.3.4 Biological functionality of Lipocalin 2 213
6.4 Conclusions 217

Chapter 7. In vitro wound healing assay 220
7.1 Introduction 220
7.2 sEnd-1 cells 222
7.3 HaCaT cells 240
7.4 Conclusion 249
Chapter 8. Conclusions 251
8.1 LIF does not have the same positive myelinating effects as EPO 251
8.2 LIF inhibited EPO-induced Mog expression 252
8.3 Socs3 expression negatively correlated with Mog induction 254
8.4 Igf1, CD36 and other genes were important in differentiation and myelination of CG4 cells 255
8.5 Tlr2 stimulation inhibited EPO-induced Mog 257
8.6 Concluding remarks 259
Chapter 9. References 262
Appendix I 305

List of Figures

Figure	Title	Page
Chapter 1		
Figure 1.1	The signalling pathways known to be involved in the neuroprotective effects of EPO	23
Figure 1.2	The four α-helical structure of EPO	28
Figure 1.3	The four α-helical structure of LIF	33
Figure 1.4	The IL-6 cytokines and their receptors	34
Figure 1.5	The JAK/STAT/Socs pathway as induced by LIF	37
Figure 1.6	Electron micrographs of myelin profiles in the optic nerve of adult mice	41
Figure 1.7	Acute demyelinating lesion be Joseph Babinsky	46
Figure 1.8	The four stages of wound healing	54
Chapter 2		
Figure 2.1	Undifferentiated CG4 cells	67
Figure 2.2	CG4 cells 24 hours after differentiation	67
Figure 2.3	Typical amplification plot from qPCR analysis	72
Figure 2.4	Schematic representing the setup of gel electrophoresis	77
Figure 2.5	Schematic representing the setup of transfer apparatus	78
Figure 2.6	Diagram representing the experimental design	79
Figure 2.7	Gene expression microarray experimental design	82
Figure 2.8	Example of a HaCaT cell scratch assay	85
Figure 2.9	Example of measuring a scratch wound area using ImageJ	86
Chapter 3		
Figure 3.1	LIF induces a bell-shaped concentration response of Mog induction in CG4 cells	89
Figure 3.2	LIF inhibited the induction of Mog expression by EPO	92
Figure 3.3	LIF inhibited the induction of Mbp expression by EPO	94
Figure 3.4	CNTF and OSM inhibited the induction of Mog expression by EPO	96

Figure 3.5 OSM, but not CNTF, induced low levels of Mog expression after low-concentration cytokine treatment. 97

Chapter 4

Figure 4.1 The inhibitory effect of LIF on EPO-induced Mog was stronger when both cytokines were added simultaneously. 702
Figure 4.2 Egr2 induction was most potent when EPO was present and was not reduced when LIF was also present 103
Figure 4.3 pERK was induced by EPO and not inhibited by the addition of Mog 106
Figure 4.4 Socs3 was induced at an early time point by LIF 107
Figure 4.5 LIF induction of Socs3 was concentration dependent 109
Figure 4.6 LIF was a more potent inducer of Socs3 than EPO 111
Figure 4.7 Low-concentration of LIF did not cause an inhibition of pSTAT3 but high concentration did after 20 minutes 113
Figure 4.8 OSM and CNTF also induced Socs3 expression 115
Figure 4.9 Socs3 siRNA failed to inhibit Socs3 expression 118
Figure 4.10 Socs3 siRNA failed to inhibit Mog expression 120
Figure 4.11 Zoledronic acid failed to inhibit Socs3 expression 121
Figure 4.12 Zoledronic acid failed to increase Mog induction 123
Figure 4.13 Zoledronic acid failed to increase Mog induction or basal Mog levels 124
Figure 4.14 PMA induced Socs3 expression when added simultaneously with EPO 126
Figure 4.15 PMA inhibited induction of Mog expression by EPO 127

Chapter 5

Figure 5.1 Egr2 and Socs3 induction in CG4 cell samples to be analysed by microarrays 133
Figure 5.2 Genes changed by the control vs undifferentiated samples at both time points 140
Figure 5.3 Genes changed by the control vs undifferentiated samples at both time points. Clusters only 141

Figure 5.4	Genes changed by the control vs undifferentiated samples at both time points plus the expression of these genes when the cells are treated with EPO expressed vs the control	144
Figure 5.5	qPCR validation of the microarray data; CD36	150
Figure 5.6	Genes changed by EPO vs the control samples at both time points	153
Figure 5.7	qPCR validation of the microarray data; Igf1	154

Chapter 6

Figure 6.1	Genes changed by EPO vs the control samples and EPO+LIF vs EPO at 1 hour	162
Figure 6.2	qPCR validation of the microarray data; Fos	165
Figure 6.3	qPCR validation of the microarray data; JunB	167
Figure 6.4	EPO+LIF vs EPO cluster analysis at 1 hour	170
Figure 6.5	EPO+LIF vs EPO cluster analysis. Clusters of genes expressed here are not changed by EPO alone but are upregulated by EPO+LIF at 1 hour	171
Figure 6.6	qPCR validation of the microarray data; Socs3	172
Figure 6.7	STRING analysis of genes unaltered by EPO but upregulated by EPO+LIF at 1 hour	175
Figure 6.8	Centre section of STRING analysis shown in Fig 6.7	176
Figure 6.9	qPCR validation of the microarray data; Tnfrsf1a	177
Figure 6.10	EPO+LIF vs EPO cluster analysis. Clusters of genes expressed here are upregulated by EPO alone and downregulated by EPO+LIF at 1 hour	180
Figure 6.11	qPCR validation of the microarray data; Inhba	182
Figure 6.12	STRING analysis of genes upregulated by EPO and downregulated by EPO+LIF at 1 hour	184
Figure 6.13	Genes changed by EPO vs the control and EPO+LIF vs EPO at 20 hours	188

Figure 6.14	Genes changed by EPO vs the control and EPO+LIF vs EPO at 20 hours. The clusters shown here are those in which genes are regulated differently by LIF and EPO+LIF treatments than EPO alone	189
Figure 6.15	qPCR validation of the microarray data; Mag	191
Figure 6.16	qPCR validation of the microarray data; Pmp2	193
Figure 6.17	qPCR validation of the microarray data; Ppargc1a	195
Figure 6.18	Genes changed by EPO+LIF vs EPO at 20 hours	199
Figure 6.19	Genes changed by EPO+LIF vs EPO at 20 hours. Selected are those unchanged by EPO alone but upregulated by EPO+LIF	201
Figure 6.20	qPCR validation of the microarray data; Tlr2	202
Figure 6.21	qPCR validation of the microarray data; Lcn2	205
Figure 6.22	STRING analysis of genes unaltered by EPO but upregulated by EPO+LIF at 20 hours	207
Figure 6.23	STRING analysis of genes unaltered by EPO but upregulated by EPO+LIF at 20 hours. Centre of Figure 6.22	208
Figure 6.24	Pam3 treatment increases the inhibitory effect of LIF on EPO-induced Mog expression	212
Figure 6.25	Lcn2 treatment did not inhibit EPO-induced Mog expression	215
Figure 6.26	High-concentration Lcn2 treatment did not inhibit EPO-induced Mog expression	216

Chapter 7

Figure 7.1	Scratch wound closure by sEnd-1 cells treated with varying concentrations of FCS	224
Figure 7.2	EPO concentration response of wound closure by sEnd-1 cells (Experiment 1)	225
Figure 7.3	EPO concentration response of wound closure by sEnd-1 cells (Experiment 2)	228
Figure 7.4	Scratch wound closure by sEnd-1 cells treated with EPO or LIF (Experiment 1)	229

Figure 7.5	Scratch wound closure by sEnd-1 cells treated with EPO or LIF (Experiment 2)	231
Figure 7.6	Scratch wound closure by sEnd-1 cells treated with EPO or LIF (Experiment 3)	232
Figure 7.7	Scratch wound closure by sEnd-1 cells treated with EPO or LIF (Experiment 4)	234
Figure 7.8	Scratch wound closure by sEnd-1 cells treated with EPO or LIF	235
Figure 7.9	Scratch wound closure by sEnd-1 cells in acute hypoxia treated with EPO or LIF	237
Figure 7.10	Scratch wound closure by sEnd-1 cells in chronic hypoxia treated with EPO or LIF	239
Figure 7.11	Scratch wound closure by HaCaT cells treated with varying concentrations of FCS	242
Figure 7.12	Scratch wound closure by HaCaT cells treated with EPO (Experiment 1)	243
Figure 7.13	Scratch wound closure by HaCaT cells treated with EPO (Experiment 2)	245
Figure 7.14	Scratch wound closure by HaCaT cells treated with EPO (Experiment 3)	246
Figure 7.15	Wound closure by HaCaT cells treated with EPO	248

Chapter 8

Figure 8.1	The signalling pathways induced by Tlr2	258
Figure 8.2	Regulation of myelination by EPO and LIF	260

List of Tables

Table	Title	Page
Chapter 2		
Table 2.1	Materials used in the project with the supplied they were purchased from	61
Table 2.2	Commonly used buffers and solutions	63
Table 2.3	Supplements used for CG4 growth medium	66
Table 2.4	Supplements used for CG4 differentiation medium	66
Table 2.5	Cycles and steps required for qPCR	72
Table 2.6	The genes measured by qPCR throughout the project and the ID number of their probe.	73
Table 2.7	Antibodies used for Western blot	77
Chapter 5		
Table 5.1	Genes differentially expressed in undifferentiated vs. differentiated cells 4 hours	137
Table 5.2	Genes differentially expressed in undifferentiated vs. differentiated cells 23 hours	138
Table 5.3	Genes differentially expressed in EPO-treated vs the control cells at both time points	147
Table 5.4	The most highly up- and downregulated genes between cells treated with EPO vs. the control at 1 hour	148
Table 5.5	The most highly up- and downregulated genes between cells treated with EPO vs. the control at 20 hours	149
Chapter 6		
Table 6.1	Genes differentially expressed in cells treated with EPO+LIF vs. EPO	164
Table 6.2	The most highly up- and downregulated genes between cells treated with EPO alone vs control and the EPO+LIF vs EPO alone at 20 hours	186
Table 6.3	The most highly up- and downregulated genes between cells treated with EPO+LIF and EPO alone at 20 hours	198

List of Abbreviations

Abbreviation	Definition
AP-1	Activator protein 1
APS	Ammonium persulfate
BBB	Blood brain barrier
bFGF	Basic fibroblast growth factor
BFU-E	Blast-forming colony-erythroid
BSA	Bovine serum albumin
Ccl20	Chemokine C-C motif
cDNA	Complementary DNA
cEPO	Carbamylated EPO
CFU-E	Colony-forming colony-erythroid
CG4	Central glia-4
CLC	Cardiotrophin-like cytokine
CNS	Central nervous system
CNTF	Ciliary neurotrophic factor
CNTFR	CNTF receptor
Ct	Cycle threshold
CT-1	Cardiotrophin-1
DM	Differentiation medium
DMEM	Dulbecco's modified eagle’s medium
dNTP	Deoxynucleotide
DTT	Dithiothreitol
Dusp6	Dual specificity phosphatase 6
EAE	Experimental autoimmune encephalomyelitis
ECL	Enhanced chemiluminescence
EDTA	Ethylene diamine tetra acetic acid
Egr2	Early growth response 2
EGTA	Ethylene glycol tetra acetic acid
EPO	Erythropoietin
EPOR	Erythropoietin receptor
ERK	Extracellular-signal regulated kinases
ESA	Erythropoiesis stimulating agent

Fads6	Fatty acid deacetylase 6
FC	Fold change
FCS	Foetal calf serum
GM	Growth medium
GM-CSF	Granulocyte macrophage-colony stimulating factor
GP130	Glycoprotein 130
HIF	Hypoxia inducible factor
Hoxc6	Homeobox C6
IGF	Insulin-like growth factor
IL	Interleukin
Inhba	Inhibin beta a
JAK	Janus-kinase
Lcn2	Lipocalin 2
LIF	Leukaemia inhibitory factor
LIFR	LIF receptor
Mag	Myelin associated glycoprotein
Mapk	Mitogen activated protein kinases
Mbp	Myelin basic protein
MCAO	Middle cerebral artery occlusion
Mog	Myelin oligodendrocyte glycoprotein
mRNA	Messenger RNA
MS	Multiple sclerosis
Myd88	Myeloid differentiation primary response gene 88
NF-κB	Nuclear factor-kappa B
OPC	Oligodendrocyte precursor cell
OSM	Oncostatin M
OSMR	OSM receptor
PAMPs	Pattern-associated recognition molecular patterns
PBS	Phosphate buffered saline
PDGF	Platelet derived growth factor
pERK	Phosphorylated ERK
PI3k	Phosphatidylinositol-3 kinase
Pkb	Protein kinase B

Plp	Proteolipid protein
PMA	Phorbol 12-myristate 13-acetate
Pmp2	Peripheral myelin protein 2
Ppargc1a	Peroxisome proliferator-activated receptor gamma
PSN	Peripheral nervous system
pSTAT	Phosphorylated STAT
qPCR	Quantitative polymerase chain reaction
RHuEPO	Recombinant Human EPO
RIPA	Radioimmunoprecipitation assay
RNA	Ribonucleic Acid
RT	Reverse transcription
SDS	Sodium dodecyl sulphate
Sh2	Src-homology 2
siRNA	Small interfering/Silencer
Socs	Suppressors of cytokine signalling
STAT	Signal transducer and activators of transcription
STRING	Search tool for the retrieval of interacting genes
TBS	Tris buffered saline
TGF	Transforming growth factor
Tlr	Toll-like receptor
TNF	Tumour necrosis factor
Tnfrsf	Tumour necrosis factor receptor super family
VEGF	Vascular endothelial growth factor
ZA	Zoledronic acid

Acknowledgements

I would like to thank my supervisors Professor Pietro Ghezzi, Professor Tony Metcalfe and Dr Simon Otter for their expertise, guidance and unwavering support throughout my PhD. I would also like to thank Professor Matteo Santin, my undergraduate supervisor who first told me about the PhD opportunity, for believing in me a long time before I believed in myself.

A special thank you to Dr Manuela Mengozzi for teaching me everything I needed to know, for her never ending patience, and mostly for being a wonderful friend and mentor the whole way through my PhD. A couple of sentences of acknowledgement can't begin to convey how grateful I am to you.

Thank you to the rest of the Ghezzi group for their advice, exchanges of knowledge and for welcoming me to be part of an incredible group of scientists.

Thank you to my office buddies, fellow PhD students and "Phamily". Aliya, Ben, Kaj, Laura, Marina, Big Matt, Little Matt, Ryan, Sonia and Sophie; not only did you guys make coming to work a pleasure but I know that we have made friendships that will last a lifetime and it wouldn't have been the same without you.

Thank you to Mum, Dad and Becca for their constant love, support and encouragement.

I dedicate my thesis to my best friend, my rock, and my whole world. Thank you, Rob.

Author's declaration

I declare that the research contained in this thesis, unless otherwise formally indicated within the text, is the original work of the author. The thesis has not been previously submitted to this or any other university for a degree, and does not incorporate any material already submitted for a degree.

Signed

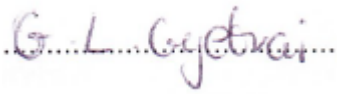

Georgina Gyetvai

Chapter 1. Introduction

1.1 Tissue protective cytokines

Cytokines are essential for the activation, differentiation, and control of the immune system, and they regulate the intensity and duration of the immune response. However, it is now understood that their functions are considerably more far-reaching and affect nearly every tissue of the body. Cytokines are small proteins produced by many cell types that affect target cells in an autocrine, paracrine or endocrine manner to provide communication throughout the body. Cytokine stimulation through a complementary receptor results in activation, differentiation, migration, or suppression of the target cell (Hiscott 2011). While the original dogma was that one cytokine stimulated one receptor, this is now known to be far from the truth; many cytokines have multiple functions, can associate with many receptors, and can interact with other cytokines. The term "tissue-protective cytokine" was first used by Ghezzi and Brines (2004) to define the cytoprotective effects erythropoietin (EPO) exerts on cells other than only maturing erythrocytes, especially in the nervous system (Ghezzi 2004). This thesis will look at the effects of EPO and other tissue protective cytokines, especially leukaemia inhibitory factor (LIF), in models of neuroregeneration and wound healing to determine how potent their effects can be within these model systems.

1.1.1 EPO

Erythropoiesis is the process through which mesenchymal stem cells in the bone marrow mature into erythrocytes. EPO is required for this process to reach completion. EPO is a 34kDa, 165 amino acid, glycoprotein which is predominantly produced by the foetal liver (Zanjani 1977) and the adult kidney (Koury 1988, Fisher *et al.* 1996) and was originally purified from the urine of patients with aplastic anaemia (Miyake 1977). The primary function of EPO is in the regulation of erythropoiesis although the first stages of erythroid cell differentiation do not require EPO. Wu *et al* (1995) created mouse knock-outs for EPO and the EPO receptor (EPOR). They found that blast-forming colony-erythroid (BFU-E) and colony

forming unit-erythroid (CFU-E) cells, the first stages of erythroid differentiation, were present in the animals but there was no further development of these cells. The animals died by embryonic day 13 due to a lack of primary erythropoiesis (Wu *et al.* 1995). Their findings demonstrate that EPO and EPOR are not needed for the initial stages of differentiation, but are crucial after that for the maturation of red blood cells. The BFU-E and CFU-E stages strongly express EPOR, again confirming that stimulation by EPO is required to progress differentiation on from this stage (Spivak 2005).

Hypoxia is the main physiological condition that stimulates EPO production and it can increase the concentration of circulating EPO by several hundred-fold (Ebert 1999). Hypoxia inducible factor (HIF)-1α and HIF-2α are the primary transcription factors responsible for the induction of EPO expression (Kapitsinou *et al.* 2010). HIF-2α is expressed widely, not just in the vasculature, although it is not as ubiquitous as HIF-1α (Wiesener 2003). The HIFs are always expressed in the circulation but under normoxic conditions they are degraded by posttranslational hydroxylation of specific proline residues, a process that is oxygen dependent. However, a lack of oxygen in hypoxic conditions means degradation of HIFs does not occur and they accumulate in the circulation. This increase of HIFs is detected by the kidneys which are stimulated to release EPO in order to increase the number of circulating erythrocytes and so allow the bloodstream to absorb, transport, and distribute more oxygen.

In the foetus the liver is the main organ that synthesises and produces EPO, but predominant production of EPO switches to the kidney after birth, with the liver remaining as a secondary producer (Koury 1991). This switch after birth is regulated at the transcriptional level. For example, there is a negative regulatory element 3' of the EPO gene that causes repression of EPO gene expression in the postnatal liver and while a kidney inducible element located 5' on the gene increases expression in the postnatal kidney (Semenza 1990).

EPO homodimerises two EPORs on the erythrocyte cell surface activating a complex network of signalling events, beginning with a conformational change in the EPOR-associated Janus-kinase (JAK)-2 by autophosphorylation (Witthuhn *et al.* 1993).

This change leads to phosphorylation of eight tyrosine residues on the EPOR which can then recruit a variety of Src-homology (SH2) domain containing proteins that activate various pathways (Fig 1.1).

One of the main pathways activated by EPO is the phosphatidylinositol-3 kinase (PI3k)/Protein kinase B (Pkb) AKT pathway (Fig 1.1). This pathway is crucial, but not sufficient, in protecting erythroid precursor cells from apoptosis (Bao 1999). The AKT pathway has substantial influence over the central nervous system. Knockout of an upstream inhibitor of AKT resulted in hypermyelination throughout the central nervous system (CNS) in mouse models (Goebbels 2010) and similar hypermyelination presented as thicker myelin and increased myelin gene expression was seen in mice that express constitutively active AKT (Flores 2008). Conversely, treatment with the AKT inhibitor rapamycin *in vitro* resulted in inhibited oligodendrocyte precursor cell (OPC) differentiation and reduced expression of myelin genes and their associated proteins (Guardiola-Diaz *et al.* 2012).

Through AKT activation EPO is able to maintain cell survival by preventing expression of pro-apoptotic genes (Chong and Maiese 2007, Hou *et al.* 2011). EPO signals through AKT to provide protection in various stress conditions, such as hypoxia (Chong 2002, Kilic 2005) and oxidative stress (Dzietko *et al.* 2004).

EPO also induces the signal transducer and activators of transcription (STAT) pathways. There are eight mammalian STATs and EPO induces STATs 1, 3, and 5. Following their binding to the EPOR, the STATs are phosphorylated by JAK2, after which they dimerise and translocate to the nucleus (Mitchell and John 2005). The major STAT molecule that EPO induces phosphorylation of is STAT5, which leads to the induction of the anti-apoptotic BCL-X_L gene, which is important in protecting proerythroblasts from apoptosis (Socolovsky 2001). STAT5 is important for the neurotrophic effects of EPO, but not its induction of neuroprotection (Byts 2008).

EPO also activates the extracellular-signal regulated kinases (ERK)/Mitogen activated protein kinases (MAPK) pathway (Fig 1.1). Binding to EPOR activates Ras and results in the phosphorylation of Raf (MAP3K) which in turn phosphorylates mitogen/extracellular signal related kinases 1 & 2 which are the upstream activators

of ERK1/2. ERK1/2 then translocates to the nucleus to regulate the expression of a number of different genes. ERK signalling has numerous effects on oligodendrocytes, including migration, differentiation, proliferation, survival, and myelination (reviewed in (Gonsalvez *et al.* 2015)). ERK1/2 knockout mice exhibited significant hypomyelination along with decreases in myelin gene expression that were not fatal but continued into adulthood (Ishii 2012). In this model, knockout mice had the same number of mature oligodendrocytes as their wild type littermates, so it was an inability of these oligodendrocytes to produce myelin that caused the hypomyelination. Overexpression of ERK1/2 was also investigated by the same group to see if it had the opposite effect to knockdown of ERK1/2. The myelin sheath of these mice was significantly thicker than controls and its density increased over time (Ishii 2013).

Activation of the ERK pathway is crucial in erythrocytes for the pro-erythropoietic effect of EPO (Arcasoy and Jiang 2005, Kuhrt and Wojchowski 2015). EPO is tissue protective in the kidney through ERK1/2 signalling, through which it has the ability to protect against apoptosis resulting from ischaemia (Zou *et al.* 2016). Finally, there is evidence of EPO-induced neuroprotection through ERK signalling in primary retinal neuronal cells (Shen *et al.* 2010).

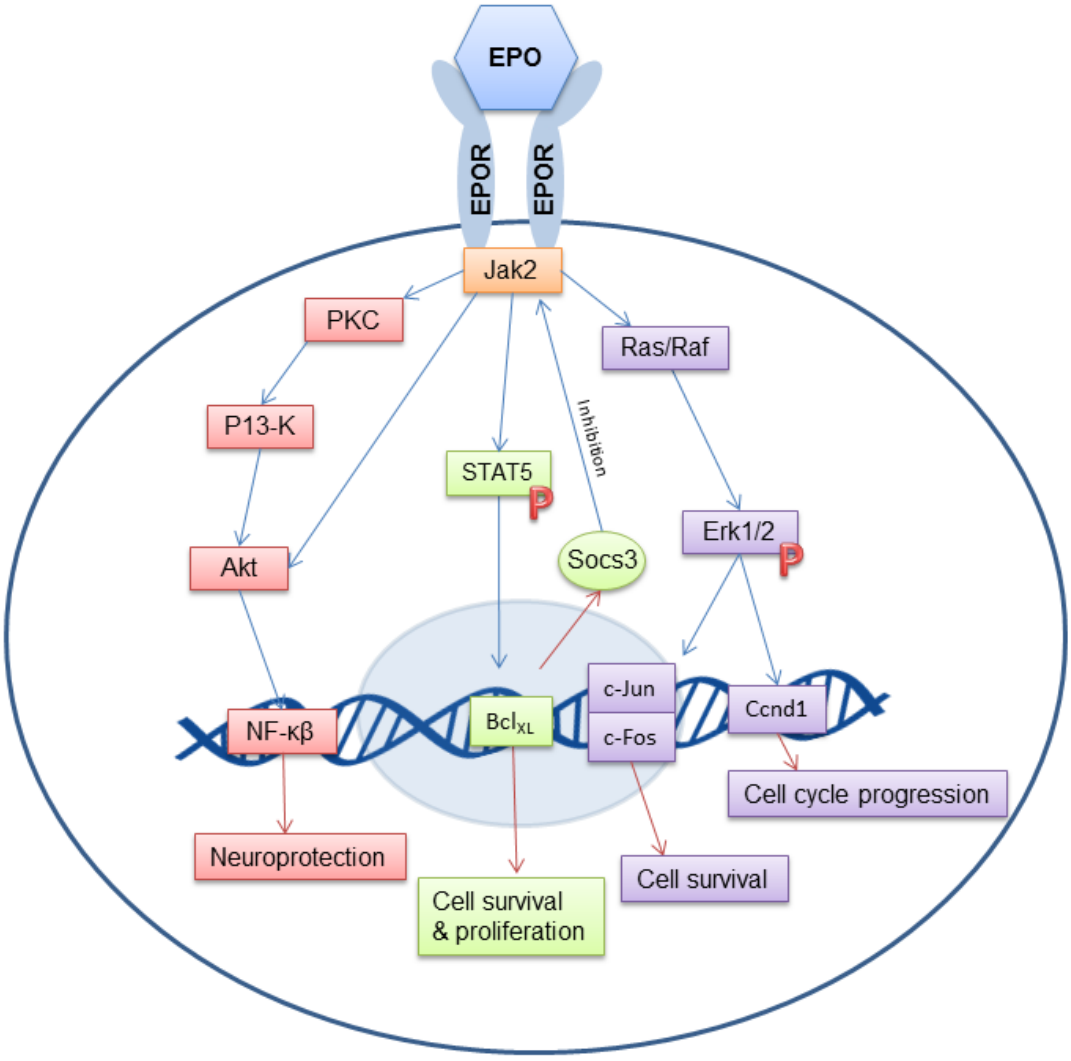

Figure 1.1: The signalling pathways known to be involved in the neuroprotective effects of EPO. JAK2 molecules that are associated with EPOR are phosphorylated following binding by a single EPO molecule at the cell surface causing a range of downstream intracellular signalling events. The phosphorylation of JAK2 results in the phosphorylation of the tyrosine residue on EPOR that then act as potential docking sites for the various pathways outlined in this figure. P=phosphorylation. Adapted from (Ghezzi 2004).

Original in colour

1.1.1.1 Non-erythropoietic functions of EPO

Despite EPO being named for its erythropoietic actions, numerous other functions for this cytokine have now been demonstrated. Elucidation of these further functions began with the finding that EPOR was expressed on cells other than just erythrocytes. For example, its expression was demonstrated on endothelial cells (Anagnostou *et al.* 1990, Anagnostou *et al.* 1994), trophoblasts (Fairchild 1999), pancreatic islets (Fenjves 2003), parathyroid cells (Ozturk 2007), and cells of the pituitary gland (Jelkmann 2005). It was Konishi *et al* (1993) who first demonstrated a non-erythropoietic function for EPO on embryonic cholinergic neurons where it promoted cell survival after the removal of serum (Konishi 1993).

After the finding that EPOR is present on various cell types came the discovery that, along with the high-affinity EPOR, there is also a second EPO receptor with an affinity for binding 6-18 times lower than EPOR that was discovered on neural cells (Masuda *et al.* 1993). It was proposed that EPO binds to a heterodimer of EPOR and this second receptor that is also used by IL-3, IL-15, granulocyte macrophage-colony stimulating factor (GM-CSF) (Jubinsky 1997). This additional receptor component was later termed tissue-protective receptor or β-common receptor (Brines 2012) and there is accumulating evidence that many of the non-hematopoietic functions of EPO are impeded by inhibition of the functions of β-common receptor (Su 2011). Many of the same signalling pathways are induced when the EPO/EPOR/β-common receptor complex is formed as when EPO binds to the EPOR homodimer, but the difference in signalling between the two receptors is not completely understood.

1.1.1.2 Neuroprotection

Masuda *et al* (1993) and Digicaylioglu *et al* (1995) found EPOR present on cells of neural origin and cerebral tissue, suggesting EPO has an effect in the nervous system (Masuda *et al.* 1993, Digicaylioglu 1995). This hypothesis was supported by Brines *et al* (2000) who showed that EPO crossed the blood-brain barrier (BBB) to protect against experimental injury in the central nervous system (CNS) in a model of cerebral ischaemia in rats (Brines *et al.* 2000), a crucial finding as EPO can be

administered peripherally and it will still exert its effects in the CNS without the need for direct administration into the brain. It is estimated that 1-2% of circulating EPO crosses the BBB (Juul 2004), although permeability of this barrier is known to increase during periods of hypoxia-ischaemia (Plateel 1997).

EPO is also neuroprotective in cerebral ischaemia as it decreases inflammation through reducing neuronal death (Villa 2003), and inducing angiogenesis and neurogenesis (Wang 2004). There is evidence that the neuroprotective properties of EPO are modulated by crosstalk between JAK2 and nuclear factor (NF)-κB pathways (Digicaylioglu 2001). Enhancement of these positive effects has been effective in treatment of infectious diseases that affect the CNS, such as cerebral malaria (Kaiser 2006).

EPO is also neuroprotective in clinically relevant models of autoimmune demyelinating diseases. Li *et al* (2004) tested the effects of systemic EPO treatment on mice with experimental autoimmune encephalitis (EAE), a model of multiple sclerosis (MS) (Li 2004). They found that daily intravenous EPO injections lowered both disease severity and duration and the spinal cord of EPO-treated mice showed less axonal damage, inflammatory cell infiltration, and demyelination. EPO was anti-inflammatory in another experiment using EAE (Agnello 2002), and also improved overall neurological recovery in this disease model (Zhang 2005). Overall, studies using EPO to treat EAE have shown that EPO halts the clinical course of the disease by targeting inflammation, demyelination, and axonal damage. It also induced neurogenesis and oligodendrogenesis in these experiments (Bartels *et al.* 2008, Sargin 2010, Cervellini *et al.* 2013b).

1.1.1.3 Functions in other tissues

EPO exerts extra-hematopoietic functions on other cell types. For example, it is present in cardiac tissue and it has protective effects on the infarcted heart by preventing apoptosis in cardiac myocytes (Parsa 2003, Depping 2005). EPO is beneficial in diabetes as it is tissue-protective on pancreatic-β cells (Fenjves 2003, Choi 2010). It is also protective in the kidney, an essential function as the kidney is

highly sensitive to hypoxia, trauma, and toxicity (Westenfelder 1999). EPO strongly reduces the inflammatory response in the kidney and prevents damage from toxins such as cyclosporine and Cisplantin (Chatterjee 2005). Furthermore, EPO has positive effects on the organ of Corti, responsible for maintaining hearing, where it increases the recovery after injury to this area in rats (Andreeva 2006, McClure 2007).

EPO is also strongly involved in the regulation of inflammation. While EPO gene expression is upregulated by HIFs, it is downregulated by NF-κB, a central transcription factor involved in the initiation and perpetuation of inflammation (La Ferla 2002). This inhibition is the common cause of anaemia seen in inflammatory diseases (Weiss 2005). Conversely, EPO inhibited NF-κB activation (Carvalho 2005) and the production of other pro-inflammatory cytokines such as TNF-α, IL-6 and IL-12/23 subunits (Nairz 2011).

EPO has direct reparative effects on wound healing. Siebert *et al* demonstrated that EPOR is expressed in both healthy and damaged skin tissue and that EPO accelerated healing *in vivo* in rats (Siebert 2011). However, too much EPO can be detrimental to the wound. Sorg *et al* (2009) found that a single high dose of 5000U/kg EPO administered systemically was beneficial and aided wound healing by accelerating wound epithelialisation and inducing angiogenesis in a model of full dermal thickness wound in hairless mice. Conversely, repeating this dose daily was detrimental as epithelialisation was delayed and newly formed blood vessels failed to properly mature (Sorg 2009). The repeated high dose prevented cell migration, which was encouraged by a single high dose. The authors also speculated that repeated EPO administration created an anti-apoptotic environment that did not allow for clearance of necrotic tissue and so prevented wound healing. Furthermore, the increase of erythrocyte mass may have caused hypertension and the negative effects of this. Clinically this study shows that the dose of EPO is important in wound healing; it is not sufficient to assume that increased EPO produces an increased positive effect.

There is also some literature on the effect of EPO in wounds of diabetic mice. Recombinant human EPO (RHuEPO) administered systemically increased vascular

endothelial growth factor (VEGF) messenger ribonucleic acid (mRNA) expression and protein in non-healing wounds of diabetic mice (Geleano 2004) as well as increasing the rate of reepithelialisation (Hong 2014). Furthermore, topical EPO treatment also decreased healing time (Hamed 2010).

1.1.1.4 Non-haematopoietic, tissue-protective EPO derivatives

A specific section of EPO's structure, not involved in interaction with the EPOR homodimer complex that mediates the erythropoietic effects of EPO, was responsible for its neuroprotective effects (Campana 1998). Therefore, it was hypothesised that molecular changes to EPOs structure would inhibit its erythropoietic effects but not alter its neuroprotective function. The first example of this was the carbamylation of lysines which resulted in the production of a neuroprotective but not erythropoietic molecule, termed carbamylated EPO (cEPO) (Leist 2004).

Non-erythropoietic derivatives also originated from the structure of EPO. EPO has a structure composed of four α helices (Fig1.2). Sections of helices A, C, and D bind to EPOR during erythropoiesis, but helix B is not implicated in binding. Therefore, it has been hypothesised that helix B is involved in neuroprotection through binding with EPOR and the common β receptor, the signal-transducing subunit shared by the granulocyte-macrophage colony stimulating factor, and the IL-3 and IL-5 receptors (Brines 2004)(Fig1.2). Based on this information derivatives of EPO have been developed that are tissue-protective but not erythropoietic. An example of such EPO derivatives is ARA290, a peptide based on the structure of helix B (Brines *et al.* 2008). This peptide was tested in a phase II study recently to see its efficacy in patients with neuropathy resulting from type II diabetes (Brines *et al.* 2014). Neuropathic symptoms improved significantly in those receiving treatment and no side-effects of the treatment were identified.

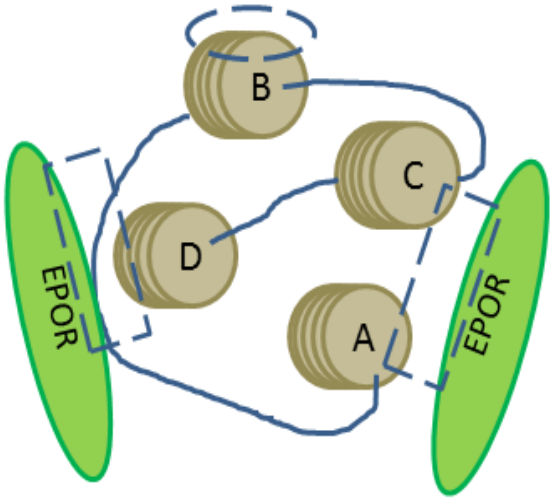

Figure 1.2: The four α-helical structure of EPO. It is believed that parts of helices A & C and helix D with the loop from A to B form the two connections with EPOR during erythropoiesis (dashed rectangles). However, when EPO binds with β-common receptor and EPOR it is part of helix B that binds to the receptors (dashed oval). It is this information that EPO derivatives have been based on. Adapted from (Vollgraf *et al.* 1999, Brines *et al.* 2008)

Original in colour

1.1.1.5 Therapeutic uses of EPO

The EPO gene was first cloned in 1985 (Jacobs 1985, Lin 1985), leading to the commercial production of RHuEPO, or epoetin, and its successful use in the treatment of patients with anaemia resulting from end-stage renal disease (Winearls *et al.* 1986). This unmodified EPO is the most successful recombinant medicine used in the treatment of anaemia, although treatment requires repeated administration. To improve the long term efficacy, molecules with the same biological functions as RHuEPO, but a longer half-life have been developed by creating specific alterations in the amino acid sequence of the molecule such as additional glycosylation sites (Egrie 2001).

RHuEPO has been used for over twenty years as a commonly used drug in the treatment of anaemia resulting from chronic kidney disease or a side-effect of chemotherapy. However, very high doses are required to reach bioactive levels in the CNS. Such large doses of any erythropoiesis stimulating agent (ESA) cause side-effects (Torup 2007). Thrombosis is a direct consequence from the increase in erythrocyte population and several animal models and patient studies have linked ESAs to thrombopoeisis (Wolf 1997, Stohlawetz 2000, Kirkeby 2008, Kato 2010).

EPO treatment may do more harm than good as it promotes vasculogenesis and angiogenesis allowing for further tumour growth in cancer patients (Hardee 2007). There has also been some suggestion that EPO acts as a growth factor for tumour progression as it has been shown to increase cell proliferation and migration (Fu 2009), however no such effect was found by other researchers (Westenfelder 2000). While the exact consequences of systemic EPO treatment are unknown, there is considerable evidence that treatment has an overall negative outcome, with the risks outweighing the benefits. A large scale meta-analysis of many trials involving the use of ESAs in the treatment of 13,933 patients with cancer showed that ESAs increased mortality during the active study period and reduced long-term survival (Bohlius *et al.* 2009). The guidelines on how extensively EPO should be used in cancer treatment have recently been updated (Rizzo 2010).

This project aimed at studying the promyelinating effects of EPO, developing on the findings by Cervellini *et al* (2013) (Cervellini *et al.* 2013a) who investigated the effect of EPO on oligodendrocyte precursor cells. They found that EPO increased myelination, a crucial marker for neurorepair. The aim of this project is to understand the mechanisms behind EPO's regenerative effects on myelination with the final aim of identifying therapeutic targets to allow the development of new drugs.

1.1.1.6 EPO in regenerative medicine

Regenerative medicine is a relatively new branch of biology that aims at using tissue engineering and molecular biology to replace, engineer, or regenerate human cells, tissues and organs that have been lost through disease or injury (Badylak *et al.* 2009). The human body has natural abilities to defend itself from insults and heal injuries, but these processes are often inefficient and incomplete. Teleost fish and urodele amphibians are unique among vertebrates as they have the ability to completely regenerate amputated limbs. Higher order animals, including humans, have replaced the ability to regenerate tissues with processes that include inflammation and scar tissue formation (Metcalfe and Ferguson 2007). Regenerative medicine approaches aim to harness these dormant regenerative mechanisms, that are believed by some to have been replaced by rapid healing processes (Metcalfe and Ferguson 2007). There are many claims of the capacity for regenerative medicine to replace lost tissue structures, although the capacity to re grow limbs is potentially overambitious. For the time being it is more realistic to look at the scope for regenerating cells and tissues; for example the field of induced pluripotent stem cells is rapidly advancing which gives the ability for adult cells to regain pluripotency and therefore replace cells that have been lost (Takahashi and Yamanaka 2006, Ohnuki and Takahashi 2015).

Angiogenesis, the formation of new blood vessels from existing ones, is one of the few regenerative mechanisms retained by humans (Carmeliet 2003). The ability of EPO to stimulate the proliferation of endothelial cells in angiogenesis is one of the mechanisms through which it has regenerative capabilities (Buemi 2002). As

discussed previously (Section 1.1.1.5) EPO may increase tumour growth through its stimulation of angiogenesis and therefore its use in the treatment of anaemic patients undergoing chemotherapy may not be appropriate (Fu 2009). While this is clearly a detrimental effect of EPO, its ability to stimulate tumour growth demonstrates its use as a tissue regenerative molecule that could potentially be applied elsewhere in the body (Buemi 2009). This project aims to investigate the regenerative capacity of EPO in the CNS beyond its angiogenic capabilities. By stimulating remyelination EPO will aid in regeneration of the myelin sheaths lost to demyelinating diseases.

1.1.2 Interleukin-6 family of cytokines

This project will develop on work on the tissue protective effect of EPO by investigating other cytokines that may share these properties. The IL-6 family of cytokines includes IL-6, LIF, ciliary neurotrophic factor (CNTF), oncostatin M (OSM), IL-11, cardiotrophin-1 (CT-1), cardiotrophin-like cytokine (CLC), and neuropoietin (Heinrich 2003, Ernst 2004) and all of these cytokines signal, in part or entirely, through the receptor glycoprotein 130 (GP130). Most of these cytokines have potent positive effects in the CNS such as increasing neurogenesis, aiding repair and regulating inflammation (Chen 2004, Erta 2012) but the experimental research presented in this thesis will mostly focus on the potential positive effects of LIF, after it was identified as another cytokine that may share the positive effects of EPO in a proof of concept bioinformatics study aimed at identifying functionally-related tissue-protective cytokines (Mengozzi 2014).

1.1.2.1 Leukaemia inhibitory factor

LIF is a pleiotropic cytokine that was first described by Ichikawa *et al* (1969) as they observed the addition of various types of conditioned medium induced cells of the murine myeloid leukaemia M1 line to differentiate into granulocytes and macrophages (Ichikawa 1969, 1970). In subsequent years, various molecules were discovered with a variety of functions and given alternative names, such as cholinergic differentiation factor, differentiation-inducing factor, and hepatocyte-

stimulating factor III (Koopman 1984, Tomida 1984, Smith 1988, Mori 1989). Slowly, it was recognised that these were all the same molecule, and the name LIF was assigned to it (Moreau 1988, Baumann 1989).

LIF is a 20kDa glycoprotein that exists as a four-helix bundle in an up-up-down-down configuration (Fig 1.3) (Robinson 1994, Hinds 1998). Along with other members of the IL-6 family, LIF interacts with a signal-transducing receptor component called GP130. Members of this family bind by forming a homodimer between two GP130 subunits or through a combination of GP130 and LIF receptor (LIFR) or another IL-6 cytokine receptor (Heinrich 2003). Although it is termed the LIF receptor, LIFR actually binds five members of the IL-6 family: LIF, OSM, CT-1, CNTF, and CLC, all of which signal through a complex of LIFR and GP130 (Fig 1.4). The pleiotropy of LIF reflects the wide array of tissues in which the LIFR is found, including the liver (Hilton 1991), bone (Gouin 1999), uterus (Ni 2002), kidney (Yoshino 2003), and CNS (Scott 2000).

LIF is secreted from a wide variety of cell types including T-cells (Shen *et al.* 1994), thymic epithelial cells (Martens *et al.* 1996), astrocytes (Aloisi 1994), neurons (Cheng and Patterson 1997), mast cells (Marshall *et al.* 1993), fibroblasts (Albrengues *et al.* 2014), keratinocytes (Paglia *et al.* 1996), epithelial cells (Morel *et al.* 2000), endothelial cells (Mi 2001), osteoblasts (Chandrasekhar and Harvey 1996), synoviocytes (Lotz 1992), and macrophages (Jasper 2011).

LIF maintains the undifferentiated state of mouse embryonic stem cells (Koopman 1984, Smith 1988, Williams 1988), and is fundamental to embryonic implantation (Stewart *et al.* 1992). Regulation of the pluripotency of stem cells by LIF makes it a useful tool in laboratory investigations and in the field of regenerative medicine. It also stimulates megakaryocyte and platelet production (Metcalf 1992), aids in embryonic implantation (Ding 2008), and enhances production of adrenocorticotropic hormone (Chesnokova 2000).

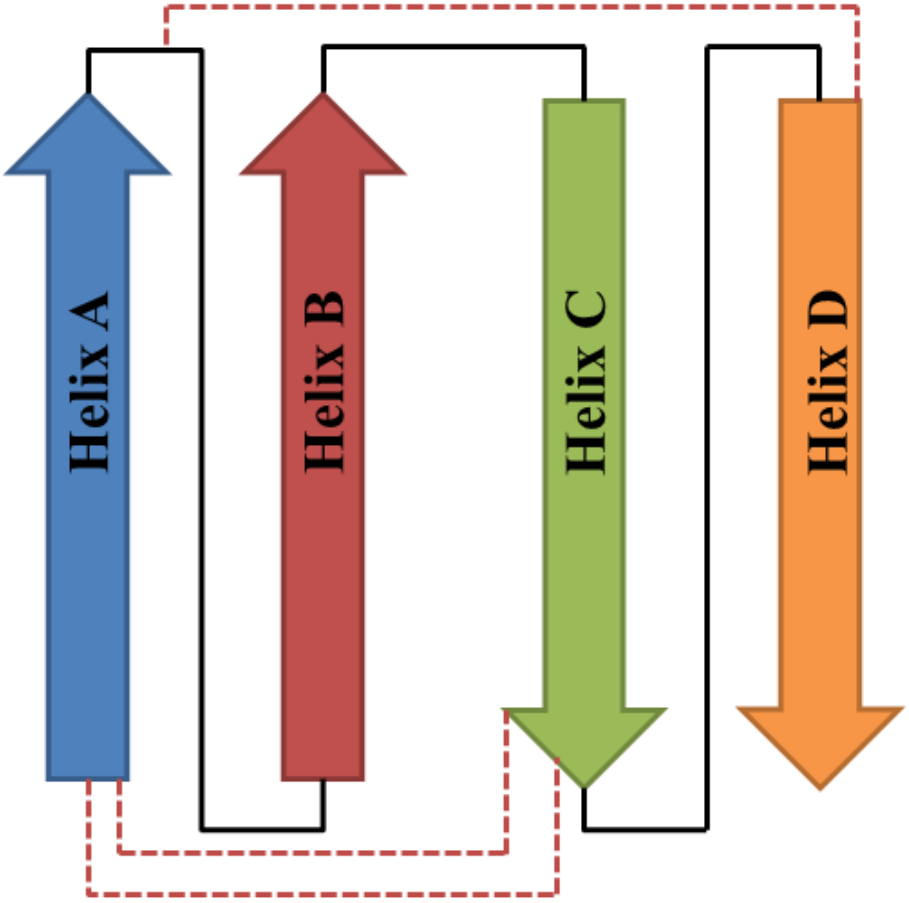

Figure 1.3: The 4 α-helical structure of LIF. The helices are arranged in an up-up-down-down formation. The red dashed lines represent disulphide bonds. The N-terminus of Helix A is important for receptor binding. Adapted from (Nicola and Babon 2015)

Original in colour

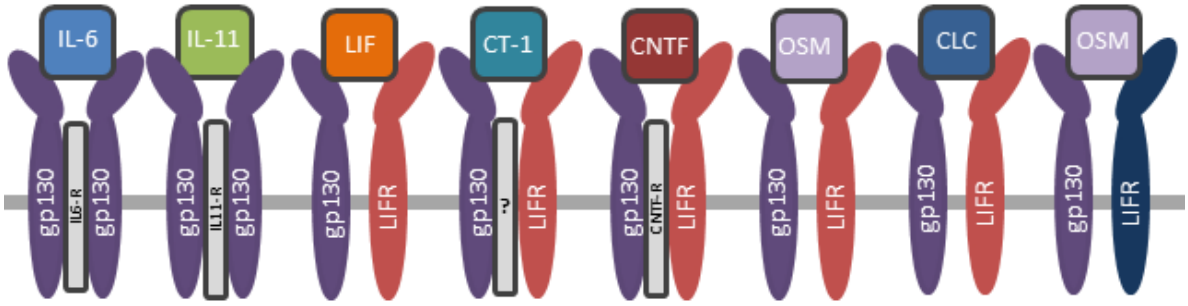

Figure 1.4: The IL-6 cytokines and their receptors. Every member of the IL-6 family signals through the GP130 receptor but the second subunit used varies, with some even using a third, smaller receptor, although this is usually not essential. Adapted from (Heinrich 2003)

Original in colour

Initially, LIF binds to LIFR with low affinity, but a high affinity connection is formed when it also binds to GP130, which is structurally related to LIFR (Gearing 1991, Xu 2010). Upon receptor dimerization, the receptors phosphorylate members of the JAK family. Three JAK kinases (JAK1, JAK2, and TYK2) are phosphorylated by IL-6-like cytokines and the combination of these activated influences the effect the cytokine has on the cell (Stahl *et al.* 1994).

In IL-6 cytokine signalling, phosphorylation of JAK2 leads to phosphorylation of STATs 3 and 5. Phosphorylated STATs dimerise and translocate to the nucleus (Matsushita 2014). A threshold level of phosphorylated STAT3 (pSTAT3) is required to maintain pluripotency (Niwa 1998, Boeuf 2001). One of the target genes pSTAT3 directly regulates is the pSTAT3 inhibitor suppressors of cytokine signalling (Socs)-3 (Naka 1997, Starr 1997) which initiates a negative feedback loop by binding between the SH2 domain of Socs3 to a motif on GP130 on $pTyr^{759}$ (Fig 1.5) (Schmitz 2000). Socs3 bound to this region prevents binding and phosphorylation by STATs. However, Socs3 can only bind to this region after it has been phosphorylated by JAK2, a process that happens after cytokine stimulation. Therefore, a cell is still able to respond to the first wave of cytokine stimulation, even if there is Socs3 present in the cytosol (Bergamin 2006).

LIF may share the tissue-protective effects of EPO. Boeuf *et al* (2001) and Duval *et al* (2000) both provided evidence that upon removal of LIF embryonic stem cells will either differentiate or apoptose within 36 hours, showing that LIF, like EPO, can be anti-apoptotic and therefore tissue-protective (Duval *et al.* 2000, Boeuf 2001).

LIFs tissue protective effects occur primarily in the nervous system where it influences neurons to become cholinergic. In a study by Joly *et al,* LIF was the most important protective cytokine in the retina where it protects the Müller glial cells from damage (Joly *et al.* 2008). The study also showed that upon removal of LIF from these cells the STAT3 pathway was inhibited and the degeneration process was accelerated.

LIF is not present in the healthy nervous system, but its expression is upregulated during various neurological disorders, including Alzheimer's disease, Parkinson's

disease (Soilu-Hanninen 2010), nerve injury (Dowsing 2001), spinal trauma (Kurek 1998), and cerebral ischaemia (Suzuki 2000). LIF reduced the clinical severity and the demyelination seen in EAE by diminishing cytokine production by T-Cells, monocytes and neutrophils (Linker 2008). In support of the promising findings in EAE models, Vanderlochte (2006) demonstrated that LIF is secreted by macrophages and T cells in the lesions characteristic of MS and that LIF limits apoptosis caused by TNF-α (Vanderlocht 2006). Furthermore, LIF mRNA was significantly increased in the spinal cords of EAE mice and neutralising anti-LIF antibodies prevented functional recovery usually seen in relapsing-remitting MS (Butzkueven 2006). They also showed that inflammatory markers had not increased therefore, the authors suggested that LIF is one of the key players in repairing damage to the CNS during relapsing-remitting MS. *In vitro,* LIF, and other IL-6 cytokines, had positive effects on myelination by aiding the final maturation of oligodendrocytes (Stankoff 2002), but inhibition of myelination has also been demonstrated (Park 2001, Ishibashi *et al.* 2006).

LIF has not been used extensively in treatment but, in contrast to EPO, LIF has relatively few side-effects when used pharmacologically, despite being such a pleiotropic cytokine. In one study (Gunawardana *et al.* 2003) it was shown to have positive effects when administered to cancer patients after they had received chemotherapy. There were some side-effects, including dizziness and hypotension, but these were mostly mild and short-term.

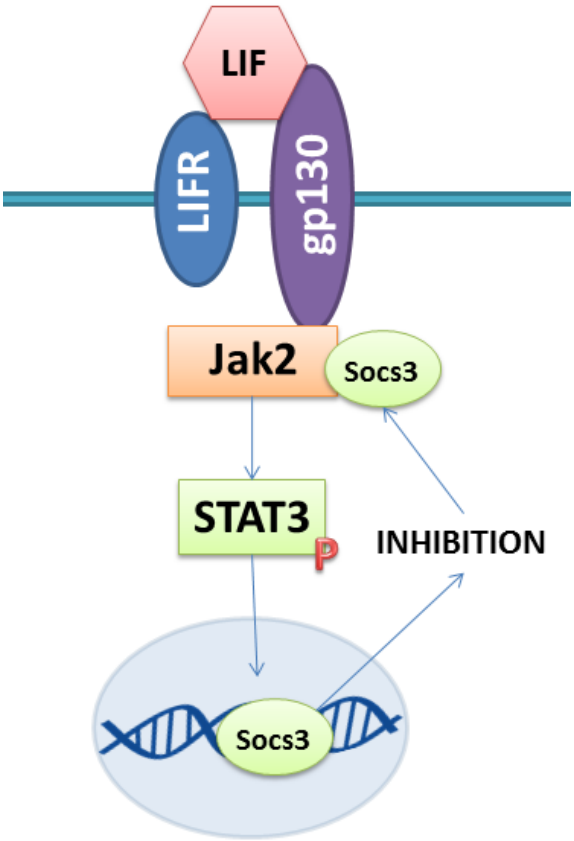

Figure 1.5: The JAK/STAT/Socs pathway as induced by LIF. Binding of LIF to LIFR and GP130 leads to conformational changes in these receptors and therefore in JAK2, leading to the availability of a Sh2 domain. STAT3 binds to this domain and becomes phosphorylated. Two pSTAT3 molecules dimerise and translocate to the nucleus where they induce, among other genes, Socs3. Socs3 can then bind to the SH2 domain on JAK2, inhibiting further STAT3 phosphorylation. P=phosphorylation

Original in colour

1.1.2.2 Other interleukin-6 cytokines and their neuroprotective properties

OSM and CNTF are other cytokines from the IL-6 family that will be considered in this thesis. Of all the IL-6 cytokines, OSM is structurally most closely related to LIF, with 27% sequence identity (Bruce 1992). OSM is unique in the cytokine family as it can bind both LIFR and OSM receptor (OSMR) along with GP130 due to a distinctive loop structure between its B and C helices that allows it to bind to either but reduces its binding affinity to both (Fig 1.3) (Chollangi 2012).

OSM inhibited neuronal death induced by N-methyl-D-aspartate by 50% when added simultaneously and inhibited death completely when neurons were pre-treated with OSM in an *in vitro* model. It also significantly reduced lesion volume in the mouse striatum, again when injury was induced by N-methyl-D-aspartate (Weiss 2006). It can be considered anti- or pro-inflammatory depending on the target cells (Tanaka 2003).

OSMR overexpression was neuroprotective in a model of ischaemic stroke while knockout of the receptor enhanced the deterioration of stroke effects. Furthermore, prophylactic treatment with OSM also provided protection (Guo 2015). However, while there is evidence that OSM is neuroprotective in certain circumstances, it appears to use different mechanisms than LIF (Moidunny 2010). OSM has been detected in MS lesions (Ruprecht 2001, Janssens 2015) and, along with LIF, is protective in EAE (Wallace 1999, Butzkueven 2002).

CNTF signals through the LIFR/GP130 complex but also a third component termed the CNTF receptor alpha (CNTFRα) (Fig.1.3) (Ip 1992, Davis 1993). CNTF is expressed by glial cells, astrocytes, Schwann cells, and skeletal muscles, and it is believed to be only secreted in response to injury (Stockli 1991, Dallner 2002). LIFR and GP130 are both expressed ubiquitously, but CNTFRα expression is limited to the brain, the retina, and skeletal muscles (Beltran 2003, Fuhrmann 2003).

The neuroprotective effects of CNTF were first identified in the PNS (Ernsberger 1989), but potent positive effects in the CNS have also been observed such as an ability to protect neurons of the rat thalamus (Clatterbuck 1993) and CNTF is the

most studied neurotrophic factor of the retina (Wen 2012). The positive effects of CNTF in the peripheral nervous system (PNS) and CNS (Pasquin 2015) led to preclinical investigations of the use of CNTF in neurodegenerative diseases, particularly Huntington's disease (Emerich 1996). After successful animal trials a phase 1 human trial demonstrated that while CNTF is pharmacologically safe, it did not show clinical efficacy (Bloch 2004). Human recombinant CNTF was also considered for the treatment of motor neuron disease after post-mortem investigations revealed patients had significantly lower expression of CNTF in the spinal cord (Anand 1995). However, a phase II clinical trial showed no improvement in pulmonary function, motility, or survival, suggesting that the positive effects of CNTF may be limited to the nervous system or it is only efficacious in mice (Miller 1996). CNTF is important in myelination (Stankoff 2002), and directly induces Mog in a mouse model of MS (Salehi 2013).

1.2 Mechanisms of repair

The process of wound healing is crucial in order to re-establish normal, efficient function after trauma has occurred. The healing process relies on several biological factors that play an active role in all stages of healing (Barrientos 2014, Kuffler 2015). The interplay between these factors and reinnervating a wound is crucial as evidenced by a lack of nerve outgrowth in hypertrophic scars (Altun 2001) and the inability of mice to heal ear-punch wounds when the ear in denervated (Buckley *et al.* 2011, Buckley *et al.* 2012). Nerves are therefore thought to be crucial for wound repair and likely critical for tissue regenerative processes (Buckley *et al.* 2012). There are a variety of cytokines, chemokines and growth factors (e.g. Transforming growth factor (TGF)-β, platelet derived growth factor (PDGF), and VEGF) that work to recruit reparative cells to the wound site (Pierce 1992, Suzuma 1998, Barrientos 2008, Penn 2012). How the balance of cytokines in the wound can affect the quality of healing and aid in faster, more complete healing with reduced scarring is being investigated (Metcalfe and Ferguson 2007). The research presented in this thesis will involve applying the tissue protective properties of EPO and LIF to aid in increasing remyelination by oligodendrocytes in models of CNS repair and in wound healing *in vitro*.

1.2.1 Myelination

Myelination is a process in the nervous system that is unique to vertebrates and which serves the purpose of aiding efficient signal transmission along axons of the nerve, protecting the axon from damage, and aiding in repair and regeneration. Myelin is essential to maintain saltatory conduction along the length of the axon to allow impulses to travel as quickly and efficiently as possible. If the myelin sheath is disrupted and not restored connections become disordered and significant loss of function results and remyelination is frequently limited in the CNS. The fundamental difference between myelination in the CNS and the PNS is that oligodendrocytes are the myelinating cell of the CNS, and it is Schwann cells that perform this function in the PNS (Martini 2010). The myelin sheath that enwraps the axon is formed of the extended membrane of the oligodendrocyte or Schwann cell from which it originates (Fig 1.6). Each Schwann cell myelinates only one axon and it does this by wrapping its cell body around it. However, one oligodendrocyte can myelinate up to twenty axons in the CNS (Mirsky 1980).

Oligodendrocytes, unlike Schwann cells (Jessen 2005), can develop and produce myelin independently of the presence of axons (Knapp 1987). They also have the capacity to migrate and find the areas in which they are needed most, unlike Schwann cells that remain adjacent to one axon their entire lifespan. OPCs are motile cells that populate the entirety of the CNS (Miller 2002).

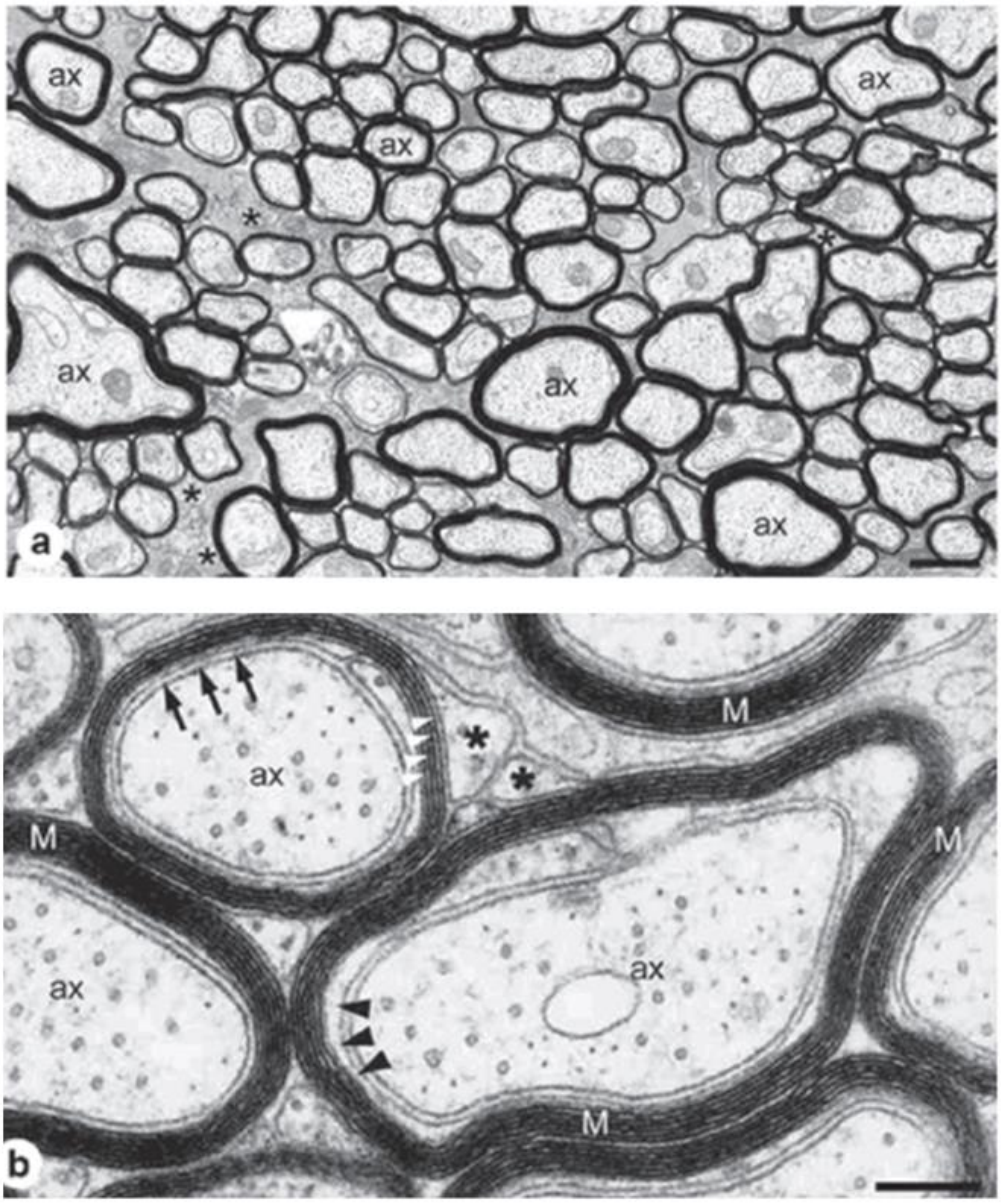

Figure 1.6: Electron micrographs of myelin profiles in the optic nerve of adult mice. The black arrows show the innermost cytoplasmic aspect of the myelinating oligodendrocytes and the arrows show the wide periaxonal space, two features that are shared with Schwann cells. However no basal lamina is visible around these cells, but it would be present in Schwann cells. Asterisks in (a) show unmyelinated axons and asterisks in (b) shows external processes. ax = axon. M = myelin. Scale bar in (a) = 1µm and in (b) = 0.2µm. Images from (Bartsch 2003) and permission to use the images was obtained from the publisher and the author.

1.2.1.1 Mechanisms that induce myelination

Oligodendrocytes respond to signals from axons (Scherer 1992), although the oligodendrocytes can be induced to express myelin *in vitro* and therefore signals from axons are not essential. Differentiation of oligodendrocytes is influenced by several ligand/receptor interactions, such as Notch and Jagged1 (Wang 1998), tropomyosin receptor kinase A and nerve growth factor (Chan 2004), PDGF receptor and PDGF (Assanah 2009), F3 and contactin (Hu 2003), polysialylated neuronal cell adhesion molecule (Charles 2000), hepatocyte growth factor and cMet (Ohya 2007), Wnt and b-catenin (Fancy 2009), leucine-rich repeat and immunoglobulin domain-containing Nogo receptor interacting protein-1 (LINGO-1)(Mi 2005), C82 and cMet (Mela 2013) and Erbb receptor tyrosine kinases and neuregulin (Brinkmann 2008). These receptor/ligand pairs interact and overlap to form an overall positive effect on differentiation and myelination. For example, Erbb4$^{-/-}$ mice show increased levels of terminal oligodendrocyte differentiation, suggesting Erbb4 has a negative effect (Sussman 2005), but LINGO-1 increases differentiation by inhibiting ErbB4 translocation (Lee 2014).

Adhesion molecules are important mediators of myelination, with the most crucial ones in the CNS being myelin associated glycoprotein (Mag), which facilitates the initial axon-oligodendrocyte interactions, and neural cell adhesion molecule which is important throughout myelination (Bartsch 1989). Once an oligodendrocyte process is in contact with an axon, an action encouraged by adhesion molecules, there are a variety of mechanisms that are adopted to change the conformation of the process from an exploratory tube to an ensheathing, flat sheet that is capable of wrapping around the axon.

Approximately 70% of the dry weight of the myelin sheath is comprised of lipids, in particular cholesterol and the glycosphingolipids galactosylceramide and its sulphated analogue sulphatide (Gielen 2006). Myelin basic protein (Mbp) and proteolipid protein (Plp) are the most abundant proteins of the myelin sheath, although the myelin-proteome is abundant, with 1200 myelin-associated proteins now known in the CNS and about 500 in the PNS (de Monasterio-Schrader 2012). Oligodendrocytes produce three times their weight in myelin and one hundred times

their weight in support membrane per day, meaning they have a high metabolic load and so are vulnerable to damage (McTigue 2008).

The addition of exogenous factors to the CNS increases myelination. The research presented in the current thesis will explore enhancing myelination by the addition of EPO, LIF, and other factors to oligodendrocyte cultures to investigate their effect on the production of myelin. The results presented here aims to understand the role these cytokines have in myelination and to characterise the mechanisms behind the effects of the cytokines.

1.2.1.2 The causes of demyelination

Demyelination is a common feature of many neurological disorders such as MS, acute-disseminated encephalomyelitis, and optic neuritis. There are many theories as to why it occurs and many factors that may interact and overlap to cause demyelination. The most common cause of demyelination is inflammation. The immune system of the CNS is largely separate from that of the rest of the body. This separation ensures systemic inflammation does not affect such a vital system (Carson 2006). However, inflammation in the CNS, neuroinflammation, can occur separately and is thought to be the mechanism behind many neuropathologies. The main cellular effectors of neuroinflammation are astrocytes and microglia, while monocytes and macrophages originating from the circulatory system also play a role. Chronic inflammation of the CNS can also be neurogenic and can lead to sustained activation of glial cells, chronic release of proinflammatory cytokines and increased permeability of the BBB (O'Callaghan 2008). While neuroinflammation is vital for the regeneration of the CNS, it can be detrimental, particularly in the brain where any excess swelling is dangerous. The inflammatory response is predominantly detrimental over the course of demyelinating disease and leads to an increase in demyelination (David 2011).

MS is the most common inflammatory demyelinating disease. MS is a chronic disease of unknown aetiology that leads to progressively worse motor, and sometimes cognitive, dysfunction. It was estimated that in 2012 there were 107,000

people in the UK living with MS and that this number is increasing by 2.4% per year due to MS patients living longer and faster diagnoses (Mackenzie 2013). The initial presentation of the disease most commonly occurs in young adults, especially females (Compston and Coles 2008, Cruz-Orengo *et al.* 2014). Initially, patients suffer from relapsing-remitting MS which manifests as acute attacks from which complete recovery is normal, with periods of relative clinical stability in-between attacks. Incomplete recovery becomes more common as the disease progresses. The disease then moves onto secondary-progressive multiple sclerosis in up to 40% of patients by 20 years after initial diagnosis (Rovaris 2006), in which neurologic decline is gradual but continuous. Primary-progressive multiple sclerosis occurs when the relapsing-remitting stage is not present. OPCs are abundant in early MS lesions and present throughout the disease progression, although their number is reduced in more advanced cases, suggesting that the lack of myelin seen in MS is not due to a lack of oligodendrocytes. Mature oligodendrocytes may be completely absent in patients who have had MS for a significant period of time.

There are two distinctly different patterns of oligodendroglial pathology in MS patients (Lucchinetti 1999). One group of patients showed preservation of oligodendrocytes in MS lesions while the other showed that about 30% of lesions had a significant loss of oligodendrocytes with the presence of oligodendrocyte apoptosis. Furthermore, work has shown oligodendrocyte death in the presence of activated microglia but little or no T cells, suggesting oligodendrocyte damage may be a causative event of MS lesion formation as opposed to an event caused by the initiation of the immune response (Barnett 2004). However, the best established explanation for the aetiology of MS is an immune attack (Steinman 1996).

Demyelination may also occur as a result of viral infection, most likely from the papovavirus or the measles virus, which cause progressive multifocal leukoencephalopathy and subacute sclerosing panencephalitis respectively. The papovavirus remains latent in B cells, the kidney and possibly the CNS but can become reactivated upon conditions that lead to reduce immune system function (Sweet 2002). Patients suffer from neurological deficits affecting functions such as speech, motor function, vision, personality, and cognition. Subacute sclerosing panencephalitis affects the whole brain and causes reduced intellectual capabilities,

personality and behavioural abnormalities. Viruses may also lead to demyelinating lesions in rare cases following systemic viral infections causing a condition called acute disseminated encephalomyelitis which is widespread throughout the CNS and results in a variety of neurological problems, principally in children (Alper 2012).

A lack of myelin also results from mutations in early growth response 2 (Egr2). Egr2 expression is associated with the onset of myelination in the PNS (Zorick *et al.* 1996) and $Egr2^{-/-}$ mice show blocked Schwann cell differentiation (Topilko 1994) and disrupted hindbrain development (Schneider-Maunoury *et al.* 1993). Furthermore, mutations in Egr2 directly lead to a lack of myelin (Warner 1998).

Hypoxia and ischaemia also cause demyelination. While in usual circumstances it is the brain tissue that suffers the most damage, sometimes it can affect myelinating oligodendrocytes. Conditions that may cause this include severe small vessel cerebrovascular disease or carbon monoxide exposure (Love 2006).

Oligodendrocyte apoptosis is another mechanism through which myelin abundance is lost (Lucchinetti 2000), as oligodendrocyte death causes an increase of Mog-specific T-cells and thus an increase in the autoimmune response against myelin (Traka 2016). This mechanism is particularly important in MS.

1.2.1.3 Why remyelination fails

Remyelination is the process in the nervous system by which the myelin sheath of demyelinated axons is restored in order to regain efficient function so impulses can pass along them correctly (Smith 1979, Smith *et al.* 1979, Jeffery 1997). Joseph Babinski was the first to propose that myelin damage might be followed by repair at the end of the nineteenth century. However it was Alastair Compston (1998) who realised that Babinski might have unintentionally observed remyelination in one of his illustrations of acute demyelinating lesions (Fig 1.7). In the drawing, the myelin surrounding the axon (labelled “a”) is being attacked by macrophages (b). However, there are uncharacteristically short sections of myelin sheath present (c) that we now know represent the appearance of remyelination (Compston 1998, Franklin 2002).

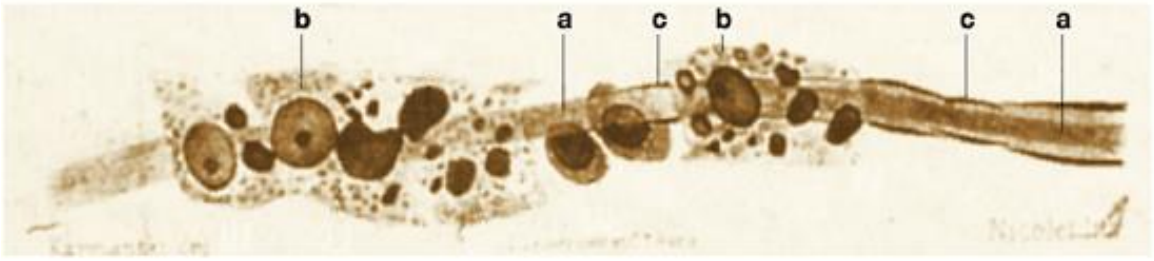

Nature Reviews | Neuroscience

Figure 1.7: Acute demyelinating lesion by Joseph Babinsky. An early drawing of demyelination by Joseph Babinsky that it is now recognised shows remyelination. a) Axon b) demyelinating macrophage c) short patch of remyelination.

(Franklin 2002)

Original in colour

Smith *et al* first demonstrated functional recovery associated with remyelination after demyelination (Smith *et al.* 1979). Remyelination reinstates saltatory conduction and functional deficits that are lost after demyelination (Jeffery 1997, Liebetanz and Merkler 2006). However, remyelination never results in the full restoration of the thickness or the length of the original myelin sheath (Prineas *et al.* 1984, Gupta *et al.* 2004).

Demyelination is associated with an increase in astrocytes and microglia which are considered to have both beneficial and detrimental roles in MS (Williams 2007, David 2011). They are involved in the migration of OPCs to the damaged area via chemoattractive signals such as basic fibroblast growth factor (bFGF) and PDGF, the same signals seen in development (Hinks 1999, Waubant 2006). However, they are also both involved in the production of TNFα which is closely linked to the pathogenesis of MS (Bitsch 2000).

For remyelination to be efficient OPCs must survive, proliferate, migrate to the lesion and differentiate into mature, myelinating oligodendrocytes (Franklin 2008). Depending on the molecular signals present in the MS plaques OPCs will either proliferate in response to PDGF, differentiate into astrocytes that contribute to the glial scar in response to bone morphogenic proteins (Fuller 2007), or differentiate into myelinating oligodendrocytes and associate with the axons. Promyelinating signals include insulin-like growth factor (IGF) -1 and -2 which promote survival and myelination of oligodendrocytes (Carson 1993, Goddard 1999, Kuhl 2002).

Remyelination is often efficient and effective, including in the early stages of multiple sclerosis (Patrikios 2006, Crawford 2013), leading to complete repair. However, in many instances, including later in MS disease progression, repair is incomplete. There are many reasons for this; in MS particularly it may be because the original cause of demyelination is still present and is therefore preventing remyelination. However, there is evidence that remyelination can fail even if there is no apparent ongoing disease activity. This may be due to a lack of reparative cells as OPCs or stem cells in the area have been depleted, a possible occurrence as adult OPCs have a more limited proliferative potential than younger ones (Wolswijk 1989).

Another hypothesis as to why remyelination fails is that OPCs have limited access to MS plaques as one third of them show limited numbers of OPCs (Lucchinetti 1999, Chang 2002, Boyd 2013). There are several factors produced at the site of injury that inhibit myelination, for example, the surrounding reactive astrocytes express elevated amounts of the chemokine CXCL1. This chemokine promotes OPC proliferation but inhibits OPC migration, therefore they convene around the plaque but are not able to enter it and produce myelin where it is required (Tsai 2002, Omari 2006).

However, around 70% of MS lesions that fail to remyelinate contain a normal number of OPCs (Wolswijk 1998, Munzel 2013), suggesting that the lack of remyelination is due to OPCs not maturing as opposed to a lack of OPC migration to the injury site. The failure of OPC maturation may be due to overexpression of molecules such as polysialic acid-containing neural cell adhesion molecule and LINGO-1, potent inhibitors of oligodendrocyte proliferation and myelination, that prevent OPCs that are close to the axon from myelinating them (Chang 2002). Furthermore, regulation of several molecules such as 9-cis retinoic acid (Huang 2011), CXCR4 (Carbajal 2011), and the bone morphogenetic protein agonist Noggin (Sabo 2011) is altered in MS and influences OPC maturation.

1.2.1.4 EPO in remyelination

Cytokines such as EPO and LIF play important roles throughout the nervous system, particularly in the regulation of myelination. EPO plays a significant role in development in the foetal brain (Juul *et al.* 1998, Knabe *et al.* 2004) and in the event of neuroinflammation, or hypoxia/ischaemia an upregulation of EPO and EPOR is observed in the nervous system (Juul *et al.* 1999, Siren 2001, Eid *et al.* 2004). EPO is anti-inflammatory in the nervous system and aids in the amelioration of symptoms of neuroinflammatory diseases such and MS/EAE, ischaemic stroke or cerebral malaria (Agnello 2002, Ehrenreich 2002, Li 2004, Kaiser 2006, Savino 2006, Bienvenu 2008, Sargin 2010). EPO significantly improves remyelination after toxic

demyelination in mice, completely ameliorating the effects of cuprizone treatment in these animals (Hagemeyer *et al.* 2012).

The first suggestion that EPO may be a useful treatment in neurodegenerative diseases came from Brines *et al* who found that EPO crossing the BBB could delay the onset, and reduce the severity of symptoms, of acute EAE, and that it could protect the brain from trauma and ischaemia and the associated inflammation (Brines *et al.* 2000). EPO may exert these functions through anti-inflammatory mechanisms as it delays the increase in TNF (Agnello 2002). As well as in a model of acute EAE (Mbp-induced in rats), EPO also protects in a model of chronic progressive EAE (Mog-induced in mice). Li *et al* (2004) found that EPO also reduced disease severity in the progressive model, even when treatment was delayed until after disease progression had begun (Li 2004). Furthermore, in the same model, EPO and two of its derivatives, CEPO and ASIALO EPO, decreased the production of proinflammatory cytokines in spinal cord lymphocytes (Erbayraktar 2003, Leist 2004, Savino 2006). Few clinical trials exist to study the impact of EPO treatment on human patients with MS, but one trial in 2008 found patients with chronic-progressive MS, the later stage of MS, presented improved cognition with no discernible increase in haemoglobin (Ehrenreich 2008).

Experimental models of stroke suggest a positive effect of EPO treatment, with evidence of increased neurogenesis and oligodendrogenesis (Gonzalez 2013). The efficacy of EPO has also been investigated in stroke patients. In the first such trial EPO was well tolerated and patients in the EPO treated group showed improved clinical outcome compared to placebo group (Ehrenreich 2002). The second trial of EPO in stroke aimed to reproduce the successful results of the first; however it showed no functional benefits of EPO treatment, and may have raised the prevalence of the need for thrombolysis (Ehrenreich 2009). Nevertheless, recent publications suggest again a positive effect of EPO treatment, while they show no decrease in long-term recurrent strokes or mortality, they did show an increased in beneficial neurological outcomes (Tsai *et al.* 2015). Furthermore, an increase in serum EPO also correlated with favourable neurological outcome in a very recent study (Åberg *et al.* 2016).

Demyelination and a failure of remyelination is a significant problem in cerebral malaria, with 40% of *post mortem* patients showing sections of demyelination in the brain and the brainstem (Medana *et al.* 2001). Several mouse models of cerebral malaria using EPO treatment have had positive outcomes (Bienvenu 2008, Hempel 2012, Bienvenu 2013, Wei *et al.* 2014). However, there has been considerable debate about the similarities, or rather the severity of the differences, between murine and human models, throwing some doubt as to whether these results provide a realistic indication of the efficacy of EPO in human cerebral malaria. However, high plasma EPO levels correlated with an >80% reduction in the chance of developing neurological complications from cerebral malaria in African children (Casals-Pascual *et al.* 2008). The potential for EPO treatment in cerebral malaria has been considered when a prospective study showing that high-dose EPO treatment, combined with quinine, assessed short-term safety and found no evidence for increased mortality and none of the expected side-effects of EPO were seen (Picot *et al.* 2009). EPO could potentially provide an anti-inflammatory benefit to cerebral malaria to limit brain damage and delay influx of inflammatory cells and the release of pro-inflammatory cytokines, its anti-apoptotic effects could prevent neuronal cell death, and its promyelinating effects could decrease the chance of neurological complications in those that survive cerebral malaria (Casals-Pascual *et al.* 2009).

1.2.1.5 LIF in remyelination

LIF is an essential protective cytokine in the CNS. It is even recognised as the most important protective molecule of the retina (Joly *et al.* 2008). The exogenous addition of LIF stimulated OPC differentiation and myelination both *in vitro* and *in vivo* (Deverman 2012).

Exogenous addition of LIF significantly reduces the clinical severity of EAE, although its positive effect seems to be mediated through prevention of oligodendrocyte loss, not an induction of remyelination. Furthermore, mutant mice that lacked both LIFR and GP130 experienced an increase in the severity of symptoms of EAE (Butzkueven 2002). Additionally, LIF has been implicated in the prevention of demyelination, while the numbers of OPCs were not altered by the

presence of LIF, highlighting that its positive effect is due to enhancing differentiation and myelination, not increasing cell migration (Marriott 2008).

LIF has been implicated in further models of neurodegeneration, for example cerebral ischaemia, where it was found expressed by neurons (Suzuki 2000), however research into the benefits of LIF in treating cerebral ischaemia is very limited. Suzuki *et al* (2005) injected either a low-dose (10ng) or a high-dose (100ng) of LIF directly into the cerebral cortex of rats immediately following middle cerebral artery occlusion (MCAO). They found the high-dose of LIF group experienced significantly less neurological deficits and ischaemic damage than the low dose or phosphate buffered saline (PBS) treated rats. Furthermore, pSTAT3 was detected at much higher levels by Western blot in the high-dose animals, showing that functional signalling is initiated by LIF (Suzuki 2005). Rowe *et al* (2005) looked at MCAO injured rats again, but this time administered LIF systemically at 6, 24, and 48 hours post-surgery. Infarct volume was significantly lower in LIF treated rats that also showed a preservation of white matter and improved functional outcomes 72 hours after surgery (Rowe 2014). Therefore, LIF limits neurodegeneration, however the dose of LIF is important.

1.2.1.6 Studying remyelination *in vitro*

The regenerative capacity of the PNS is much greater than the CNS. Due to this the majority of studies into nerve repair have been conducted in the PNS (Faroni *et al.* 2015). The restoration of function of severed nerves is possible through microsurgical repair but the regrowth of a damaged myelin sheath cannot be physically encouraged. The application of endogenous factors is the best way to encourage this. Unlike nerve repair, remyelination is possible in both the PNS and CNS.

The finding that oligodendrocytes can be induced to myelinate *in vitro* in the absence of axons (Mirsky 1980) allowed the development of many experimental procedures for studying demyelination and remyelination *in vitro.* Separation of cultures of pure OPCs from rat CNS further allowed the study of these cells individually (Chen

2007). *In vitro* models of OPCs and their capacity to myelinate are the first steps to understanding the process of myelination, why remyelination fails in diseased patients, and how remyelination can be encouraged and improved upon.

A key breakthrough in the development of *in vitro* cultures was the identification of stage-specific markers which are identical in OPC cultures as they would be *in vivo* (Baumann 2001). The CG4 cell line is OPCs that can be differentiated and the myelinating capacity of these cells measured through a variety of markers such as myelin oligodendrocyte glycoprotein (Mog) (Solly 1996, 1997). Proteins such as Mog can then be used to accurately quantify the myelinating capacity of the cells *in vitro* and comparisons can be made as to how various conditions affect the myelination of the cells. Mbp is another frequently used marker of myelination that is expressed earlier than other proteins such as Mog (Nakahara 2001). However, it should be noted that while comparisons can be made between cells under various treatments *in vitro* this is not a comparative representation of the myelinating capacity of these cells *in vivo* as each oligodendrocyte in the body can produce approximately 500 times the area of myelin membrane than an oligodendrocyte in culture (Pfeiffer 1993).

1.2.2 Wound healing

1.2.2.1 Normal wound healing process

The second method of tissue regeneration to be investigated in this thesis is wound healing. The wound healing process has four overlapping stages, originally proposed by Quinn and Wells (1998): haemostasis, inflammation, proliferation, and remodelling (Fig 1.8) (Quinn 1998). The initial stage, haemostasis, aims to prevent blood loss in order to reduce the immediate danger, and to provide the right environment to allow healing to progress. Vasoconstriction occurs immediately due to an increase of cytoplasmic calcium levels (McMurtry 1975) leading to tissue hypoxia and acidosis. This induces the release of nitric oxide, adenosine and other vasodilatory molecules which, along with an influx of histamine, cause subsequent vasodilation to allow entry of inflammatory cells into the wound space. Further

blood loss is prevented by the formation of a clot from the transformation of fibrin from fibrinogen and the activation of thrombin and platelets (Mosesson 2005).

The second stage, inflammation, then aims to prevent infection. Chemotaxis encourages neutrophils to migrate to the wound and subsequently destroy debris and bacteria. Later, phagocytosis of the wound area is performed primarily by macrophages which also provide various growth factors that are important in controlling inflammation (Velnar 2009). Inflammation is crucial and will continue as long as debris and bacteria are present, but a prolonged inflammatory response has a negative effect and can lead to the formation of a chronic wound.

The third stage, proliferation, follows in which the aim switches from preventing further damage to repair. Angiogenesis, granulation tissue formation, collagen deposition, epithelialisation, and wound contraction are all components that stimulate wound closure in this phase (Greaves 2013).

Remodelling is the final stage. It involves the formation of a normal epithelium and of scar tissue below the epithelium and can take up to two years before completion. A balance between degradation and synthesis ensues during remodelling allowing type 1 collagen to be deposited by fibroblasts and myofibroblasts during the previous stages to be slowly replaced with type 3 collagen (Profyris 2012) to replicate the basket-weave collagen structure seen in unwounded tissue. This latter stage is not often orchestrated properly in an attempt to heal the wound quickly without too much inflammation. In this situation, the type 1 collagen is often laid down by the fibroblasts in excess and in a dense parallel arrangement of the matrix that leads to the development of a scar.

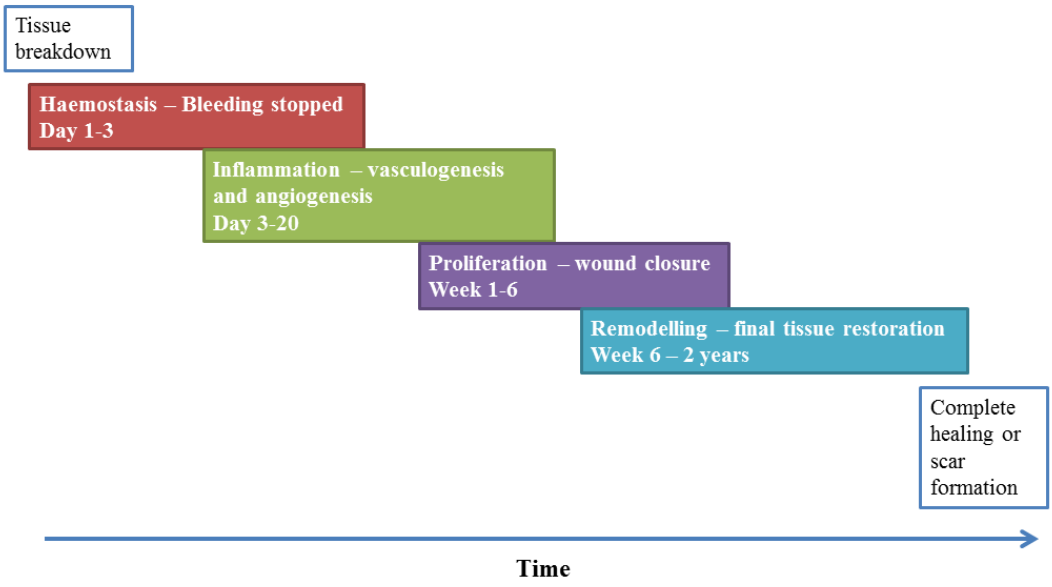

Figure 1.8: The four stages of wound healing. The wound progresses through haemostasis, inflammation, proliferation, and remodelling to form a fully closed wound and reinstate skin integrity. Adapted from (Martin 2013)

Original in colour

If the stages of wound healing fail to progress as expected, and the injury does not heal beyond the inflammatory phase, a chronic wound can develop. Chronic wounds are of particular problem to people suffering from diabetes mellitus who experience neuropathy in their extremities. The lack of sensation in the extremities caused by the neuropathy means a wound, commonly on the sole of the foot, could go unnoticed and so untreated. Furthermore, the wounds of people with diabetes mellitus have very different biochemical characteristics; including reduced growth factor secretion (Galkowska 2006), decreased angiogenesis (Glaiano 2004) and decreased macrophage function (Gibran 2002). These combined symptoms enhance the development of chronic wounds. It is estimated that in 2010 there were 280 million people living with diabetes mellitus and it is projected that 360 million people will suffer by 2030 (Shaw 2009, Whiting 2011). The estimates of how many of these will suffer from a foot ulcer vary but some believe it could be as high as 25% (Boulton 2005). Treatments for foot ulcers range from off-loading strategies which move pressure on the foot away from the affected area (Boulton 2004), to hyperbaric oxygen therapy which exposes the wound to 100% oxygen for intermittent periods of time (Oliveira 2014), and specialised wound dressings (Boateng 2007).

More than 85% of foot amputations are caused by diabetic foot ulcers (Snyder 2009). Chronic wounds fail to heal because excess inflammation does not allow for the regeneration of new tissue. Therefore, a wound dressing that can decrease healing time could help to reduce the huge personal, social, and economic burden of diabetic foot ulcers. This work will look at potentially incorporating tissue protective cytokines into wound healing strategies as the topical application of tissue protective cytokines directly to a wound has the potential to reduce inflammation, speed up wound healing, and prevent formation of chronic wounds. The use of tissue protective cytokines in regenerative medicine could aid in faster healing and potentially the restoration of skin that more closely mimics the original tissue, instead of scars that lack the tensile strength and flexibility of normal skin.

The repair of damaged skin is an extensive topic of research within regenerative medicine. This research extends beyond just improving wound healing, but also the development and use of skin substitutes to replace tissue that has been damaged or

lost, such as patients suffering from 3rd degree burns (James *et al.* 2009). Skin substitutes such as grafts or artificial skin could be more effective and have a greater chance of success if tissue protective cytokines could be incorporated into their application to reduce apoptosis and inflammation and increase angiogenesis to the area.

1.2.2.2 EPO in wound healing

The effects of EPO on cell survival and proliferation mean it has potent positive effects on wound healing. The anti-apoptotic effect of EPO increases wound healing and the non-erythropoietic derivatives of EPO are also effective at aiding wound healing by suppression of apoptosis (Ghezzi 2004, Erbayraktar 2009). Furthermore, the effects that EPO has on the nervous system could be beneficial in a wound setting. Denervated tissues fail to heal wounds (Buckley *et al.* 2012) so treating a wound by encouraging the formation of fully mature and myelinated nerves would likely help to increase wound healing efficiency. In fact it is thought that the presence of infiltrating nerves within the regenerating blastemal-like structure of wounds made in the ears of mice promotes tissue regeneration (Buckley *et al.* 2012). In this situation the nerves were observed to infiltrate the regenerating ear structure in advance of neovascularisation. Conversely in the same animals that had wounds made on the dorsum, blood vessels infiltrated in advance of the nerves growing into the wound space, and those wounds healed with a scar (Buckley *et al.* 2011, Buckley *et al.* 2012). From these and other studies in urodeles, it would appear that nerves are critical for tissue regenerative processes (Kumar and Brockes 2012).

EPO can stimulate the coagulation phase of wound healing. It is a causative agent in platelet aggregation and can stimulate the bone marrow to increase platelet production, aiding in the immediate stage after wounding has occurred (Demetz *et al.* 2014).

The anti-inflammatory effects of EPO may aid in progression through the inflammatory phase of wound healing. This phase is important, but can regularly become chronic, preventing the wound from moving to the next stages. Sorg *et al*

treated mice with a repeated low-dose or a single high-dose of EPO and found the wound healing time was significantly decreased because the inflammatory phase was considerably shorter (Sorg 2009). EPO also inhibits the production of pro-inflammatory cytokines (Brines 2008, Strunk 2008).

EPOR was found on endothelial cells and so can directly stimulate angiogenesis (Anagnostou *et al.* 1994). It is also capable of indirectly stimulating angiogenesis by upregulating the expression of VEGF (Arroyo 1998). The effect of EPO on wound vasculogenesis can also be attributed to endothelial cell mitosis, recruitment of endothelial progenitor cells, and of mesenchymal stem cells (Heeschen 2003, Chen *et al.* 2008). Furthermore, EPO influences the remodelling phase as it orchestrates the TGF-β pathway and myofibroblast differentiation (Siebert 2011). However, EPO could potentially have negative impacts on the final stage of wound healing because the formation of scar tissue relies on apoptosis of myofibroblasts, endothelial cells and other cell types involved in the formation of granulation tissue, and decreased apoptosis could lead to the formation of hypertrophic scarring (Desmoulière *et al.* 1995, Sarrazy 2011).

The conclusion of many animal studies on EPO in wound healing is that it positively influences healing. In the first study of this kind, Fatouros *et al* (1999) found that EPO increased the wound breaking strength seven days after injury of Wistar rats (Fatouros *et al.* 1999). Haroon *et al* (2003) could later attribute this greater tensile strength to an increase in granulation tissue (Haroon *et al.* 2003). Further studies provide evidence that EPO is protective throughout the wound healing process and that this is due to an increase in VEGF-induced angiogenesis and a decrease in inflammation (Buemi 2002, 2004, Bohr *et al.* 2013). These results suggest that EPO could be an important regenerative tool in the restoration of tissue function

The improvement of wound healing observed with the administration of some tissue protective cytokines in animal studies have led to many human trials of the benefit of EPO in the healing of human wounds. The first findings were a side-effect of using EPO for the treatment of anaemia resulting from chronic kidney disease; these patients exhibited increased healing of chronic pressure ulcers due to increased oxygenation and the non-hematopoietic effects of EPO (Keast 2004). Topical

application of EPO was also beneficial in patients with deep split-thickness skin grafts, pressure sores, and venous ulcers as EPO stimulated an increased formation of granulation tissue and aided complete epithelialisation (Bader 2011). A large trial on 150 burns patients in currently ongoing to investigate how regular EPO treatment affects the time it takes until re-epithelialisation is complete (Günter *et al.* 2013). Furthermore, diabetic patients treated with the EPO peptide ARA290 reported reduced symptoms from neuropathy (Brines *et al.* 2014). These results of EPO in wound healing suggest that it is a viable molecule for regenerative therapies.

1.2.2.3 LIF in wound healing

The first evidence of LIF in the skin was its expression in a squamous carcinoma skin cell line (Baumann 1989). LIF was later identified in healthy human keratinocytes of the epidermis, that were also expressing LIFR, suggesting LIF has autocrine effects on these cells (Paglia *et al.* 1996). LIF is expressed constitutively in the epidermis, a rare event for cytokines in the skin, however its very low normal release (1 to 1.5 pg/ml) (Paglia *et al.* 1996) is severely increased in keratinocytes of tumour cells lines (1 to 2 ng/mL) (Szepietowski *et al.* 2001).

There is little evidence of LIF in wound healing, although LIF transfection did increase skin collagen production and angiogenesis (Akita *et al.* 2004). Furthermore, IL-6 which shares the GP130 receptor with LIF has been implicated. IL-6 is essential in wound healing as IL-$6^{-/-}$ mice as wound injuries remained larger than wild type mice and complete reepithelialisation took 14 days in knockout mice compared to 10 days in the wild types (Lin 2003).

STAT3 is expressed in keratinocytes and is essential for keratinocyte migration, but not proliferation (Sano *et al.* 1999, Quadros 2004). Socs3, which is a downstream negative regulator of STAT3, a function that is also present in wound healing. Socs3 knockout mice exhibited impaired wound healing, prolonged secretion of chemokines, a hyperproliferative epidermis, and neutrophil infiltration into wounds through irregular STAT3 phosphorylation (Zhu *et al.* 2008). Findings such as this provide evidence that LIF may also have an impact on wound healing. The work

presented here will look at the effects of EPO and LIF on wound healing, developing on work in models of oligodendrocyte myelination.

1.2.3 Applications of this thesis

The current work presented here will investigate the role of tissue protective cytokines, particularly EPO and LIF, in increasing myelination by oligodendrocytes and in increasing the rate of wound healing.

The aims of this thesis are to study the mechanisms through which EPO increases myelination. To do this the myelinating properties of LIF, another tissue protective cytokine, will be investigated both separately and simultaneously with EPO. The comparisons between the cytokines, and the effects that they have synergistically, will help to study molecular mechanisms and help to eventually identify therapeutic targets for demyelinating diseases.

The use of tissue protective cytokines in wound healing was also investigated. Chronic wounds develop primarily when wounds remain in the inflammatory phase. Here a cycle can develop where inflammation causes tissue necrosis, which in turn causes more inflammation. The application of a tissue protective cytokine could prevent apoptosis and inflammation and so aid in the development of the wound beyond the inflammatory stage. If a tissue protective cytokine could be incorporated into a wound dressing it could be administered topically and therefore avoid the side effects associated with systemic delivery. Again, EPO and LIF will both be tested in a simple wound healing model to determine if there are any improvements in cellular repair brought about by either of these cytokines and therefore show their potential uses in regenerative medicine.

The hypothesis at the start of this project was that LIF shares the pro-myelinating effects of EPO and that it may synergise with EPO or serve as a viable alternative for EPO in the treatment of demyelinating diseases. Furthermore, tissue protective cytokines such as EPO and LIF may be effective in treating chronic wounds.

1.3 Aims

1. To thoroughly test EPO and LIF in a previously established model of neurorepair
   1.1. To determine if LIF has the same positive effects on Mog induction as EPO and to test the synergistic effect of adding the cytokines simultaneously
   1.2. To define the mechanisms of action in terms of signal transduction pathways of these tissue protective cytokines by measuring the phosphorylation or the expression of specific proteins
   1.3. To study the gene expression profile involved in the differential effects of the cytokines on myelination using microarrays by comparing CG4 cells treated with EPO, LIF and their combination
   1.4. To validate by qPCR gene expression changes detected by microarray analysis
   1.5. To determine if the detected genes have any functional impact on Mog expression by studying the effect of their proteins on differentiating CG4 cells
2. To test these cytokines in models of wound repair using scratch assays to see if they have a significant effect on wound healing

Chapter 2. Materials and Methods

2.1 Materials and Suppliers

Material	Supplier
Acrylamide/Bis	Bio-Rad Laboratories
APS	Sigma-Aldrich
bFGF	Invitrogen
Biotin	Sigma-Aldrich
Brilliant III qPCR master mix	Agilent technologies
Bromophenol Blue	Sigma-Aldrich
BSA	Sigma-Aldrich
Chloroform	Sigma-Aldrich
CNTF	Peprotech
DMEM/F12+Glutamine	Sigma-Aldrich
DMEM	Sigma-Aldrich
dNTP	GE Healthcare Life Sciences
DTT	Invitrogen
ECL	GE healthcare Life Sciences
EDTA	Thermo Fisher Scientific
EGTA	Sigma-Aldrich
EPO	Sigma-Aldrich
Ethanol	Sigma-Aldrich
FCS	Invitrogen
Glucose	Sigma-Aldrich
Glycerol	Melford Laboratories
Glycine	Sigma-Aldrich
Glycogen	Invitrogen
High performance autoradiography film	GE Healthcare Life Sciences
Insulin	Sigma-Aldrich
Isopropanol	Sigma-Aldrich
Lcn2	Adipogen
LIF	Sigma-Aldrich
Lipofectamine	Invitrogen
Methanol	Thermo Fisher Scientific
M-MLV-RT	Invitrogen
miRNeasy Mini Kit	Qiagen
N1 supplement	Sigma-Aldrich
Nitrocellulose blotting membrane	GE healthcare Life Sciences
OSM	Peprotech
Pam3	Axxora
PBS	Fisher

PDGF	Invitrogen
Pen/Strep	GIBCO
PhosphoSTOP	Roche Life Sciences
Plates and flasks for CG4 cells	Falcon
Plates and flasks for HaCaT and Send-1 cells	Corning
PMA	Sigma-Aldrich
Poly-L-ornithine	Sigma-Aldrich
Progesterone	Sigma-Aldrich
Protease inhibitors	Roche
Putrescine	Sigma-Aldrich
QIAzol	QIAGEN
Opti-MEM	Thermo Fisher Scientific
Random primers	Promega
RIPA buffer	Thermo Fisher Scientific
RNAse OUT	Invitrogen
RNAse-free H_2O	Thermo Fisher Scientific
SDS	Sigma-Aldrich
Socs3 siRNA "1"	Ambion
Socs3 siRNA "2"	Thermo Fisher Scientific
Sodium selenite	Sigma-Aldrich
Taqman probes and primers	Thermo Fisher Scientific
Temed	Sigma-Aldrich
Thyroxine	Sigma-Aldrich
Transferrin	Sigma-Aldrich
Trizma base	Sigma-Aldrich
Tween-20	Sigma-Aldrich
ZA	Sigma-Aldrich
β-mercaptoethanol	Sigma-Aldrich

Table 2.1: Materials used in the project with the manufacturing supplier that they were purchased from.

2.2 Commonly used buffers and solutions

Product	Dilution	Volume	Composition
qPCR master mix		10µl/sample	RT-PCR buffer, $MgCl_2$, nucleotides, stabilisers, mutant Taq DNA polymerase
Running buffer	10X	1L	250mM Tris pH 8.3, 144.13g glycine, 1% SDS
Running gel		1 gel	Acrylamide/bis solution 1650µl (9% gel) or 1850µl (10% gel), running gel buffer 1375µl, SDS 10% 55µl, APS 55µl, Temed 5.5µl, H_2O 2420µl (9% gel) or 2260µl (10% gel).
Running gel buffer	4X	100ml	1.5M Trizma® (tris)-hydrochloride (HCl) pH 8.8
Sample buffer	6X	10ml	375mM Tris-HCl, 12% SDS, 60% glycerol, 0.02% bromophenol blue, pH 6.8
Stacking gel		1 gel	Acrylamide/bis solution 417.5µl, stacking gel buffer 625µl, SDS 10% 25µl, APS 37.5µl, Temed 2.5µl, H_2O 1430µl.
Stacking gel buffer	4X	100ml	500mM Tris-HCl, pH 6.8
Supplemented RIPA buffer		1ml	Glycerol 50µl, EDTA 2µl (1mM), EGTA 25µl (1mM), Protease inhibitors 143µl, PhosphoSTOP 100µl, RIPA buffer 680µl
Tris buffered saline	10X	1L	Tris base 200mM (24.2g/l), NaCl 1.37M (80g/l)

Table 2.2: Commonly used buffers and solutions

2.3 Cell lines

2.3.1 CG4 cell line

Central Glia-4 (CG4) cells, rat oligodendrocyte precursor cells that have the ability to differentiate into mature, myelinating oligodendrocytes or type-2 astrocytes, were used to assess the pro-myelinating properties of LIF in comparison to EPO (Figs 2.1 and 2.2). While these are a cell-line, they are viable OPCs as when transplanted into myelin-deficient rats or into regions of experimental demyelination they develop into mature oligodendrocytes and remyelinate the affected neurons (Tontsch *et al.* 1994, Franklin *et al.* 1995). They have served as a good model by our group and by others for the study of the mechanisms regulating the expression of myelin components, signalling factors, and transcription factors (Anderson 1994, Solly 1997, Bichenkov 1999, McNulty *et al.* 2001, Annenkov *et al.* 2011, Wang *et al.* 2011, Cervellini *et al.* 2013a).

Based on previous work, CG4 cells overexpressing EPOR were used. The development of these was described previously (Cervellini *et al.* 2013a). Briefly, CG4 cells were transduced with the mouse *EPOR* gene in a constitutive lentiviral vector modified to include the V5 epitope, the mouse encephalomyocarditis internal ribosome entry site and the enhanced green fluorescent protein reporter. The cells were screened for EPOR expression by qPCR. The overexpression of EPOR in these cells should be considered when analysing results, but they reflect *in vivo* oligodendrocytes that express EPOR (Ott *et al.* 2015). In this thesis the cells are referred to as "CG4"; however throughout the CG4 EPOR cells are used.

The cells were cultured on plates coated with poly-L-ornithine in PBS (15µg/ml). To coat the plates enough poly-L-ornithine was added to coat the base of the plate and then they were incubated at 37°C for 1 hour before two washes in PBS.

CG4 cells were seeded in growth medium (GM) consisting of Dulbecco's modified eagle medium (DMEM) supplemented with Biotin, basic fibroblastic growth factor (bFGF), platelet derived growth factor (PDGF), N1 supplement, and 30% conditioned medium from neuroblastoma B104 cells (Table 2.3). The conditioned

medium was obtained by culturing B104 cells to confluence in DMEM supplemented with 10% foetal bovine serum (FBS) before changing their medium to N1 supplemented DMEM without serum. They were then incubated for three and a half days before the medium was aspirated, centrifuged, filtered and then split into aliquots of 15ml and stored at -80^{o}C.

The CG4 cells were not allowed to exceed 80% confluence and so were passaged every other day, although with plating at a lower density passage could occur after 3 days, in which case half the medium was changed on the second day. Trypsin was used to passage the cells but, because of a lack of serum in the medium, trypsin inhibitor was required throughout culture.

CG4 cells were plated in 24-well plates at a density of $4x10^4$ cells/ml in 1ml GM in experiments measuring Mog and at $8x10^4$ cells/ml in experiments measuring signalling pathways. Each condition was sampled in quadruplicate. For both myelin investigations and signalling investigations they were incubated in GM for 24 hours before GM was removed and they were washed in serum-free DMEM twice. Differentiation medium (DM) was then added which contained DMEM/F12+glutamine supplemented with: progesterone, putrescine, sodium selenite, insulin, transferrin, biotin, thyroxine, glucose, and penicillin/streptomycin (Table 2.4).

Component	Volume for 50ml	Final concentration
B104-conditioned N1 medium	15ml	
N1 supplement	500µl	X1
Biotin	50µl	10ng/ml
bFGF	50µl	5ng/ml
PDGF	50µl	1ng/ml
HEPES 1M	500µl	
NEAA	500µl	
DMEM+glutamine+pen/strep	≈32.5ml	

Table 2.3: Supplements used for CG4 growth medium.

Component	Volume for 50ml	Final concentration
Progesterone	7.5µl	3ng/ml
Putrescine	2.5µl	5µg/ml
Sodium selenite	44.5µl	4µg/ml
Insulin	62.5µl	12.5µg/ml
Transferrin	50µl	50µg/ml
Biotin	50µl	10ng/ml
Thyroxine	20µl/ml	0.4µg/ml
Glucose	333.5µl	3%
DMEM/F12=glutamine+pen/strep	49ml	

Table 2.4: Supplements used for CG4 differentiation medium.

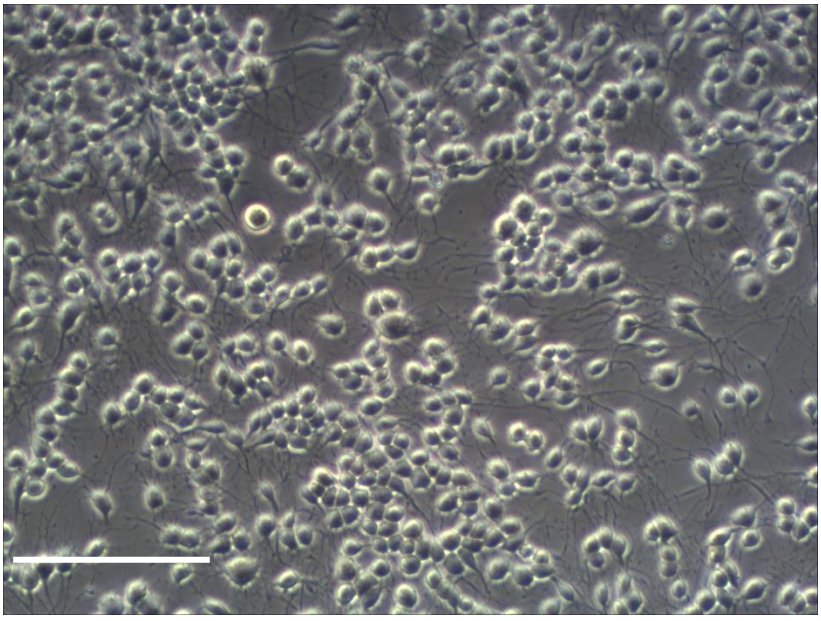

Figure 2.1: Undifferentiated CG4 cells. The cells were grown in GM on Poly-L-Ornithine coated plates. Scale bar represents 400µm.

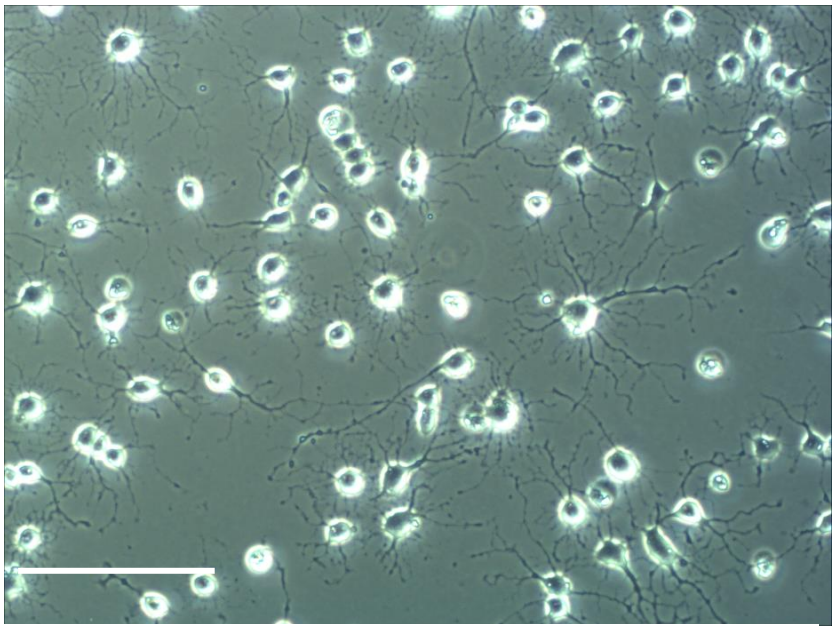

Figure 2.2: CG4 cells 24 hours after differentiation. After incubation for 24-hours in GM the cells were washed twice in serum-free DMEM then DM was added. Scale bar represents 400µm.

Original in colour

2.3.2 sEnd-1 cell line

sEnd-1 cells are a mouse skin endothelial cell line used here for scratch assay models. The cells are derived from subcutaneous haemangioma and show morphology similar to that of *in vivo* endothelial cells (Boraschi *et al.* 1991). They were maintained in DMEM supplemented with 10% FCS and 1% penicillin/streptomycin. The cells were cultured in T75 flasks and passaged once ~80% confluent. Upon splitting the cells in a 1:5 ratio, passage would usually be carried out every 2 days, but if plated at a lower density and passaged less frequently they remained viable. The cells were not sufficiently robust to survive centrifugation. Therefore, the medium was changed the day after thawing and the day after passage to remove any remaining DMSO or trypsin.

2.3.3 HaCaT cell line

HaCaT cells are a human keratinocyte cell line that maintains full epidermal differentiation capacity and the ability to keratinise. Furthermore, when transplanted onto nude mice they form an epidermal tissue that mimics that of normal keratinocytes (Boukamp 1988). The cells were maintained in DMEM supplemented with 10% FCS and 15 penicillin/streptomycin in T75 flasks. Upon splitting 1:5 ~80% confluence would be achieved after 2-3 days.

2.4 *In vitro* oligodendrocyte myelination model

2.4.1 Myelination and signalling investigations

The effect of various cytokines on CG4 cell myelination was investigated by three day incubation immediately following cell differentiation. Half the medium was changed at day 2, along with the supplemented cytokines. In the experiments in which the earlier signalling events were being observed the cells were incubated for 24-hours in DM before addition of the cytokine(s). The cells were then incubated for 1 hour before the experiment was stopped.

2.4.1.1 RNA extraction

Following cell stimulation, DM was removed and cells were thoroughly washed and resuspended in 400µl of QIAzol. Two wells were then pooled into one single sample in RNAse-free Eppendorf tubes.

Total RNA extraction began with the addition of 160µl cold chloroform per 800µl sample. Each Eppendorf microcentrifuge tube was shaken vigorously to homogenise the solution. The samples were then centrifuged at 12,000xg at 4°C for 15 minutes after which a separation between the upper, colourless aqueous phase and the lower, pink phenol-chloroform phase was obvious. Also visible was the layer of DNA and protein which appeared solid white around the edge of the tube in the upper phase. The top 200µl of the aqueous phase was transferred to a new Eppendorf for each sample, with care taken not to touch the interphase or the phenol-chloroform layers. Added to this new Eppendorf microcentrifuge tube was 1µl of glycogen as an inert co-precipitant to increase the yield of RNA, and 200µl of cold isopropanol. The samples were inverted gently to mix then incubated at 4°C overnight to allow RNA precipitation.

The next day the samples were centrifuged at 12,000xg at 4°C for 30minutes after which an opaque pellet of RNA precipitate was visible at the bottom of the tube. The supernatant was completely aspirated, with care taken not to disturb the pellet. One millilitre of cold 75% ethanol was then added and the tubes were vortexed briefly until the pellet was detached. The samples were then centrifuged at 7,500xg at 4°C for 15minutes to wash. The supernatant was again removed completely, before air-drying until the tubes were completely dry and the RNA pellets were no longer visible at the bottom of the tube. The samples were then resuspended in 12µl RNAse-free H_2O before incubation at 60°C for 10 minutes. The Nanodrop ND-1000 was used to determine the RNA quality and quantity by determining the ratio of absorbance at 260nm and at 280nm. Samples with a ratio below 1.7 were discarded.

2.4.1.2 Reverse transcription

Reverse transcription (RT) is a process through which complementary DNA (cDNA) is synthesised from an RNA template, producing cDNA that mimics the original DNA of the cell (Sanders *et al.* 2014).

RT was carried out to obtain single-stranded cDNA from the extracted RNA for use in quantitative polymerase chain reaction (qPCR) analysis. The RT reaction began with incubation of the samples with 500ng random primers and 0.6mM dNTP for 10 minutes at 60°C. To this RT buffer, DTT 10mM, RNAse OUT 40 U, and M-MLV-RT 200 U was added before incubation for 10 minutes at 25°C, then 60 minutes at 37°C, and finally 15 minutes at 70°C.

2.4.1.3 Quantitative polymerase chain reaction

PCR was originally invented by Kary Mullis in 1988 as a method to amplify fragments of nucleic material (Saiki 1988). Specific primers for a sequence between a 3' and a 5' marker are used to amplify a certain length of target sequence. Once the sequence has been recreated a Taq polymerase enzyme synthesizes it into a continuous strand. In this manner a measurable quantity of DNA is acquired that will correlate with the occurrence of this sequence in the original cDNA. Traditional PCR is not quantitative as only a final measurement is taken. This would not take into account quantification reaching a plateau earlier in some samples than others. Therefore, qPCR was developed in which the measurement is taken at the exponential increase stage, before the amplification plateaus, thus allowing accurate quantification and comparison between samples (Nolan 2006).

For the qPCR, brilliant III qPCR master mix and Taqman probes were used. For each sample, assayed in duplicate, a mix of 10µl master mix, 1µl 20X gene expression assay mix, 7µl H_2O, and 2µl cDNA was used. The qPCR was carried out on the MX 3000P sequence Detection System and analysis of the results was carried out using the $2^{-\Delta\Delta CT}$ Method (Livak 2001) in which the number of cycles required to reach a threshold where the quantity of DNA is deemed to be significantly different

from baseline is measured (Fig 2.3). The housekeeping gene (Hprt1) was measured for every sample in order to provide a normalised background measurement that should be uniform across all samples. The cycles and steps required for qPCR are outlined in Table 2.5.

The analysis of the qPCR data begins with subtracting the cycle threshold (Ct) of the housekeeping gene from that of the gene of interest for the same sample, therefore normalising the gene expression against the housekeeping gene, obtaining the ΔCt. From here the results are normalised versus one control sample which is the calibrator, providing the ΔΔCt value, which for the calibrator will be 0. Once the difference between the samples and the control is obtained and the values are expressed as a fold change the $2^{-\Delta\Delta Ct}$ value is obtained, providing a measure of how much that gene was amplified above baseline. Statistical significance between these samples was determined using the unpaired two-tailed student t-test. The genes measured by qPCR for the myelination experiments are Mog, Socs3, Mbp and Egr2 and the full list of genes measured by qPCR and their probes ID numbers is in table 2.6.

Cycles #	Cycle setting	Cycle purpose
1 cycle	3 minutes at 95°C	**Initialisation step**: the Taq polymerase is activated
40 Cycles	15 seconds at 95°C	**Denaturation step:** the cDNA template is divided to obtain two single strands of DNA
	20 seconds at 60°C	**Annealing-extension step:** Taq DNA polymerase extends the DNA from the primers

Table 2.5: Cycles and steps required for qPCR. The cycles remained the same for each primer used.

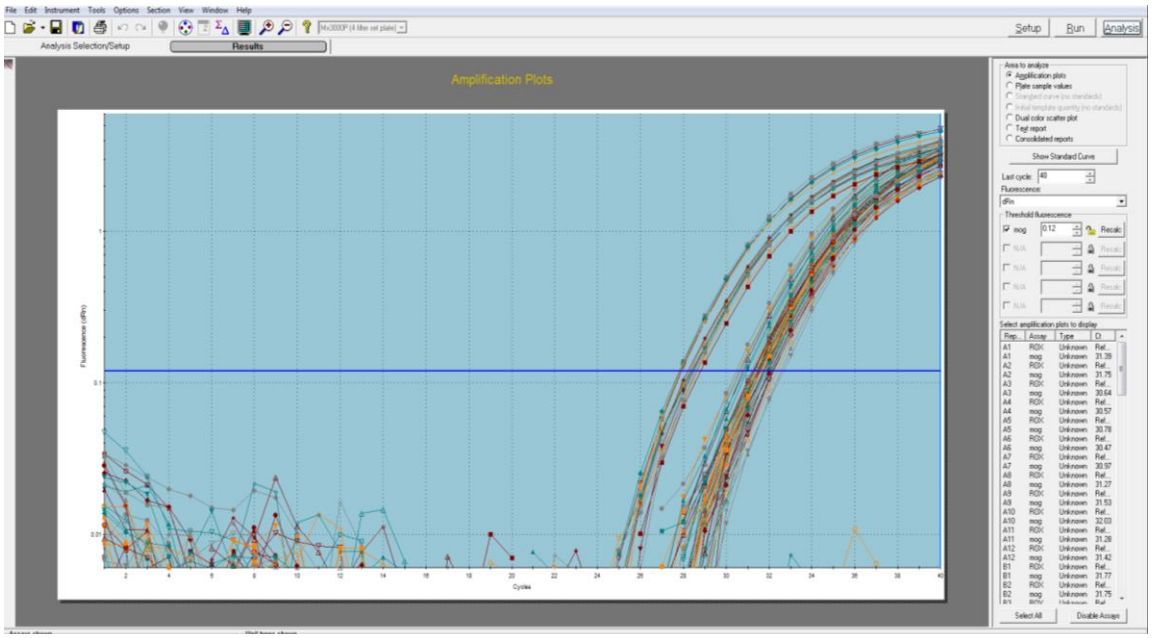

Figure 2.3: Typical amplification plot from qPCR analysis. The plot measures the number of cycles required to reach the threshold, shown as the blue horizontal line. The more cycles required for samples to cross the threshold indicates lower expression of the gene in that sample.

Probe	ID number
Hprt1	Rn01527840_m1
Mog	Rn00575354_m1
Socs3	Rn00585674_s1
Mbp	Rn00690431_m1
CD36	Rn01442639_m1
Igf1	Rn00710306_m1
Fos	Rn00487426_g1
JunB	Rn00572994_s1
Tnfrsf1a	Rn01492348_m1
Inhba	Rn01538592_m1
Mag	Rn01457782_m1
Pmp2	Rn01457054_m1
Ppargc1a	Rn00580241_m1
Tlr2	Rn02133647_s1
Lcn2	Rn00590612_m1

Table 2.6: The genes measured by qPCR throughout the project and the ID number of their Taqman probe. All probes purchased from Thermo Fisher Scientific.

2.4.1.4 Western Blot Analysis

Western blots were set up as a method to separate proteins using gel electrophoresis. The samples are loaded into the top of an acrylamide gel and a current passed through the gel. The samples were negatively charged due to sodium dodecyl sulphate (SDS) in the sample buffer, therefore they migrate through the gel towards the positively charged electrode. Smaller proteins migrate faster through the gel, so the proteins become separated based on size. The concentration of acrylamide in the gel is altered to change the density of the gel depending on the size of the protein of interest; for a high molecular weight the percentage is lowered so the larger proteins will not remain stationary at the top of the gel, and for lower molecular weights the percentage of acrylamide is increased so the proteins do not run through the whole gel. The charge is removed as the smallest proteins reach the bottom of the gel and the remaining proteins remain in the gel. After running, the proteins are transferred from the gel to a nitrocellulose membrane for detection by antibodies (Towbin *et al.* 1979, Burnette 1981).

For creating protein samples for Western blot analysis, CG4 cells were plated at a density of $2x10^5$ cells/ml in 24-well plates, and differentiated after 24 hours. After a further 24 hours they were treated with the required cytokine(s) for 10-80 minutes before the experiment was stopped by putting the plate on ice. The medium was completely removed and 120µl of supplemented radioimmunoprecipitation assay buffer (RIPA) was added per well. The supplemented buffer contained: RIPA buffer, glycerol, EDTA 1mM, EGTA 1mM, protease inhibitors and PhosphoSTOP phosphatase inhibitors. The samples were left on ice for ten minutes then the surface was scraped to collect the cell extracts and transferred to new Eppendorf tubes. These were left on ice for 30 minutes then centrifuged at top speed at 4°C for 15 minutes. The supernatant was collected and transferred to a new Eppendorf tube for each sample. Protein concentration was measured using the BIOrad colorimetric protein assay which is based on the Bradford dye-binding method (Bradford 1976). The colour change of Coomassie blue is measured as the binding of this dye to protein causes a shift in the absorption maximum of the dye. The samples were incubated with the dye at room temperature for 15 minutes. A series of dilutions of BSA were prepared to create a standard curve against which sample proteins could

be compared. Absorption was then measured using the Synergy HT Plate Reader (Biotek) and quantification of proteins was used to ensure 30µg of cellular proteins were used for the Western blot.

Acrylamide gels were made using Acrylamide/Bis solution (percentage of final solution varied depending on the size of the protein to be measured), running gel buffer (1.5M Tris/HCL pH8.8), SDS 10%, APS, tetramethylethylenediamine, and H_2O. 10X running buffer is composed of Trizma base, glycine, and 1% SDS. It is then diluted to 1X in H_2O before use (table 2.2). The running buffer was added to the Western apparatus first and allowed to polymerise at room temperature. The stacking gel was then added on top and the comb inserted. The gel was then incubated at 4°C and either used after a minimum of half an hour or could be left overnight before use.

Samples were prepared for Western blot by dilution to 30µg of protein in 25µl in sample buffer with the remaining volume made up of distilled water. To this, 5µl sample buffer is added with 10% β-mercaptoethanol, as the gels were to be subjected to electrophoresis under reducing conditions. The samples were then boiled at 100°C for 5 minutes before being spun down briefly. Each well was loaded with 28µl of sample plus 10µl molecular weight markers in one well before electrophoresing at 150V until the blue dye front reached the bottom of the gel (approximately 60 minutes) (Fig 2.4).

After performing the electrophoresis of the protein samples, the gel was transferred to nitrocellulose blotting membranes by sandwiching the gel and the membrane between two pieces of blotting paper and two sponges in the transfer apparatus (Fig 2.5). The apparatus was placed in a tank and submerged in cold transfer buffer (Table 2.1). The Western blot transfer was subjected to a current of 400mA for 90 minutes.

After transfer the nitrocellulose membrane was blocked in 5% bovine serum albumin (BSA) in tris buffered saline (TBS) for 1 hour rocking at room temperature to coat the membrane in excess non-specific protein to prevent the antibody from binding to the membrane itself. The membrane was then incubated with the primary antibody at

the concentration specified by the manufacturer in TBS with 5% BSA and 0.1% tween-20 overnight at 4°C (Table 2.7).

The next morning the membrane was washed 3x5 minutes in TBS+0.1% tween-20. The secondary antibody was then added at the required concentration (Table 2.6) in TBS with 5% BSA and 0.1% tween-20 for 1 hour at room temperature. The membrane was then washed again in TBS+0.1% tween-20 3x5 minutes before incubating in ECL for 5 minutes, continuously washing the ECL over the membrane. The membrane was then exposed to autoradiography film and developed using SRX-101A Developer (Konica Minolta).

Antibody	Working dilution	Molecular weight	Secondary antibody	Working Dilution	Antibody solution
pSTAT3	1:1000	80kDa	α-rabbit	1:25,000	TBS + 5% BSA + 0.1% Tween
TotalSTAT3	1:1000	80kDa	α-mouse	1:5000	TBS + 5% Milk + 0.1% Tween
pERK1/2	1:1000	44/42kDa	α-rabbit	1:25,000	TBS + 5% BSA + 0.1% Tween
TotalERK1/2	1:1000	44/42kDa	α-rabbit	1:25,000	TBS + 5% Milk + 0.1% Tween

Table 2.7: Antibodies used for Western blot analyses. All antibodies purchased from cell signalling.

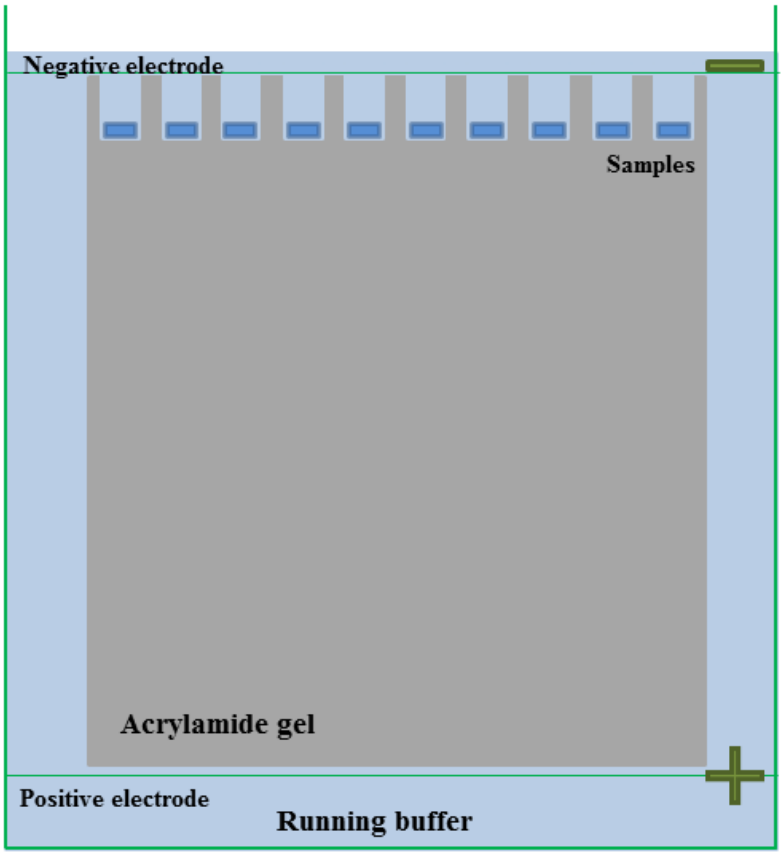

Figure 2.4: Schematic representing the setup of gel electrophoresis. Samples were loaded into the wells at the top of the acrylamide gel before a current is passed through. The negatively charged proteins in the samples travel through the gel towards to positively charged electrode. They are separated by weight as the smaller proteins travel further through the gel.

Original in colour

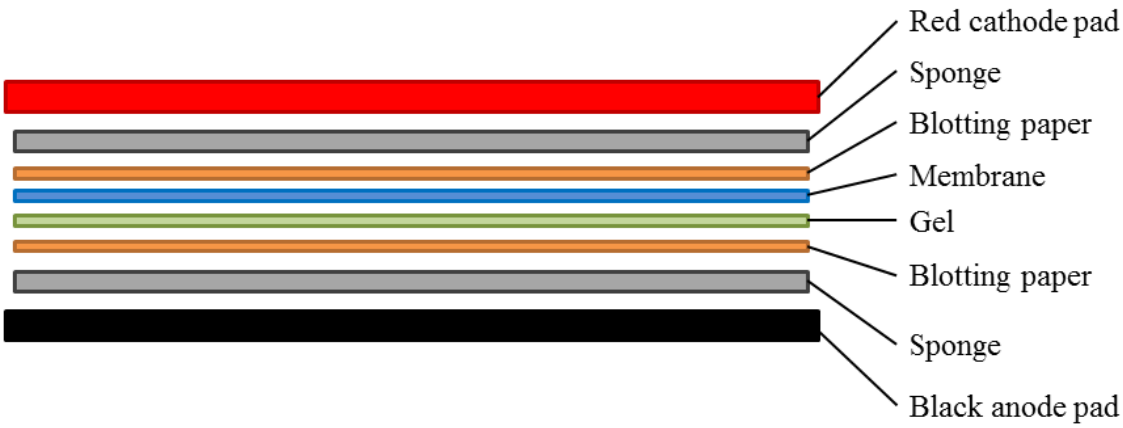

Figure 2.5: Schematic representing the setup of transfer apparatus. The proteins from the gel were transferred to the membrane using the setup shown. The current passed from the anode to the cathode to transfer the proteins from the gel to the membrane from where it could be developed. The sponges and pieces of blotting paper ensure the gel and membrane are pressed together tightly, protected from damage, and that the current passed evenly through them.

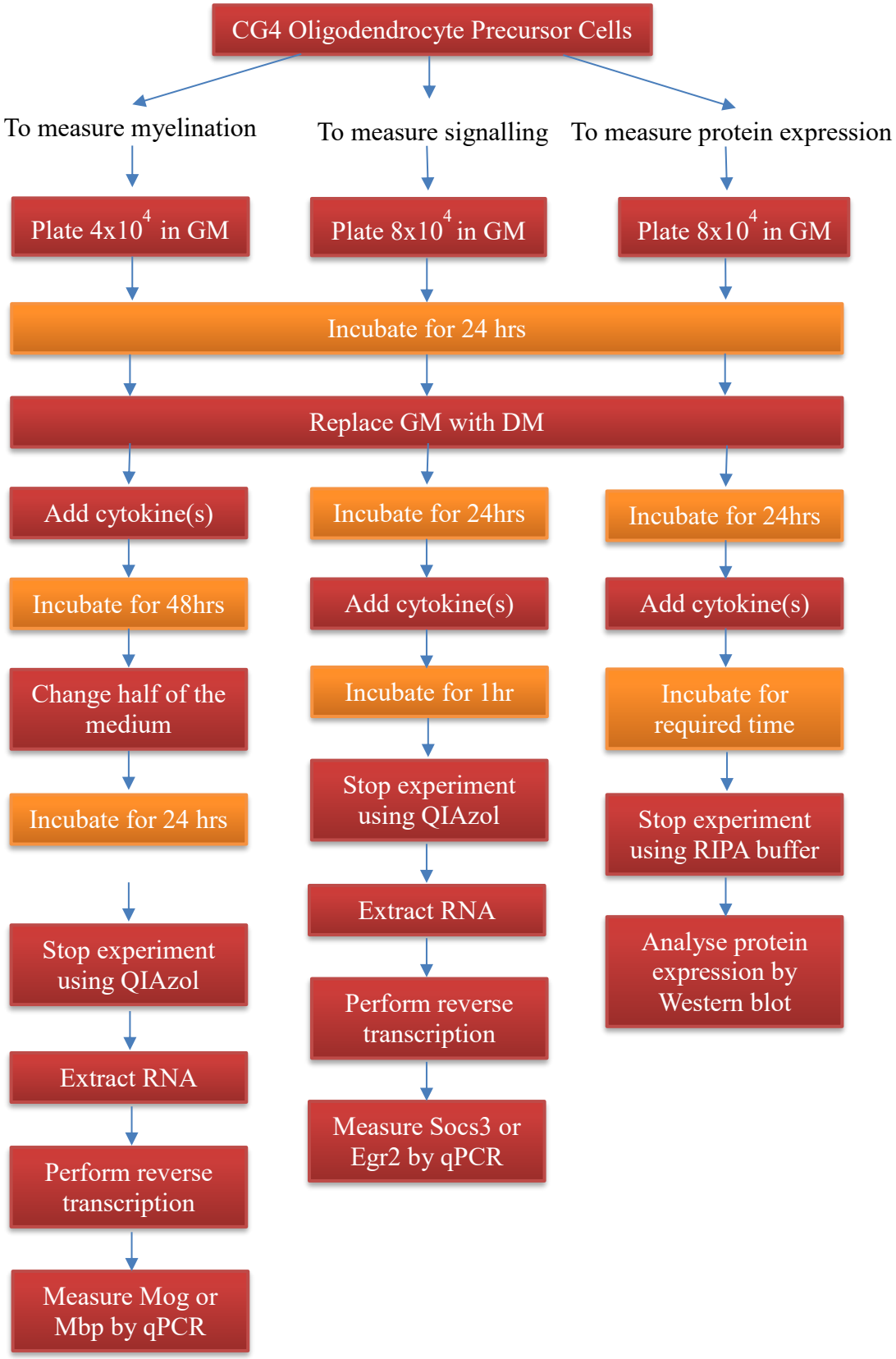

Figure 2.6: Diagram representing the experimental design. The myelinating capacity, the signalling mechanisms and the protein expression of CG4 cells were measured and the diagram represents the different protocols used to achieve the different outcomes.

Original in colour

2.4.1.5 Gene silencing by siRNA transfection

Gene silencing was used to inhibit Socs3 expression. To do this CG4 cells were forward transfected with silencer RNAs for Socs3. Forward transfection protocols involve adding the transfection mixture to previously plated cells, as opposed to reverse transfection in which the cells are added to a plate already containing the transfection mixture.

CG4 cells were plated at a density of $4x10^4$ cells/well and $8x10^4$ cells/well for Mog and Socs3 analysis respectively. siRNA was used at a concentration of 60nM. Two Socs3 siRNAs were attempted, either in combination or individually, plus a negative control siRNA. Two solutions were required for siRNA transfection and for each well the two transfection mixtures were:

- 3.6µl siRNA (either 3.6µl of one siRNA, or 1.8µl of each of two siRNAs) in 50µl Opti-MEM
- 1µl Lipofectamine in 50µl Opti-MEM

The two solutions were mixed together and incubated at room temperature for 15 minutes.

The GM was removed from the cells 24 hours after plating and they were differentiated using 500µl DM per well. One hundred microliters of transfection mixture was then added to every well and resuspended gently to mix. After incubation at 37°C for 24 hours the medium was removed and 1ml DM plus cytokines was added for the remainder of the experiment. This method of plating the cells then waiting 24 hours before transfection is known as forward transfection.

2.5 Gene expression microarrays

Analysis of gene expression microarrays was used to further elucidate the mechanisms that resulted in changes of expression of Mog after CG4 cells are treated with EPO, LIF, or both. Microarray technology was first described in 1995 by Brown *et al.* as a way of measuring a large number of genes at once (Schena 1995). The profiling of thousands of genes simultaneously allows for the detection of

subtle changes in transcript variants and for the identification of genes that may not have been previously implicated in the specified condition.

CG4 oligodendrocyte precursor cells were cultured at a density of $3.5x10^5$ cells/well on poly-L-ornithine coated six-well plates in GM as described in Section 2.1.1. The cells were incubated overnight before being washed twice with serum-free DMEM after which the medium was replaced with DM, also described earlier, to induce a switch from proliferation to differentiation. They were incubated for 3 hours before treatment; no cytokine (control), EPO 10ng/ml, LIF 0.2ng/ml, LIF 10ng/ml, or EPO+LIF 10ng/ml, each condition in quadruplicate. At 1 or 20 hours the experiment was terminated using QIAzol by adding 1ml to each well after medium was aspirated. The bases of the wells were washed thoroughly then the QIAzol was transferred to new Eppendorfs. Each sample was vortexed for 1 minute and left at room temperature for 15 minutes. Total RNA was extracted using the miRNeasy Mini Kit in which the samples were centrifuged with chloroform. Then the upper aqueous phase was transferred to the supplied collection tubes, washed thoroughly with 100% ethanol then transferred to an RNeasy MinElute spin column in a collection tube. Several washing stages followed and were repeated several times upon advice from the manufacturer. RNA quality and concentration were determined using Nanodrop ND-1000 by determining the ratio of absorbance at 260nm and at 280nm.

Microarray analysis was carried out by Oxford Gene Technology (Oxford Gene Technology, Begbroke, Oxfordshire, UK. The raw data has been entered into the Gene Expression Omnibus (GEO) database for NCBI and are accessible through GEO series accession number GSE84687 (www.ncbi.nlm.nih.gov/geo). Raw data were normalised and analysed using GeneSpring (Agilent) and Excel softwares. For each sample one excel file with normalised gene expression data (gProcessed Signal) was obtained. Eight samples were analysed simultaneously on each array plate. The organisation of this was planned to ensure that treatment duplicates were spread out over the plates to minimise the effect of a problem with one plate. The samples were also normalised between array plates. 30367 transcripts were analysed. Samples were labelled according to the cytokine used and organised into groups and separated into 1 and 20 hours documents.

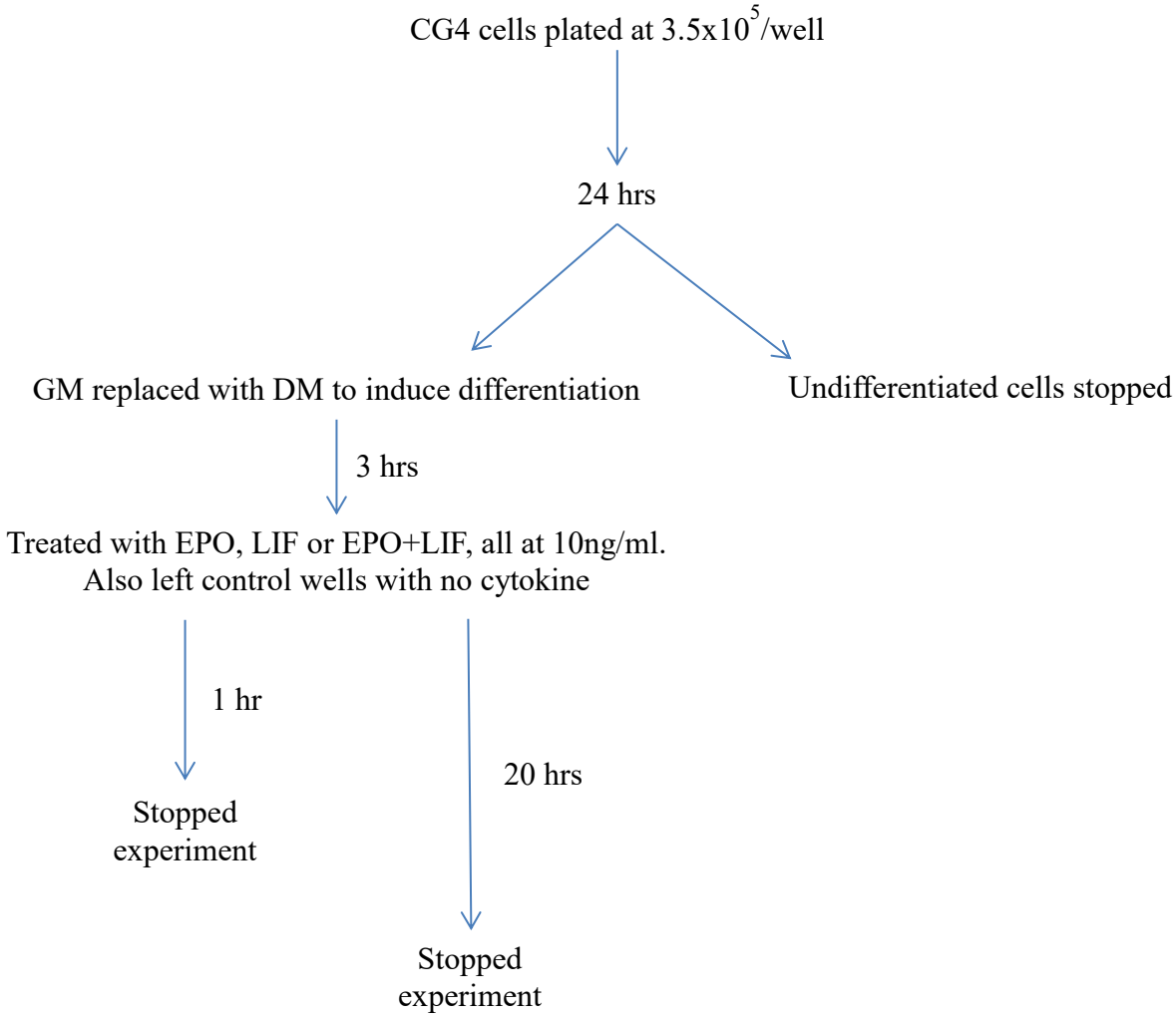

Figure 2.7: Gene expression microarray experimental design. In total eight different conditions were tested for the effects they had on CG4 cell gene expression. Each condition was tested in quadruplicate and each cytokine was added at 10ng/ml.

Hypothesis-driven filtering strategies and unbiased cluster and pathway analysis was used. Gene expression between the experimental groups was compared by Student's *t* test on the Log_2 of the gProcessed Signal. Fold change in the expression was calculated as the ratio between the averages of the gProcessed Signals of the various groups and expressed as Log_2 ratio. To identify genes with shared expression patterns among the experimental groups of interest, hierarchical cluster analysis was performed using the Genesis software. Genesis is a software package that produces a heat map of the up or downregulation of the genes to group those that have a similar expression profile together (Sturn 2000). Once a list of differentially expressed genes between experimental groups is identified STRING software was used to identify functional associations between genes (Szklarczyk 2015). A selection of genes was validated by qPCR analysis, performed on the same samples used for the microarrays.

2.6 Scratch assay

The scratch assay is a model of *in vitro* wound healing that measures migration of a monolayer of cells in a tissue-culture plate after an artificial wound is made down the centre (Liang 2007). Two cell types were used to try to obtain the best model of wound healing: Send-1 mouse endothelial skin cells and HaCaT cells which are human keratinocytes (kindly donated by Dr Ferdinand Lali, Blond McIndoe Research Foundation, East Grinstead).

Twelve-well plates coated with poly-L-ornithine were used. The cells were plated at a concentration of $10x10^4$ cells/well in DMEM supplemented with 1% pen/strep and 10% FCS. Six replicates were used for each condition to ensure as minimal variability as possible. Cells were incubated overnight or until confluent. Achieving confluence was important because cell-cell interactions are an essential aspect of wound healing *in vivo* and should be replicated as closely as possible in these experiments.

Horizontal lines were drawn along the underside of the plate as a marker half-way up each well. A sterile ruler was then laid vertically over the top of the wells and a scratch was made down the centre of the cell monolayer using a P1000 pipette tip.

Care was taken to ensure the angle of the tip was as similar as possible between wells so that the width of the scratch was uniform among the replicates. The cells were then washed twice in serum-free DMEM before being replaced with DMEM plus various concentrations of serum, most commonly 0.1% or 1%. The serum concentration was varied in an attempt to find a concentration at which the cells were healthy but did not migrate too quickly for measurements to be made. The cytokine being investigated was added at this stage.

Scratches were then photographed immediately (T0) using an inverted microscope and the 4X objective. The position of the photograph was normalised using the horizontal line drawn on the underside of the plate, with this line always aligned with the bottom of the image. The cells were incubated at 37°C and further photographs taken of the scratches at later time points ensuring the picture is taken at the same place by aligning the horizontal line with the bottom of the image again (Fig 2.7).

Analysis of wound closure was made by anonymising images and measuring the area of the scratch in each picture using Image J software (Fig 2.8) before calculating the percentage closure between the time points and the T0 measurement of the same well. The treated scratches can then be compared to the control ones to determine if the addition of a cytokine has any effect on the speed of wound closure.

2.7 Statistics

Results are expressed as mean ± standard deviation. Student's *t* test was used to compare the means of cytokine-treated samples with the mean of the control samples or EPO-treated samples in some circumstances. The results were considered significantly different when $P<0.05$, and absolute $FC>1.5$ ($Log_2 >0.58$ or <-0.58) although $P<0.01$ and $P<0.001$ were also used to decrease the chance of false positive where possible.

Student's *t* test was also used for analysis of gene expression microarray results. This is because the gene expression microarray was used only as an initial discovery step to indicate genes not previously impflicated in demyelination. After genes had been identified the results were validated by qPCR so *t* test analysis reduced the number of false negative results.

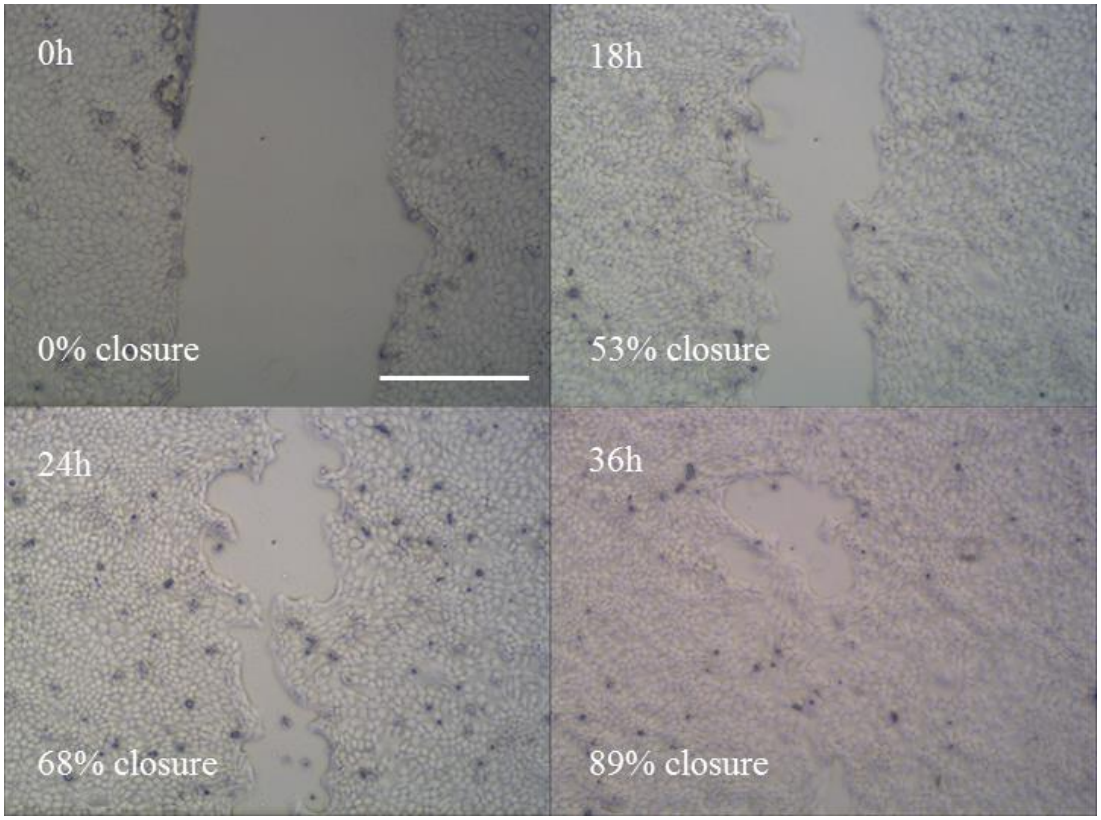

Figure 2.8: Example of a HaCaT cell scratch assay. A wound was created down the centre of a monolayer of cells using a p1000 pipette tip. The rate of wound closure was then measured at intervals and compared to time 0h to measure percentage closure. Figure 2.4 represents images taken at 1, 18, 24, and 36 hours. White scale bar represents 1mm.

Original in colour

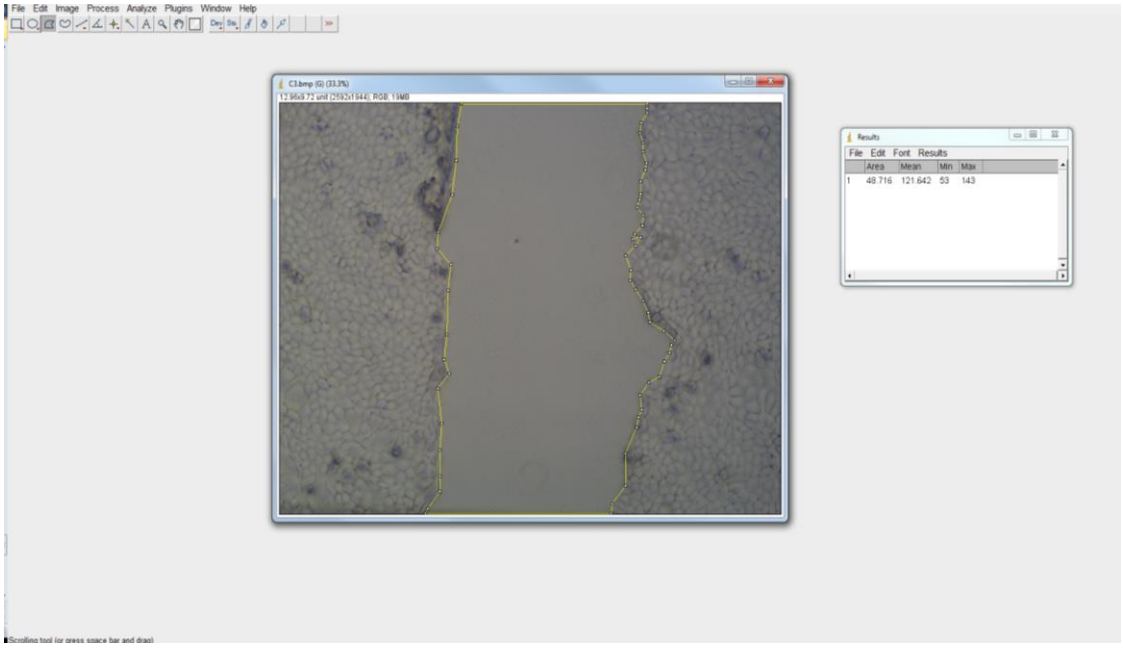

Figure 2.9: Example of measuring a scratch wound area using ImageJ. The area of the wound was drawn out using the drawing tool and marked with a yellow line. The scale was set to 200 pixels per unit and the area within the yellow line was obtained. These arbitrary units were then used to calculate percentage closure.

Original in colour

Chapter 3. The effect of LIF on CG4 cells

3.1 Introduction

LIF has potent positive tissue protective effects in the nervous system (Section 1.1.2.1). It is the most important neuroprotective cytokine in the retina (Joly *et al.* 2008), and it reduces the clinical severity of EAE (Linker 2008). Furthermore, mutant mice that lacked LIFR and GP130 demonstrated an increase in severity of the symptoms of EAE (Deverman 2012). The exogenous addition of LIF stimulated OPC differentiation and myelination both *in vitro* and *in vivo* (Deverman 2012).

Cervellini *et al* (2013) demonstrated that EPO increases Mog expression in CG4 EPOR cells (used throughout the project but referred to as only "CG4" from here) by at least 8-fold (Cervellini *et al.* 2013a). Mog expression is a good marker for oligodendrocyte maturation because, unlike other myelin genes, it is only expressed after 1-2 days of differentiation in culture, so represents the later stages of maturation (Scolding 1989). Furthermore, expression of Mog is related to myelin deposition, not just process extension, and it is upregulated by CG4 cells only when they are producing myelin (Solly 1996). The initial purpose of this work was to determine if LIF has a synergistic effect with EPO on the myelinating capacity of these cells.

3.2 LIF induced Mog expression via a bell-shaped concentration response curve

CG4 cells were originally plated at a density of $3x10^4$ cells/ml as in the protocol used by Cervellini *et al*; however RNA yields were typically too low for analysis. Furthermore, it was found that, for three day experiments, $4x10^4$ cells/ml did not become confluent enough to run the risk of becoming astrocytic, therefore the higher density of cells was used. Twenty-four hours after plating, the cells were differentiated and treated immediately with LIF. To ascertain the optimal concentration of LIF the cells were treated with a range of concentrations of LIF. It had been found that 8ng/ml was the optimum concentration of EPO for Mog upregulation in these cells and at higher concentrations (up to 400ng/ml was investigated) Mog expression reached a plateau (Cervellini *et al.* 2013a). I initially

tested LIF over a wide range of concentrations (0.004-10ng/ml), based on the same concentrations as used for EPO.

As seen in Figure 3.1, 0.2ng/ml was the optimum concentration of LIF in terms of Mog expression, although the induction was only around 1.5-fold. Interestingly, conversely what was observed with EPO, 2 and 10ng/ml LIF induced less Mog (1.6 FC, SD 0.2 and 1.2FC, SD 0.4 respectively) expression than the optimum concentration of 0.2ng/ml (2.9 FC, SD 0.4). The highest concentration, 10ng/ml, did not induce any significant increase in Mog expression when compared to the control group. This suggests that there was potentially a feedback mechanism that was preventing Mog expression from reaching increased levels of induction when the concentration of LIF increased. Furthermore, this feedback mechanism was not present following EPO stimulation, as concentrations up to at least 400ng/ml did not cause any reduction in Mog induction (Cervellini *et al.* 2013a). These findings are supported by work by Ishibashi (2006) who also found a negative feedback at higher concentrations of LIF (Ishibashi *et al.* 2006). A very low concentration of 0.004ng/ml LIF was used to see if such a low concentration had an effect on Mog expression. However, 0.004ng/ml LIF induced less Mog (1.8 FC, SD 0.5) than 0.2ng/ml suggesting that LIF produced an increase in Mog expression that correlates with the concentration of LIF. The resulting graph (Fig. 3.1) showed a clear bell-shaped response curve to increased concentrations, demonstrating the negative effect LIF had at higher concentrations that was not present at lower concentrations. The experiment was repeated twice with successful replication of the results.

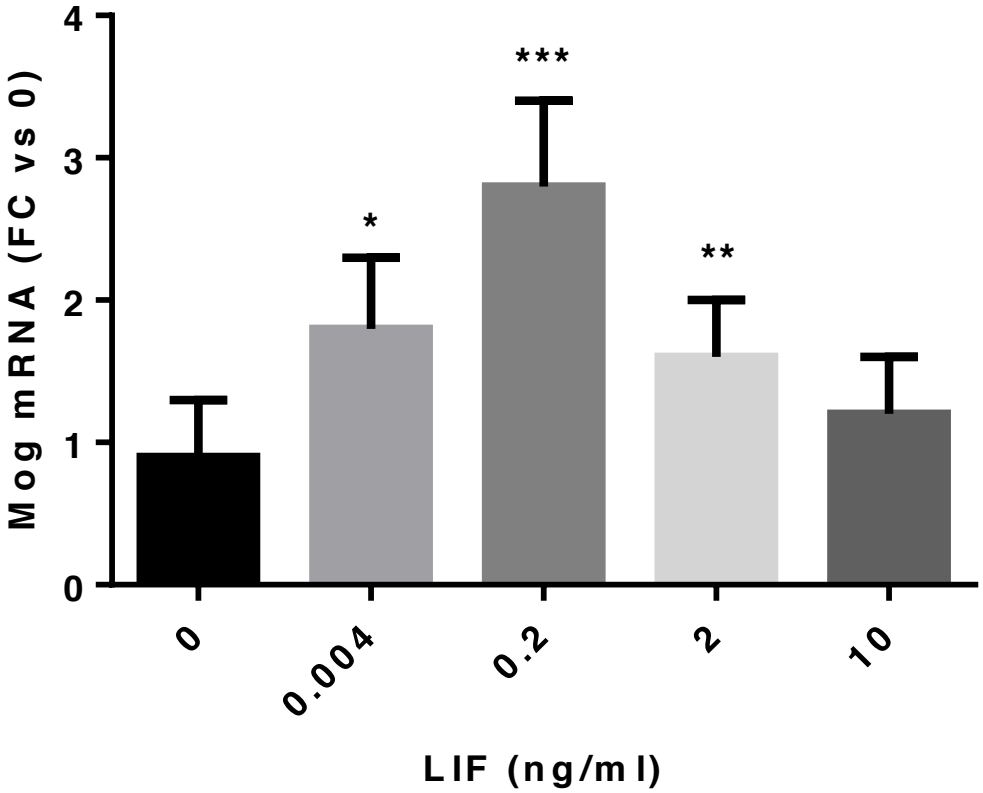

Figure 3.1: LIF induced a bell-shaped concentration response of Mog induction in CG4 cells. CG4 cells were plated at a density of $4x10^4$ cells/well and differentiated for three days after treatment with indicated concentrations of LIF. Mog mRNA was measured by qPCR and results are expressed as arbitrary units versus 0ng/ml LIF. Data represented here are the mean ± SD of quadruplicate samples. * P<0.05, ** P<0.01, ***P<0.001 versus 0ng/ml by Student's *t*-test.

LIF (ng/ml)	Mog Mean	SD	P value
0	0.8	0.3	
0.004	1.8	0.5	0.184
0.2	2.9	0.4	0.0001
2	1.6	0.2	0.0071
10	1.2	0.4	0.2163

3.3 LIF inhibited the induction of Mog by EPO

The potential for a synergistic effect that EPO and LIF have on Mog induction was investigated. An understanding of how LIF affects EPO-induced Mog will help in elucidating the mechanisms behind Mog induction in these cells and therefore the mechanisms behind their myelinating capacity. It was hypothesised that LIF would cause an increase of the promyelinating effect of EPO on Mog expression.

EPO and LIF were added both individually and simultaneously immediately after differentiation of CG4 cells as in the previous LIF experiments. The use of the cytokines individually in these experiments allowed for a direct comparison between the effects of the two cytokines to also be assessed in this experiment. EPO was added at 10ng/ml to be comparable to the previous LIF concentration response experiments in which 10ng/ml LIF was used as the upper limit and is the concentration when the reduced effect of LIF is clearly visible. As EPO and LIF have roughly the same molecular weight, using the same concentration was justified. Furthermore, in previous EPO experiments all concentrations between 8ng/ml and 400ng/ml were shown to act similarly, so 10ng/ml should be expected to act the same as 8ng/ml which was defined as the optimum concentration of EPO in that work (Cervellini *et al.* 2013a). The experimental procedure took three days to complete and Mog expression was analysed by qPCR.

The experiments showed clearly that LIF did not reproduce the same positive effect on Mog expression as EPO as the individual LIF treatments did not increase Mog expression as much as EPO when each cytokine was used individually (Fig 3.2). Furthermore, the increase seen at 0.2ng/ml LIF was not observed here, although the induction was trending towards significance (P=0.08). The experiment using 10ng/ml LIF confirmed that this concentration did not induce Mog.

The surprising result from these experiments was that LIF did not induce a synergistic effect of Mog induction when added simultaneously to EPO. On the contrary, LIF inhibited the positive effect of EPO on Mog expression, which was a new finding and had not been seen in the literature before.

The treatment with EPO and LIF simultaneously induced significantly less Mog expression than with EPO alone; 0.2ng/ml LIF significantly inhibited the positive effect of EPO on Mog expression by about half, despite the fact that, when added alone, LIF increased the induction of Mog, although not significantly in this experiment. Ten ng/ml LIF almost completely abolished induction of Mog by EPO, however Mog was still significantly induced when compared to the control (P=0.0001). The reduction of EPO-induced Mog expression by LIF suggests that LIF induced negative feedback mechanisms that inhibited the production of myelin by these cells. The results presented here showed that these pathways were induced by LIF and not by EPO, but that they had the capability to inhibit the positive effects of both cytokines. The experiments were repeated twice with successful replication of the results.

3.4 The effects of EPO and LIF on Mog were consistent in other myelin genes

Mbp is another protein that is expressed by myelinating oligodendrocytes. It is the second most abundant myelin protein in the CNS and comprises about 10% of the dry weight of myelin (Boggs 2006). It was decided to use Mog expression as a measure of myelination because treatment of these cells with EPO induces a bigger fold-change increase in Mog than in Mbp expression (Cervellini *et al.* 2013a) and Mog is expressed later in myelination than Mbp. However, it was important to check that changes in Mog expression were reflected in Mbp expression so that it could be concluded that Mog was a reliable representation of myelin genes. Therefore, qPCR was re-run on samples in which Mog had previously been measured but this time Mbp was measured. As hypothesised, the expression of Mbp reflected that of Mog; Mbp was also increased by EPO treatment but reduced when LIF was present simultaneously (Fig 3.3). The consistency in myelin gene expression shows that Mog gene expression is a good gene indicator for overall myelin production.

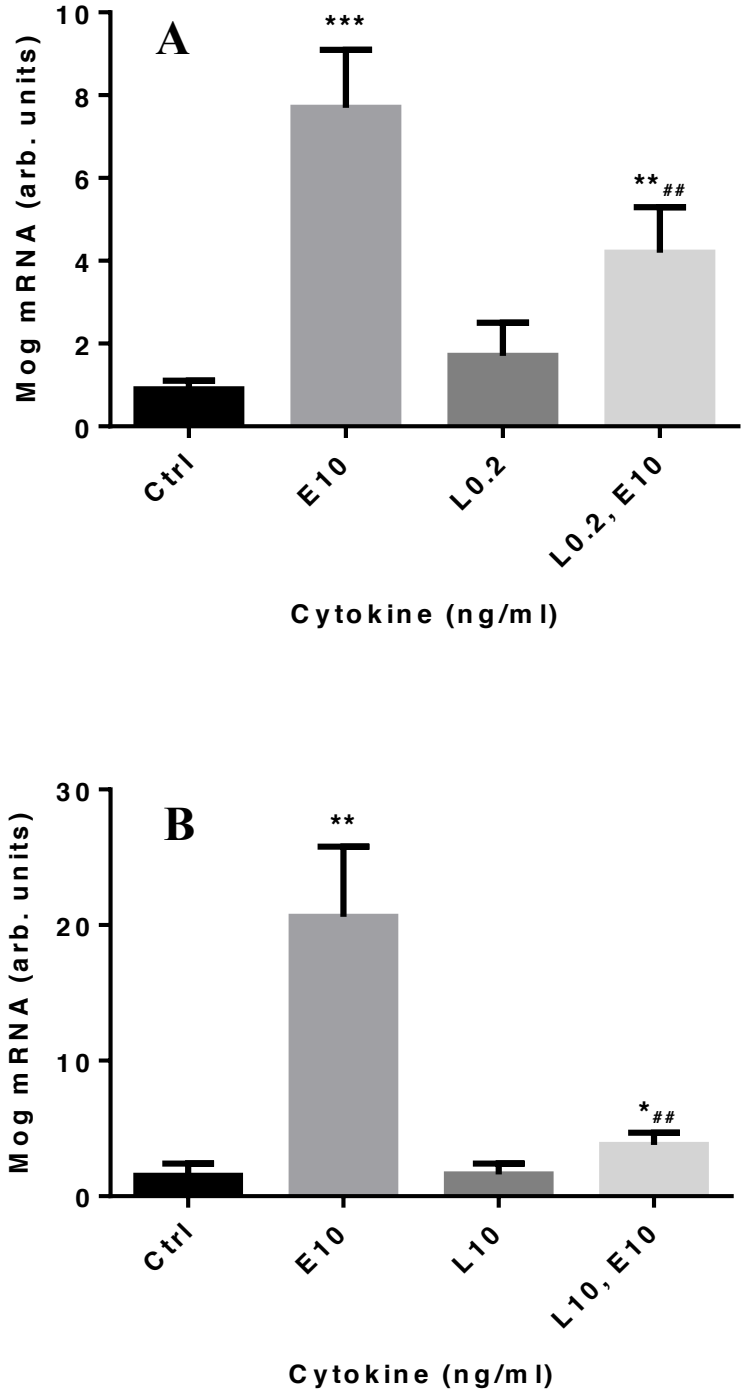

Figure 3.2: LIF inhibited the induction of Mog expression by EPO. CG4 cells were plated at a density of $4x10^4$ cells/well and differentiated for three days after treatment with indicated cytokine. LIF (L) was used at 0.2ng/ml in panel A and at 10ng/ml in panel B, and the concentration of EPO (E) is always 10ng/ml. Mog mRNA was measured by qPCR and results are expressed as arbitrary units versus the control. Data represented here are the mean ± SD of quadruplicate samples. *P<0.05, **P<0.01, *** P<0.001 versus the control and #P<0.05, ##P<0.01 versus EPO alone….

Figure 3.2 cont.: LIF inhibited the induction of Mog expression by EPO.

Graph A data:

Cytokine (ng/ml)	Mog Mean	SD	P value
0	0.9	0.2	
0L, 10E	7.7	1.4	0.0001
0.2L, 0E	1.7	0.8	0.0873
0.2L, 10E	3.9	0.9	0.0327

Graph B data:

Cytokine (ng/ml)	Mog Mean	SD	P value
0	1.5	0.9	
0L, 10E	20.6	5.2	0.0016
10L, 0E	1.6	0.8	0.8975
10L, 10E	3.9	0.9	0.0327

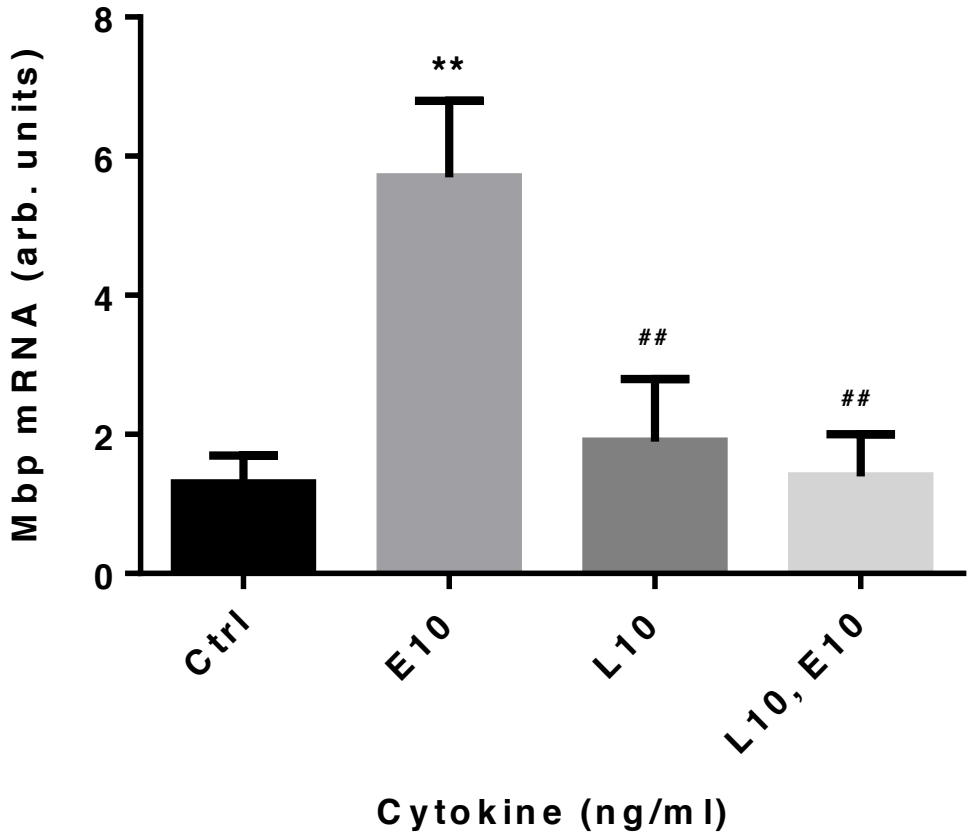

Figure 3.3: LIF inhibited the induction of Mbp expression by EPO. CG4 cells were plated at a density of $4x10^4$ cells/well and differentiated for three days after treatment with the indicated cytokine. Mbp mRNA was measured by qPCR and results are expressed as arbitrary units versus the control. Data represented here are the mean ± SD of quadruplicate samples. ** P<0.01 versus the control and ##P<0.01 vs EPO alone.

Cytokine (ng/ml)	Mbp Mean	SD	P value
0	1.3	0.4	
0L, 10E	5.7	1.1	0.0013
0.2L, 0E	1.9	0.9	0.3383
0.2L, 10E	1.4	0.6	0.7971

3.5 Other IL-6 cytokines had the same effect on Mog expression as LIF

LIF is part of a pleiotropic group of cytokines, the IL-6 cytokine family, which perform a wide array of frequently overlapping functions around the body (Section 1.1.2.2). LIF is the primary cytokine that associates with LIFR but CNTF, CT-1, OSM, and CLC can also bind to this receptor. For this reason, I decided to see if CNTF and OSM shared the inhibitory effect caused by LIF on EPO-induced Mog. The experiment was conducted using the same protocol as the previous LIF and EPO experiments with the cytokines added at equimolar concentrations to 10ng/ml and also carried out for three days after the cells underwent differentiation.

OSM and CNTF clearly inhibited the effect of EPO on Mog expression as there was a marked inhibition of EPO-induced Mog when the GP130-user cytokine was added simultaneously (Fig.3.4). Furthermore, neither cytokine induced any increase in Mog expression when added individually. Both of these results reflected the effect of LIF addition to the cell culture conditions. The experiment was repeated and the results replicated.

To determine if the effects of CNTF and OSM correlated consistently with those of LIF, a low-concentration treatment was also added to the CG4 cells. As seen in previous experiments, at the low concentration, 0.2ng/ml, LIF induced a 1.5-2 fold increase in Mog expression. OSM was consistent with this and even seemed to induce slightly more Mog expression, although the difference between LIF and OSM was not significant (P=0.17) (Fig.3.5). Interestingly, CNTF did not induce an increase in Mog expression, despite the fact that CNTF decreased the effect of EPO, indicating that it did have a functional effect in these cells. Also of note, as seen in Fig.3.4, CNTF did not completely block EPO-induced Mog as did OSM, suggesting that CTNF had reduced functionality in these cells. This may be due to CNTF's use of a third receptor, as well as the GP130/LIFR complex it shares with LIF and OSM, that was perhaps not abundant enough in these cells to produce the complete effect of CNTF.

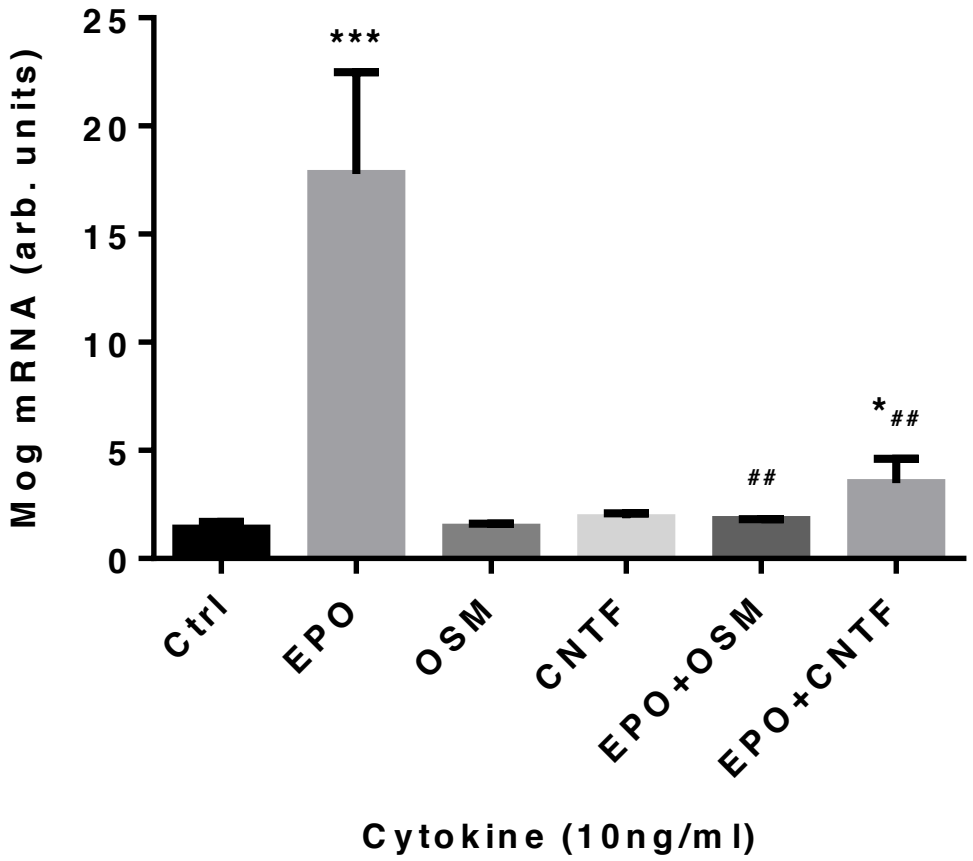

Figure 3.4: CNTF and OSM inhibited the induction of Mog expression by EPO. CG4 cells were plated at a density of $4x10^4$ cells/well and differentiated for three days after treatment with indicated cytokine. Mog mRNA was measured by qPCR and results are expressed as arbitrary units versus the control. Data represented here are the mean ± SD of quadruplicate samples. *P<0.05, ** P<0.001 versus the control and # P<0.05, ## P<0.01 versus EPO alone.

			P value	
Cytokine	**Mog Mean**	**SD**	**vs Ctrl**	**vs EPO**
0	1.4	0.3		
EPO	17.8	4.7	0.0004	
OSM	1.4	0.2	0.8745	
CNTF	1.9	0.2	0.0543	
EPO+OSM	1.6	0.3	0.3001	0.0022
EPO+CNTF	3.5	1.1	0.0117	0.0011

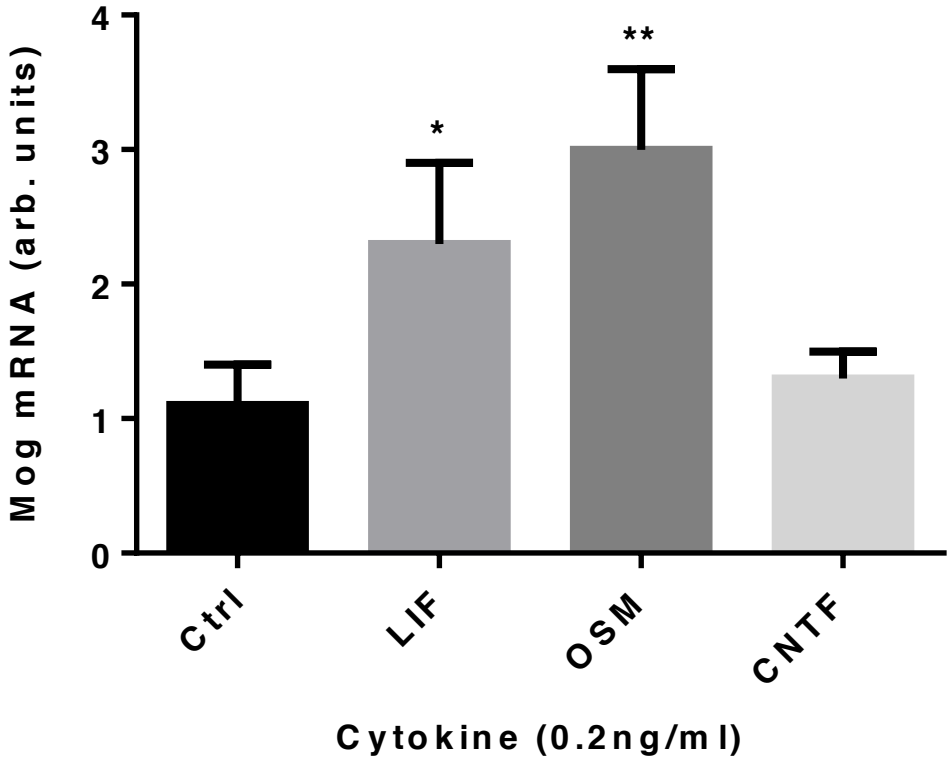

Figure 3.5: OSM, but not CNTF, induced low levels of Mog expression after low-concentration cytokine treatment. CG4 cells were plated at a density of $4x10^4$ cells/well and differentiated for three days after treatment with indicated cytokine. Mog mRNA was measured by qPCR and results are expressed as arbitrary units versus the control. Data represented here are the mean ± SD of quadruplicate samples. *P<0.05, ** P<0.001 versus the control.

Cytokine (ng/ml)	Mog Mean	SD	P value
Ctrl	1.1	0.3	
LIF	2.3	0.6	0.0101
OSM	3.0	0.6	0.0016
CNTF	1.3	0.2	0.1874

3.6 Conclusions

- LIF treatment produced a bell-shaped response curve of Mog mRNA expression
- LIF inhibited EPO-induced Mog expression
- OSM and CNTF shared the inhibitory effect of LIF on EPO-induced Mog expression

LIF induced Mog expression in CG4 cells, a result that is in agreement with previous literature in which LIF increased myelination (Deverman 2012, Mashayekhi 2015, Rittchen 2015). However, high concentrations of LIF, 10ng/ml, induced less Mog expression than the optimum concentration of 0.2ng/ml, producing a bell-shaped response curve from the cells to increasing concentrations of LIF. Ishibashi (2006) also found that higher concentrations, above 5ng/ml, caused an inhibition of myelin, although they were observing Mog protein by immunocytochemistry (Ishibashi *et al.* 2006). Mog mRNA expression was measured by qPCR, which may explain why Mog was sensitive to lower concentrations in the experiments presented in this thesis compared to the results obtained by Ishibashi through immunohistochemistry (2006). Less inhibition was required to inhibit at the transcriptional level than to maintain the inhibition after translation, and so produce an inhibition of Mog protein. The finding of the inhibitory effect of higher concentrations of LIF on cells at the mRNA level is novel to this work.

When EPO and LIF were added simultaneously LIF inhibited induction of Mog expression by EPO, as CG4 cells treated with the cytokines simultaneously showed a reduced induction of Mog. This novel finding shifted the focus of my research towards understanding the mechanisms that resulted in the observation of the bell-shaped concentration response curve of LIF and its inhibition of the positive effect of EPO on Mog induction.

It was also found that OSM, another IL-6 cytokine that uses exactly the same receptors as LIF, inhibited the positive effect of EPO, as seen with LIF. CNTF, that uses the GP130/LIFR complex but plus an additional receptor subunit, inhibited the

effects of EPO but did not induce complete inhibition as OSM did and did not increase Mog expression at low levels as LIF and OSM did.

High concentrations (10ng/ml) of LIF did not induce increases in Mog, suggesting the concentration of LIF is delicately balanced and potentially finding the correct concentration for use in treatment would be difficult. However, the interaction between EPO and LIF is interesting and the inhibition of EPO's promyelinating effects by LIF should be considered when using EPO in treatment. Endogenous factors present in the body that might be able to inhibit EPO *in vivo* should be considered to obtain the maximum positive effect of EPO, without this effect being inhibited.

Taken together, there are a number of novel findings presented in this chapter which suggest that there is a signalling mechanism, or multiple mechanisms, that are induced by LIF and OSM, but not by EPO, that have an inhibitory effect on the myelinating capacity of the CG4 cells. Furthermore, it appears that while this inhibitory mechanism is not induced by EPO, it has the ability to inhibit the positive effect of EPO as mentioned previously. The interplay between these cytokines is very interesting and has not been investigated before; therefore the subsequent work in this thesis will use various methods to determine the mechanisms that LIF utilises to inhibit EPO-induced Mog.

The following chapter will look at known signalling mechanisms Egr2 and Socs3 to determine if they can be linked to the inhibition by measuring their expression and the phosphorylation of their upstream components. Furthermore, the expression of Egr2 and Socs3 will be modified to identify their role in the regulation of Mog expression by EPO and LIF.

Chapter 4. Signalling mechanisms

4.1 Introduction

In this chapter the downstream signalling mechanisms responsible for the inhibition of EPO-induced Mog will be explored. After initial binding of the LIF/LIFR/GP130 complex on the cell surface a variety of signalling pathways are activated (Section 1.1.2.1). Possibly the main inhibitory signalling mechanism that is induced by LIF involves Socs3, a protein that is activated by STAT3 and binds to JAK2 to prevent further phosphorylation of STATs (Nicholson 2000, Babon 2014). Socs3 limits the ability of LIF to prevent demyelination *in vivo* (Emery 2006). There is evidence to suggest that Socs3 can bind to EPOR and prevent signalling resulting from its phosphorylation (Sasaki 2000, Hortner 2002). However, it binds with around a ten-fold lower affinity than for the GP130 (Babon 2014) and no evidence for its binding in the CNS has been detected. Previous work, all conducted in the early 2000s, focussed only on the effect of Socs3 on erythropoiesis (Marine *et al.* 1999, Krebs and Hilton 2000, Hortner 2002, Jegalian 2002). The current work will investigate how signalling induced by LIF inhibited EPO-induced Mog expression

4.2 The inhibitory mechanisms of LIF are induced immediately

The time point at which LIF was added to the EPO-treated CG4 cells was different from the original experiments (Chapter 3) where EPO and LIF were added simultaneously to clarify whether it was an early or late signalling event that caused the inhibition. The experiment was performed exactly as before (Section 3.3) but, along with immediate addition of LIF, it was also added 24 and 48 hours later. This experiment was carried out using the high-concentration of LIF (10ng/ml) as it was the concentration that had the greatest inhibitory effect on EPO-induced Mog expression.

The most complete inhibition of Mog expression was seen when LIF was added at the same time as EPO (Fig.4.1). Incomplete inhibition was seen when LIF was added

at 24 and 48 hours, suggesting that it was an early signalling mechanism that was required to inhibit EPO. The experiment demonstrated that a signalling mechanism initiated at a later time point could not completely inhibit all of the effects of EPO, possibly because the pathways required to induce Mog expression are early events, with Mog induction being initiated later. If the negative feedback seen when LIF was present was not initiated immediately the inhibition of EPO was not complete. The mechanism that inhibited EPO needed to be present immediately to completely inhibit EPO-induced Mog expression.

4.3 Egr2 mRNA expression did not correlate with inhibition of Mog

The first signalling mechanism that was investigated was the pathway involving Egr2. Egr2 is a protein that is crucial in promoting myelination in the PNS (Topilko 1994, Decker 2006), but in oligodendrocytes it appears to work as a feedback inhibitor (Cervellini *et al.* 2013a). Recent work has shown the importance of Egr2 in response to EPO stimulation (Mengozzi 2012). Egr2 is also induced by LIF (Mengozzi 2014), so the effect of the addition of both cytokines on Egr2 expression was investigated as it could be a protein that could affect Mog induction.

CG4 cells were plated at $8x10^4$ cells/well and the cytokines were added after 24 hours of differentiation. The higher cell count was used because the experiment was only run for one day after differentiation. This is because Egr2 is expressed much earlier than Mog and so a higher cell count would ensure that a sufficient quantity of RNA would be present after the experiment had been run. The experiment was stopped after 1 hour and RT and qPCR performed to measure Egr2 expression. LIF and EPO both induced significant increases in Egr2 expression (Fig.4.2), although EPO induced nearly 100-fold more Egr2 expression than LIF. However, the level of Egr2 expressed remained elevated when LIF and EPO were added simultaneously with no decrease when compared to EPO treatment alone (P=0.77), suggesting that Egr2 expression is not inhibited by LIF. Therefore, as Egr2 levels are increased in cells treated with EPO+LIF, it can be concluded that induction of Egr2 alone was not sufficient to cause an increase in Mog. Furthermore, Egr2 was not the protein responsible for the inhibition of EPO-induced Mog by the addition of LIF.

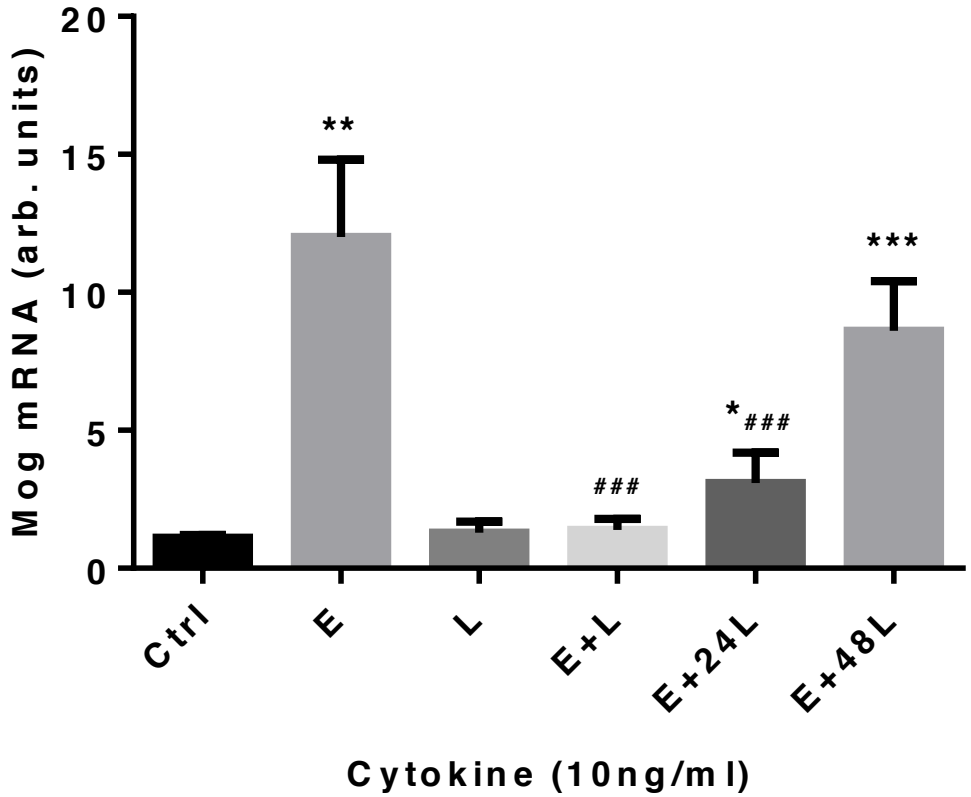

Figure 4.1: The inhibitory effect of LIF on EPO-induced Mog was strongest when both cytokines were added simultaneously. CG4 cells were plated at a density of $4x10^4$ cells/well and differentiated for three days after treatment 10ng/ml LIF (L) or EPO (E) or both, with LIF added either simultaneously or 24, or 48 hours later. Mog mRNA was measured by qPCR and results are expressed as arbitrary units versus the control. Data represented here are the mean ± SD of quadruplicate samples. * P<0.05, ** P<0.01, ***P<0.001 versus the control and ###P<0.001 vs EPO alone by Student's *t*-test.

			P value	
Cytokines	**Mog mean**	**SD**	**vs Ctrl**	**vs EPO**
0	1.1	0.1		
EPO	12.0	2.8	0.0012	
LIF	1.3	0.4	0.3122	
EPO+LIF	1.4	0.4	0.2420	0.0003
EPO+24h LIF	3.1	1.1	0.0221	0.0010
EPO+48h LIF	8.6	1.8	0.0009	0.0888

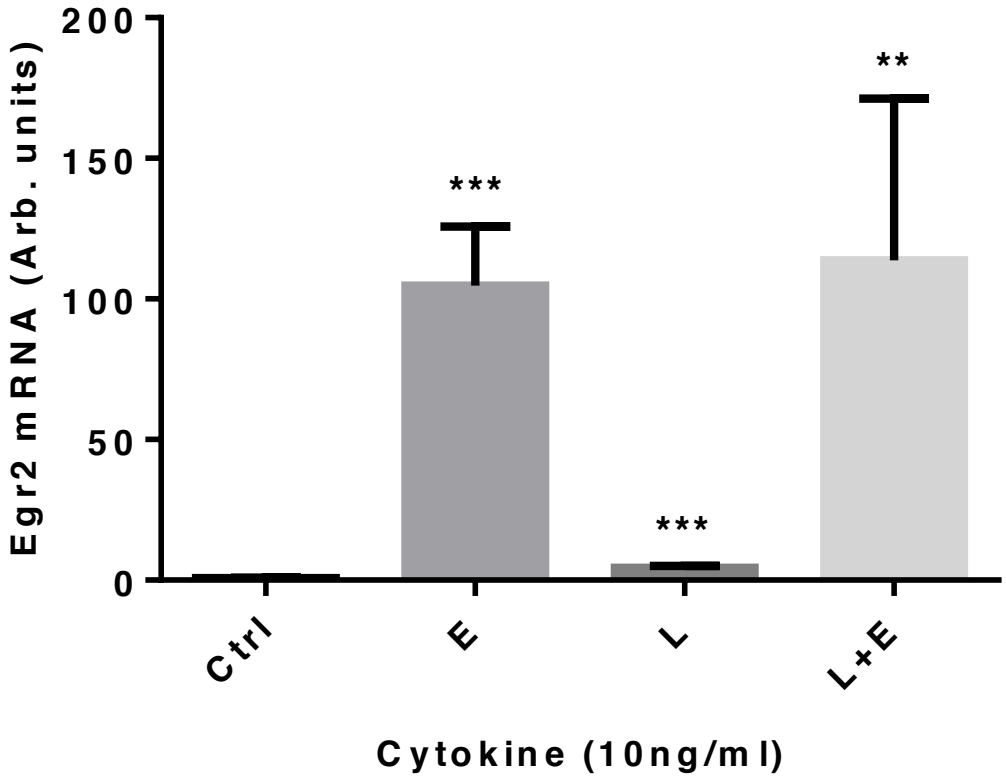

Figure 4.2: Egr2 induction was most potent when EPO was present and was not reduced when LIF was also present. CG4 cells were plated at a density of $8x10^4$ cells/well and differentiated for one day before 10ng/ml LIF or EPO or both were added for one hour. Data represented here are the mean ± SD of quadruplicate samples. ** P<0.01, *** P<0.001 versus the control.

Cytokine (ng/ml)	Mog Mean	SD	P value
0	0.8	0.1	
EPO	104.7	21.1	0.00006
LIF	4.4	0.6	0.00002
LIF+EPO	113.7	57.5	0.00774

4.4 ERK1/2 phosphorylation did not correlate with inhibition of Mog

ERK is downstream of Raf and MEK1/2 (Gaesser 2016). Activation of these MAPKs results in the phosphorylation of ERK (pERK). Once phosphorylated, pERK translocates to the nucleus to regulate the expression of several genes, including Egr2. There is evidence that ERK1/2 has significant effects on myelination; ERK1/2 knockout mice exhibited significant hypomyelination (Ishii 2012) and, conversely, sustained activation of ERK1/2 leads to increased thickness of the myelin sheath (Ishii 2013). EPO induces pERK1/2 while LIF supresses its phosphorylation (Xu 2015, Cherepkova 2016). For the purposes of this study, the phosphorylation of ERK was measured to confirm that it is linked to increased myelination and to determine if it is suppressed when LIF is present and so provide an explanation for a lack of Mog induction.

CG4 cells were plated at a density of $2x10^5$ cells/well on 24-well plates. They were differentiated 24 hours after plating and stimulated with EPO, LIF, or both 24 hours after differentiation. The experiment was stopped 10 or 30 minutes after the addition of the cytokines and the protein content was measured before pERK1/2 was measured by Western blot.

As hypothesised, EPO induced high levels of pERK1/2 as bands were seen at 44/42 kDa respectively at both time points (Fig.4.3). LIF seemed to induce pERK1/2 strongly at 10 minutes but this expression had diminished by 30 minutes, indicating that LIF had an immediate but unsustained effect on pERK1/2. This could show that LIF did not maintain pERK1/2 long enough to produce the positive effect on Mog as induced by EPO. Perhaps pERK1/2 only increased Mog when its levels were increased continuously.

Stimulation with the cytokines simultaneously had an additive effect on pERK1/2. It was certainly not diminished and so was still increased in conditions where Mog induction was inhibited, meaning that here an increase in pERK1/2 was seen in conditions where Mog was both increased and inhibited. The increased expression by EPO that remained elevated when LIF was also present suggested that pERK1/2

was important, but not sufficient, for Mog induction, as its presence did not guarantee that Mog expression would increase.

In conclusion, it appeared that pERK1/2 might be involved in the increase in Mog induction by EPO but its presence alone was not sufficient to ensure that Mog expression remained increased, as high levels were still present when the cells were treated with LIF. Therefore, it appears as though it was not involved in the inhibition of EPO-induced Mog by LIF.

4.5 Socs3 induction occurred early in LIF signalling

Other pathways classically known to be induced by LIF and other IL-6 cytokines were investigated. The JAK-STAT-Socs pathway is one of the most important signalling mechanisms induced by IL-6 cytokines so may partly be responsible for the observed inhibition seen in the CG4 cell model.

A time course experiment was performed to determine the chronology of Socs3 induction. CG4 cells were plated at a density of $8x10^4$ cells/well and differentiated as before. As the induction of Socs3 was expected to be quick and it was important that the differentiation state of the cells did not affect its expression, the cells were allowed to differentiate for 24 hours before LIF was added to induce Socs3 expression. The experiment was stopped after 30 minutes, 1 hour, 4 hours, or 24 hours and Socs3 expression was measured by qPCR.

Socs3 was induced significantly at 30 minutes compared to the control and to LIF treatment at later time points (Fig 4.4). It was induced at high levels at 1 hour compared to the control, and still maintained a high increase in expression. Furthermore, while the expression was reduced further at 4 and 24 hours, it still remained significantly elevated compared to the control ($P<0.001$). The results indicated that Socs3 was significantly induced by LIF and that its expression remained increased for an extended period of time. The experiment was repeated and the same results obtained.

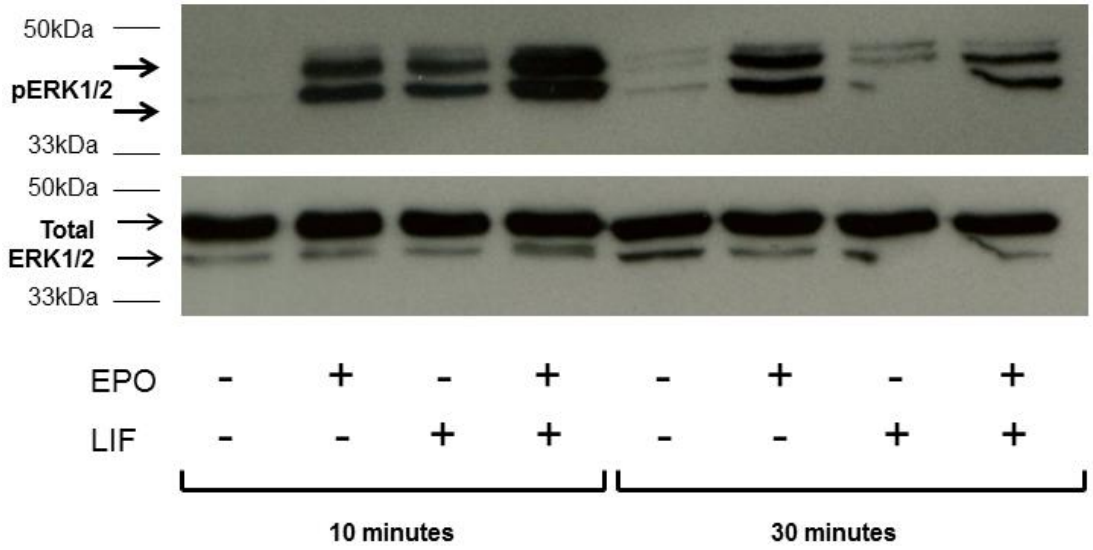

Figure 4.3: pERK was induced by EPO and not inhibited by the addition of Mog. CG4 cells were plated at a density of $2x10^5$ cells/well and differentiated for 24 hours before EPO, LIF, or both were added at a density of 10ng/ml for 10 or 30 minutes. pERK1/2 protein density was measured by Western blot and total ERK1/2 was used as a loading control. The proteins of ERK1/2 can be seen at 44 and 42kDa respectively.

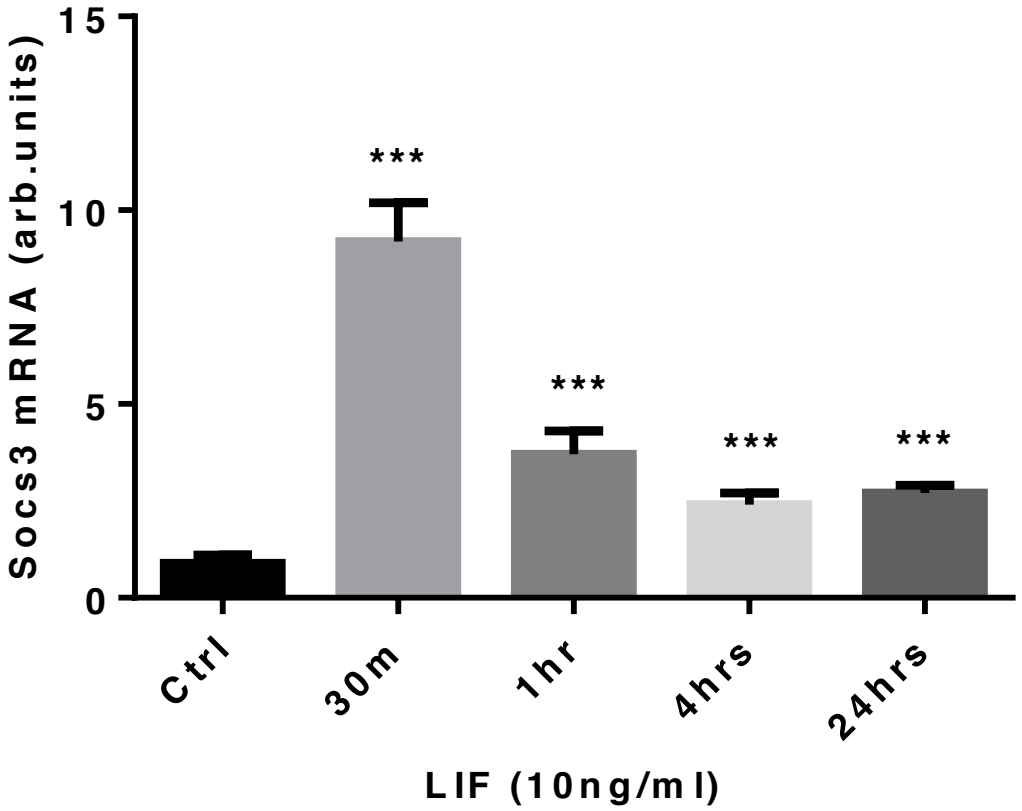

Figure 4.4: Socs3 was induced at an early time point by LIF. CG4 cells were plated at a density of $8x10^4$ cells/well and differentiated for one day before LIF was added for the time specified. Socs3 mRNA was measured by qPCR and results are expressed as arbitrary units versus the control. Data represented here are the mean ± SD of quadruplicate samples. ***P<0.0001 versus the control.

LIF (10ng/ml)	Socs3 Mean	SD	P value
0	0.9	0.2	
30mins	1.0	1.0	3.34E-06
1hr	0.6	0.6	6.88E-05
4hrs	0.3	0.3	0.0002
24hrs	0.2	0.2	5.99E-06

4.6 Induction of Socs3 correlated with decreased Mog induction

The previous experiment confirmed that Socs3 was induced by LIF and that it was best to measure the expression of Socs3 at an early time point. Therefore Socs3 expression was measured after varying concentrations of LIF. This would determine if Socs3 expression correlated with the induction of Mog because a signalling protein that correlated with Mog expression could be causing the inhibition of Mog expression at high concentrations of LIF. To measure Socs3 induction $8x10^4$ CG4 cells were plated per well of 24-well plates and differentiated as in Section 4.3. The cytokines were added 24 hours after differentiation and the experiment was stopped after one hour of cytokine treatment. Socs3 expression was measured by qPCR.

The initial experiment showed that Socs3 induction increased as the concentration of LIF increased (Fig. 4.5). The concentrations used here match those used to measure Mog induction by LIF in Section 3.1. From the two graphs it was observed that 0.2ng/ml, which is the optimum concentration of LIF for Mog induction, induced significantly less Socs3 than 2 and 10ng/ml of LIF, both of which inhibited LIF-induced Mog (Fig.3.1). The increased Socs3 expression at the higher concentration of LIF may offer an explanation as to why 10ng/ml LIF induces less Mog than 0.2ng/ml. This experiment was repeated and the results remained the same.

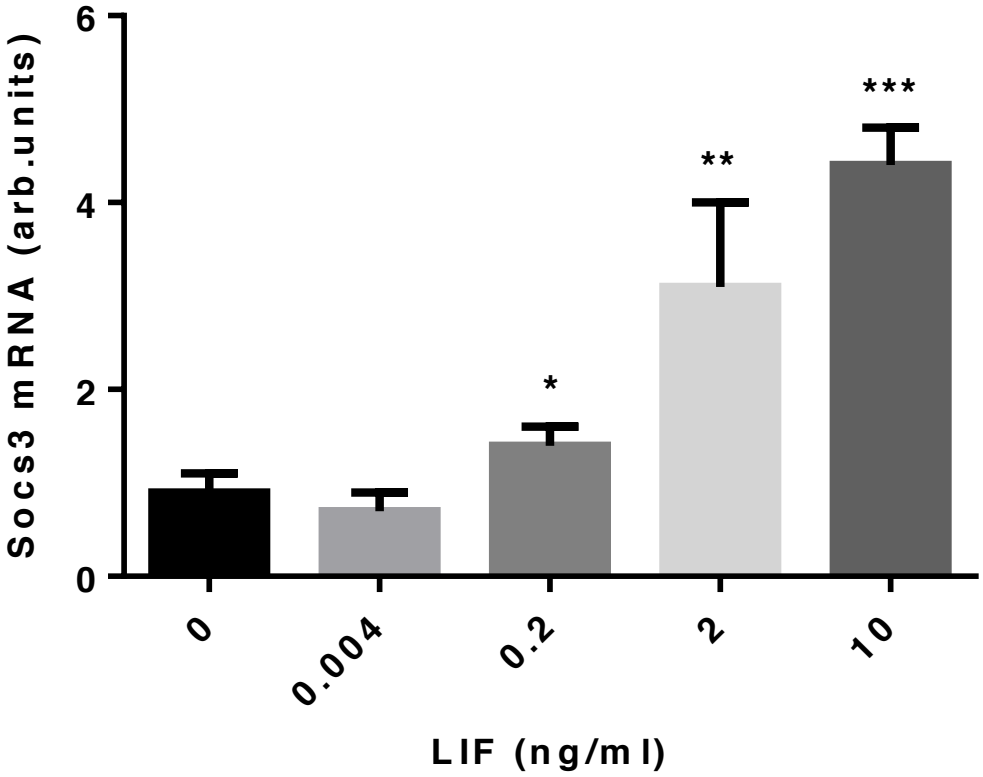

Figure 4.5: LIF induction of Socs3 was concentration dependent. CG4 cells were plated at a density of $8x10^4$ cells/well and differentiated for one day before the indicated concentration of LIF was added for one hour. Socs3 mRNA was measured by qPCR and results are expressed as arbitrary units versus the control. Data are mean ± SD of quadruplicate samples. *P<0.05, ** P<0.01, ***P<0.001 versus the control.

LIF (ng/ml)	Socs Mean	SD	P value
0	0.9	0.2	
0.004	0.7	0.2	0.2066
0.2	1.4	0.2	0.0108
2	3.1	0.9	0.0039
10	4.4	0.4	0.00007

Secondly, Socs3 induction was measured upon EPO treatment and simultaneous treatment with EPO and LIF to assess if it was upregulated when they were added simultaneously. Again, the cytokines were added 24 hours after differentiation, both at 10ng/ml, and the experiment was stopped one hour later.

The increase of Socs3 expression by 10ng/ml LIF was confirmed in this experiment (Fig.4.6). Furthermore, the results showed that EPO induced significantly less Socs3 expression than LIF (P=0.0001). Finally, the increase in Socs3 expression induced by LIF was still present when the cytokines were added simultaneously; the presence of EPO did not prevent LIF from inducing high levels of Socs3. The experiment was repeated and the same results were obtained.

The results shown in Figures 4.5 and 4.6 demonstrated that Mog negatively correlated with Socs3 induction. Therefore, the treatments that induced less Mog, i.e. LIF 10ng/ml and EPO+LIF, are those that induced greatest Socs3 expression. It can be implied from this result that Socs3 was an inhibitory feedback mechanism that prevented the induction of Mog. It seemed that the quantity of Socs3 induced was important as EPO treatment alone, which induced a large increase in Mog, also induced some Socs3. Potentially if this small amount of Socs3 induction was inhibited, then the expression of Mog would be increased even further. However, the results simply show a correlation, more work was needed to prove causation.

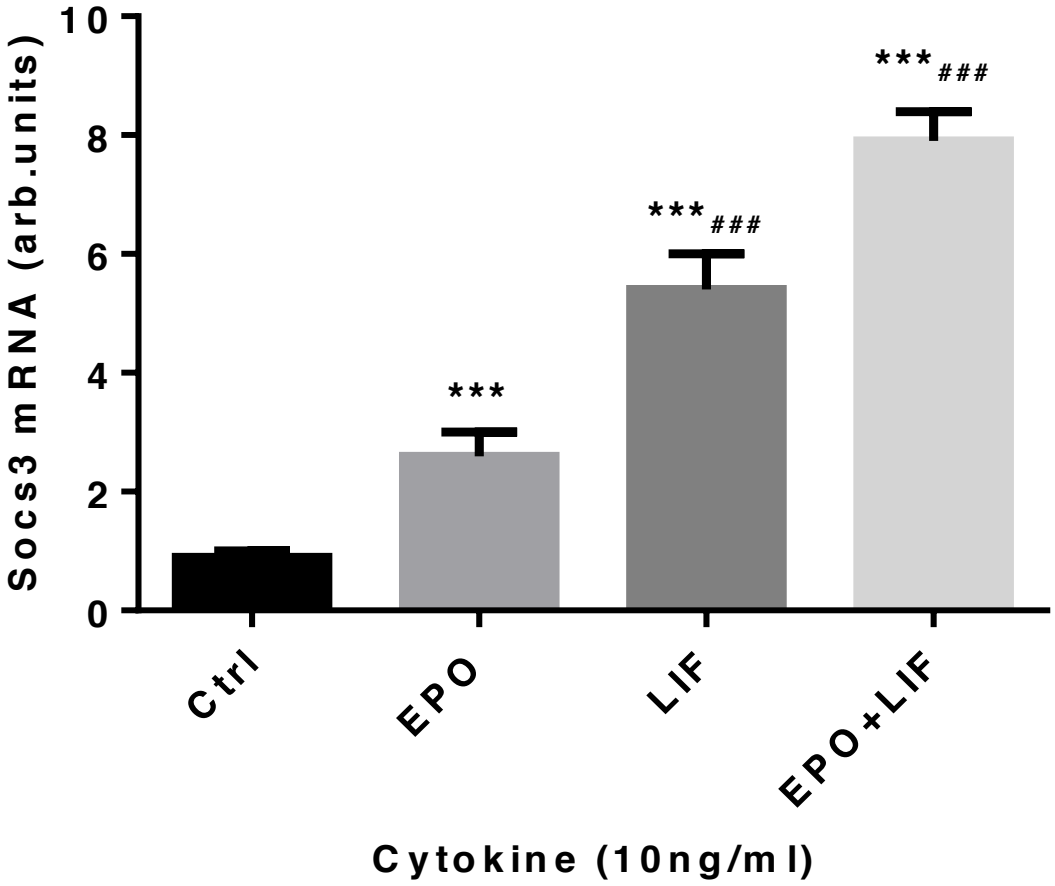

Figure 4.6: LIF was a more potent inducer of Socs3 than EPO. CG4 cells were plated at a density of $8x10^4$ cells/well and differentiated for one day before the indicated cytokine was added for one hour. Socs3 mRNA was measured by qPCR and results are expressed as arbitrary units versus the control. Data represented here are the mean ± SD of quadruplicate samples. *P<0.05 **P<0.001 ***P<0.0001 versus the control.

			P value	
Cytokine	**Socs Mean**	**SD**	**vs Ctrl**	**vs EPO**
Ctrl	0.9	0.1		
EPO	2.6	0.4	0.0003	
LIF	5.4	0.6	4.56E-06	0.0002
EPO+LIF	7.9	0.5	1.72E-07	3.74E-06

4.7 Inhibition of STAT3 phosphorylation occurred only after a high concentration of LIF

More evidence was required to prove that Socs3 was having an effect in the CG4 cells and that the observed effects were not simply as a result of an inert induction of the Socs3 signalling cascade. Analysis of STAT3 phosphorylation would show if Socs3 was preventing STAT3 phosphorylation and therefore its further downstream effects. STAT3 phosphorylation was measured by Western blot.

CG4 cells were plated at a density of $2x10^5$ cells/well. The cells were differentiated after 24 hours and then treated with 0.2ng/ml or 10ng/ml of LIF 24 hours after that. LIF was added to the cells at eight 10-minute intervals to provide a thorough time course of STAT3 phosphorylation. Total cellular extracts were prepared using RIPA buffer.

At both concentrations of LIF, STAT3 was phosphorylated by the ten-minute time point, as seen by bands at the expected molecular weight of 85kDa (Fig 4.7). At 0.2ng/ml LIF the levels of pSTAT3 remained elevated for the whole time-course, up to 80 minutes. In contrast, when the cells were treated with 10ng/ml LIF the levels of pSTAT3 only remained elevated for 20 minutes, by 30 minutes the quantity of protein was decreasing and by 40 minutes there was very little detection. These results suggest that at the higher concentration there is a negative feedback that is not present at 0.2ng/ml. This finding fits the hypothesis that it is Socs3 that caused the inhibition of Mog induction as Socs3 was transcriptionally regulated by pSTAT3. Therefore, at 10ng/ml, enough STAT3 was phosphorylated and translocated to the nucleus to induce Socs3 expression that in turn prevented further phosphorylation of STAT3. At 0.2ng/ml, Socs3 expression did not increase enough to cause an inhibition of pSTAT3.

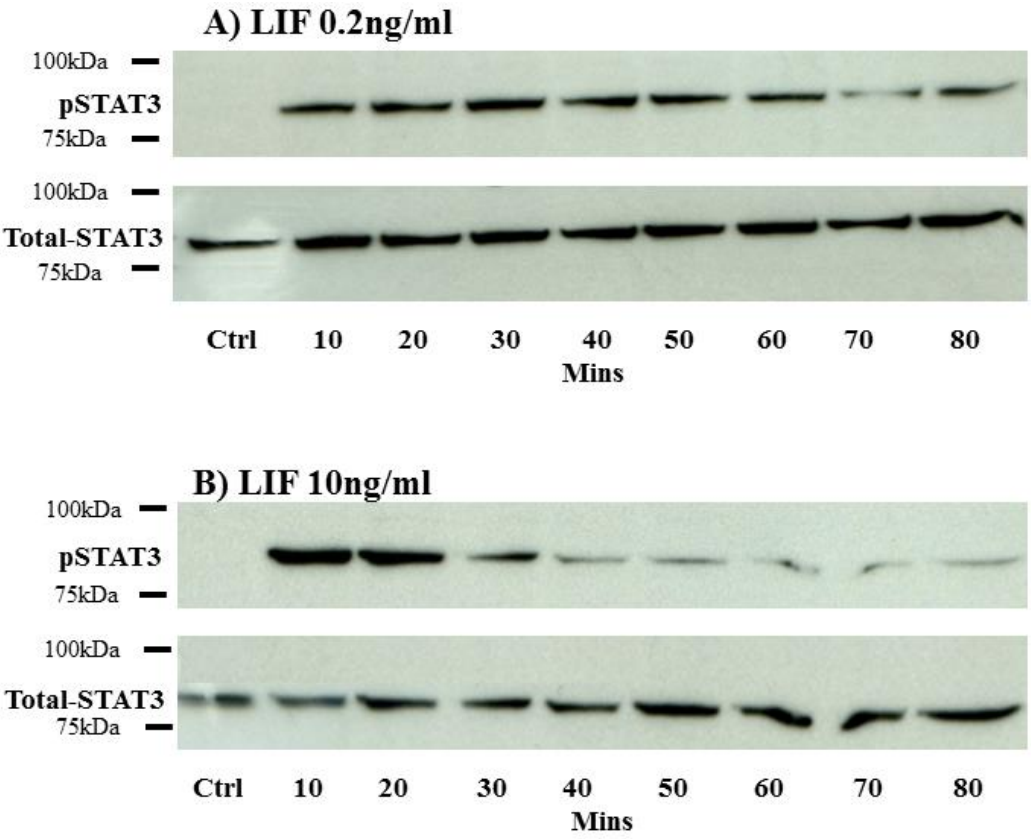

Figure 4.7: Low-concentration of LIF did not cause an inhibition of pSTAT3 but high concentration did after 20 minutes. CG4 cells were plated at a density of $10x10^4$ cells/well and differentiated for 24 hours before 0.2 or 10ng/ml LIF were added for the time indicated. pSTAT3 protein density was measured by Western blot and total STAT3 was used as a loading control. STAT3 protein is 80kDa.

4.8 Socs3 was also induced by OSM and CNTF

Section 3.5 demonstrated that OSM and CNTF, IL-6 family cytokines that share LIFR, induced inhibition of EPO-induced Mog in the same way as LIF. For this reason the expression of Socs3 by cells treated with OSM and CNTF was measured. The experiment was performed identically to experiments measuring Socs3 induction by LIF, and OSM and CNTF were added at and equimolar concentration to LIF.

OSM and CNTF both induced significant quantities of Socs3 ($P=0.00016$ and $P=0.002$ respectively), as did LIF ($P=0.00001$) (Fig 4.8). CNTF seemed to induce less Socs3 that the other two cytokines. In Section 3.5 it was noted that CNTF did not induce as much Mog as LIF or OSM and it did not completely inhibit EPO-induced Mog as LIF and OSM did. The slightly reduced effects of CNTF when compared to LIF and OSM could be due to a third receptor that CNTF utilises; the CNTFR. Both LIF and OSM signal through only LIFR and GP130, while CNTF also uses the CNTFR. The CG4 cells used here could express less CNTFR, and so explain why the effect of CNTF on these cells was slightly reduced. The experiment was repeated and the same results obtained.

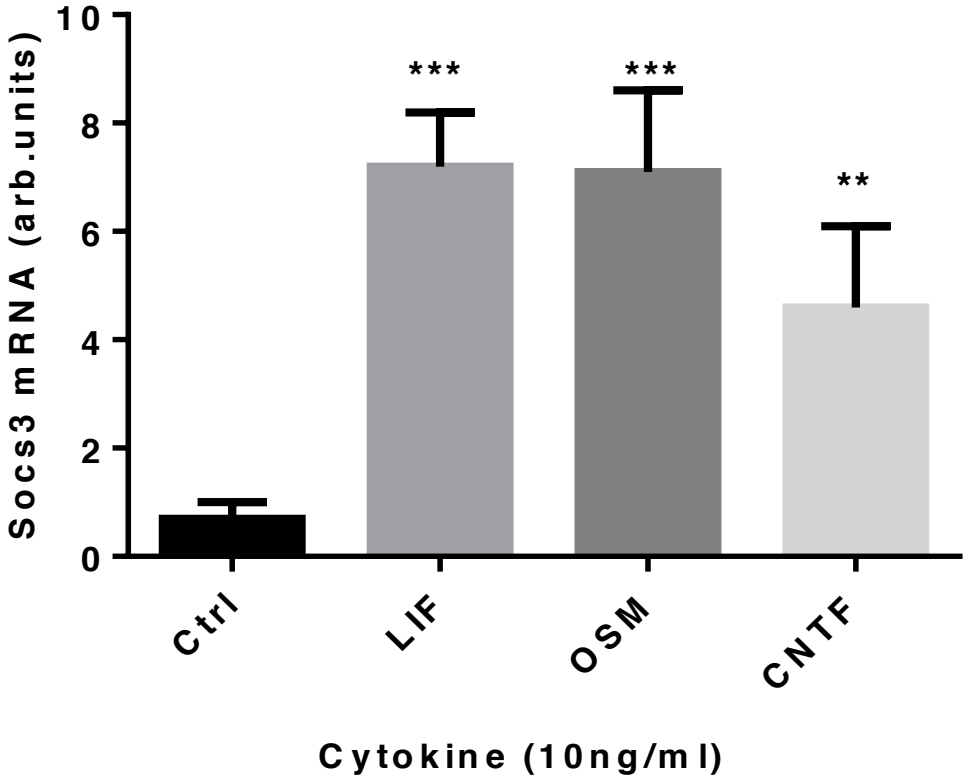

Figure 4.8: OSM and CNTF also induced Socs3 expression. CG4 cells were plated at a density of $8x10^4$ cells/well and differentiated for one day before 10ng/ml LIF and equimolar concentrations of OSM and CNTF were added for one hour. Socs3 mRNA was measured by qPCR and results are expressed as arbitrary units versus the control. Data represented here are the mean ± SD of quadruplicate samples. **P<0.01, ***P<0.001 versus the control.

Cytokine (ng/ml)	Mog Mean	SD	P value
Ctrl	0.7	0.3	
LIF	7.2	1.0	0.00002
OSM	7.1	1.5	0.0002
CNTF	4.6	1.5	0.0021

4.9 Inhibition of Socs3

To investigate the relationship between Socs3 and Mog, Socs3 was inhibited. I hypothesised that inhibition of Socs3 would cause an increase in Mog. The method used to inhibit Socs3 was the use of small interfering RNA (siRNA). Fire *et al* (1998) found that protein expression of endogenous genes could be restricted by endogenous injection of double stranded RNA in *Caenorhabditis elegans,* the molecule injected was later named siRNA (Fire 1998, Elbashir 2001). The siRNA can block gene expression by binding to the complementary RNA sequence and so preventing translation of this sequence (Matranga 2005). To produce this effect *in vitro* Lipofectamine 2000 transfection of the siRNA into the genome of the cells was used (Gopalakrishnan 2009).

CG4 cells were plated at a density of $4x10^4$ cells/well on 24-well plates and differentiated after 24 hours. The transfection mixture consisted of Lipofectamine 2000 and Opti-MEM. Two siRNAs were used individually and in combination. Furthermore, a control siRNA was used as a negative control. Twenty four or forty eight hours after transfection 10ng/ml LIF was added to each well. Two time points were used to ensure that the siRNA would have been properly incorporated into the mRNA and that this would have led to a translational decrease in Socs3 expression. The experiment was stopped 1 hour after the addition of LIF and Socs3 mRNA expression was measured by qPCR.

The siRNA did not successfully inhibit Socs3 expression (Fig 4.9). At 24 hours, the cells that were treated with siRNA2, either alone or in combination with siRNA1, even expressed more Socs3 mRNA than those that were not transfected and only treated with LIF. The upregulation seen showed that the siRNAs were not inert; it is possible that there was an overcompensation of Socs3 expression after the attempted inhibition.

To confirm that the siRNA was not inhibiting post-transcriptional Socs3, Mog was also measured after transfection with the Socs3 siRNA. Cells were plated at a density of $3x10^4$cells/well and transfected 24 hours later. In this experiment the two siRNAs were used in combination and the control siRNA was used again. EPO and LIF were

added 24 hours after transfection and the cells were incubated for 3 days before Mog expression was measured by qPCR. Socs3 siRNA did not have any effect on Mog expression (Fig 4.10). If the siRNA had inhibited Socs3 it would be expected that the inhibition of EPO-induced Mog by LIF would be prevented, however, the inhibition was still seen when cells treated with EPO+LIF simultaneously were transfected with the Socs3 siRNA. Furthermore, the control siRNA showed no difference in effect over the Socs3 siRNA, leading to the conclusion that the siRNA transfection was not successful.

Another method used to inhibit Socs3 was the use of a chemical inhibitor, Zoledronic acid (ZA). ZA is an amino-bisphosphonate that is approved for use in the USA for treatment of Paget's disease, postmenopausal osteoporosis, multiple myeloma, and bone metastases from solid tumours (Ibrahim 2003). ZA is a known inhibitor of Socs3 (Scheller 2011) so it was used in another attempt to inhibit Socs3.

CG4 cells were plated at a density of $8x10^4$ cells/well in a 24-well plate. They were allowed to proliferate for 1 day at which point differentiation medium and a range of concentrations of ZA was added. After overnight incubation, 10ng/ml LIF was added and the experiment was stopped 1 hour after the addition of LIF. Socs3 mRNA expression was measured by qPCR.

ZA had no effect on Socs3 induction in CG4 cells at any of the concentrations added (Fig.4.11). There was no variation in the results between concentrations of ZA and none produced a significantly different change from the control.

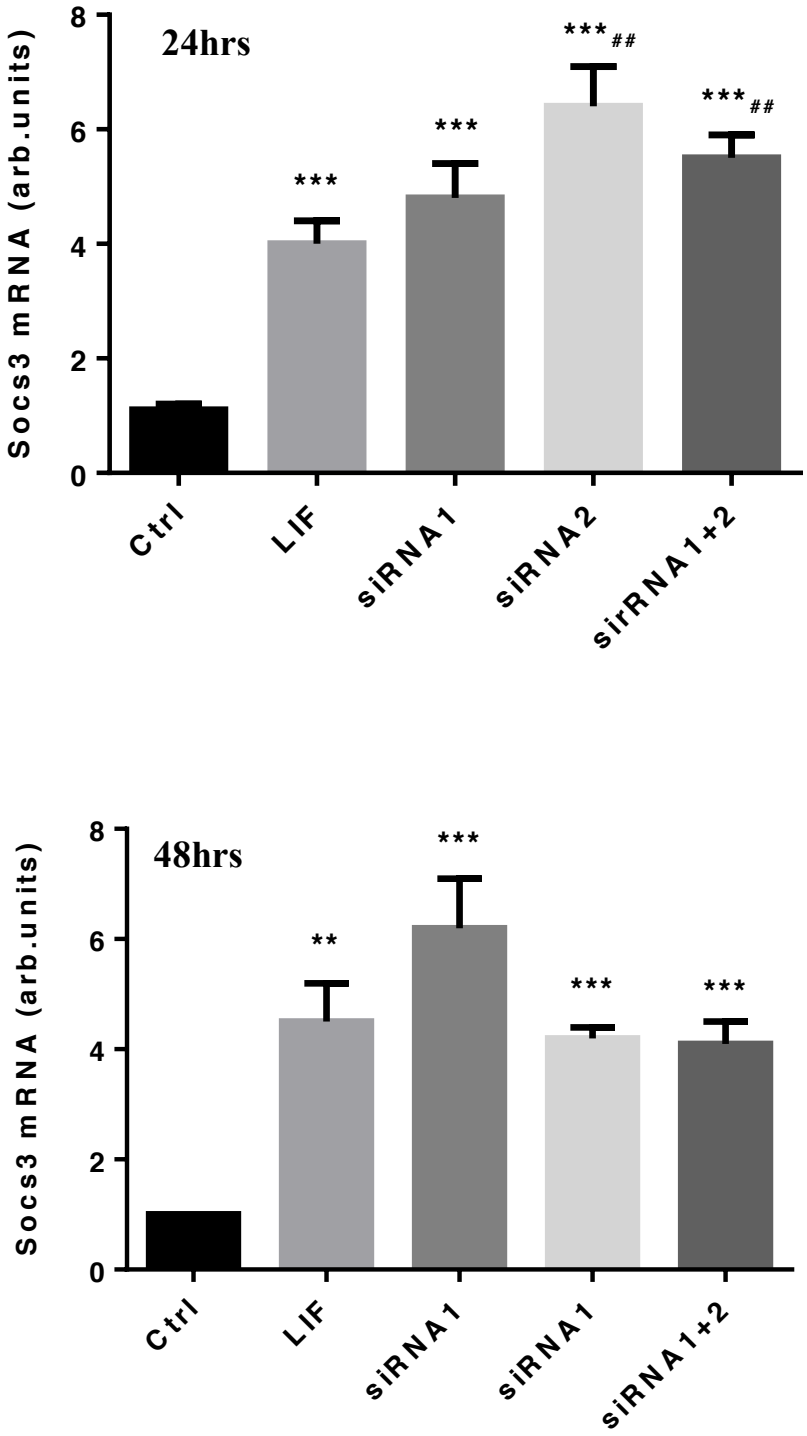

Figure 4.9: Socs3 siRNA failed to inhibit Socs3 expression. CG4 cells were plated at a density of $4x10^4$ cells/well and differentiated and transfected 24hours later. LIF was added 24 or 48 hours after transfection and the experiment was stopped 1 hour after the addition of LIF. Socs3 mRNA was measured by qPCR and results are expressed as arbitrary units versus the control. Data represented here are the mean ± SD of quadruplicate samples. ***P<0.001 versus the control and ##P<0.01 versus EPO alone…

Figure 4.9 cont.:

24hr data:

			P value	
Cytokine (ng/ml)	**Socs3 Mean**	**SD**	**vs Ctrl**	**vs EPO**
Ctrl	1.1	0.1		
LIF	4.0	0.4	0.0003	
siRNA1	4.8	0.6	0.0006	0.1331
siRNA2	6.4	0.7	0.0002	0.0068
siRNA1+2	5.5	0.4	0.00004	0.0097

48hr data:

			P value	
Cytokine (ng/ml)	**Socs3 Mean**	**SD**	**vs Ctrl**	**vs EPO**
Ctrl	1.0	0.0		
LIF	4.5	0.7	0.0012	
siRNA1	6.2	0.9	0.0006	0.0665
siRNA2	4.2	0.2	0.00001	0.5235
siRNA1+2	4.1	0.4	0.0002	0.4324

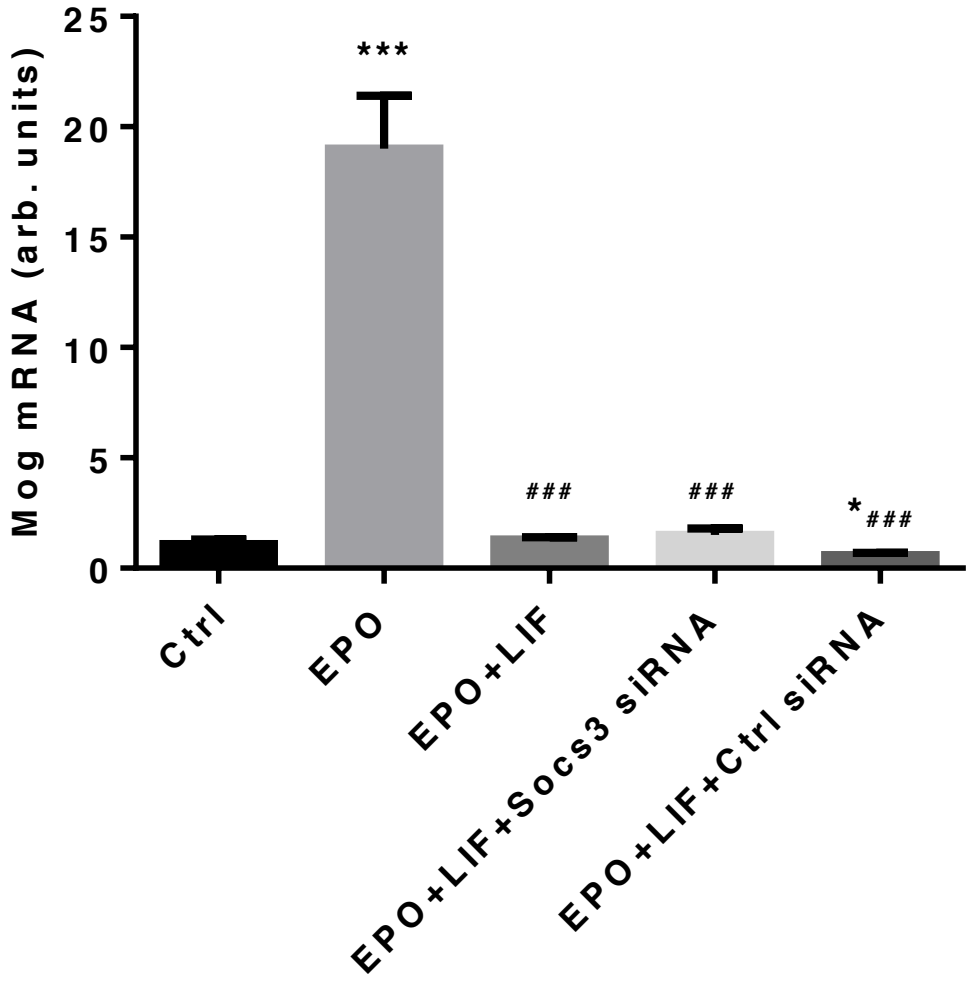

Figure 4.10: Socs3 siRNA failed to inhibit Mog expression. CG4 cells were plated at a density of $4x10^4$ cells/well and differentiated and transfected 24hours later. LIF was added 24 hours after transfection and the experiment was stopped 3 days later. Mog mRNA was measured by qPCR and results are expressed as arbitrary units versus the control. Data represented here are the mean ± SD of quadruplicate samples. *P<0.05 ***P<0.001 versus the control and ###P<0.001 versus EPO alone.

			P value	
Cytokine (ng/ml)	**Mog Mean**	**SD**	**vs Ctrl**	**vs EPO**
Ctrl	1.1	0.2		
EPO	19.0	2.4	5.5E-06	
EPO+LIF	1.3	0.1	0.2035	5.75E-06
EPO+LIF+Socs3si	1.5	0.3	0.0816	6.41E-06
EPO+LIF+Ctrlsi	0.6	0.1	0.0299	4.74E-05

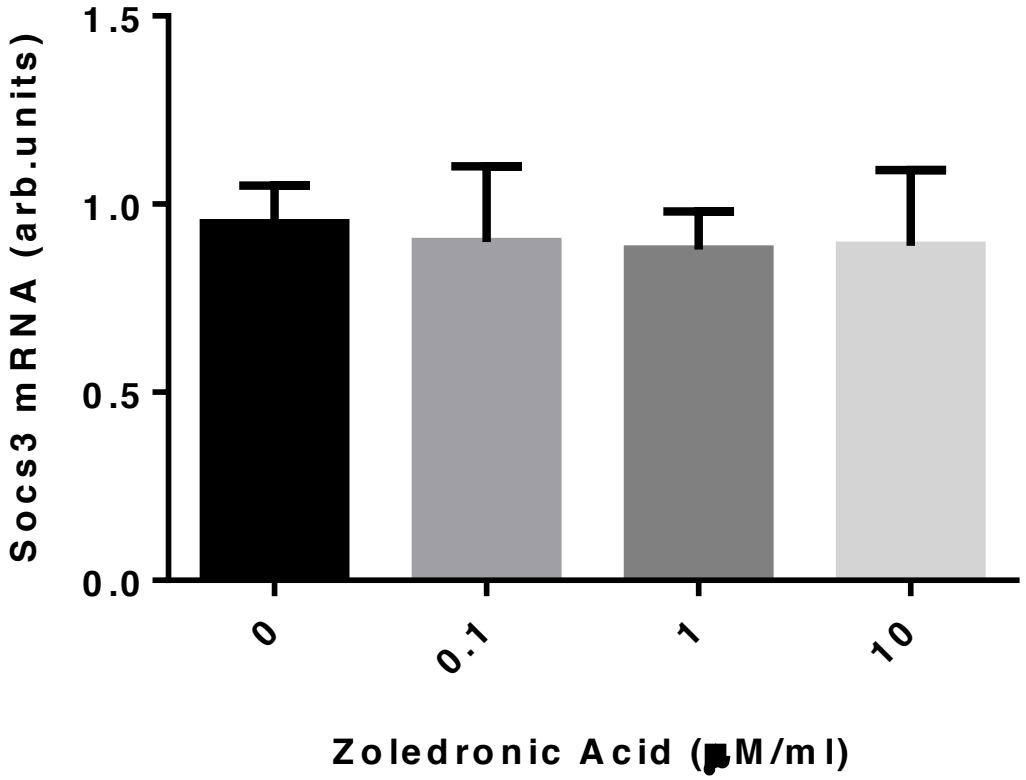

Figure 4.11: Zoledronic acid failed to inhibit Socs3 expression. CG4 cells were plated at a density of $8x10^4$ cells/well and differentiated 24 hours later, at which point ZA was added. LIF was added 24 hours later and the experiment was stopped 1 hour after this addition. Socs3 mRNA was measured by qPCR and results are expressed as arbitrary units versus the control. Data represented here are the mean ± SD of quadruplicate samples. No statistical significance.

ZA (µM/ml)	Socs3 mean	SD	P value
0	0.9	0.1	
0.1	0.9	0.2	0.6451
1	0.9	0.1	0.4141
10	0.9	0.2	0.6448

Potentially the reason there was no effect of ZA seen here was that it affects Socs3 post-translationally, preventing formation of the active protein as opposed to expression of the mRNA. Therefore it was decided to measure Mog output when ZA was present to see if it was having an effect on the final outcome of the treatment with EPO and LIF. It was hypothesised that, because ZA blocks Socs3 protein there would not be a decrease in Mog when EPO+LIF were added simultaneously.

CG4 cells were plated at a density of $4x10^4$ cells/well in 24-well plates. They were differentiated 24 hours later and ZA was added at both 1 and 10 μM/ml to the cells that required it. After overnight incubation EPO alone or EPO+LIF were added and the experiment was run for an additional 3 days. Mog mRNA expression was measured by qPCR.

The pre-treatment of these cells with ZA failed to prevent the inhibition of EPO-induced Mog by LIF (Fig 4.12). The samples treated with ZA as well as EPO+LIF showed the same reduction in Mog expression as those that were not. It appears that ZA had no effect on these cells.

To finally confirm that ZA had no effect in these cells the basal expression of Mog after ZA treatment was investigated. CG4 cells were plated at $3x10^4$ cells/ml. They were differentiated after 24 hours and ZA was added to the wells that required it at a concentration of 10μM/ml. Twenty four hours later EPO was added and the experiment was run for 3 days. Mog mRNA expression was measured by qPCR.

The results seen in Figure 4.13 show that ZA had no effect on either basal Mog expression or on the increased Mog induction by EPO. The graph appears to show a difference between EPO treatment alone and EPO and ZA treatment, but this difference was not statistically significant (P=0.069). The combined results after ZA treatment show that it had no effect on Socs3.

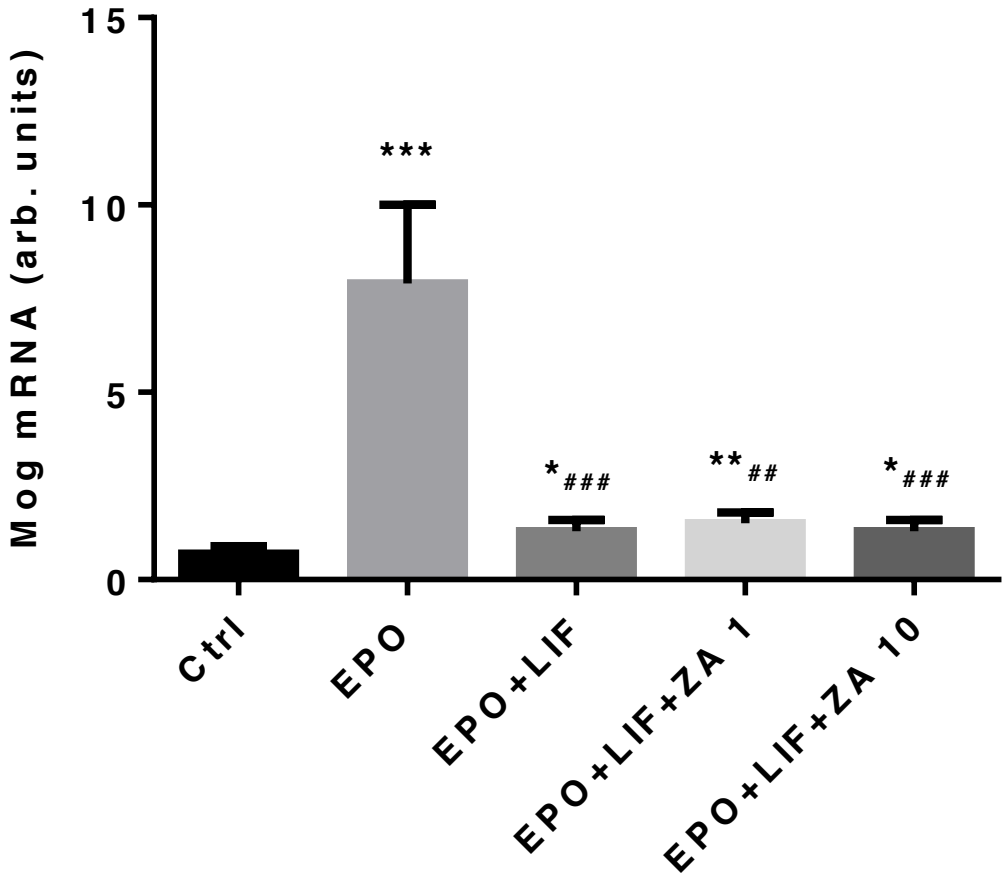

Figure 4.12: Zoledronic acid failed to increase Mog induction. CG4 cells were plated at a density of $4x10^4$ cells/well and differentiated 24 hours later, at which point ZA was added. EPO and LIF were added 24 hours after ZA treatment. The experiment was run for 3 days after the addition of the cytokines. Mog mRNA was measured by qPCR and results are expressed as arbitrary units versus the control. Data represented here are the mean ± SD of quadruplicate samples. *P<0.05, **P<0.01 and ***P<0.001 versus the control and ##P<0.01 and ###P<0.001.

			P value	
Samples	**Mog Mean**	**SD**	**vs Ctrl**	**vs EPO**
Ctr	0.7	0.2		
EPO	7.9	2.1	0.0005	
EPO+LIF	1.3	0.3	0.0210	0.0007
EPO+LIF+ZA1	1.5	0.3	0.0038	0.0035
EPO+LIF+ZA10	1.3	0.3	0.0132	0.0008

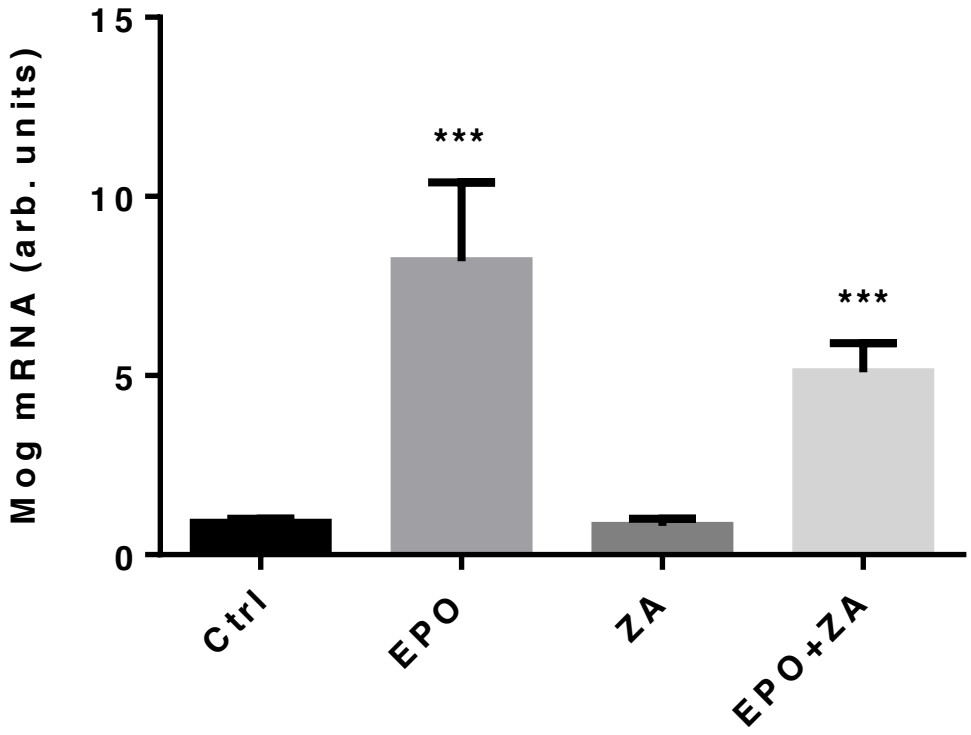

Figure 4.13: Zoledronic acid failed to increase Mog induction or basal Mog levels. CG4 cells were plated at a density of $3x10^4$ cells/well and differentiated 24 hours later, at which point ZA was added. EPO was added 24 hours after ZA treatment. The experiment was run for 3 days after the addition of EPO. Mog mRNA was measured by qPCR and results are expressed as arbitrary units versus the control. Data represented here are the mean ± SD of quadruplicate samples. ***P<0.001 versus the control.

			P value	
Samples	**Mog Mean**	**SD**	**vs Ctrl**	**vs EPO**
Ctrl	0.9	0.1		
Ctrl+ZA	0.8	0.2	0.1909	
EPO	8.2	2.2	0.0005	
EPO+ZA	5.1	0.8	0.0001	0.0693

4.10 A known inducer of Socs3 also inhibited EPO-induced Mog

As inhibition of Socs3 was not successful (Section 4.9) it was decided to induce Socs3 to provide further evidence that it caused inhibition of EPO-induced Mog expression by LIF. If an inducer of Socs3 also causes the inhibition of EPO-induced Mog it would show that Socs3 has the capacity to induce inhibition.

Phorbol 12-myristate 13-acetate (PMA) inhibits IL-6 signalling by inducing expression of Socs3 (Terstegen 2000). For this reason it was used to replace LIF in the simultaneous treatment with EPO. To confirm that it induced Socs3 in these cells, PMA was added at 10ng/ml individually and simultaneously with EPO 24 hours after differentiation of CG4 cells. They were treated for 1 hour before Socs3 mRNA expression was measured by qPCR.

PMA induced very high levels of Socs3 expression when added simultaneously with EPO (Fig 4.14). Interestingly, and dissimilar to LIF, it did not induce Socs3 when added alone suggesting that in this instance it is a combined effect of EPO and PMA that caused a high increase in Socs3 expression.

The effect of this significant increase in Socs3 expression by PMA and EPO simultaneously was investigated by measuring the influence on Mog expression after these treatments. CG4 cells were plated at a density of $4x10^4$ cells/well and PMA was used at the same concentration as EPO and added at the same time. The experiment proceeded for three days to allow for the induction of Mog expression, which was measured by qPCR.

PMA caused a decrease in EPO-induced Mog, reflecting the inhibition seen by LIF (Fig 4.15). The similarities between induction of Mog by PMA and by LIF suggest that a signalling pathway that is common to these two molecules was involved in the inhibition of EPO-induced Mog. As Socs3 is known to be present downstream of both of these molecules it can be assumed that it was working in the same way after PMA treatment as it did after LIF treatment. The conclusion drawn here was that Socs3 was involved in LIF's inhibition of EPO-induced Mog. The experiment was repeated and the same results obtained.

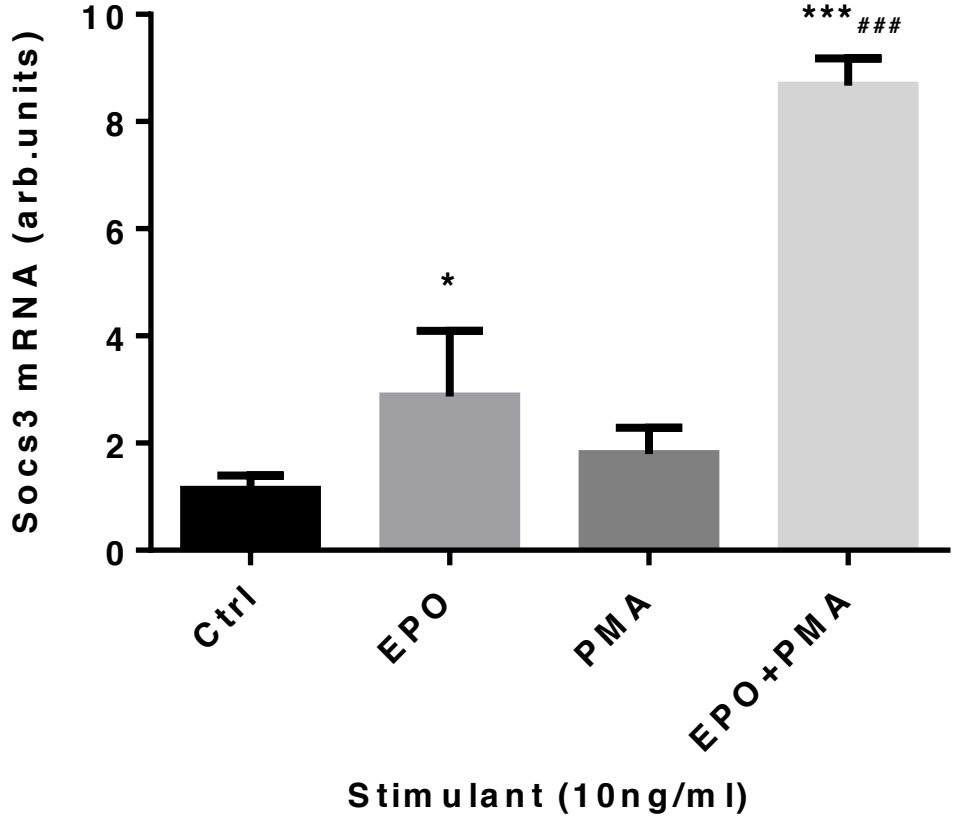

Figure 4.14 PMA induced Socs3 expression when added simultaneously with EPO. CG4 cells were plated at a density of $8x10^4$ cells/well and differentiated for one day before treatment with EPO, PMA or both at 10ng/ml. Socs3 mRNA was measured by qPCR and results are expressed as arbitrary units versus the control. Data represented here are the mean ± SD of quadruplicate samples. *P<0.05, ***P<0.001 versus the control and ###P<0.001 versus EPO alone.

			P value	
Samples	**Socs3 Mean**	**SD**	**vs Ctrl**	**vs EPO**
Ctrl	1.1	0.3		
EPO	2.9	1.2	0.0327	
PMA	1.8	0.5	0.0525	0.1582
EPO+PMA	8.7	0.5	2.033E-07	0.0001

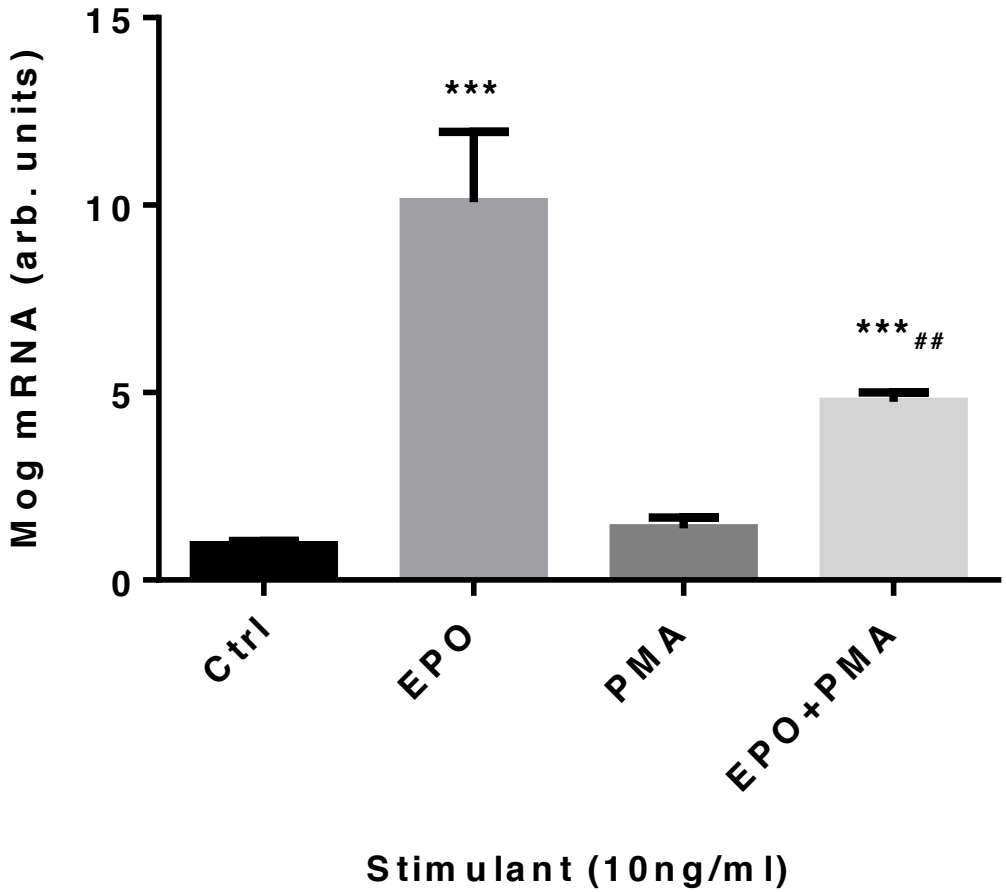

Figure 4.15: PMA inhibited induction of Mog expression by EPO. CG4 cells were plated at a density of $4x10^4$ cells/well and differentiated for three days after treatment with PMA, EPO, or both at 10ng/ml. Mog mRNA was measured by qPCR and results are expressed as arbitrary units versus the control. Data represented here are the mean ± SD of quadruplicate samples. **P<0.001 versus the control and ##P<0.001 versus EPO alone.

			P value	
Samples	**Mog Mean**	**SD**	**vs Ctrl**	**vs EPO**
Ctrl	3.0	0.1		
EPO	10.1	1.9	0.0011	
PMA	1.4	0.3	0.0539	
EPO+PMA	4.8	0.3	2.3226E-06	0.0021

4.11 Conclusions

- Socs3 expression correlated with decreased Mog expression
- A known inducer of Socs3 also inhibited Mog expression
- Egr2 and ERK1/2 were not involved in the inhibition of EPO-induced Mog, despite being previously linked to myelination

The purpose of the experiments presented in this chapter was to investigate the signalling mechanisms that lead to the inhibition of EPO-induced Mog by the addition of LIF. It was confirmed that it is an early signalling event that caused the inhibition of EPO-induced Mog because only LIF added simultaneously with EPO caused a complete inhibition of Mog; it did not when it was added at later time points.

Socs3 is known to be induced by IL-6 cytokines. The results here confirmed that Socs3 is an early-induced protein and so could be causing the inhibition seen. Socs3 expression was then shown to negatively correlate with Mog induction. The conditions that demonstrated the lowest Mog induction (LIF 10ng/ml and EPO+LIF) showed the highest levels of Socs3 expression, while EPO alone and LIF 0.2ng/ml, conditions that increased Mog induction, resulted in lower levels of Socs3. Furthermore, with treatment of 0.2ng/ml LIF phosphorylation of STAT3 was sustained up to 80 minutes, whereas 10ng/ml LIF initially increased the phosphorylation of STAT3 but inhibition was observed after 20 minutes, suggesting that Socs3 was expressed at high enough concentrations to cause an inhibitory feedback.

In attempting to prove that the interaction between Socs3 and Mog is not just coincidental, Socs3 was intentionally upregulated by PMA. EPO-induced Mog was also inhibited by PMA and an increased expression of Socs3 was induced when added simultaneously with EPO.

Furthermore, neither Egr2 nor pERK1/2 correlated with the suppression of Mog induction seen when the CG4 cells were treated with EPO+LIF, demonstrating that this signalling pathway was not involved in the inhibition.

Taken together, these results suggest a functional implication for Socs3 expression and an explanation for how LIF inhibits EPO-induced Mog. Suppression of EPO by Socs3 has not been investigated in a model of neurorepair so from this series of experiments it can be concluded that a novel feedback mechanism has been identified.

The identification of Socs3 as a viable inhibitor of EPO has implications for treatment of demyelinating diseases. If there is a chance that EPO treatment is being inhibited by Socs3 expression as induced by endogenous cytokine stimulation, then the use of EPO in regenerative medicine could be less efficacious than if Socs3 were not present. If Socs3 expression was inhibited, less EPO would be required in treatment. Therefore, given a reduced quantity of EPO would be required for therapeutic efficacy, it is likely that the side-effects of EPO would be reduced.

The current chapter focussed on signalling mechanisms previously investigated as downstream consequences of EPO and/or LIF stimulation. While this approach did lead to potential answers for what caused inhibition of EPO-induced Mog by LIF, I only explored known signalling mechanisms. To investigate a much wider variety of genetic effects of EPO and LIF, chapter 5 will characterise the genetic profile of the cytokine treated CG4 cells using gene expression microarrays. In the analysis that follows, hierarchical clustering and gene association software were used to screen over 30,000 genes to identify those that may have a functional impact on myelination in these cells.

Chapter 5. Gene expression microarray analysis of EPO-regulated genes

5.1 Introduction

Microarray technology was first described in 1995 by Schena *et al.* as a method of profiling the expression of a large number of genes simultaneously (Schena 1995). The analysis of thousands of genes concurrently allowed for the detection of subtle changes in transcript variants and for the identification of genes that may not have been previously implicated in the specified condition.

Previous work by Cervellini *et al,* and confirmed by experiments undertaken in this project, investigated the effect of EPO on CG4 OPCs, showing that EPO consistently upregulated myelin genes such as Mog in these cells (Cervellini *et al.* 2013a).

The mechanisms that control OPC differentiation and myelination are complex and rely on the interaction between many signalling pathways that act in synergy to produce an overall increase in myelination. Individual signalling pathways may have opposing effects on myelination but the optimal conditions and combination of orchestrated signalling pathways induces a genetic profile in OPCs that leads to a pro-myelinating phenotype.

Microarray gene technologies have been used to study the oligodendrocyte genome previously, leading to a greater understanding of basic mechanisms of oligodendrocyte development. Using this technology, SRY-box containing gene 17 was identified as a gene whose expression was coordinated with that of four myelin genes (Sohn 2006). Furthermore, oligodendrocytes demonstrated overall a large change in gene expression as the cells prepared to commit to a myelinating phenotype including upregulation of myelin structural genes, cholesterol biosynthesis genes and actin cytoskeleton regulatory genes (Nielsen 2006). Oligodendrocyte differentiation was also investigated by microarrays, and patterns in transcription factor expression were identified (Dugas 2012). Comparisons between the two latter datasets showed that 70% of the upregulated transcription factors

important in differentiation identified by Dugas *et al* were also identified as important in myelination by Nielsen *et al* (Joseph A. Nielsen *et al.* 2010).

EPO had protective properties in models of cerebral ischaemia (Mengozzi 2012). The genes responsible for its ability to provide this protective effect have been investigated previously by gene expression microarrays, introducing Arc, Bdnf, Egr1 and Egr2 as important regulators of synaptic plasticity. The pro-myelinating effects of EPO on oligodendrocytes have been investigated previously, and confirmed in this thesis. CG4 cells treated with EPO show an increased expression of the myelin gene Mog, but the genetic expression that results in its ability to increase myelination is not well understood.

Analysis of the genes whose expression is altered by differentiation and by the addition of EPO will elucidate the mechanisms that are most important in contributing to maturation and myelination. Developing a greater understanding of these mechanisms will clarify potential therapeutic targets that could be used to increase OPC differentiation and myelination in disease models. Furthermore, by investigating two time points; 1 hour and 20 hours, genes that were induced immediately could be investigated as well as those induced later. Genes that are induced early will be compared to gene expression profiles at the later time point to identify concomitant effects upon gene regulation. The results obtained by microarray analysis alluded to several regulatory mechanisms and validation of genes involved in such regulatory pathways by qPCR was largely confirmed.

5.2 Confirmation of the effect of EPO and LIF on CG4 cells

Gene expression microarray analysis was conducted to investigate the effects of EPO, LIF and EPO+LIF simultaneously on gene expression in CG4 cells. The cells were plated at a density of $3.5x10^5$ cells/well in 6-well plates. Twenty-four hours after plating they were differentiated and 3 hours after that the cytokines were added. Half of the experiment was stopped at 1 hour and the same number of samples was stimulated for 20 hours. The use of two time points would allow comparisons between the genes that are induced immediately, those whose expression remains

elevated throughout the time-course, and those that are only altered at later time points, representing downstream effects. The experiment was stopped using QIAzol and total RNA extracted using miRNeasy Mini Kit (Qiagen) and the quality and quantity measured using Nanodrop ND-1000. Gene expression microarray analysis was carried out by Oxford Gene Technologies (Section 2.5).

Before the samples were sent away for analysis by microarrays it needed to be confirmed that the experiment showed the same results as those seen in previous work from this project (Chapters 3&4). As the longest time point of the experiment was 20 hours, Mog could not be used to confirm the experiment worked as it is measured at 3 days. Therefore, expression of Socs3 and Egr2 in the 1 hour samples were analysed by qPCR and these results compared to previous data from Chapter 4 (Fig 5.1). The patterns of expression observed support those seen in the previous work. Crucially, Socs3 expression was increased by LIF and EPO+LIF, suggesting again that it is a causative agent of the inhibition of EPO-induced myelination. Therefore these samples were suitable for the microarray analysis.

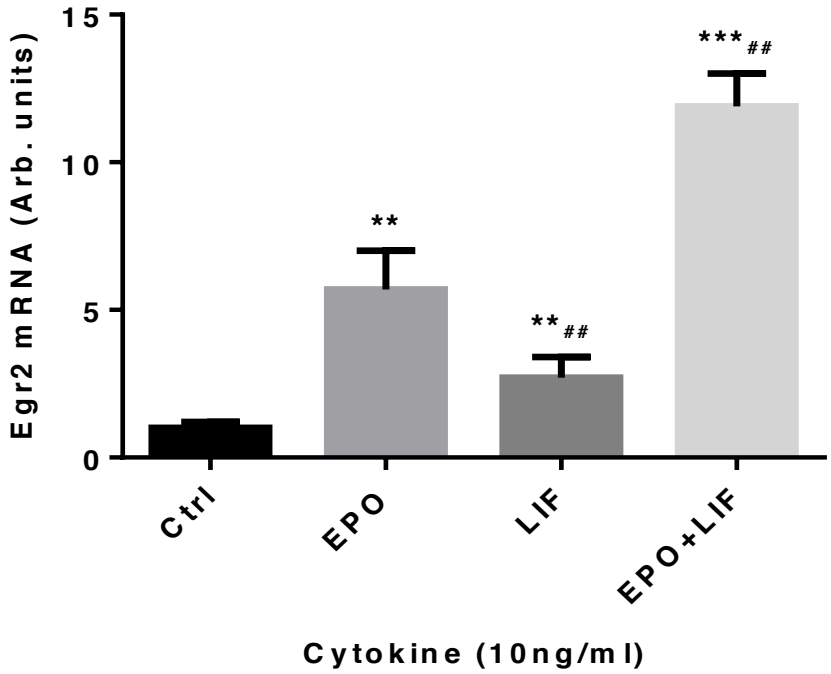

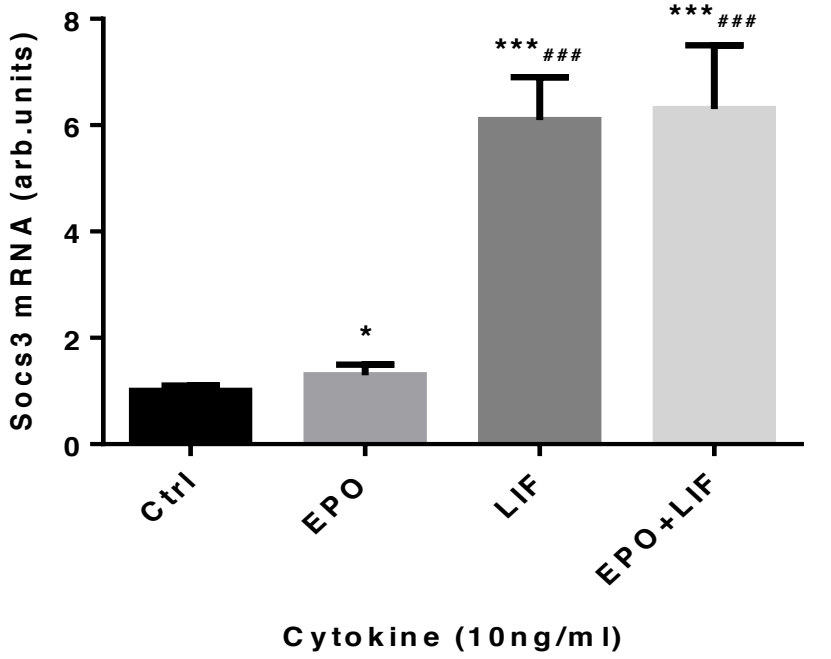

Figure 5.1: Egr2 and Socs3 induction in CG4 cell samples to be analysed by microarrays. CG4 cells were plated at a density of $35x10^4$ cells/well and differentiated for 3 hours before 10ng/ml LIF or EPO or both were added for one hour. Data represented here are the mean ± SD of quadruplicate samples. *P<0.05, ** P<0.01, *** P<0.001 versus the control & ##P<0.01, ###P<0.001 versus EPO alone by Students *t* test…

Figure 5.1 cont.:

Egr2 results:

			P value	
Cytokine (ng/ml)	**Egr2 Mean**	**SD**	**vs Ctrl**	**vs EPO**
Ctrl	1.0	0.2		
EPO	5.7	1.3	0.0006	
LIF	2.7	0.7	0.0030	0.0086
LIF+EPO	11.9	11	1.4881E-06	0.0011

Socs3 results:

			P value	
Cytokine (ng/ml)	**Socs3 Mean**	**SD**	**vs Ctrl**	**vs EPO**
Ctrl	1.0	0.1		
EPO	1.3	0.2	0.0487	
LIF	6.1	0.8	1.3101E-05	0.0002
LIF+EPO	6.3	1.2	0.0001	0.0010

5.3 Transcripts that are altered by differentiation

A group of undifferentiated samples that were not treated with cytokines were included in the gene expression microarray analysis. The inclusion of these samples allowed analysis of the genes that were altered by differentiation. The cells used for the undifferentiated samples were plated at the same time as the cells for the other samples but were not induced to differentiate and were not treated with either EPO or LIF. The experiment was stopped after culture for 48 hours and the total RNA was extracted. The undifferentiated samples were not considered to be at either time point because the time point measured time since the addition of the cytokines. As such they were only considered in analysis versus the control samples i.e. those that were differentiated but were not stimulated by cytokines.

There were 30367 transcripts analysed in the microarrays. Those that had no mapped EntrezGene IDs and those with no functional annotation were removed and 21575 transcripts remained. The fold change between each control sample at both time points versus the mean of the undifferentiated samples was calculated. The mean of the control fold changes was calculated and filtered for control versus undifferentiated at both time points separately with parameters for significance set at a fold change greater than or equal to 1.5 (Log_2 FC ±0.58) and $p<0.05$ by Student's *t* test. For the purpose of comparing the differentiated samples to the undifferentiated ones it should be noted that the early time point is 4 hours of differentiation and the second time point is 23 hours. The 1 hour and 20 hour time points throughout the rest of the analysis refer to those samples treated with cytokines, as these were the time points after cytokine addition. After the 4 hour samples were filtered for significance 2134 genes remained. After the same filter was applied to the 23 hours samples 3761 genes remained. More genes were altered at 23 hours than 1 hour when comparing the control to undifferentiated because the cells have had an extra 19 hours of differentiation that increased their maturity.

Filters were applied to both time points simultaneously, and 982 genes remained. Analysis was difficult with so many genes and the large number meant that a more conservative test needed to be applied. Therefore the p value was reduced to less than or equal to 0.01 by Students *t* test, a parameter which left 580 genes remaining.

By increasing the level of significance the chance of a false positive was also reduced, as only those within a 1% confidence interval were included. The significant genes were ordered for mean fold change at both time points separately and then ten most highly up- and downregulated at each time point are shown in Tables 5.1 and 5.2.

Firstly of note from the analysis presented in table 5.2 is that Mbp was the second most highly upregulated gene at 23 hours. In previous experiments Mbp expression was the same as Mog expression when induced by EPO and LIF (Section 3.4). Mbp is the second most abundant protein in the CNS myelin, after proteolipid protein, and is the only protein known to be essential for myelination (Readhead *et al.* 1990). Its gene expression as determined by our analysis as such a highly upregulated gene supports evidence for its role in maturation of OPCs.

The most highly upregulated gene at 4 hours was fatty acid deacetylase 6 (Fads6). While this gene has not been linked specifically to myelination, the enzymes that it codes for have been implicated in demyelinating diseases. The Fads family of genes is important in the development of cerebral white matter (Peters 2014).

Chemokine C-C motif (Ccl20) appeared among the most highly downregulated in both tables 5.2 and 5.3. It was the only gene to appear in both tables that may have a functional relation to oligodendrocytes. Ccl20 is a chemokine involved in immunity and inflammation. Neurodegenerative injury led to increased Ccl20 expression, and it was toxic to neurons and oligodendrocytes (Das *et al.* 2011, Leonardo 2012). The downregulation of Ccl20 in differentiated cells suggests that it reduced cell viability and supported the hypothesis that it is detrimental to oligodendrocyte development.

Hes5 was one of the most highly downregulated genes at 1 hour. It is downstream of the Notch pathway, which is crucial to oligodendrocyte development (Morrison *et al.* 2000). Notch is selectively downregulated in oligodendrocytes that begin myelinating and it is upregulated during demyelination (Woodhoo 2007, Aparicio *et al.* 2013). Furthermore, it is expressed in oligodendrocytes that fail to remyelinate in MS plaques (John 2002).

		1hr		20hrs	
Gene name	**Accession number**	**Average Log_2 FC**	**P value**	**Average Log_2 FC**	**P value**
Upregulated					
Fads6	NM_001107064	6.45	0.00002180	1.20	0.00528068
Crym	NM_053955	5.01	0.00052411	3.41	0.00359519
Rpe65	NM_053562	4.99	0.00000000	5.22	0.00000001
Shroom2	NM_001047893	4.54	0.00001449	3.46	0.00005107
Prr15	NM_001104527	4.44	0.00003671	3.57	0.00015374
Hs3st6	NM_001109450	4.37	0.00003525	1.27	0.00415522
Txnip	NM_001008767	3.54	0.00007228	5.83	0.00000678
Bmp4	NM_012827	3.53	0.00000053	2.50	0.00000383
Btbd17	NM_001134534	3.38	0.00028875	2.89	0.00066828
Kcnj12	NM_053981	3.18	0.00073958	3.09	0.00051745
Downregulated					
Skor2	XM_003751807	-2.32	0.00330278	-2.17	0.00436327
Trib3	NM_144755	-2.35	0.00001099	-2.88	0.00000092
Tfrc	NM_022712	-2.39	0.00037228	-1.70	0.00086615
Bdnf	NM_012513	-2.41	0.00001348	-1.94	0.00015074
Fam212b	NM_001107713	-2.66	0.00015119	-1.78	0.00030249
Hes5	NM_024383	-3.36	0.00015832	-2.60	0.00020626
Ccl20	NM_019233	-3.58	0.00005855	-2.72	0.00003949
Egr1	NM_012551	-3.69	0.00019517	-1.90	0.00279780
Spry4	NM_001106150	-4.59	0.00000022	-1.14	0.00014540
Samd9l	XM_001069386	-5.05	0.00000011	-1.35	0.00010806

Table 5.1: Genes differentially expressed in undifferentiated vs. differentiated samples at 4 hours. Genes were filtered for significant changes between the control and undifferentiated cells at both time points. Ordered for fold change at 4 hours and the most highly up- and downregulated are shown here. Significance was defined as a p value less than 0.05 and fold change greater than 1.5. P value was calculated using Students *t* test.

		1hr		20hrs	
Gene name	**Accession number**	**Average Log_2 FC**	**P value**	**Average Log_2 FC**	**P value**
Upregulated					
Txnip	NM_001008767	3.54	0.00007228	5.83	0.00000678
Mbp	NM_001025289	1.53	0.00014749	5.42	0.00000023
Ninj2	NM_021595	2.82	0.00000383	5.40	0.00000020
Rpe65	NM_053562	4.99	0.00000000	5.22	0.00000001
Sema5a	NM_001107659	1.49	0.00000548	4.61	0.00000002
Sim2	NM_001107108	2.98	0.00005752	4.48	0.00000927
Mid2	NM_001191889	1.63	0.00012772	3.83	0.00000262
P2ry12	NM_022800	1.23	0.00169351	3.65	0.00000900
Prr15	NM_001104527	4.44	0.00003671	3.57	0.00015374
Arrdc3	NM_001007797	1.67	0.00083525	3.54	0.00000581
Downregulated					
Ccl20	NM_019233	-3.58	0.00005855	-2.72	0.00003949
Acvr1c	NM_139090	-0.88	0.00726047	-2.86	0.00055348
Ldlrad4	NM_001271365	-1.03	0.00889526	-2.86	0.00005705
Trib3	NM_144755	-2.35	0.00001099	-2.88	0.00000092
Slc37a2	XM_006242809	-0.85	0.00033732	-2.89	0.00003887
Mdfic	NM_001105668	-0.88	0.00627783	-2.92	0.00003656
Tac1	NM_001124769	-1.34	0.00045308	-3.81	0.00002348
Gjb2	NM_001004099	-2.20	0.00004985	-4.54	0.00000187
Slc7a11	NM_001107673	-0.89	0.00040854	-4.69	0.00000078
Wdr16	NM_001100968	0.92	0.00008156	-4.72	0.00000035

Table 5.2: Genes differentially expressed in undifferentiated vs. differentiated samples at 23 hours. Genes were filtered for significant changes between the control and undifferentiated cells at both time points. Ordered for fold change at 23 hours and the most highly up- and downregulated are shown here. Significance was defined as a p value less than 0.05 and fold change greater than 1.5.

The genes significantly changed at both time points between undifferentiated versus control samples were analysed by hierarchical clustering. The fold change values of the control samples were expressed versus the mean of the undifferentiated samples. The heat map image that was produced showed that most genes behaved similarly between 4 hours and 23 hour analysis (Fig 5.2). The trend appeared to be that a stronger expression was observed at 23 hours than 4 hours, as in general the red or the green tiles were brighter on the right side of the heat map image. This signifies genes that are expressed from an early time point whose expression only increases with time. There were areas of the gene expression tiling of the image where the 4 hours panel showed the greater expression, perhaps indicating that those genes were induced strongly and very quickly but after initial induction their expression was not sustained. It must be noted that only genes that were altered at both time points were represented here, therefore any that were unaltered compared to undifferentiated levels were excluded.

At the top of the image however were two clusters that represented opposing effects at each time point (Fig 5.3). Cluster 1 represented genes that were upregulated at 4 hours but downregulated at 23 hours and cluster 2 showed genes whose expression was induced in the opposite effect. Included in these clusters were genes Vegfa, a growth factor that influences cell maturity and differentiation, although most of what is known is in endothelial cells (Hirashima 2009). ErbB2 also appeared which has potent effects on myelination of Schwann cells so may have a similar effect on oligodendrocytes (Basak 2015). Both of these genes were downregulated at 4 hours but upregulated at 23 hours.

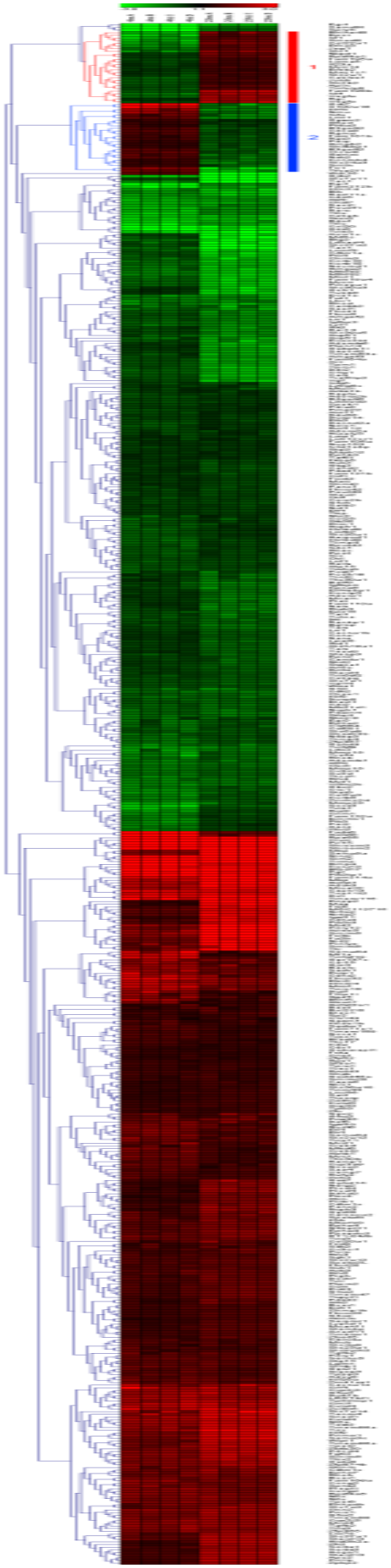

Figure 5.2: Genes changed by the control vs. undifferentiated samples at both time points. Hierarchical clustering and heat map of the differentially expressed transcripts identified by comparing control vs. undifferentiated at a threshold of 1.5 fold change (Log_2 FC±0.58) and P<0.01. Each sample represents the expression change compared to the mean Log_2 of undifferentiated. Red indicates an increase and green indicates a decrease in expression compared to controls. Average linkage clustering analysis was performed using Genesis software. The whole image is shown to give a full overview of the analysis. Individual clusters are shown later. Four columns of each treatment are biological replicates. The first four columns represent 4 hour samples and the final four the 23 hour analysis. Bars 1&2 indicate clusters of interest.

Original in colour

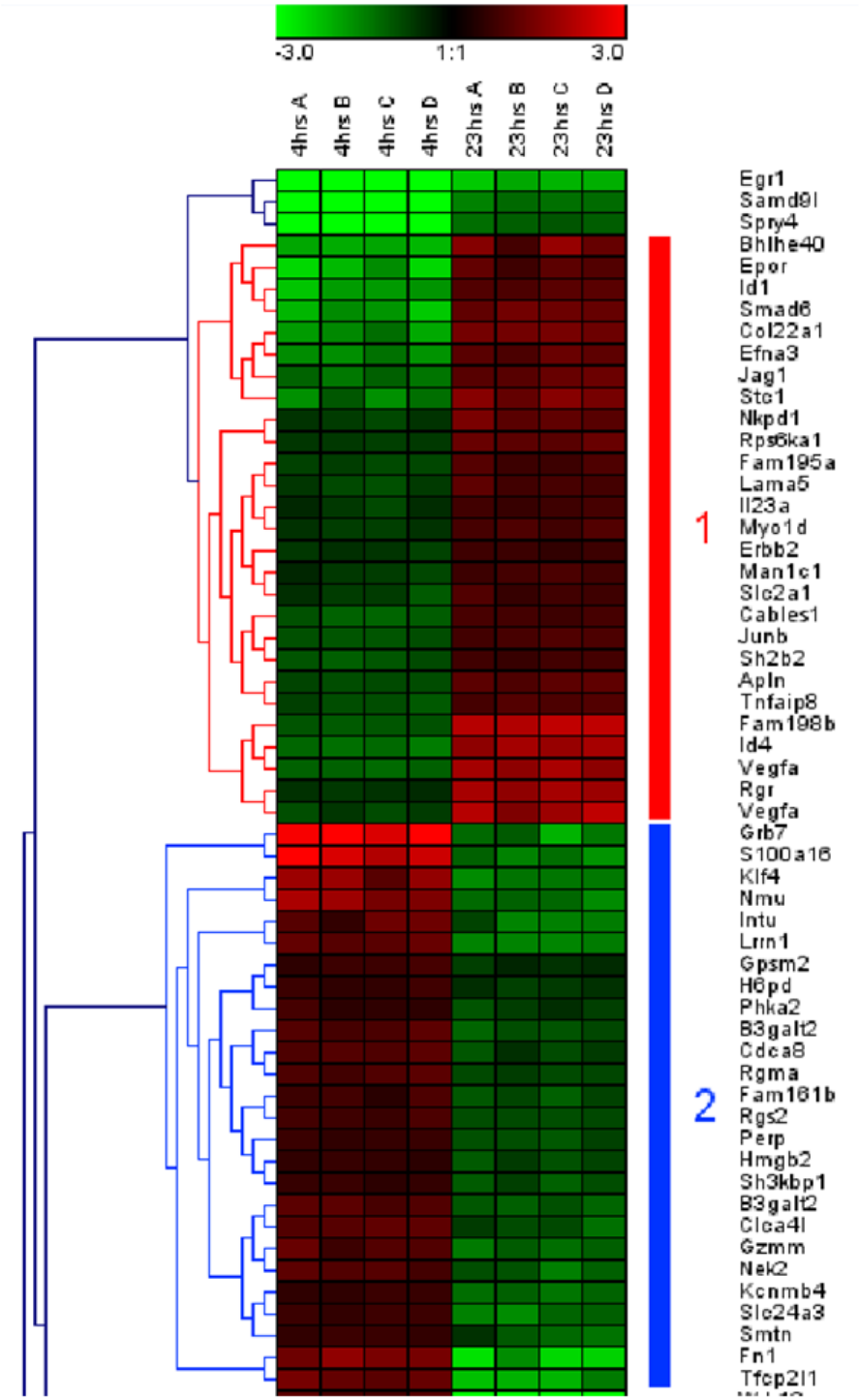

Figure 5.3: Genes changed by the control cells vs. undifferentiated samples at both time points. Clusters only. Hierarchical clustering and heat map of the differentially expressed transcripts identified by comparing the control vs. undifferentiated at a threshold of 1.5 fold change (Log_2 FC±0.58) and P<0.01. Each sample represents the expression change compared to the mean Log_2 of undifferentiated. Red indicates an increase and green indicates a decrease in expression compared to controls. Average linkage clustering analysis was performed using Genesis software. Two clusters of interest labelled as 1 &2. Four columns of each treatment are biological replicates.

Original in colour

5.4 Transcripts that are altered by differentiation and by EPO

The gene expression microarray analysis was also used to elucidate how EPO affected gene expression when it was used to stimulate CG4 OPCs. Previous experimental work presented in Chapter 3 of this thesis, and that carried out by Cervellini *et al* (2013), showed that EPO significantly increased expression of two myelin genes, Mog and Mbp, by differentiating CG4 cells (Cervellini *et al.* 2013a). Therefore, analysis of the genes significantly altered by EPO could provide crucial information about the mechanisms that mediate the EPO's promyelinating effect.

The same filters employed in Section 5.2 were applied so that only the transcripts significantly changed between the controls at both time points and the undifferentiated samples were present. Again, the parameters of significance were set at fold change greater than 1.5 (Log_2 FC±0.58) and a P value less than or equal to 0.01 as determined by the Students *t* test. In addition to being expressed as control versus undifferentiated, the same genes were also filtered for EPO versus control. This provided a comparison of how the addition of EPO affected these genes that were important in differentiation.

Hierarchical cluster analysis was performed on the genes that were significantly altered between control at both time points and undifferentiated samples, this time with the additional values for EPO versus control (Fig 5.4). The clusters on the right of the heat map image, controls versus undifferentiated, were not altered by the addition of the EPO-treated samples to the analysis. On the whole the clusters look the same including the two clusters near the top of the image where the genes were altered differently between the two time points. Furthermore, the right side of the image is mostly dark in colour intensity with very few tiles showing an increased or decreased expression. The conclusion to be drawn from this was that on the whole the genes that were altered during differentiation were not those that were altered during EPO-induced myelination.

However, there were a few small clusters in which genes were altered between differentiated and undifferentiated samples and were then altered in the same way by EPO compared to differentiated samples. One such gene was tumour necrosis factor

receptor super family (Tnfrsf)-9, also known as Cd137, which was downregulated at both conditions. Upregulation of this ligand in the CNS has been linked to oligodendrocyte apoptosis and mice knockout models for this gene showed reduced severity of EAE (Yeo *et al.* 2012). Another gene that was modulated in the same way between both conditions was myelin associated glycoprotein (Mag). The upregulation of Mag was important because it is a myelin gene and so its expression is related to the myelinating capacity of the cells. Its expression profile here demonstrated that the myelin produced by the cells increased upon differentiation and was further amplified upon stimulation with EPO, although this effect was only seen at 20 hours.

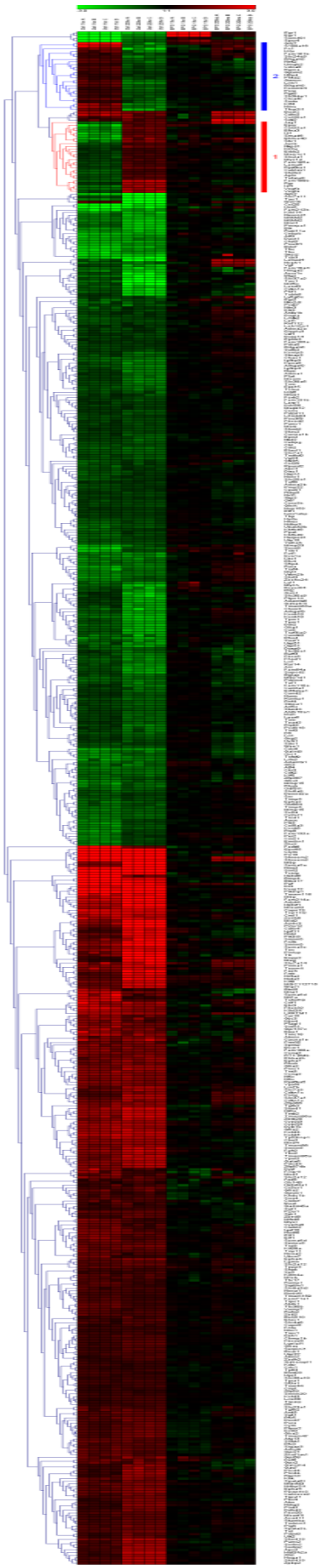

Figure 5.4: Genes changed by the control vs. undifferentiated samples at both time points plus the expression of these genes when the cells are treated with EPO expressed vs the control. Hierarchical clustering and heat map of the differentially expressed transcripts identified by comparing the control vs. undifferentiated at a threshold of 1.5 fold change (Log_2 FC±0.58) and P<0.01. Samples treated with EPO are also included; the values shown represent EPO vs the control. Each sample represents the expression change compared to the mean Log_2 of undifferentiated or the control. Red indicates an increase and green indicates a decrease in expression compared to the controls. Average linkage clustering analysis was performed using Genesis software. The whole image is shown to give a full overview of the analysis. Four columns of each treatment are biological replicates. The conditions are; Ctrl 1hr, ctrl 20hrs, EPO 1hr, and EPO 20hrs. Bars 1&2 indicate clusters of interest.

Original in colour

5.5 Transcripts that are altered by the addition of EPO

Section 5.4 looked at the effect that EPO had on only those genes that were altered during differentiation. One of the further aims of the gene expression microarray analysis was to determine the effect of EPO on all genes to study the mechanism behind the promyelinating effect of EPO. It was important to investigate the effects of EPO at both time points, and the comparison between the two time points, to ascertain any patterns of gene expression that were consistent for the duration of the experiment. Initially, the transcripts were sorted for EPO versus control with parameters for significance set at fold change greater than or equal to 1.5 ($Log_2FC \pm 0.58$) and P value less than or equal to 0.05 by Student's *t*-test and these filters applied to both time points. Only 12 transcripts remained after these two filters, all of which are represented in Table 5.3 with their average FC values and P values. The low number of genes that had significant P values across both time points suggests that it was not the same genes initiating myelination as those sustaining it.

The most highly upregulated gene was H19, which is a non-coding RNA that is linked closely to development (Gabory *et al.* 2010). The significant upregulation of H19 by EPO at 20 hours could demonstrate that EPO induced a pro-developmental genotype, which could lead to the increase in myelination. Peripheral myelin protein 2 (Pmp2) appeared as the second most highly upregulated gene in the table. Pmp2 is a myelin gene and although it is primarily known for myelination in the PNS (Zenker *et al.* 2014), it is expressed in the CNS (Gould *et al.* 2008) and the presence of it so highly upregulated by EPO represented the potent pro-myelinating effects of EPO.

The expression of these genes in differentiated versus undifferentiated sample analysis was investigated to determine if any genes were consistently changed across both sets of analyses. Those genes changed in both analyses would be important in both the differentiation of the cells and the myelinating effect of EPO. Again, Pmp2 was present throughout both time points, highlighting its importance in developing a pro-myelinating phenotype.

The time points were also considered separately. The same parameters were applied to the individual time points. At 1 hour 159 genes were significantly different and at 20 hours 617 genes were significantly changed by EPO. The genes were filtered for fold change and the ten most highly up- and downregulated genes for each time point are shown in Tables 5.4 & 5.5.

Cd36 was one of the most highly upregulated genes at 20 hours. It is important in cellular differentiation and so could explain how EPO increased the myelinating capacity of the CG4 cells (Christiaens *et al.* 2012). Therefore, qPCR was performed on the samples used in the microarrays to confirm the expression seen. The validation was successful as the large upregulation of Cd36 seen in cells treated with EPO seen in the microarrays was replicated in the qPCR validation (Fig 5.5).

		1hr		20hrs	
Gene name	**Accession number**	**Average Log_2 FC**	**P.value**	**Average Log_2 FC**	**P.value**
H19	NR_027324	2.43	0.00000518	12.53	0.00000024
Pmp2	NM_001109514	0.86	0.00711807	5.29	0.00000058
Arl4a	NM_019186	0.91	0.00000791	1.85	0.00000004
Cish	NM_031804	0.83	0.02744074	1.75	0.00000273
Ccdc166	NM_001163519	-0.75	0.02514777	0.92	0.00863588
Fos	NM_022197	1.91	0.00000507	0.90	0.00001360
Ovch2	XM_003748959	-0.82	0.01749556	0.87	0.01979570
Irx2	NM_001039505	0.73	0.00801204	0.83	0.00151167
Spry4	NM_001106150	1.27	0.00145496	0.77	0.00006127
Fam222a	NM_001109067	-0.75	0.00666498	0.59	0.04166606
Olr841	NM_001000405	-0.69	0.02647437	-1.32	0.03298333
Bcl6	NM_001107084	-0.60	0.00153975	-1.34	0.00000001

Table 5.3: Genes differentially expressed in EPO-treated vs the control samples at both time points. Genes were filtered for significant changes between EPO and the control treatments at both time points. Significance was defined as a P value less than or equal to 0.05 and fold change greater than 1.5.

		1hr		20hrs	
Gene name	**Accession number**	**Average Log_2 FC**	**P value**	**Average Log_2 FC**	**P value**
Upregulated					
Egr1	NM_012551	4.60	0.00000056	0.48	0.00578004
H19	NR_027324	2.43	0.00000518	12.53	0.00000024
Hoxc6	XM_006226279	2.00	0.00175606	0.07	0.54237074
Fos	NM_022197	1.91	0.00000507	0.90	0.00001360
Pstpip1	NM_001106824	1.43	0.03506725	0.09	0.72003330
Vsig8	NM_001105972	1.29	0.00062659	0.05	0.65808805
Spry4	NM_001106150	1.27	0.00145496	0.77	0.00006127
Wfdc3	NM_001106541	1.08	0.00303977	-0.30	0.40864902
Ptpn22	NM_001106460	1.06	0.01714175	0.04	0.75196221
Has2	NM_013153	1.03	0.00048971	-0.49	0.02806679
Downregulated					
Usp17l5	XM_219062	-1.11	0.00280315	0.52	0.14905731
Olr1678	NM_001000893	-1.11	0.04172825	0.05	0.59491368
Olr813	NM_001000846	-1.16	0.04339875	-0.37	0.10163985
Cldn7	NM_031702	-1.25	0.03816708	0.05	0.62358439
Sptb	NM_212522	-1.26	0.00028376	1.04	0.26304015
Tchh	XM_006224200	-1.26	0.00269190	0.19	0.45776918
Cntnap2	XM_006236412	-1.26	0.02828578	0.04	0.75580201
Krtap8-1	XM_002724689	-1.31	0.00347626	0.04	0.76468505
Tmem119	NM_001107155	-1.37	0.00347876	-0.03	0.90302842
Gpx3	NM_022525	-1.41	0.01333592	0.08	0.80757283

Table 5.4: The most highly up- and downregulated genes between cells treated with EPO vs. the control at 1 hour. Genes were filtered for significant changes between EPO and the control treatments. Significance was defined as a P value less than 0.05 and fold change greater than 1.5. The corresponding values for the genes at 20 hours, again EPO vs ctrl, are also shown.

		1hr		20hrs	
Gene name	**Accession number**	**Average Log_2 FC**	**P value**	**Average Log_2 FC**	**P value**
Upregulated					
H19	NR_027324	2.43	0.00000518	12.53	0.00000024
Cd36	NM_031561	-0.07	0.50432600	5.92	0.00000004
Pmp2	NM_001109514	0.86	0.00711807	5.29	0.00000058
Htr2c	NM_012765	-0.07	0.49929561	5.14	0.00000000
Tnfrsf11a	NM_001271235	0.54	0.05497056	4.37	0.00000000
Ptpre	NM_053767	-0.31	0.18143596	4.01	0.00000033
Mrvi1	NM_001105210	-0.09	0.38085052	3.96	0.00000788
Igf2	NM_178866	-0.22	0.04840662	3.68	0.00000006
Trpc4	NM_080396	-0.29	0.11010510	3.42	0.00000085
Angpt1	NM_053546	-0.01	0.97020816	3.41	0.00000298
Downregulated					
Mtnr1b	NM_001100641	-0.20	0.48074189	-1.07	0.03269191
Crb2	NM_001135761	-0.12	0.68727106	-1.07	0.00118175
Hist2h2ab	NM_001111341	-0.19	0.22948236	-1.07	0.00811987
Npy	NM_012614	-0.03	0.72601068	-1.11	0.00010454
Btnl7	NM_212488	-0.13	0.61080050	-1.13	0.00080593
Rpl10l	XM_003750173	-0.61	0.17480689	-1.20	0.03785364
Slco1a2	NM_131906	-0.18	0.42477322	-1.22	0.00575591
Olr841	NM_001000405	-0.69	0.02647437	-1.32	0.03298333
Bcl6	NM_001107084	-0.60	0.00153975	-1.34	0.00000001
Cryab	NM_012935	0.03	0.88450361	-1.54	0.00000481

Table 5.5: The most highly up- and downregulated genes between cells treated with EPO vs. the control at 20 hours. Genes were filtered for significant changes between EPO and the control treatments. Significance was defined as a P value less than 0.05 and fold change greater than 1.5. The corresponding values for the genes at 1 hour, again expressed as EPO vs ctrl, are also shown.

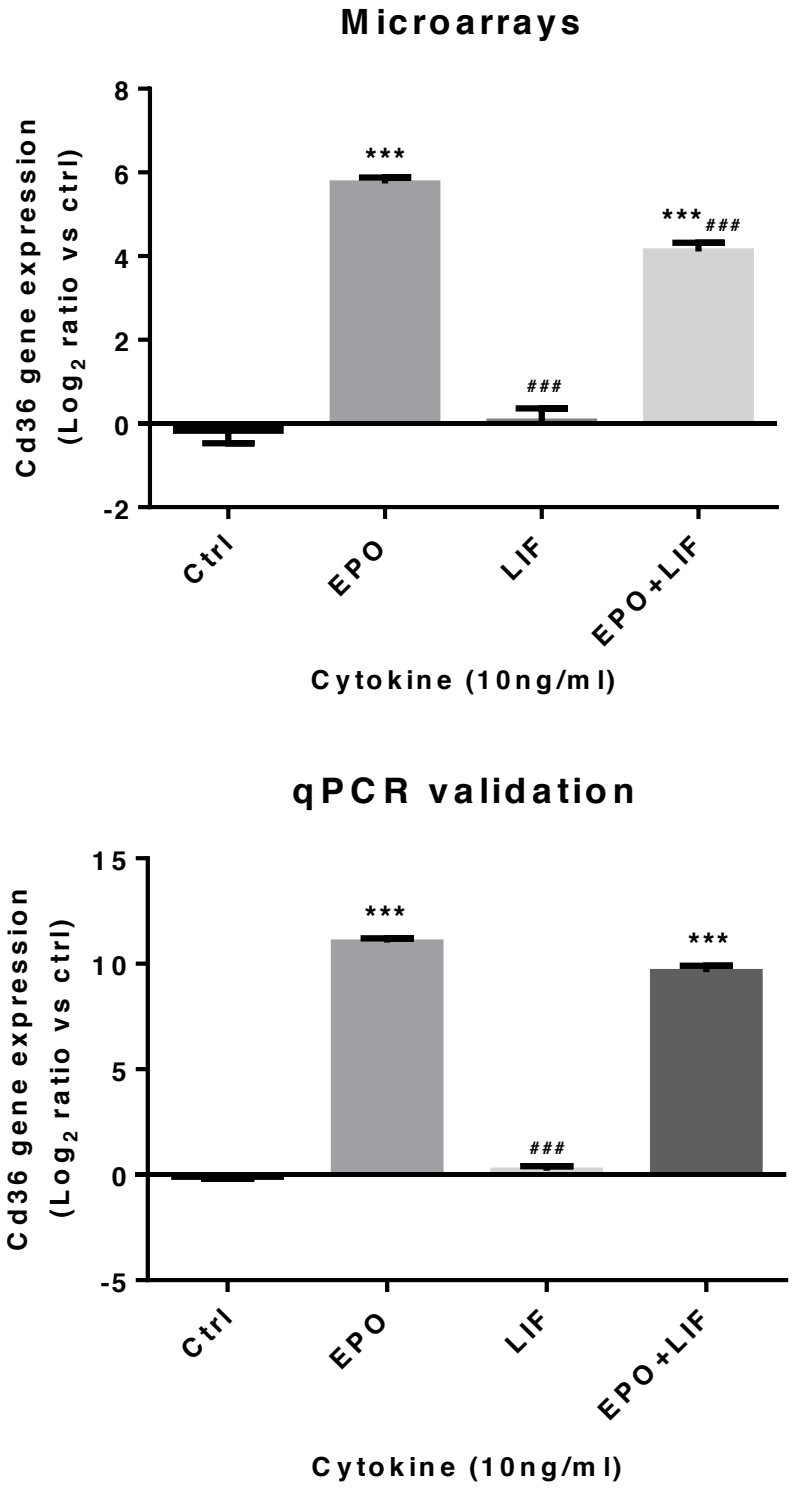

Figure 5.5: qPCR validation of the microarray data; CD36. Each graph compares the mean Log_2 FC of each gene after the specified cytokine treatment (10ng/ml) versus the control sample "B"±SD performed in quadruplicate. RT and qPCR were performed on the same samples as those used in the microarray. **P<0.01, ***P<0.001 vs ctrl & #P<0.05 ###P<0.001 vs EPO alone…

Figure 5.5 cont.:

Microarray results:

			P value	
Cytokine (ng/ml)	**CD36 Mean**	**SD**	**vs Ctrl**	**vs EPO**
Ctrl	-0.2	0.3		
EPO	5.7	0.1	3.65E-08	
LIF	0.05	0.3	0.4833	3.57E-06
LIF+EPO	4.1	0.2	8.68E-07	1.59E-05

qPCR validation results:

			P value	
Cytokine (ng/ml)	**CD36 Mean**	**SD**	**vs Ctrl**	**vs EPO**
Ctrl	-0.1	-0.1		
EPO	11.0	11.0	7.06E-11	
LIF	0.2	0.2	0.0188	1.52E-10
LIF+EPO	9.6	0.3	0.0001	0.00012

A direct comparison was needed to analyse the effect on genes between time points. To do this the parameters for significance were applied individually, but when the genes were analysed by hierarchical clustering the corresponding values at both time points were represented. This allowed visualisation of the effect of EPO treatment between one time point, where the change was significant, and the other time point, regardless of significance (Fig 5.6). At both time points very little occurred at the time point that was not filtered for, as little green or red was visible from that side of the heat map cluster analysis. Again this showed that it was not the same genes that induced an early increase in myelination as those that maintain its increase for the long term.

Igf1 codes for a member of the IGF protein family that is involved in growth and differentiation. It is known that IGF1 plays an important role in oligodendrocyte development and myelin formation (McMorris 1988, Beck 1995, Shinar 1995) and is protective to oligodendrocytes in models of cerebral injury (Lin *et al.* 2005, Pang *et al.* 2007). In Schwann cells, Igf1 downregulation is one of the key mechanisms through which demyelination occurs (Hao 2015). Igf1 appeared in image B (Fig 5.6) approximately half way down, and was the 14th most highly-upregulated gene by EPO versus control at 20 hours. Therefore, it was decided to validate it to confirm that the expression seen in the microarrays corresponded with its expression profile by qPCR. The validation was successful as it reflected the large increase in Igf1 induced by the addition of EPO (Fig 5.7).

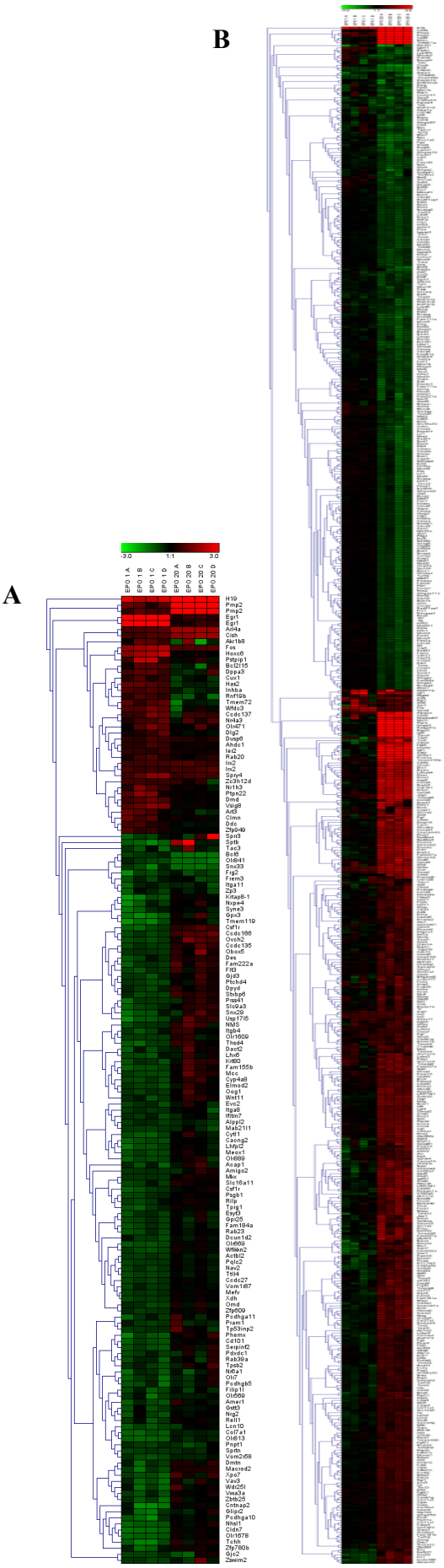

Figure 5.6: Genes changed by EPO vs the control samples at both time points. Hierarchical clustering and heat map of the differentially expressed transcripts identified by comparing EPO vs. the control at a threshold of 1.5 fold change (Log_2 FC±0.58) and P<0.05. Each sample represents the expression change compared to the mean Log_2 of the control. Red indicates an increase and green indicates a decrease in expression compared to the controls. Average linkage clustering analysis was performed using Genesis software. Panel A is filtered for EPO vs the control at 1 hour with the expression levels at 20 hours also shown and panel B is filtered for EPO vs the control at 20 hours with the expression levels at 1 hour also shown. Four columns of each treatment are biological replicates. The whole image is shown to give a full overview of the analysis.

Original in colour

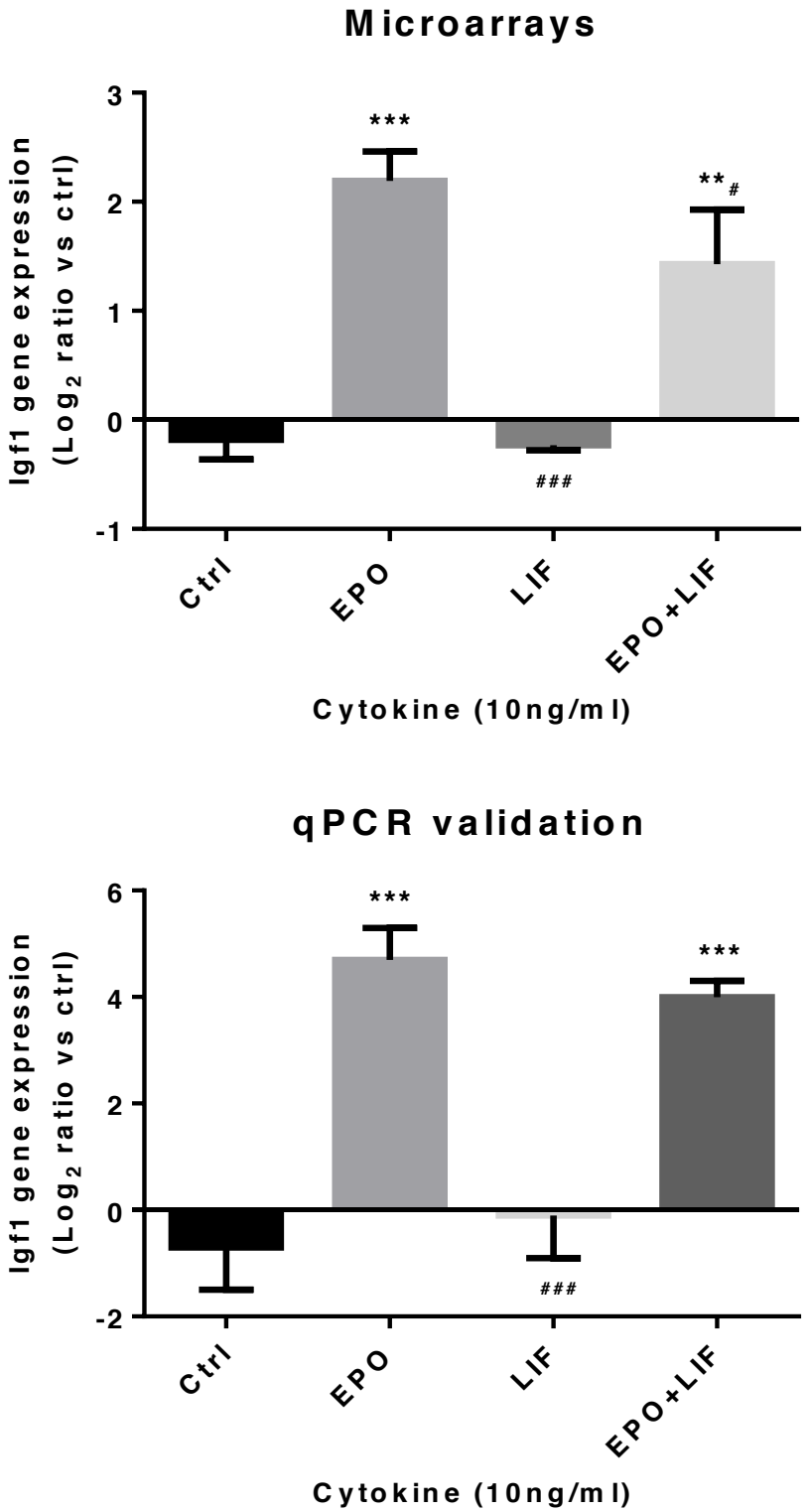

Figure 5.7: qPCR validation of the microarray data; Igf1. Each graph compares the mean Log_2 FC of each gene after the specified cytokine treatment (10ng/ml) versus the control sample "B"±SD performed in quadruplicate. RT and qPCR were performed on the same samples as those used in the microarray. **P<0.01, ***P<0.001 vs ctrl & #P<0.05 ###P<0.001 vs EPO alone.

Figure 5.7 cont.:

Microarray results:

			P value	
Cytokine (ng/ml)	**Igf1 Mean**	**SD**	**vs Ctrl**	**vs EPO**
Ctrl	-0.19	0.19		
EPO	2.19	0.27	3.03E-05	
LIF	-0.24	0.05	0.3598	6.72E-06
LIF+EPO	1.44	0.50	0.0045	0.0399

qPCR validation results:

			P value	
Cytokine (ng/ml)	**Igf1 Mean**	**SD**	**vs Ctrl**	**vs EPO**
Ctrl	-0.7	0.8		
EPO	4.7	0.6	0.0001	
LIF	-0.1	0.8	0.3663	9.14E-05
LIF+EPO	4.0	0.3	8.87E-05	0.1067

5.6 Conclusion

- Expression of Egr2 and Socs3 in the microarray analysis corresponded with results obtained previously in this thesis (Sections 4.3 and 4.6)
- Genes that are important in CG4 cell differentiation were identified
- Genes that are important in increasing myelination were identified

Microarray analysis was carried out to determine the genetic profile behind a differentiating and pro-myelinating phenotype of CG4 OPC cells. Gene expression microarray analysis technology was used for this project to expand on previous results. In preliminary experiments I had investigated the role of Egr2, induced by EPO at high levels in these cells (Cervellini *et al.* 2013a) and of Socs3 which is induced by LIF. These are well known pathways. Therefore, microarrays were used to identify genes and mechanisms that had not previously been associated with this work. The large quantity of transcripts measured in the microarrays provided a broad spectrum of data that would be impossible to replicate by other techniques.

Initial analysis of the microarrays looked at the difference between the cells that had been induced to differentiate and those that had not. The genes expressed in this analysis provided information into the maturation process of oligodendrocytes from their precursor state. From ordering genes so that those with the largest fold changes were represented at both time points Ccl20 was identified as a gene that was dramatically downregulated at both time points. Ccl20 is a chemokine that is neurotoxic after neurodegeneration (Das *et al.* 2011, Leonardo 2012). Its significant downregulation by differentiating oligodendrocytes supported the hypothesis that it was detrimental to oligodendrocyte development and showed that it could potentially exacerbate neurological insult by preventing the replenishment of the number of mature oligodendrocytes.

Hierarchical cluster analysis was used to investigate the differentiated cells at both time points versus undifferentiated cells. The output showed that for most of the genes the expression, either up- or downregulated, was consistent across the time points. Furthermore, the expression seemed to be stronger at 20 hours, suggesting that the effect was amplified as maturation continued (Fig 5.2). This suggested that

maintaining expression of pro-myelinating signals was more important to the final development of mature oligodendrocytes than early, but unsustained expression.

Hierarchical cluster analysis was used to compare the expression of the genes altered by differentiation to the expression of the same genes by the addition of EPO. The tiles representing the expression induced by EPO showed very little in this analysis suggesting that it is not the genes that are altered by differentiation providing the pro-myelinating effect of EPO.

The effect of EPO on these cells was then investigated without first filtering for gene expression significantly changed by differentiation. There were only 12 genes that were altered significantly by EPO treatment versus control at both 1 hour and 20 hours showing that, for myelination, maintaining expression of genes expressed early is not as important as it was for differentiation. Instead, the positive effect of EPO on myelination seemed to result from an induction of genes at later time points than early ones as there were more genes remaining after filtering at 20 hours than 1 hour.

From hierarchical cluster analysis of the genes that were significantly changed between EPO and control at each individual time point, it was clear that at 1 hour more gene regulation involved suppression of anti-myelinating genes than upregulation of pro-myelinating ones. However, at 20 hours the expression of these genes is more even suggesting a balance between upregulating pro-myelinating signals and downregulating anti-myelinating signals (Fig 5.6). H19, Pmp2 and Cd36 were identified as genes that may be involved in the promyelinating effect of EPO.

In the next chapter, the microarray analysis was used to investigate the causes of inhibition of EPO-induced Mog by the addition of LIF. To do this, the gene expression of samples treated with EPO+LIF were compared to those treated by EPO alone. Filtering for the genes altered significantly between these two treatments elucidated genes that were induced in conditions where Mog was inhibited, and thus allowed identification of mechanisms that decrease the myelinating capacity of these oligodendrocytes.

Chapter 6. Gene expression microarray analysis of inhibition of EPO-induced Mog by LIF

6.1 Introduction

LIF is a potent pro-myelinating cytokine within the CNS. However, LIF inhibited EPO-induced Mog when both cytokines were added simultaneously, reducing the promyelinating effect of EPO. Microarray analysis was used to determine any changes in gene expression that may be involved in LIF-induced inhibition of Mog and other myelin genes.

To initiate signalling, LIF binds to a complex of the LIFR and GP130, a common signalling component used by every member of the IL-6 cytokine family. Binding initiates tyrosine phosphorylation of the receptors which in turn results in the phosphorylation of JAKs 1, 2, and TYK2, which are present on both receptors, which leads to a variety of downstream signalling events.

The most important signalling pathway initiated by LIF is the STAT pathway, with STAT3 being the most important of the seven STATs known to be involved in LIF signalling. STATs, which are always present in the cytoplasm, bind to the cytokine receptors through their Sh2 domain, a mechanism that is only possible after receptor phosphorylation. After phosphorylation, the STATs dimerise and translocate to the nucleus, where they induce Socs3. Socs3 contains a Sh2 domain that competes to bind to JAK2 and thus prevents further STAT3 phosphorylation (Section 1.1.2) (Babon 2014). Previous work, described in Chapter 4, implicated Socs3 in the inhibition of EPO-induced Mog by LIF, as increased Socs3 expression correlated with decreased Mog induction.

LIF also induces the PI3K signalling cascade. The PI3k enzyme modifies certain phosphatidylinositides so that protein kinase B/Akt is recruited to the plasma membrane. Substrates of Akt include Bcl-2/Bcl-X_L-antagonist, causing cell death, the phosphorylation of which leads to increased cell survival and growth. The PI3k pathway is crucial for survival responses to cytokine stimulation (Alonzi 2001).

The SHP2 domain on the LIFR is responsible directly for initiation of MAPK cascades, including the ERK/Egr pathway. Similarly to STATs, activation of these pathways involves recruitment of signalling components to the activated LIFR, in this case Ras/Raf signalling leads to MAPK signalling. Interestingly, while LIF induces MAPK, STAT3, and PI3k, in embryonic stem cells, the latter two pathways are responsible for maintaining pluripotency while MAPK has the opposite effect. However, the outcome of LIF stimulation on these cells is preserving pluripotency, suggesting that MAPK is subservient to the other two pathways (Section 1.1.2) (Burdon *et al.* 1999, Meloche 2004).

Gene expression analysis was carried out using microarrays on cells treated with EPO, LIF, and both cytokines simultaneously in order to examine the genes whose expression was induced by each cytokine and the interactions that may happen between these genes. Filtering strategies and gene association software such as hierarchical cluster analysis and the STRING database were used to analyse the gene expression arrays and to elucidate connections and interactions between the genes.

When CG4 cells were treated with EPO there was an eight-fold increase in Mog expression and when they were treated with LIF there was a minor increase in Mog expression at a concentration of 0.2ng/ml but no increase at a high concentration of 10ng/ml. When both cytokines were added simultaneously LIF inhibited EPOs positive effect as there was a significant decrease in Mog expression compared to EPO treatment alone. The purpose of the gene expression microarray analysis was to determine other mechanisms that may be involved in inhibiting Mog expression. To do this the genetic regulation of CG4 cells after stimulation with EPO, LIF, and both cytokines together was investigated. By looking at which genes were expressed differently by cells treated with both EPO and LIF than those treated with only EPO the genes that are differentially expressed between the treatments were elucidated and their involvement in the inhibition of EPO-induced Mog could be hypothesised. Furthermore, two time points were analysed; 1 hour and 20 hours after treatment with EPO and LIF. This allowed investigations into early induced genes at 1 hour and later induced genes at 20 hours and comparisons between genes that are altered

between the two time points. This chapter will look at the two time points separately. The results found by microarrays were validated by qPCR.

6.2 Analysis of genes altered after cytokine treatment for 1 hour

6.2.1 Transcripts altered by EPO and by EPO+LIF treatment

30367 transcripts were analysed by microarrays. After the probes with no mapped EntrezGene IDs and those with no functional annotation were removed 21575 transcripts remained. Initial parameters used to indicate significance were a P value less than 0.05 determined by a Student's *t*-test and a fold change greater than 1.5. Initially transcripts that were significantly different between EPO and the control were filtered and 159 genes remained. Secondly, these 159 genes were filtered for those that were significantly different between the EPO+LIF group and the EPO only group, using the same parameters, with 45 genes remaining.

The 45 remaining significant genes were clustered using hierarchical clustering software. This software uses hierarchical clustering analysis to determine clusters of genes with similar expression patterns (Fig 6.1). Two clusters were identified in these analyses that have some significance to this investigation. Cluster 1 revealed genes that were upregulated by EPO but expression returned to the control level when treated with EPO+LIF. These could be genes whose activation was important in myelination but that are then inhibited by the presence of LIF. Homeobox C6 (Hoxc6) has been linked to Schwann cell differentiation and so could potentially link to maturation and the myelinating capacity of oligodendrocytes too (Zhang *et al.* 2007).

Cluster 2 revealed genes that were downregulated by EPO but did not differ from the control when the cells were treated with EPO+LIF. These could be genes that inhibited myelination as their expression was decreased by EPO alone but upregulated by the presence of LIF, when myelination was decreased. Other genes of interest that are significantly changed both by EPO versus the control and EPO+LIF versus EPO are Egr1 and Fos that appeared at the top of the image. These were

significantly upregulated by EPO, confirming previous results obtained in a rat model of cerebral ischaemia (Mengozzi 2012).

It was noteworthy that Socs3 was not present after both of these filters had been applied. In the previous work in this project a clear link was seen between Socs3 induction and a reduction in myelination. Therefore, it was expected that Socs3 would be important to the microarray analysis. However, because the first filter applied in this analysis meant that only genes significantly different between EPO and the control were present, and because Socs3 was not induced significantly by EPO (Section 4.6, Figure 4.6), Socs3 did not appear in this initial analysis, suggesting that in order to properly understand the gene expression patterns induced by LIF treatment, genes that are not significantly different between EPO and the control also needed to be included.

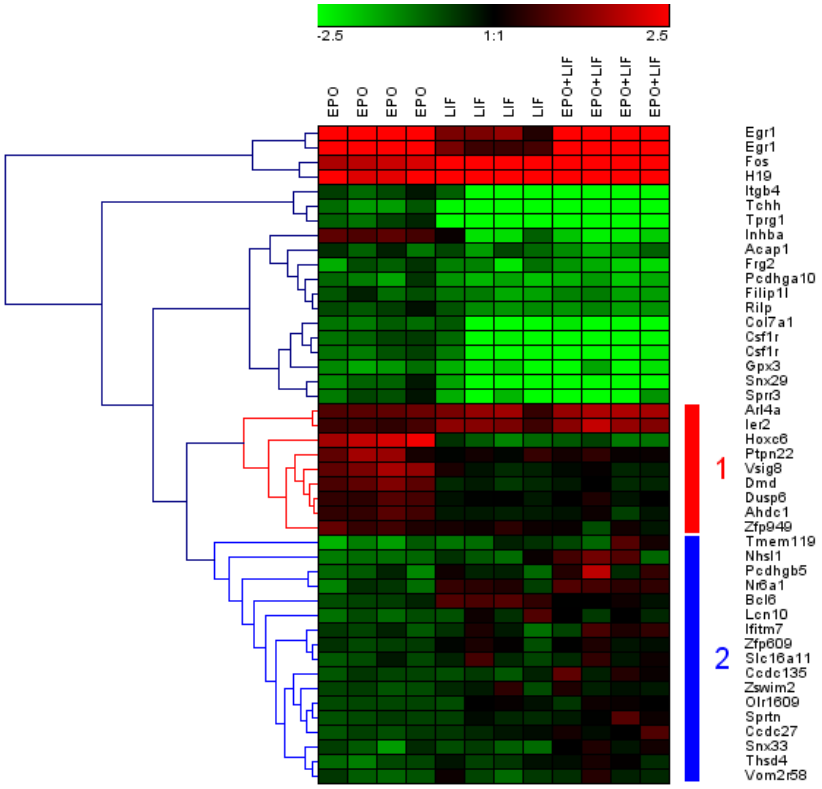

Figure 6.1: Genes changed by EPO vs control samples and EPO+LIF vs EPO at 1 hour. Hierarchical clustering and heat map of the differentially expressed transcripts identified by comparing EPO vs. the control and then EPO+LIF vs. EPO at a threshold of 1.5 fold change (Log_2 FC±0.58) and $P<0.05$. Expression changes in LIF treated samples vs. the control are also shown. Each sample represents the expression change compared to the mean Log_2 of the control. Red indicates an increase and green indicates a decrease in expression compared to the controls. Average linkage clustering analysis was performed using Genesis software. Bars 1&2 represent clusters. Four columns of each treatment are biological replicates.

Original in colour

6.2.2 Transcripts altered by treatment with EPO+LIF compared to EPO alone

Genes that were altered by EPO+LIF versus EPO were explored, regardless of whether they were significantly changed between EPO and the control. Therefore, genes whose only effect was an inhibition of myelination would still be present in the analysis. Filtering thus would allow investigation into those genes that may have been involved in the inhibitory effect of LIF on EPO-induced Mog.

The 21575 transcripts from the data set were filtered to leave only those significantly different between the samples treated with EPO+LIF and those treated with EPO alone. The parameters of a fold change greater than 1.5 and P value less than 0.05 by Student's *t*-test were used again, after which 632 transcripts remained. These genes were ordered by fold change between EPO+LIF and EPO and the ten most highly upregulated and the 10 most highly downregulated are shown in table 6.2.

JunB and Fos appeared among the most highly upregulated. While the Jun proteins are known to have positive effects on Schwann cells, their effects in the CNS are less clear with evidence of a correlation between c-Jun induction and apoptosis in oligodendrocytes (Ladiwala 1998). Here they were considerably upregulated by treatment with EPO+LIF compared to EPO alone, suggesting that they induced a significant inhibitory effect.

It was decided to validate both Fos and JunB as they appeared so highly upregulated in this analysis. Furthermore, they form a heterodimer to produce the transcription factor activator protein 1(AP-1), a complex that has been implicated in myelin gene expression (Dobretsova *et al.* 2004). Validation by qPCR was performed on the same samples that had been used for microarray analysis. The validation was successful for both Fos and JunB genes as the results from the qPCR validation reflected those for the microarrays (Fig 6.2 and 6.3).

		EPO vs Ctrl		EPO+LIF vs EPO	
Gene name	**Accession Number**	**Average Log_2 FC**	**P.value**	**Average Log_2 FC**	**P.value**
Upregulated					
Gpx2	NM_183403	-1.27	0.90475438	5.04	0.00000004
Bcl3	NM_001109422	-1.81	0.00845620	4.83	0.00000000
H19	NR_027324	-3.20	0.00000518	4.16	0.00000090
Atf3	NM_012912	-0.83	0.15629416	3.20	0.00000000
Trib1	NM_023985	-1.29	0.15653837	3.12	0.00000835
Reg3b	NM_053289	-0.37	0.36307107	3.11	0.00000255
JunB	NM_021836	-1.32	0.00427060	3.02	0.00000357
Fos	NM_022197	-1.92	0.00000507	2.89	0.00000109
Bhlhe40	NM_053328	-2.97	0.88340288	2.84	0.00001004
Arid5a	NM_001034934	-0.97	0.14387640	2.77	0.00000003
Downregulated					
Itgb4	NM_013180	4.65	0.04297722	-5.14	0.00000038
Try10	NM_001004097	3.85	0.44264247	-5.15	0.00000064
Spink5	NM_001170606	5.89	0.04848904	-5.96	0.00000003
Fads6	NM_001107064	4.79	0.24102092	-6.08	0.00000339
Col17a1	NM_001106366	6.02	0.14983697	-6.16	0.00000002
S100a6	NM_053485	6.47	0.87984925	-6.40	0.00000002
Hspb1	NM_031970	6.53	0.13518615	-6.69	0.00000001
Lor	XM_001057506	6.62	0.29951528	-6.85	0.00000001
Krt10	NM_001008804	7.99	0.31945128	-8.07	0.00000005
Krt17	NM_212545	8.39	0.16122838	-8.53	0.00000001

Table 6.1: Genes differentially expressed in cells treated with EPO+LIF vs. EPO alone at 1 hour. Genes were cut for significant changes between EPO+LIF and EPO. Significance was defined as a p.value less than 0.05 and fold change greater than 1.5. P.value calculated using Students *t* test.

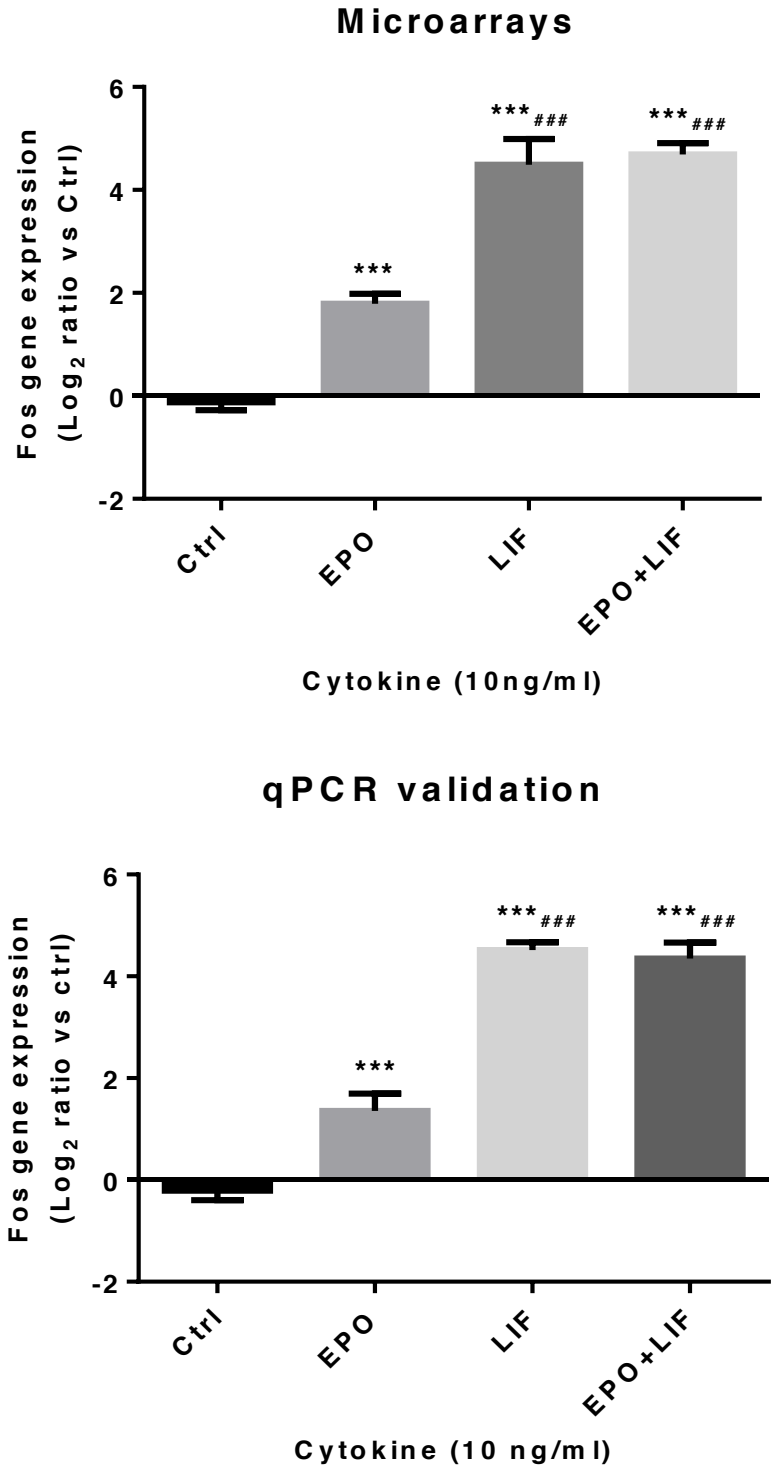

Figure 6.2: qPCR validation of the microarray data; Fos. Each graph compares the mean Log_2 FC of Fos after the specified cytokine treatment (10ng/ml) versus 1 control sample ±SD performed in quadruplicate. RT and qPCR were performed on the same samples as those used in the microarrays. **P<0.01, ***P<0.001 vs ctrl & ###P<0.001 vs EPO alone…

Figure 6.2 cont.:

Microarray results:

			P value	
Cytokine (ng/ml)	**Fos Mean**	**SD**	**vs Ctrl**	**vs EPO**
Ctrl	-0.1	0.2		
EPO	1.8	0.2	5.07E-06	
LIF	4.5	0.5	2.21E-06	5.49E-05
LIF+EPO	4.7	0.2	3.71E-08	1.09E-06

qPCR validation results:

			P value	
Cytokine (ng/ml)	**Fos Mean**	**SD**	**vs Ctrl**	**vs EPO**
Ctrl	-0.2	0.2		
EPO	1.4	0.3	0.0002	
LIF	4.5	0.2	1.78E-08	2.61E-06
LIF+EPO	4.4	0.3	2.74E-07	1.31E-05

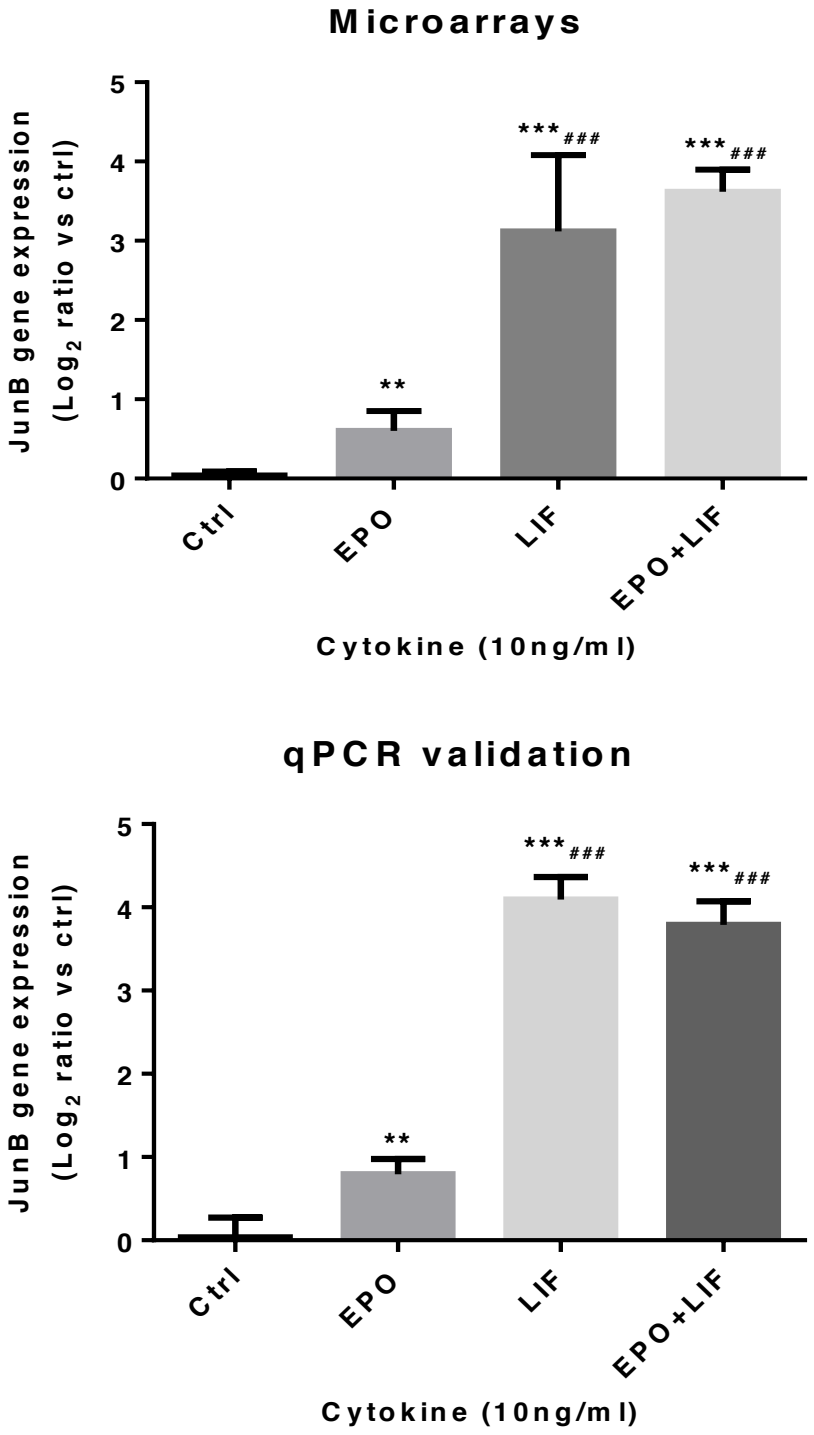

Figure 6.3: qPCR validation of the microarray data; JunB. Each graph compares the mean Log_2 FC of JunB after the specified cytokine treatment (10ng/ml) versus 1 control sample ±SD performed in quadruplicate. RT and qPCR were performed on the same samples as those used in the microarrays. **P<0.01, ***P<0.001 vs ctrl & ###P<0.001 vs EPO alone.

Figure 6.3 cont.:

Microarray results:

			P value	
Cytokine (ng/ml)	**JunB Mean**	**SD**	**vs Ctrl**	**vs EPO**
Ctrl	0.04	0.04		
EPO	0.6	0.2	0.0042	
LIF	3.1	0.9	0.0007	0.0023
LIF+EPO	3.6	0.3	2.54E-07	3.57E-06

qPCR validation results:

			P value	
Cytokine (ng/ml)	**JunB Mean**	**SD**	**vs Ctrl**	**vs EPO**
Ctrl	0.0	0.2		
EPO	0.8	0.2	0.0024	
LIF	4.1	0.3	5.08E-07	9.56E-07
LIF+EPO	3.8	0.3	1.01E-06	2.22E-06

6.2.2.1 Transcripts unaltered by EPO but upregulated by EPO+LIF

The transcripts that were significantly different between EPO+LIF and EPO were analysed by hierarchical clustering software. The resultant image showed groups of genes that were expressed in a similar manner under these treatments (Fig 6.4). Seven clusters that are marked on the image using blue bars were selected for further investigation (Fig 6.4).

The first criteria for the selection of clusters from Figure 6.4 was genes that were not altered by EPO but upregulated by EPO+LIF (Fig 6.5). Treatment with a high concentration of LIF (10ng/ml) decreased the expression of EPO-induced Mog, therefore investigation into those genes that were upregulated by LIF would clarify mechanisms through which LIF induced inhibitory mechanisms. The presence of such a high number of genes that fit this criteria was evidence that LIF had a strong effect on gene expression and was potentially inducing inhibition through a variety of mechanisms.

As expected, Socs3 was present here; it appeared in cluster 1. It was strongly upregulated by both the LIF 10 group and the EPO+LIF group but was unchanged by treatment with EPO alone. This reflected the previous work, shown in Chapter 4, where Socs3 expression by CG4 cells was significantly increased by treatment with a high concentration of LIF (10ng/ml). Socs3 expression in these samples was validated by qPCR to confirm that the results are reproducible when measured by different experimental procedures (Fig 6.6).

Myeloid differentiation primary response gene 88 (Myd88) was also identified in cluster 1. Myd88 is an adapter protein that is used by almost all toll-like receptors (TLRs), of which Tlr2 is also present in cluster 1 (Deguine 2014). It has a role in neurological differentiation and in EAE, as $Myd88^{-/-}$ mice were completely resistant to the disease progression (Miranda-Hernandez 2011), and Tlr2 inhibits oligodendrocyte maturation and remyelination, an effect not shared by all the Tlrs (Sloane 2010).

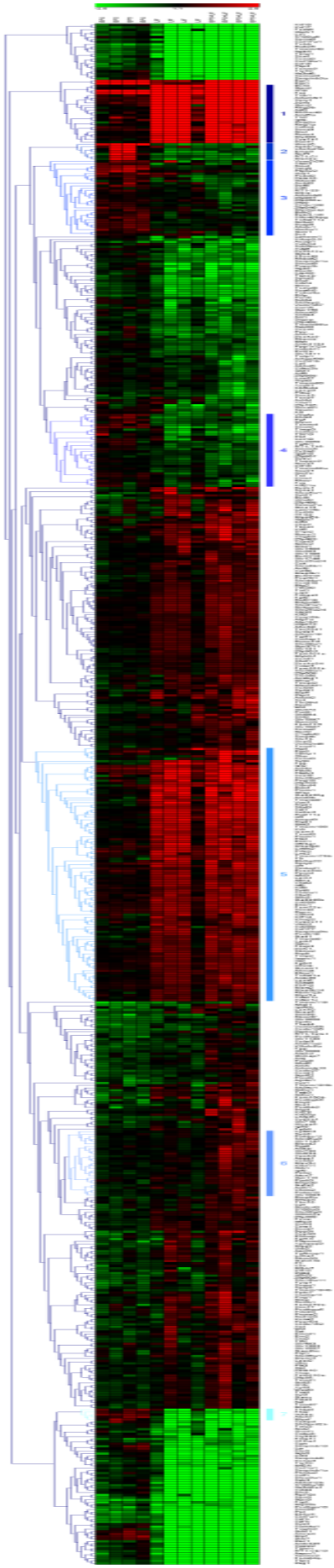

Figure 6.4: EPO+LIF vs EPO cluster analysis at 1 hour. Hierarchical clustering and heat map of the differentially expressed transcripts identified by comparing EPO and LIF vs. EPO at 1hr at a threshold of fold change greater than 1.5 and $P<0.05$. Expression changes in EPO treated samples and LIF treated samples are also shown expressed vs the control. Each sample represents the expression change compared with the mean of four control samples. Red indicates an increase and green indicates a decrease in expression compared to the controls. Average linkage clustering analysis was performed using Genesis software. The whole image is shown to give a full overview of the analysis. Individual clusters are shown later. Numbered blue bars mark the position of clusters. Four columns of each treatment are biological replicates.

Original in colour

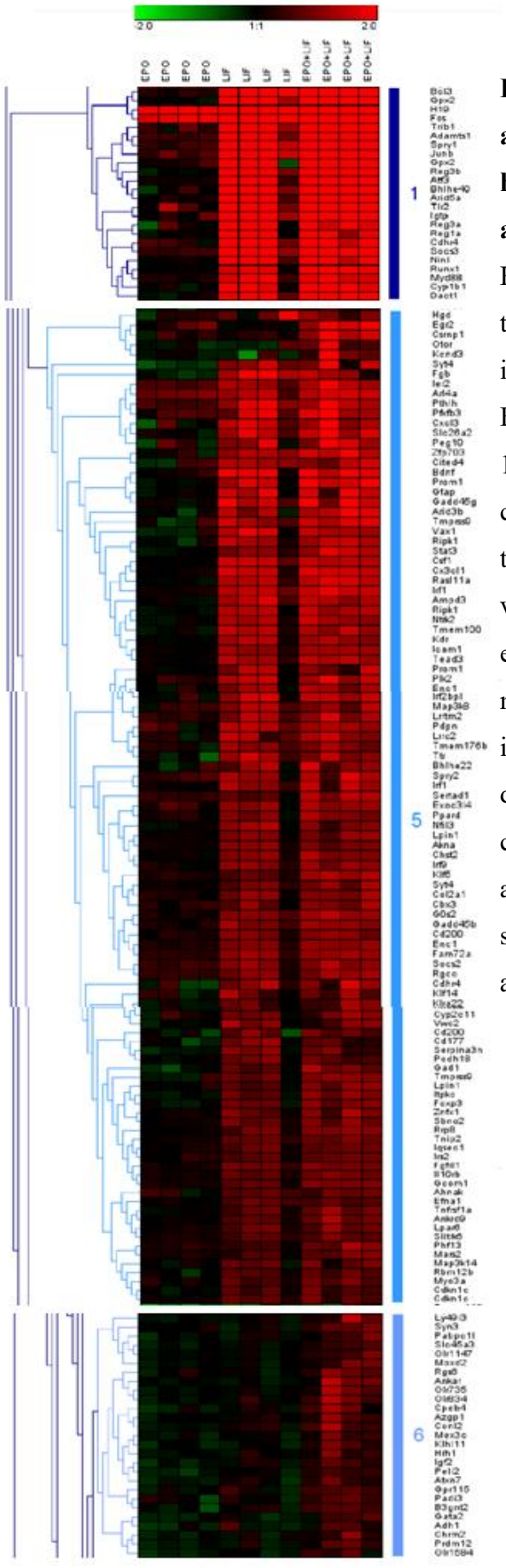

Figure 6.5: EPO+LIF vs EPO cluster analysis. Clusters of genes expressed here are not changed by EPO alone but are upregulated by EPO+LIF at 1 hour. Hierarchical clustering and heat map of the differentially expressed transcripts identified by comparing EPO+LIF vs. EPO at 1hr at a threshold of greater than 1.5 fold change and $P<0.05$. Expression changes in EPO treated samples and LIF treated samples are also shown expressed vs the control. Each sample represents the expression change compared with the mean of four control samples. Red indicates an increase and green indicates a decrease in expression compared to the controls. Average linkage clustering analysis was performed using Genesis software. Four columns of each treatment are biological replicates.

Original in colour

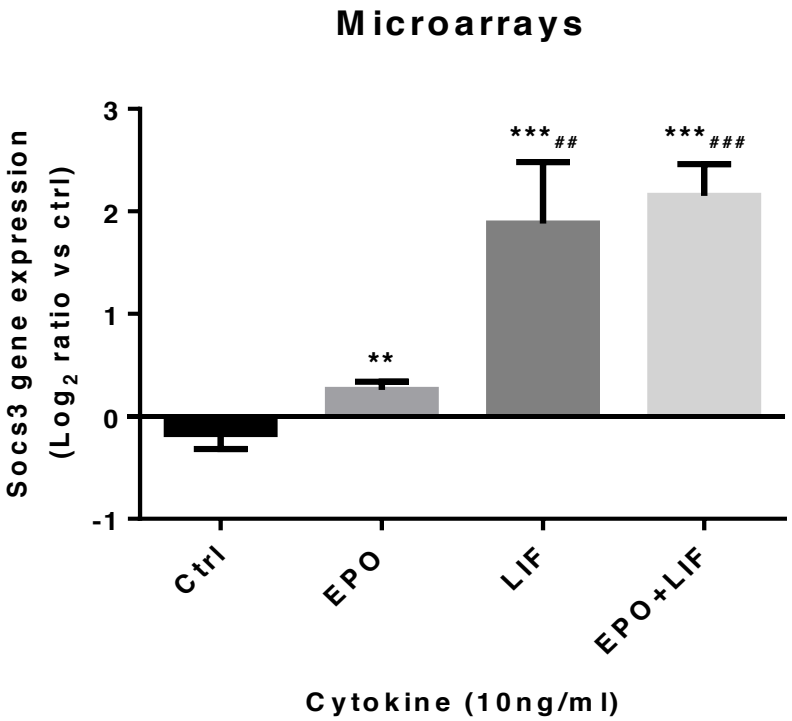

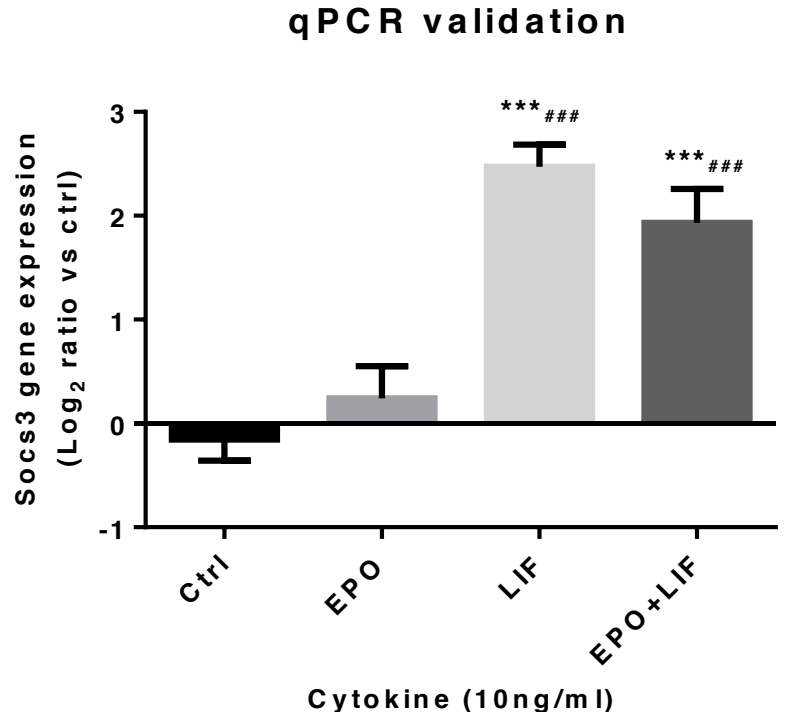

Figure 6.6: qPCR validation of the microarray data; Socs3. Each graph compares the mean Log_2 FC of Socs3 gene expression after the specified cytokine treatment (10ng/ml) versus 1 control sample ±SD performed in quadruplicate. RT and qPCR were performed on the same samples as those used in the microarrays. **P<0.01, ***P<0.001 vs ctrl & ##P<0.01, ###P<0.001 vs EPO alone.

Figure 6.6 cont.:

Microarray results:

			P value	
Cytokine (ng/ml)	**Socs3 Mean**	**SD**	**vs Ctrl**	**vs EPO**
Ctrl	-0.2	0.2		
EPO	0.3	0.1	0.0024	
LIF	1.9	0.6	0.0005	0.0018
LIF+EPO	2.2	0.3	1.19E-05	2.58E-05

qPCR validation results:

			P value	
Cytokine (ng/ml)	**Socs3 Mean**	**SD**	**vs Ctrl**	**vs EPO**
Ctrl	-0.2	0.2		
EPO	0.2	0.3	0.079	
LIF	2.5	0.2	2.06E-06	2.17E-05
LIF+EPO	1.9	0.3	3.47E-05	0.0003

All the genes present in these clusters were entered into STRING: software that interrogates functional protein association networks in order to analyse the genes which may be have functional association with each other and therefore provide links to further genes that should be considered. STRING is a database of interactions, both direct and indirect, between proteins that provide a visual representation of the interactions between a list of proteins. All the genes identified in the clusters that are not altered by EPO but upregulated by EPO+LIF by hierarchical cluster analysis (Fig 6.5) were entered into STRING (Fig 6.7).

The STRING analysis highlighted a group of functionally connected genes centred around Stat3 and Socs3 (Fig 6.8). It further suggested that they could have an effect on other signalling mechanisms. Egr2 was also present, another signalling mechanism that has previously been investigated. Myd88 and Tlr2 are also highlighted by this analysis suggesting their potential importance in the inhibition of EPO-induced Mog.

A gene identified from this STRING image is Tnfrsf1a as it is linked to both Stat3 and Myd88. TNF is an inflammatory cytokine that has been linked to MS, including being found overexpressed in the brain of MS patients at autopsy (Hofman 1989) and its expression correlated with MS disease severity (Rieckmann 1995). The receptor coded for by the Tnfrsf1a gene is one of the major receptors responsible for TNF signal transduction and is implicated in the pathogenesis of EAE (Archambault 2006) and is crucial for normal disease pathology as Tnfrsf1a$^{-/-}$ mice were completely resistant to EAE (Suvannavejh 2000). This suggests that oligodendrocytes that produced less myelin were more susceptible to TNF. Validation by qPCR was successful as an increase in Tnfrsf1a expression was seen in samples treated with LIF and those treated with EPO+LIF, reflecting the upregulations seen in the microarrays (Fig 6.9). The increase of a key receptor for TNF in the conditions in which myelination is reduced is evidence for the association between inflammation and demyelination.

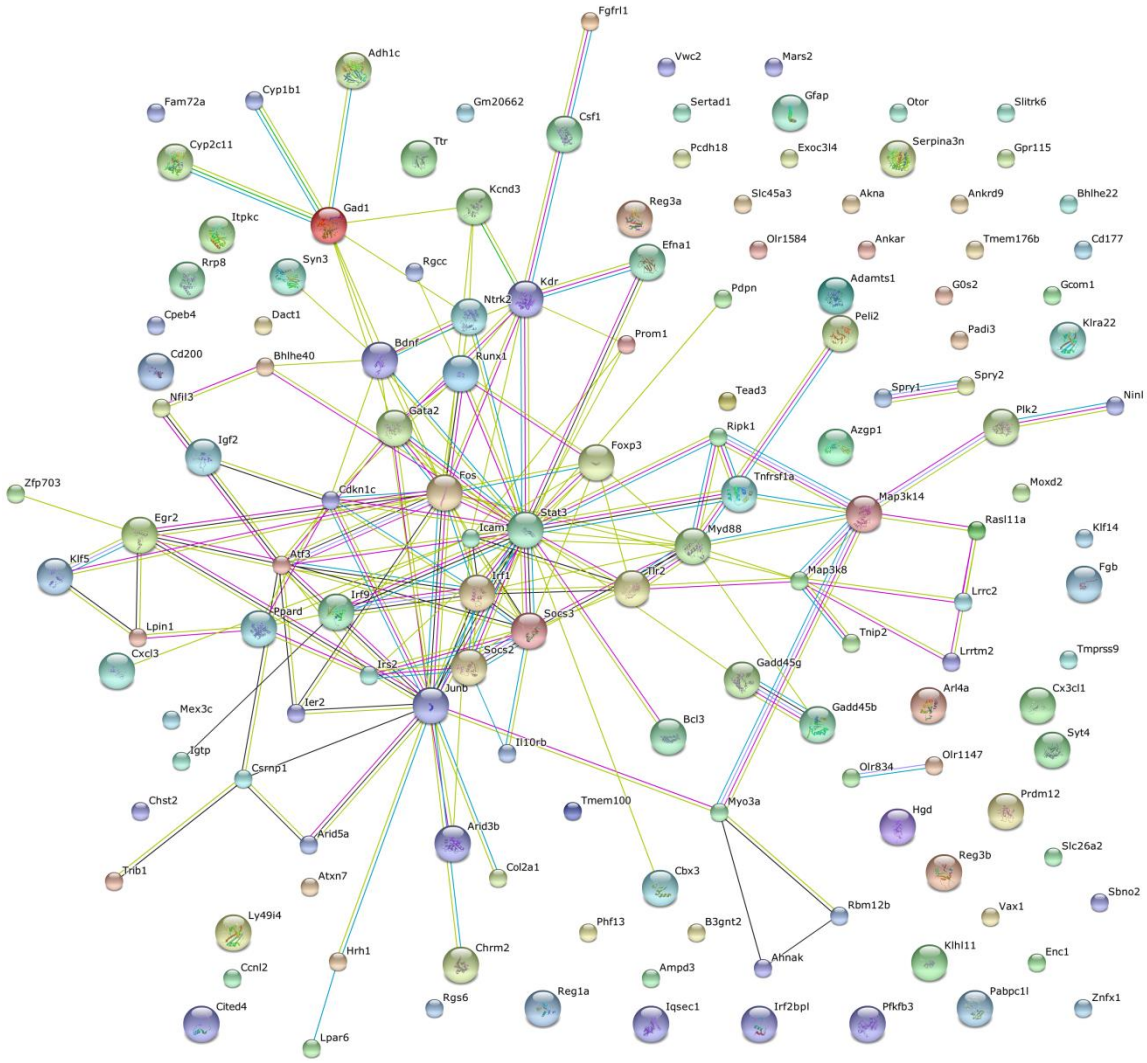

Figure 6.7: STRING analysis of genes unaltered by EPO but upregulated by EPO+LIF at 1hour. All transcripts were filtered for EPO+LIF vs EPO with parameters of fold change greater than 1.5 and $p<0.05$. The genes represented here were selected from a hierarchical cluster analysis where clusters that were not changed by EPO but upregulated by EPO and LIF were identified. The nodes represent the proteins encoded by the genes and the lines between the nodes represent functional interactions between them. Confidence score >0.4 with text mining.

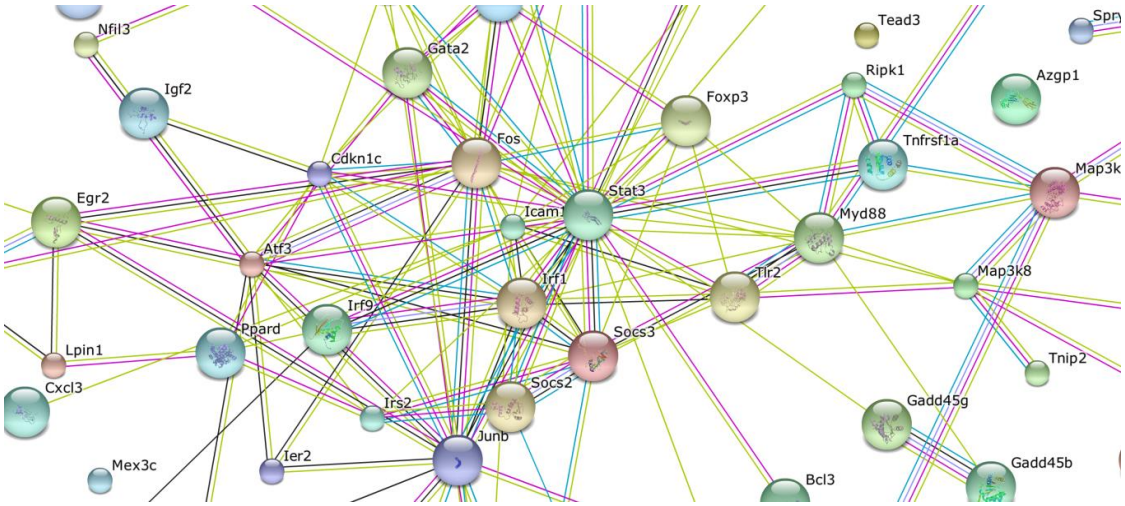

Figure 6.8: Centre section of STRING analysis shown in Fig 6.7. Genes shown here are not altered by EPO and upregulated by EPO+LIF at 1 hour. The nodes represent the proteins encoded by the genes and the lines between the nodes represent functional interactions between them. Confidence score >0.4 with text mining.

Original in colour

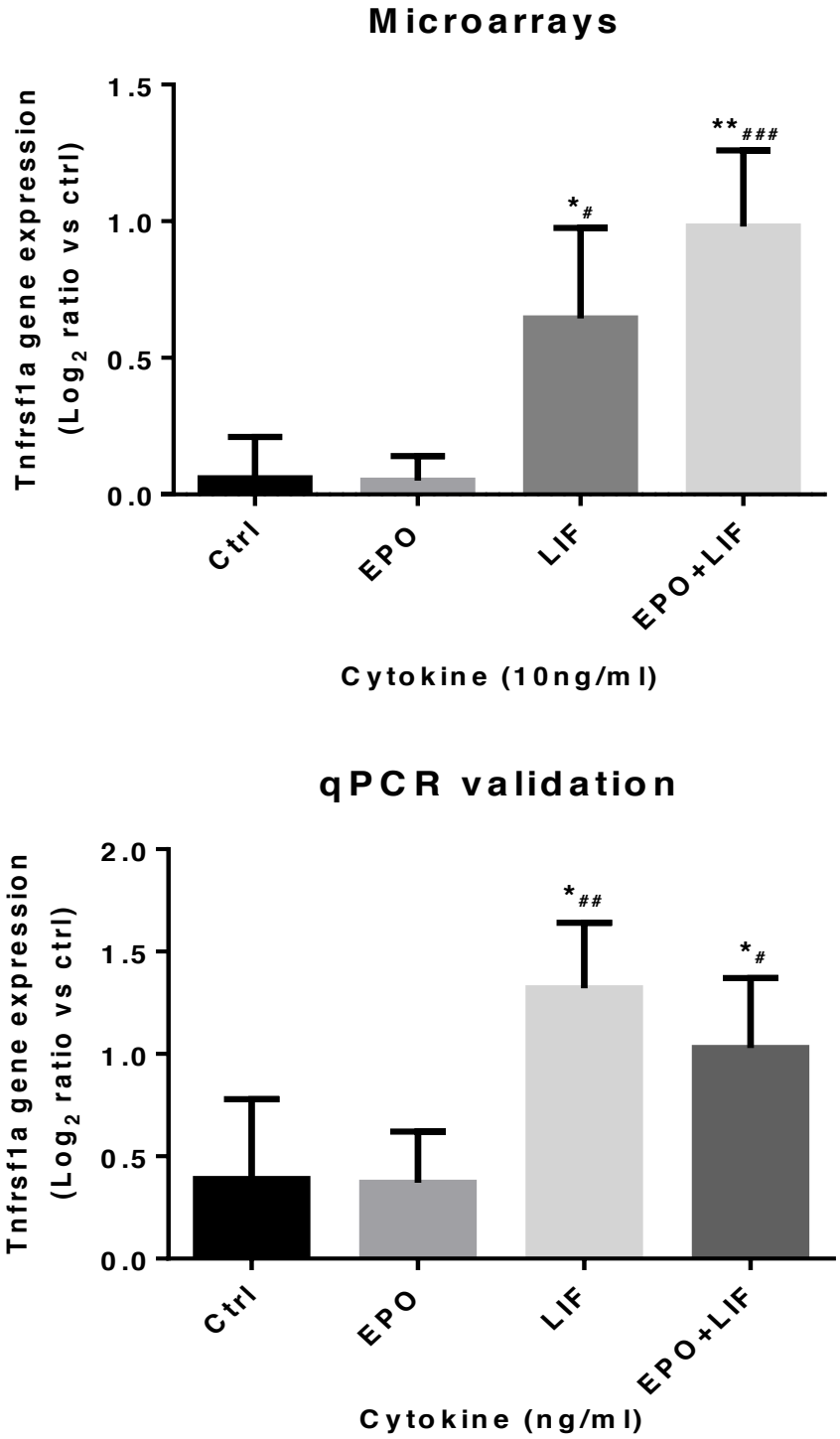

Figure 6.9: qPCR validation of the microarray data; Tnfrsf1a. Each graph compares the mean Log_2 FC of Tnfrsf1a gene expression after the specified cytokine treatment (10ng/ml) versus 1 control sample ±SD performed in quadruplicate. RT and qPCR were performed on the same samples as those used in the microarray. *P<0.05, **P<0.01 vs ctrl & #P<0.05, ##P<0.01, ###P<0.001 vs EPO alone.

Figure 6.9 cont.:

Microarray results:

			P value	
Cytokine (ng/ml)	**Tnfrsf1a Mean**	**SD**	**vs Ctrl**	**vs EPO**
Ctrl	0.1	0.2		
EPO	0.1	0.1	0.8930	
LIF	0.6	0.3	0.0193	0.0142
LIF+EPO	1.0	0.3	0.0012	0.0008

qPCR validation results:

			P value	
Cytokine (ng/ml)	**Tnfrsf1a Mean**	**SD**	**vs Ctrl**	**vs EPO**
Ctrl	0.4	0.4		
EPO	0.4	0.3	0.9387	
LIF	1.3	0.3	0.0106	0.0035
LIF+EPO	1.0	0.3	0.0501	0.0215

6.2.2.2 Transcripts upregulated by EPO but downregulated by EPO+LIF

The second condition for clusters selected from the significant genes between EPO+LIF and EPO at 1 hour (Fig 6.4) was genes that were upregulated by treatment with EPO alone but downregulated by treatment with EPO+LIF (Fig 6.10). Genes regulated thus were considered in Section 6.2.1 however in that section only genes that were significantly different between EPO and the control remained after filtering. Therefore, the rest of this chapter will consider a wider range of genes that were present after only filtering of EPO+LIF versus EPO. Genes that were regulated in this way are of interest to the analyses undertaken here because they could be important in increasing myelination, as represented by an increase when EPO treatment alone was present. In contrast the presence of LIF actively downregulated these compared to their basal levels in the control samples, suggesting that LIF was inhibiting these pro-myelinating genes.

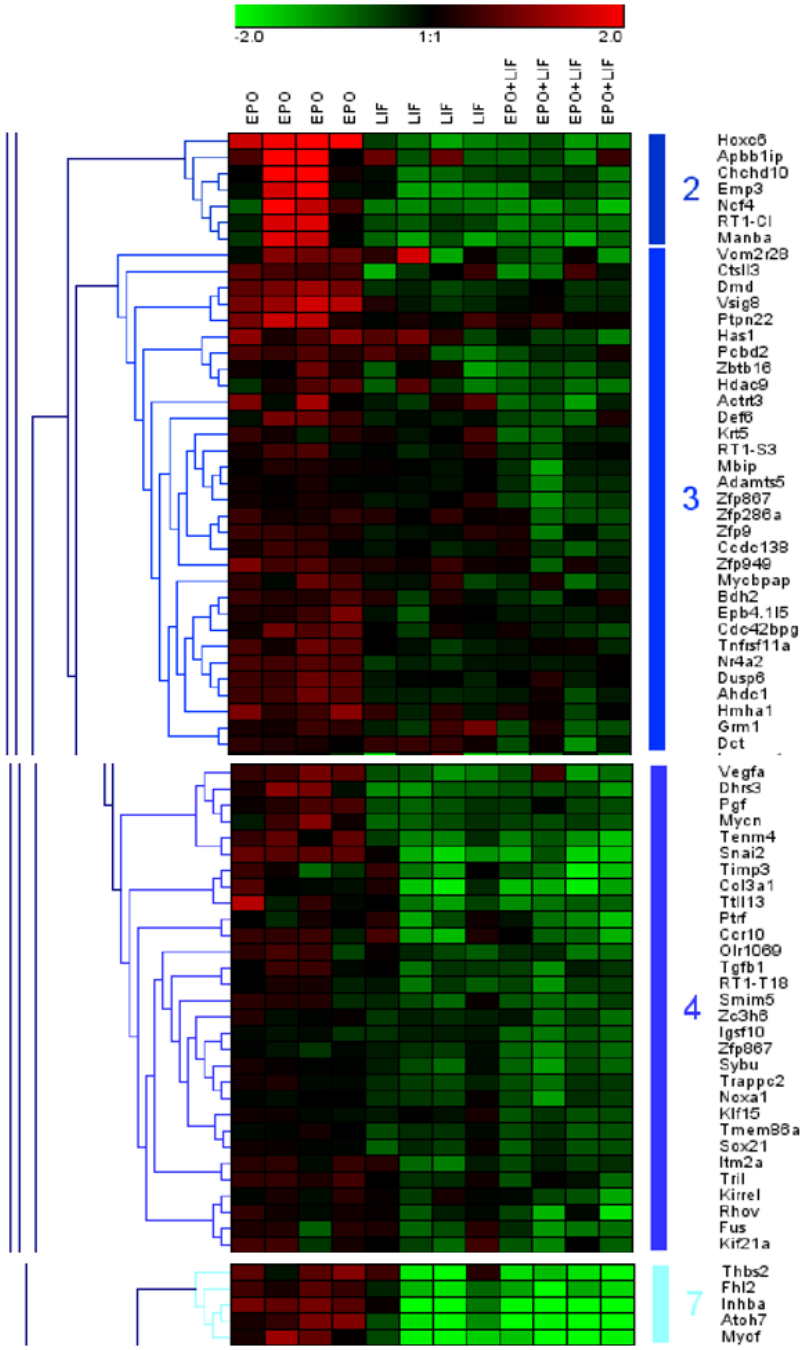

Figure 6.10: EPO+LIF vs EPO cluster analysis. Clusters of genes expressed here are upregulated by EPO alone and downregulated by EPO+LIF at 1 hour. Hierarchical clustering and heat map of the differentially expressed transcripts identified by comparing EPO and LIF vs. EPO at 1hr at a threshold of 1.5 fold change and $P<0.05$. Expression changes in EPO treated samples and LIF treated samples are also shown expressed vs the control. Each sample represents the expression change compared with the mean of four control samples. Red indicates an increase and green indicates a decrease in expression compared to the controls. Average linkage clustering analysis was performed using Genesis software. Four columns of each treatment are biological replicates and the blue bars indicate clusters of interest.

Original in colour

There were several genes identified by the analysis that will be discussed further. As mentioned in Section 6.2.1, Hoxc6 and Dusp6 were both present in this cluster. In cluster 7, Inhibin beta a (Inhba) was identified which creates a homodimer to form ActivinA, a molecule that is secreted by inflammatory macrophages and is known to be important in remyelination and differentiation of oligodendrocytes and was also present in the cluster analysis when transcripts had been filtered for EPO versus the control and EPO+LIF versus EPO (Miro 2013). qPCR validation was performed on Inhba, however, it was unsuccessful as LIF and EPO+LIF groups were upregulated in the validation while they were downregulated in the microarrays (Fig 6.11). The failure of validation was potentially due to a very low expression. This result meant that Inhba would be considered no further.

STRING analysis of the clusters that are upregulated by EPO but downregulated by EPO+LIF was carried out to determine functional connections between the proteins coded for by the genes present (Fig 6.12). The majority of the information this analysis provided was just confirmation of the functional connections between the genes that had been selected from the cluster analysis. However, at the centre of this image was Vegfa, which had not been previously recognised. Vegfa is involved in migration but not proliferation of OPCs (Hayakawa 2012) and it is expressed by astrocytes and neurons in the CNS (Ogunshola 2000, Argaw 2006). However, there is no previous evidence that it is expressed by oligodendrocytes, suggesting that the upregulation of Vegfa by EPO seen in the microarrays was a novel finding.

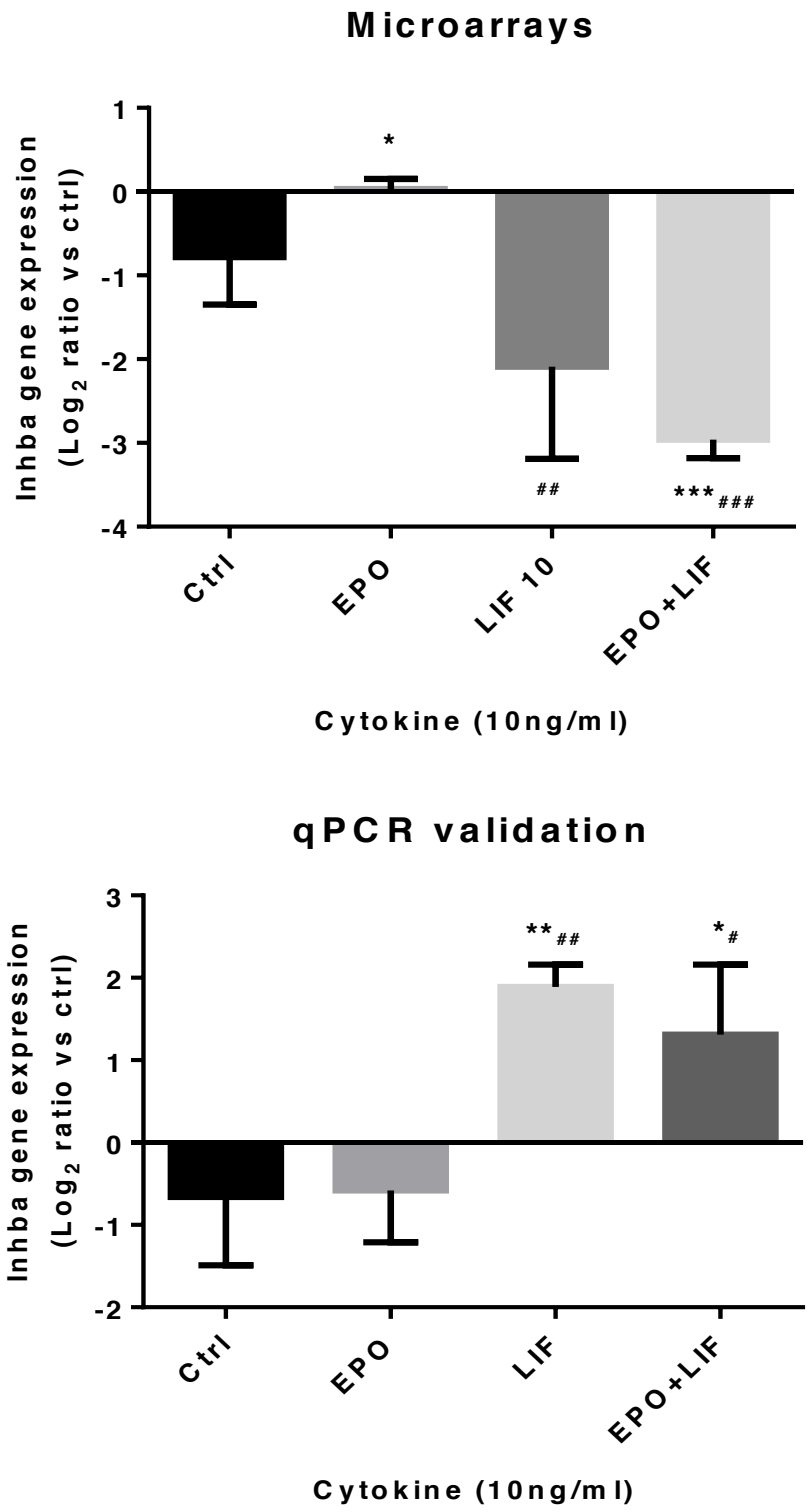

Figure 6.11: qPCR validation of the microarray data; Inhba. Each graph compares the mean Log_2 FC of Inhba gene expression after the specified cytokine treatment (10ng/ml) versus 1 control sample ±SD performed in quadruplicate. RT and qPCR were performed on the same samples as those used in the microarray. **P<0.01, ***P<0.001 vs ctrl & ##P<0.01, ###P<0.001 vs EPO alone.

Figure 6.11 cont.:

Microarray results:

			P value	
Cytokine (ng/ml)	**Inhba Mean**	**SD**	**vs Ctrl**	**vs EPO**
Ctrl	-0.8	0.6		
EPO	0.0	0.1	0.0327	
LIF	-2.01	1.1	0.0788	0.0086
LIF+EPO	-3.0	0.2	0.0004	3.36E-07

qPCR validation results:

			P value	
Cytokine (ng/ml)	**Inhba Mean**	**SD**	**vs Ctrl**	**vs EPO**
Ctrl	-0.7	0.8		
EPO	-0.6	0.6	0.8771	
LIF	1.9	0.3	0.0011	0.0004
LIF+EPO	1.3	0.8	0.0158	0.0117

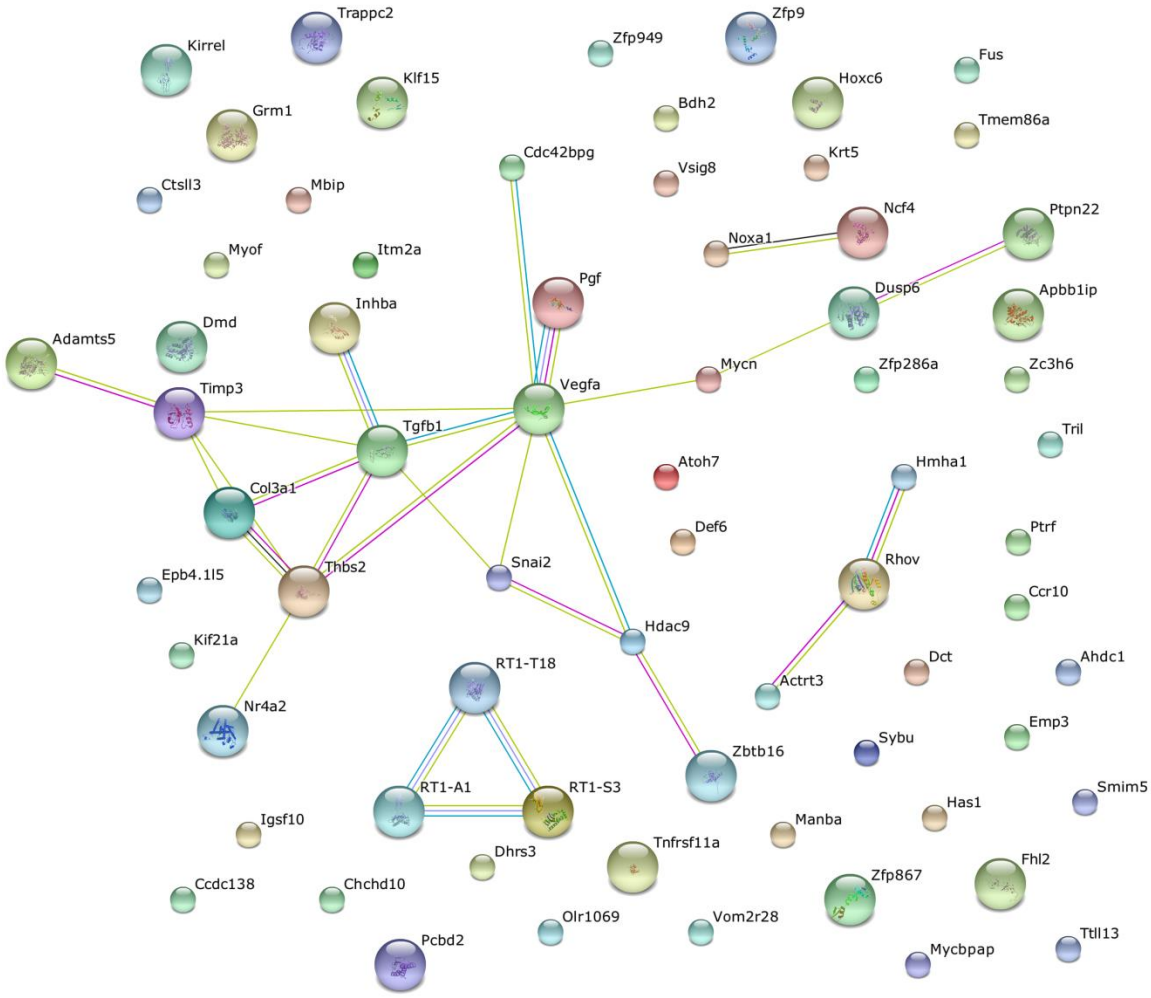

Figure 6.12: STRING analysis of genes upregulated by EPO and downregulated by EPO+LIF at 1hour. All transcripts were filtered for EPO+LIF vs EPO with parameters of fold change greater than 1.5 and $p<0.05$. The genes represented here were selected for from hierarchical cluster analysis where clusters that were upregulated by EPO and downregulated by EPO+LIF. The nodes represent the proteins encoded by the genes and the lines between the nodes represent functional interactions between them. Confidence score >0.4 with text mining.

6.3 Analysis of genes altered after cytokine treatment for 20 hours

6.3.1 Transcripts altered by EPO vs the control and EPO+LIF vs EPO

Analysis of the effects of EPO and LIF at a late time point, 20 hours, would allow identification of those genes that were induced further downstream than those seen at 1 hour that may have affected the myelinating capacity of the CG4 cells. The same number of transcripts were analysed at 20 hours as 1 hour, again leaving 21575 transcripts after those that were unnamed or had no functional annotation were removed. The same parameters applied to the 1 hour analysis were used initially with significance being defined as a fold changed greater than 1.5 and P value less than 0.05 by Student's *t*-test. The first filter was for EPO vs ctrl, after which 617 genes remained. The second filter was for EPO+LIF vs EPO after which 341 genes remained. The remaining genes were ordered for fold change between EPO+LIF and EPO and the top ten most highly up- and downregulated are shown in Table 6.2.

Analysis of Table 6.2 showed that genes that were most highly upregulated by the addition of LIF were also upregulated when EPO alone was present suggesting that the addition of LIF simply exaggerated any effect of EPO on the expression of these genes. However, this was not true of the genes most highly downregulated upon the addition of LIF. While some of these downregulated genes were also downregulated by EPO, there were a few that were instead upregulated by EPO, including CD36 and Htr2c which showed a high fold change of 4.85 and 5.14 respectively. These genes may have some relevance in mediating the myelinating effects of EPO.

		EPO vs Ctrl		EPO+LIF vs EPO	
Gene Name	**Accession number**	**Average Log_2 FC**	**P Value**	**Average Log_2 FC**	**P Value**
Upregulated					
Itga9	XM_006244173	1.54	0.00072575	4.46	0.00000210
Bcl3	NM_001109422	0.96	0.00000775	4.38	0.00000000
Tmem176b	NM_134390	2.40	0.00004984	3.45	0.00000018
Il33	NM_001014166	0.85	0.00012281	3.00	0.00000001
Fos	NM_022197	0.90	0.00001360	2.96	0.00000001
Anxa2	NM_019905	1.06	0.00205820	2.89	0.00000856
Ampd3	NM_031544	1.14	0.00069063	2.84	0.00000493
Atp1b2	NM_012507	0.69	0.00002644	2.67	0.00000002
Klhl31	NM_001108170	0.92	0.03864935	2.60	0.00001855
Vgf	NM_030997	1.16	0.00096804	2.35	0.00000109
Downregulated					
Ppargc1a	NM_031347	1.48	0.00016825	-1.43	0.00006620
Depdc1	XM_001080406	-0.71	0.03851175	-1.48	0.00120565
Nek2	NM_053691	-0.65	0.00129277	-1.52	0.00138468
Shroom2	NM_001047893	1.73	0.00017057	-1.52	0.00012310
Bub1	NM_001106507	-0.69	0.02338221	-1.54	0.00192689
Nod1	NM_001109236	-0.83	0.01821738	-1.56	0.00099279
Pgf	NM_053595	1.46	0.00498708	-1.56	0.00145360
Cd36	NM_031561	4.85	0.00000002	-1.78	0.00002427
Esam	NM_001004245	-0.80	0.00769477	-1.86	0.00022118
Htr2c	NM_012765	5.14	0.00000000	-1.98	0.00000201

Table 6.2: The most highly up- and downregulated genes between cells treated with EPO alone vs control and then EPO+LIF vs EPO alone at 20 hours. Genes were first cut for significant changes between EPO and the control and then between EPO+LIF and EPO. Significance was defined as a P value less than 0.05 and fold change greater than 1.5.

Hierarchical cluster analysis was performed on the genes that remained after the filters were entered to produce a heat map that is an aid to defining clusters of genes that were expressed similarly to each other (Fig 6.13). There were two clusters that were identified from this figure (Fig 6.14 shows just these two clusters). Genes in cluster 1 were upregulated by EPO but not altered when the cells were treated with both EPO+LIF, suggesting that they were important in inducing myelination, and so upregulated by EPO, but that the presence of LIF inhibited them. Genes in cluster 2 were downregulated by EPO but unaltered by EPO+LIF, possibly suggesting inhibitory genes that treatment with EPO diminished.

Genes of note that appeared in cluster 1 (Fig 6.14) included Igf1, which is known to be important in myelination and cerebral development (Beck 1995) as discussed in Chapter 5. Mag, another myelin gene, and peroxisome proliferator-activated receptor gamma (Ppargc1a) which is important in metabolism and so crucial to the high metabolic load required for myelin production and deposition were also in Figure 6.14.

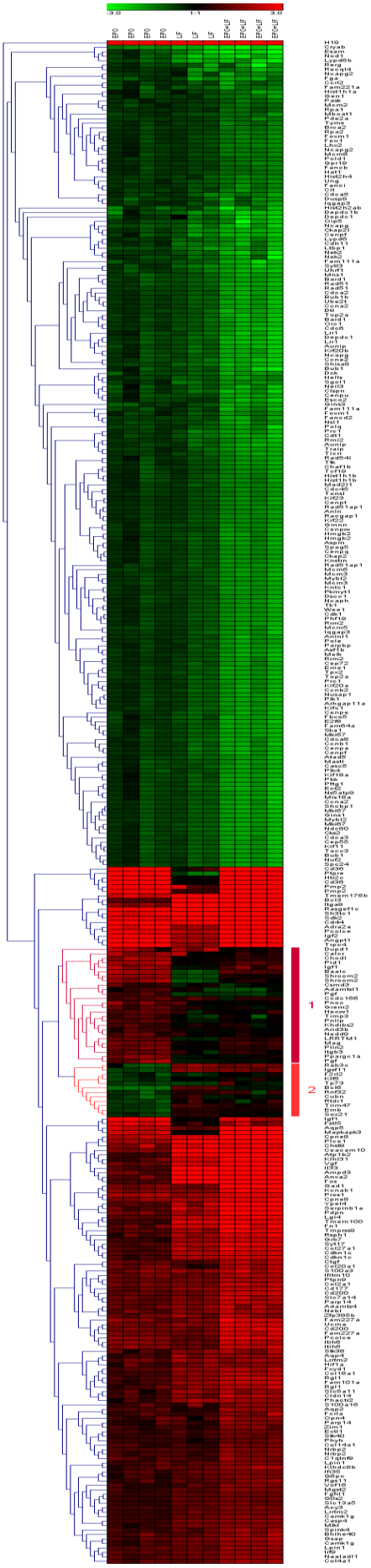

Figure 6.13: Genes changed by EPO vs the control and EPO+LIF vs EPO at 20 hours. Hierarchical clustering and heat map of the differentially expressed transcripts identified by comparing EPO vs. the control and then EPO+LIF versus EPO at a threshold of 1.5 fold change (Log_2 FC 0.58) and $P<0.05$. Expression changes in LIF treated samples are also shown expressed vs the control. Each sample represents the expression change compared to the mean Log_2 of the control. Red indicates an increase and green indicates a decrease in expression compared to the controls. Average linkage clustering analysis was performed using Genesis software. Four columns of each treatment are biological replicates. The whole image is shown to give a full overview of the analysis. Bars 1&2 indicate clusters of interest.

Original in colour

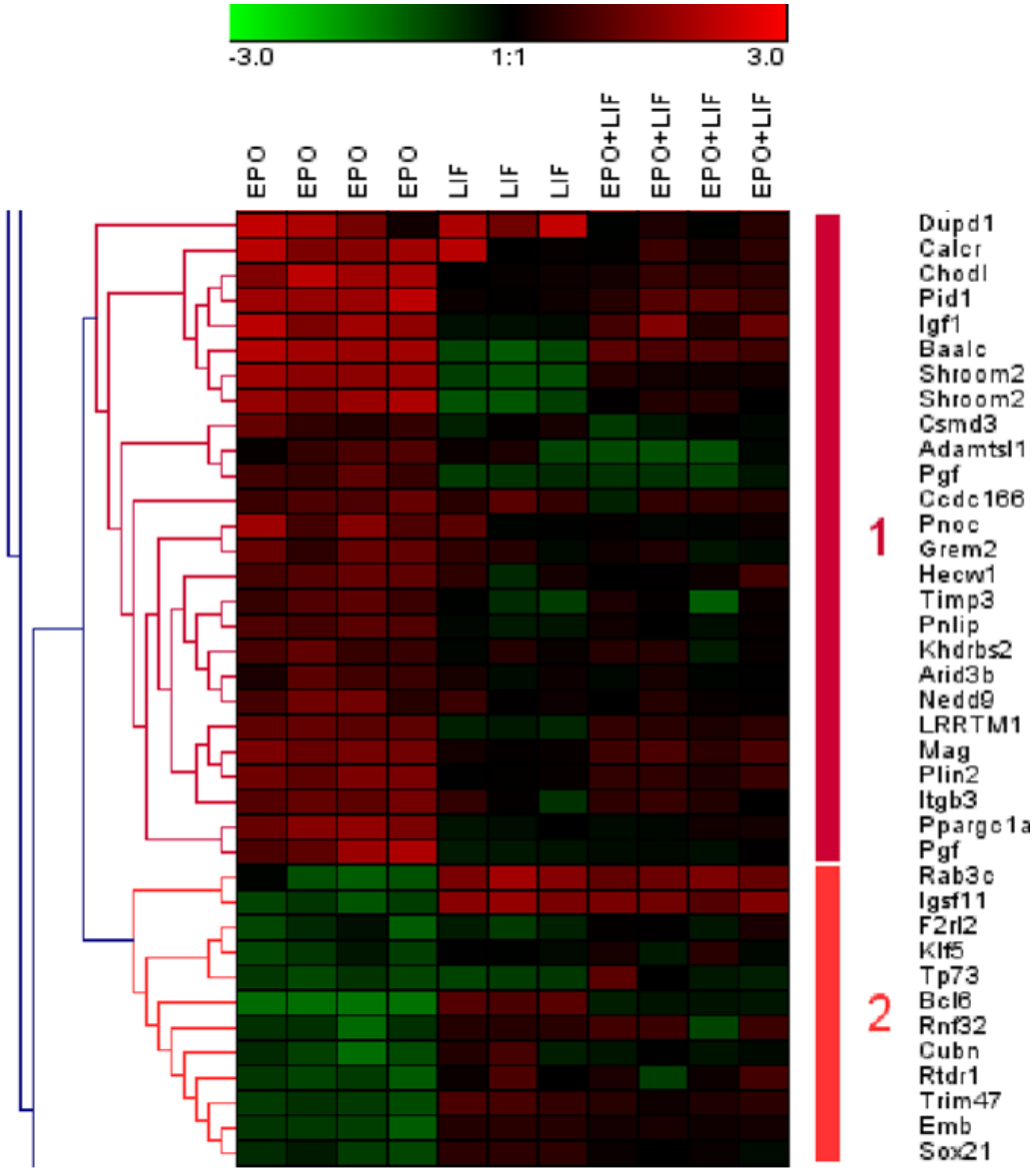

Figure 6.14: Genes changed by EPO vs the control and EPO+LIF vs EPO at 20 hours. The clusters shown here are those in which genes are regulated differently by LIF and EPO+LIF treatments than EPO alone. Hierarchical clustering and heat map of the differentially expressed transcripts identified by comparing EPO vs. the control and then EPO+LIF versus EPO at a threshold of 1.5 fold change (Log_2 FC 0.58) and $P<0.05$. Expression changes in LIF treated samples are also shown expressed vs the control. Each sample represents the expression change compared to the mean Log_2 of the control. Red indicates an increase and green indicates a decrease in expression compared to controls. Average linkage clustering analysis was performed using Genesis software. Bars 1&2 indicate clusters of interest. Four columns of each treatment are biological replicates.

Original in colour

Mag expression was validated by qPCR as it was important to show that a gene associated with myelination acted in the same way in these samples as Mog had in the other experimental work that comprises this thesis. Mog was not present in the microarray analysis because it is a very late-induced gene, so other myelin genes had to be selected from the analysis for confirmation that the microarray analysis reflected the work seen previously in the lab. The qPCR validation of Mag was not successful, as although the data replicated that seen in the microarray analysis, the difference between EPO+LIF and EPO was not significant (P=0.326), therefore no inhibition of this myelin gene by LIF was seen (Fig 6.15).

It was important to successfully validate a myelin gene from the microarrays to create a link directly to the previous work from this project that warranted the microarray analysis. Pmp2 is a myelin gene that was detected in the microarrays to be expressed in the same way as Mog is in the current project, so qPCR validation was carried out on it. The validation was successful as EPO induced large amounts of Pmp2 while both LIF and EPO+LIF treatment groups induced significantly less than EPO (P=0.000001 and P=0.0025 respectively), showing significant inhibition of EPO-induced myelination (Fig 6.16).

Also seen in cluster 1 (Fig 6.14) is Ppargc1a, which was mentioned in Section 6.3.1, where it was still present after cuts for both EPO versus the control and EPO+LIF versus EPO. It is a transcription factor, also known as Pgc-1α, which is a master regulator of metabolism, and therefore may play a crucial role in the production of myelin, and is associated with mitochondrial function (Lindholm 2012). The expression of Ppargc1a was validated by qPCR (Fig 6.17). Crucially, treatment with EPO+LIF significantly changed Ppargc1a expression when compared to EPO in the microarray analysis (P=0.00006) but there was considerably less significance between these two groups in the qPCR validation (P=0.01). Consequently, Ppargc1a will not be investigated further.

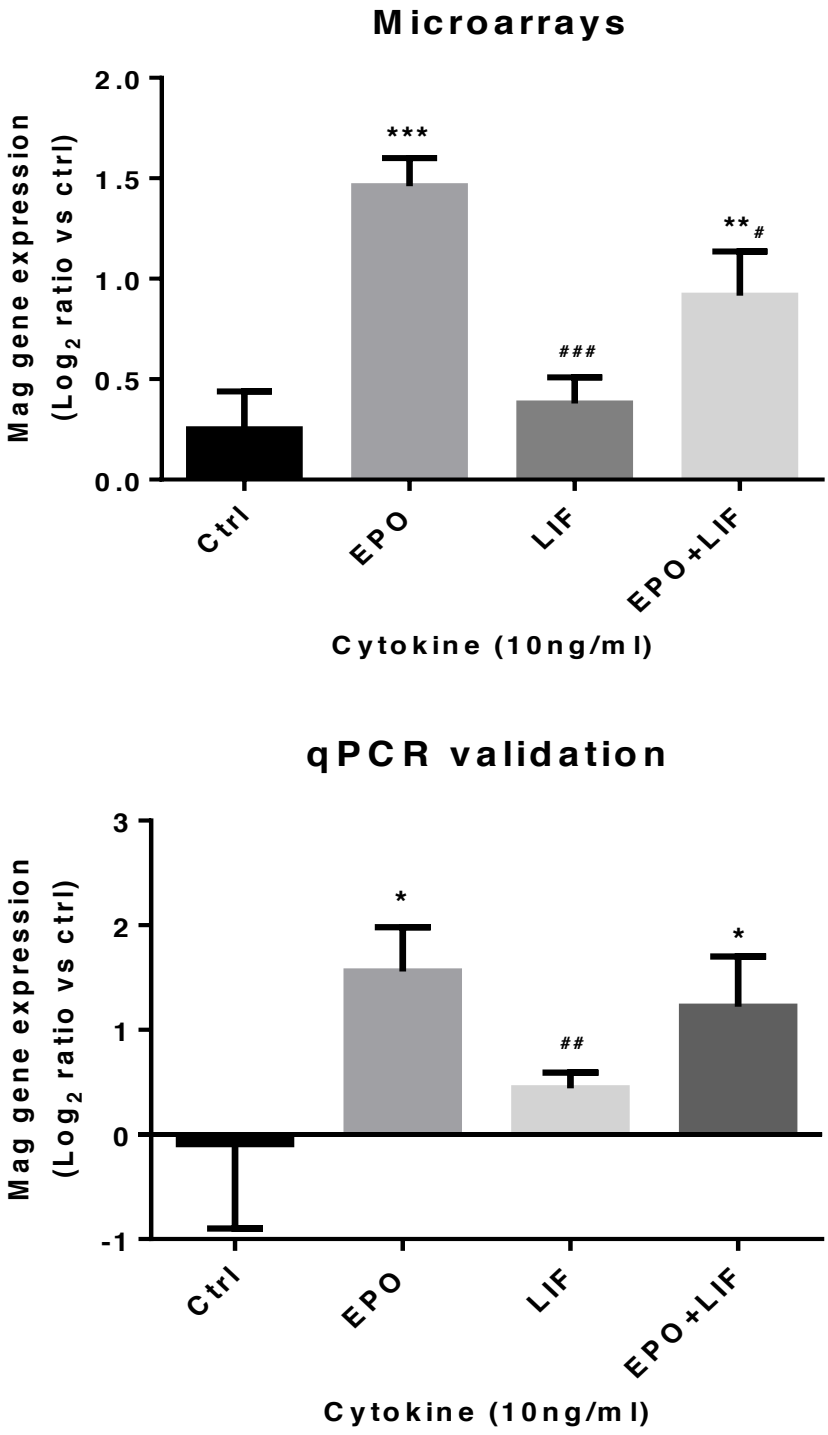

Figure 6.15: qPCR validation of the microarray data; Mag. Each graph compares the mean Log_2 FC of Mag gene expression after the specified cytokine treatment (10ng/ml) versus control sample "B"±SD performed in quadruplicate. RT and qPCR were performed on the same samples as those used in the microarray. *P<0.05, **P<0.01, ***P<0.001 vs ctrl & #P<0.05, ##P<0.01, ###P<0.001 vs EPO alone.

Figure 6.15 cont.:

Microarray results:

			P value	
Cytokine (ng/ml)	**Mag Mean**	**SD**	**vs Ctrl**	**vs EPO**
Ctrl	-0.19	0.2		
EPO	0.27	0.3	3.03E-05	
LIF	0.05	0.1	0.3598	6.71E-06
LIF+EPO	0.50	0.5	0.0045	0.0399

qPCR validation results:

			P value	
Cytokine (ng/ml)	**Mag Mean**	**SD**	**vs Ctrl**	**vs EPO**
Ctrl	-0.1	0.8		
EPO	1.6	0.4	0.0114	
LIF	0.4	0.2	0.2506	0.0024
LIF+EPO	1.2	0.5	0.0328	0.3255

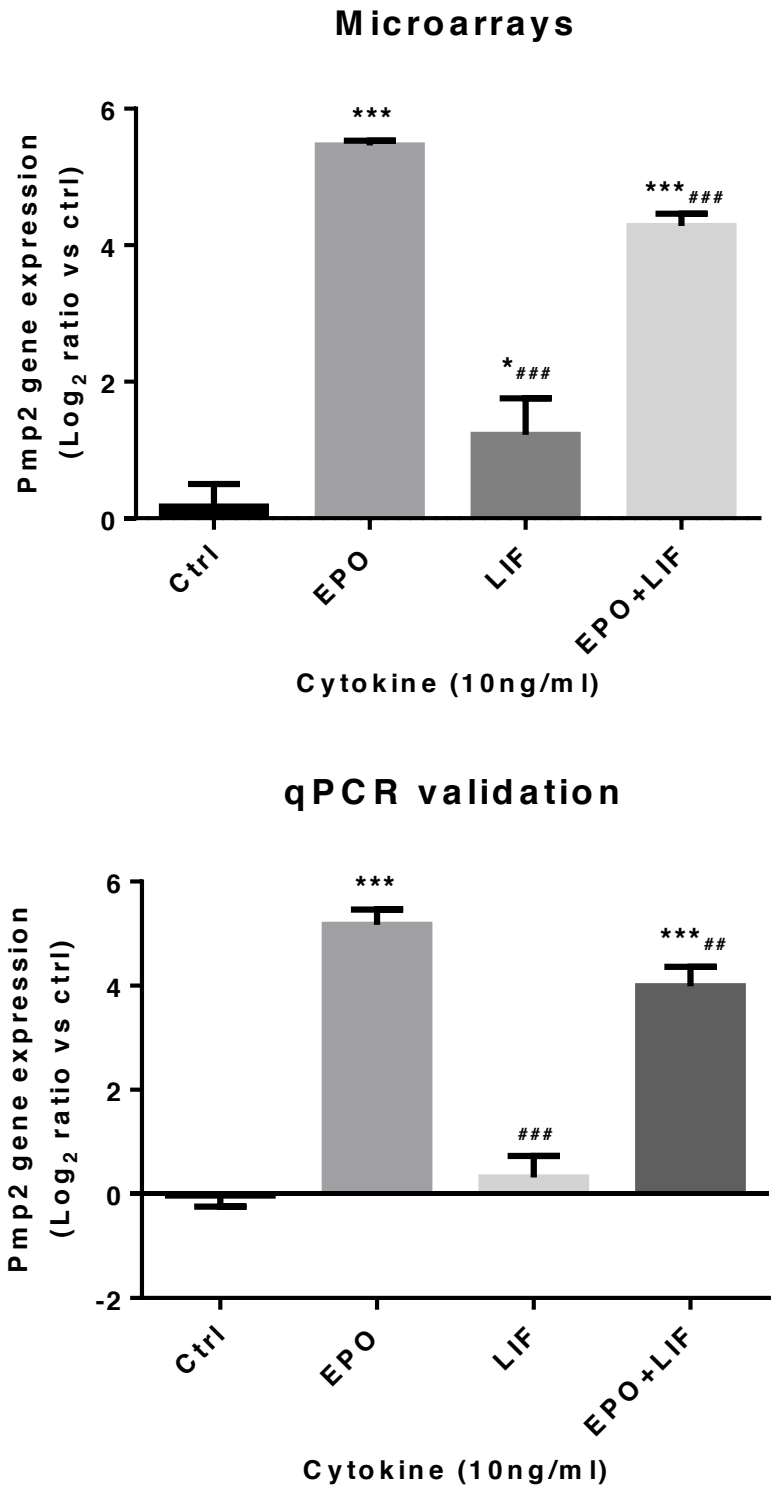

Figure 6.16: qPCR validation of the microarray data; Pmp2. Each graph compares the mean Log_2 FC of Pmp2 gene expression after the specified cytokine treatment (10ng/ml) versus control sample "B"±SD performed in quadruplicate. RT and qPCR were performed on the same samples as those used in the microarray. **P<0.01, ***P<0.001 vs ctrl & ##P<0.01, ###P<0.001 vs EPO alone.

Figure 6.16 cont.:

Microarray results:

			P value	
Cytokine (ng/ml)	**Pmp2 Mean**	**SD**	**vs Ctrl**	**vs EPO**
Ctrl	0.2	0.3		
EPO	5.5	0.1	5.76E-07	
LIF	1.2	0.5	0.0316	1.46E-05
LIF+EPO	4.3	0.2	3.66E-06	2.24E-05

qPCR validation results:

			P value	
Cytokine (ng/ml)	**Pmp2Mean**	**SD**	**vs Ctrl**	**vs EPO**
Ctrl	0.0	0.2		
EPO	5.2	0.3	1.14E-07	
LIF	0.3	0.4	0.1828	1.34E-06
LIF+EPO	4.0	0.4	1.36E-06	0.0025

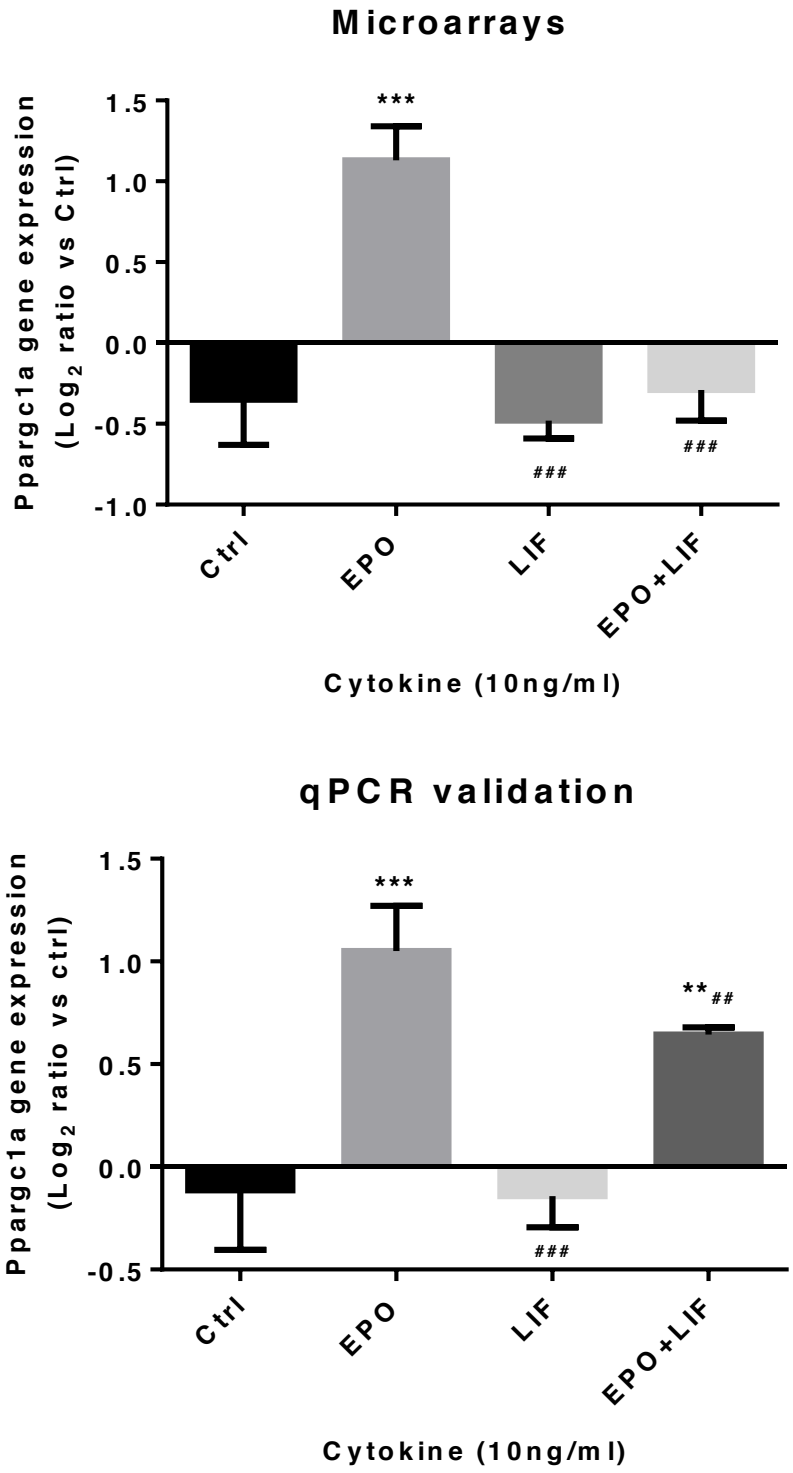

Figure 6.17: qPCR validation of the microarray data; Ppargc1a. Each graph compares the mean Log_2 FC of Ppargc1a gene expression after the specified cytokine treatment (10ng/ml) versus control sample "B"±SD performed in quadruplicate. RT and qPCR were performed on the same samples as those used in the microarray. **P<0.01, ***P<0.001 vs ctrl & ##P<0.01, ###P<0.001 vs EPO alone.

Figure 6.17 cont.:

Microarray results:

			P value	
Cytokine (ng/ml)	**Ppargc1a Mean**	**SD**	**vs Ctrl**	**vs EPO**
Ctrl	-0.4	0.3		
EPO	1.1	0.2	0.002	
LIF	-0.5	0.1	0.4771	8.01E-05
LIF+EPO	-0.3	0.2	0.7742	6.62E-05

qPCR validation results:

			P value	
Cytokine (ng/ml)	**Ppargc1a Mean**	**SD**	**vs Ctrl**	**vs EPO**
Ctrl	-0.1	0.3		
EPO	1.1	0.2	0.0007	
LIF	-0.1	0.2	0.8668	0.0001
LIF+EPO	0.6	0.0	0.0021	0.0104

6.3.2 Transcripts altered by treatment with EPO+LIF compared to EPO alone

As with the 1 hour analysis it was decided to analyse just those genes altered between treatment of cells with EPO+LIF combined and EPO alone as this would give a clearer explanation of the causes behind the inhibition of EPO-induced Mog by LIF. The transcripts were filtered initially using the same parameters as before (fold change greater than 1.5 and P value less than or equal to 0.05). However, after this 1169 transcripts remained which were too many to analyse. Also, as there is such a large quantity it is possible to increase the level of significance and so only be left with genes that show a substantial effect. Therefore, the P value was lowered first to less than or equal to 0.01, which still left 961 genes remaining, before it was decided to use less than or equal to 0.001, after which 688 genes remained, a number low enough that it could be properly analysed without fear that important interactions might be missed. The remaining genes were ordered for fold change between EPO+LIF versus EPO and the ten most highly up- and downregulated genes are shown in Table 6.3.

Table 6.3 differs from table 6.2 in that it shows genes that are not significantly changed by the addition of EPO, whereas those in table 6.2 were significantly changed between EPO and the control and between EPO+LIF and EPO. By comparing the two tables it can be seen that the three most highly upregulated genes by EPO+LIF were not significantly changed by EPO alone, suggesting that these could be inhibitory genes that required LIF for activation.

The remaining genes and their expression values versus the control were analysed by hierarchical cluster analysis (Fig 6.18). It appeared from the image that downregulated genes would provide little information here as shown by the large section of green tiles which suggest that in this analysis genes that were downregulated by EPO were only further downregulated by EPO+LIF. Genes that acted in this way did not correlate with, or offer an explanation for, the inhibition seen by EPO+LIF so would not be considered in this analysis.

		EPO vs Ctrl		EPO+LIF vs. EPO	
Gene name	**Accession Number**	**Average Log_2 FC**	**P.value**	**Average Log_2 FC**	**P.value**
Upregulated					
Gfap	NM_017009	0.05	0.7581313	6.70	0.0000000
Gpx2	NM_183403	-0.40	0.1826736	5.66	0.0000001
Emp3	NM_030847	0.06	0.8565486	4.74	0.0000003
Itga9	XM_006244173	1.54	0.0007258	4.46	0.0000021
Bcl3	NM_001109422	0.96	0.0000078	4.38	0.0000000
Prom1	NM_021751	0.08	0.7467147	4.23	0.0000007
Cxcl14	NM_001013137	-0.21	0.1784740	4.08	0.0000001
Tmem176a	NM_001039008	0.08	0.5659822	3.96	0.0000000
Ccl20	NM_019233	-0.69	0.3883343	3.94	0.0000333
Tmem176b	NM_134390	2.40	0.0000498	3.45	0.0000002
Downregulated					
Fam64a	NM_001113781	-0.53	0.0018208	-1.45	0.0000072
Shroom2	NM_001047893	1.73	0.0001706	-1.52	0.0001231
Ndnf	XM_006236609	-0.20	0.4210522	-1.55	0.0001464
Nod1	NM_001109236	-0.83	0.0182174	-1.56	0.0009928
Dct	XM_006222052	-0.06	0.6137649	-1.58	0.0000062
Pcp4	NM_013002	-0.64	0.0642694	-1.62	0.0006832
Cd36	NM_031561	4.85	0.0000000	-1.78	0.0000243
Esam	NM_001004245	-0.80	0.0076948	-1.86	0.0002212
Htr2c	NM_012765	5.14	0.0000000	-1.98	0.0000020
Slc15a1	NM_057121	0.50	0.0084439	-2.30	0.0004087

Table 6.3: The most highly up- and downregulated genes between cells treated with EPO+LIF and EPO alone at 20 hours. Genes were first cut for significant changes between EPO+LIF and EPO. Significance was defined as a p.value less than 0.001 and fold change greater than 1.5.

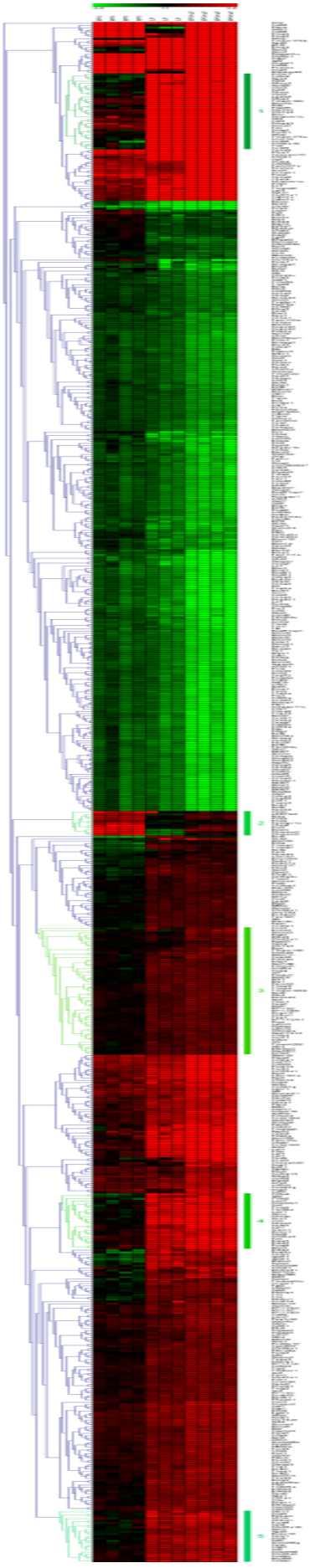

Figure 6.18: Genes changed by EPO+LIF vs EPO at 20 hours. Hierarchical clustering and heat map of the differentially expressed transcripts identified by comparing EPO+LIF versus EPO at a threshold of 1.5 fold change and $P<0.001$. Each sample represents the expression change compared to the mean Log_2 of the control. Red indicates an increase and green indicates a decrease in expression compared to the controls. Average linkage clustering analysis was performed using Genesis software. Four columns of each treatment are biological replicates. The whole image is shown to give a full overview of the analysis. Green bars indicate clusters of interest.

Original in colour

6.3.2.1 Transcripts upregulated by EPO+LIF

Several clusters of interest were identified here that were unaltered by EPO but upregulated by EPO+LIF, therefore representing potential genes that are inhibitory to myelin production (Fig 6.19). Cluster 1 included Fos, as mentioned in the 1 hour analysis where its expression was stronger so it was successfully validated at that time point. Also in this cluster was Tlr2 which was also of importance in the 1 hour analysis. Furthermore, Myd88 and Irf1 which are both downstream of Tlr2 appeared in clusters 5 and 3 respectively. Tlr2 was validated because it, and its downstream signalling components, were present in both 1 hour and 20 hour analysis and because it is more abundant on oligodendrocyte precursor cells than mature oligodendrocytes. Furthermore, stimulating Tlr2 with hyaluronan blocked maturation of the immature cells (Sloane 2010). The qPCR validation was successful (Fig 6.20) as samples treated with LIF and those treated with EPO+LIF expressed significantly more Tlr2 than the control samples or those treated with EPO alone, reflecting the results seen in the microarrays. Tlr2 will be investigated further to see if the results here have elucidated a biological functionality (Section 6.3.3).

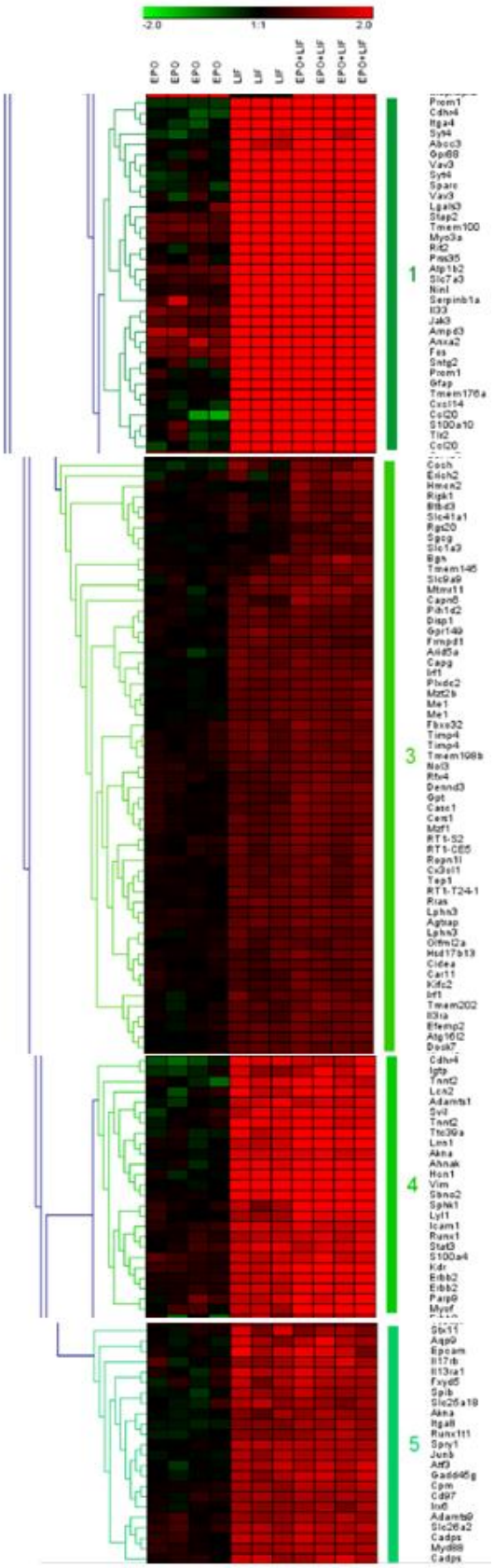

Figure 6.19: Genes changed by EPO+LIF vs EPO at 20 hours. Selected are those unchanged by EPO alone but upregulated by EPO+LIF. Hierarchical clustering and heat map of the differentially expressed transcripts identified by comparing EPO+LIF versus EPO at a threshold of 1.5 fold change and $P<0.001$. Expression changes in EPO treated samples and LIF treated samples are also shown expressed vs the control. Each sample represents the expression change compared to the mean Log_2 of the control. Red indicates an increase and green indicates a decrease in expression compared to the controls. Average linkage clustering analysis was performed using Genesis software. Four columns of each treatment are biological replicates. Bars 1, 3, 4, & 5 indicate clusters of interest.

Original in colour

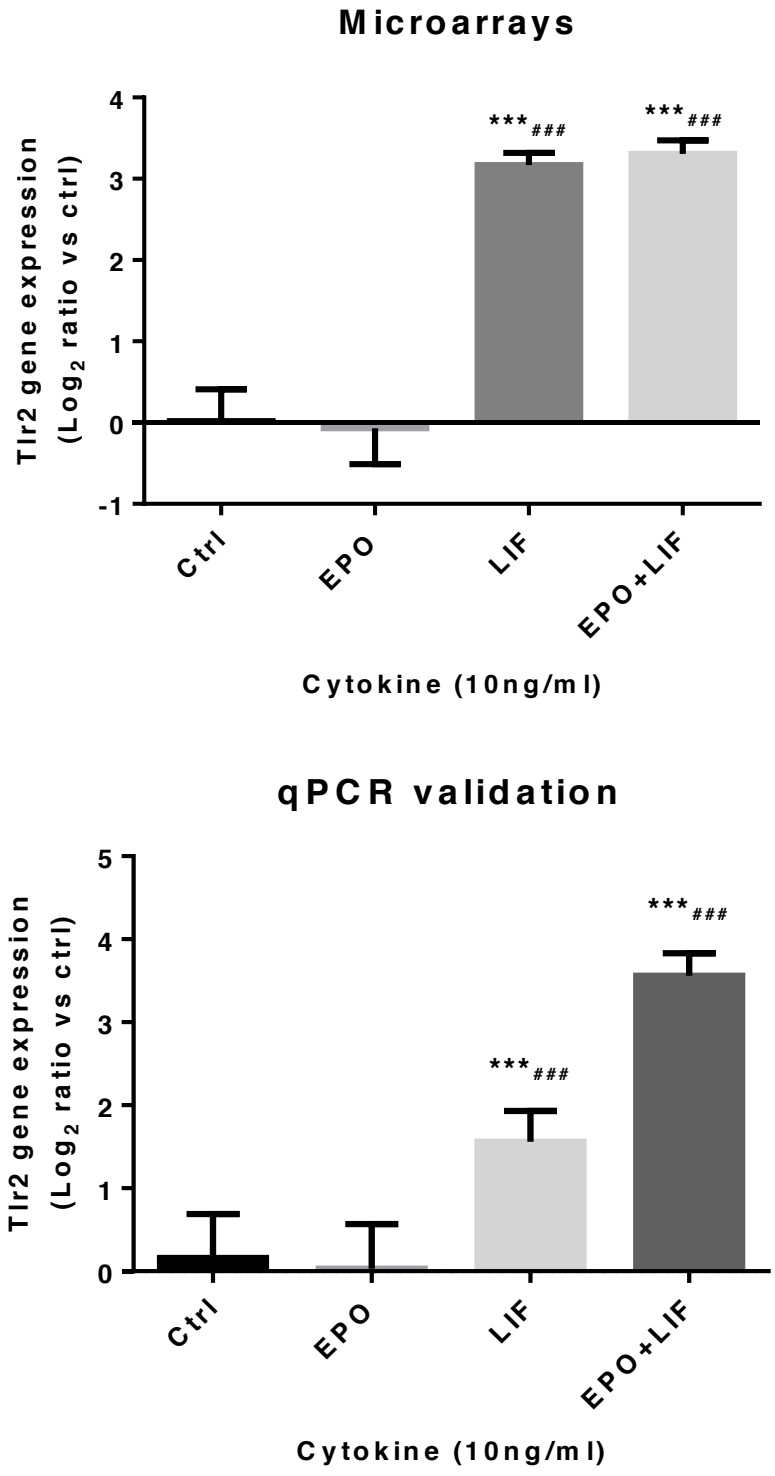

Figure 6.20: qPCR validation of the microarray data; Tlr2. Each graph compares the mean Log_2 FC of Tlr2 gene expression after the specified cytokine treatment (10ng/ml) versus 1 control sample ±SD performed in quadruplicate. RT and qPCR were performed on the same samples as those used in the microarrays. ***P<0.001 vs ctrl & ###P<0.001 vs EPO alone.

Figure 6.20 cont.:

Microarray results:

			P value	
Cytokine (ng/ml)	**Tlr2 Mean**	**SD**	**vs Ctrl**	**vs EPO**
Ctrl	0.0	0.4		
EPO	-0.1	0.4	0.7525	
LIF	3.2	0.1	4.78E-05	7.13E-05
LIF+EPO	.3.	0.2	4.66E-06	7.29E-06

qPCR validation results:

			P value	
Cytokine (ng/ml)	**Tlr2 Mean**	**SD**	**vs Ctrl**	**vs EPO**
Ctrl	0.2	0.5		
EPO	0.0	0.5	0.7496	
LIF	3.2	0.4	9.28E-05	7.44E-05
LIF+EPO	3.6	0.3	2.92E-05	2.4E-05

Lipocalin 2 (Lcn2) also appears in cluster 4. LCN2 is an iron-trafficking protein that, among multiple other functions, has been linked in several studies to demyelinating diseases. $Lcn2^{-/-}$ mice exhibit an amelioration of the symptoms of EAE and are less susceptible to white matter damage after subarachnoid haemorrhage, damage which in wild type mice caused an increase in Lcn2 (Egashira 2014, Nam 2014). There is debate about whether Lcn2 is neuroprotective or neurodetrimental. It is known that it is upregulated after neuronal injury but the consequences of this are unclear. These links of Lcn2 to demyelinating diseases justified validation of Lcn2 as it could provide novel evidence to a causative agent of demyelination. The validation was successful (Fig 6.21). Expression of Lcn2 was significantly increased by LIF and EPO+LIF treatment both in the microarrays and in the qPCR validation. Investigation into the potential biological functionality of Lcn2 would be carried out further (Section 6.3.4).

The genes represented in clusters unaltered by EPO but upregulated by EPO+LIF were entered into STRING to provide evidence of functional connections between the proteins they code for (Fig 6.22, a close-up of the centre of the STRING analysis is shown in Fig 6.23). Tlr2, Myd88, and Irf1 again feature prominently in the centre of the image. After being identified from both the 1 hour and 20 hours analysis this pathway will feature prominently in further investigation. JunB, Fos, and Stat3, all identified in previous work, are also in the centre of this image with a large number of functional connections to other proteins.

In the STRING image, Lcn2 had a functional connection to Tlr2 and Tlr2 has been shown to increase the expression of Lcn2 in epithelial cells and macrophages (Eller 2013). Lcn2 also has a connection here to Erb-b2 receptor tyrosine kinase-2 (Erbb2) which is a receptor upstream of the MAPK and Pi3K pathways, among others (Yarden 2001), which has been linked to Schwann cell myelination (Basak 2015).

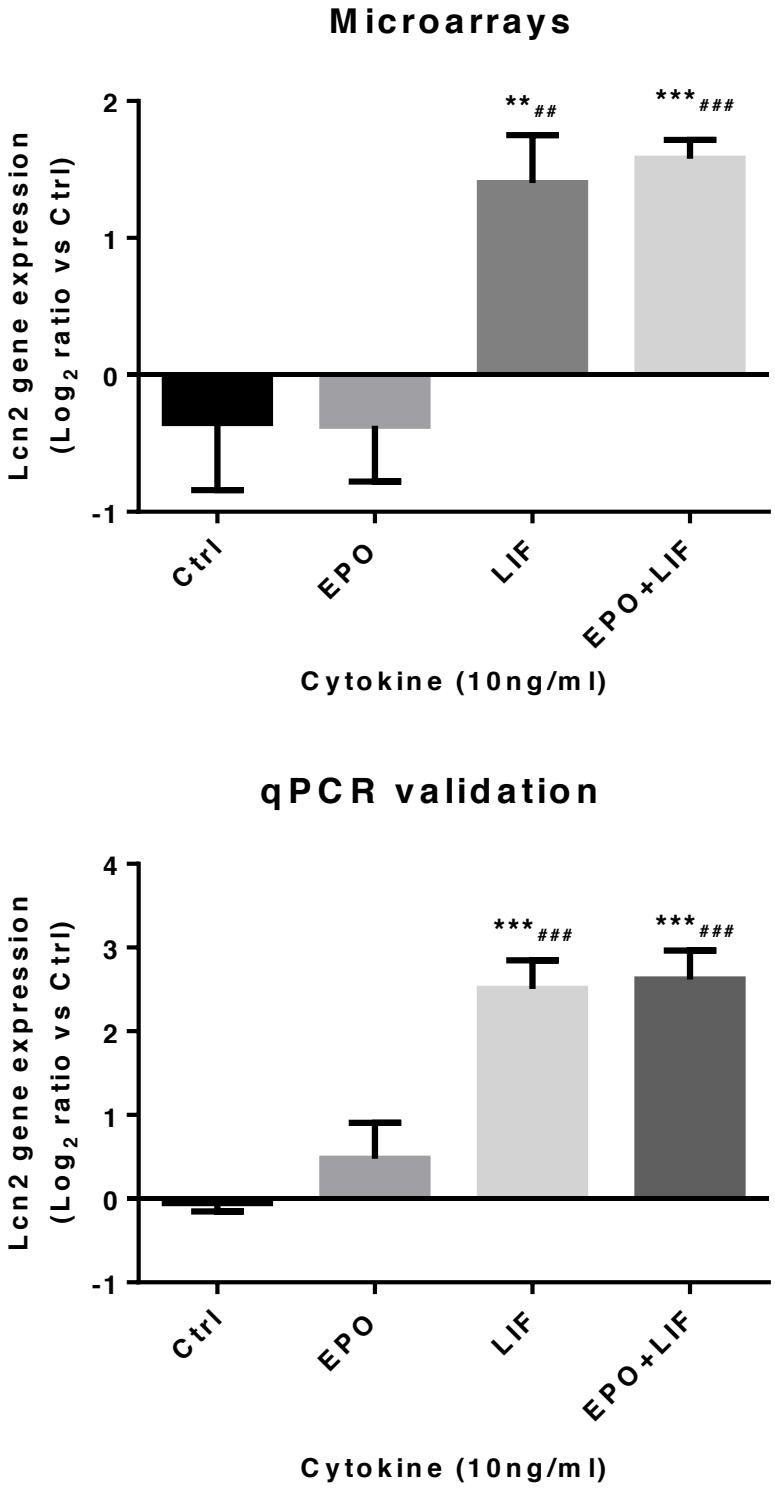

Figure 6.21: qPCR validation of the microarray data; Lcn2. Each graph compares the mean Log_2 FC of Lcn2 gene expression after the specified cytokine treatment (10ng/ml) versus 1 control sample ±SD performed in quadruplicate. RT and qPCR were performed on the same samples as those used in the microarrays. **P<0.01, ***P<0.001 vs ctrl & ##P<0.01, ###P<0.001 vs EPO alone…

Figure 6.21 cont.:

Microarray results:

			P value	
Cytokine (ng/ml)	**Lcn2 Mean**	**SD**	**vs Ctrl**	**vs EPO**
Ctrl	-0.4	0.5		
EPO	-0.4	0.4	0.9697	
LIF	1.4	0.4	0.0035	0.0019
LIF+EPO	1.6	0.1	0.0002	0.0001

qPCR validation results:

			P value	
Cytokine (ng/ml)	**Lcn2 Mean**	**SD**	**vs Ctrl**	**vs EPO**
Ctrl	0.0	0.1		
EPO	0.5	0.4	0.0546	
LIF	2.5	0.3	7.38E-06	0.0003
LIF+EPO	2.6	0.3	6.3E-06	0.0002

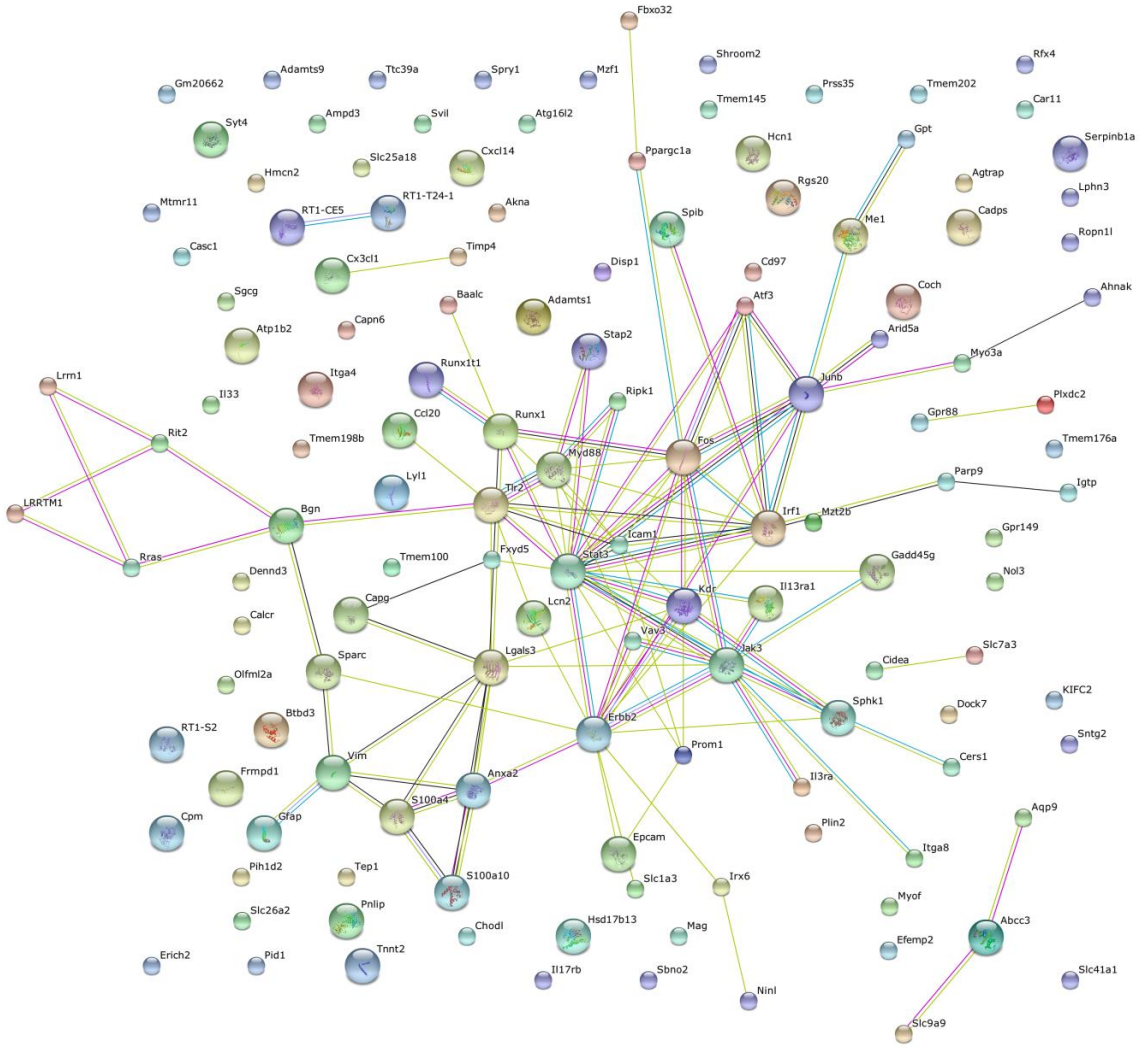

Figure 6.22: STRING analysis of genes unaltered by EPO but upregulated by EPO+LIF at 20 hours. All transcripts were filtered for EPO+LIF vs EPO with parameters of fold change greater than 1.5 and $p<0.001$. The genes represented here were selected for from hierarchical cluster analysis where clusters that were unaltered by EPO but upregulated by EPO+LIF were identified. The nodes represent the proteins encoded by the genes and the lines between the nodes represent functional interactions between them. Confidence score >0.4 with text mining.

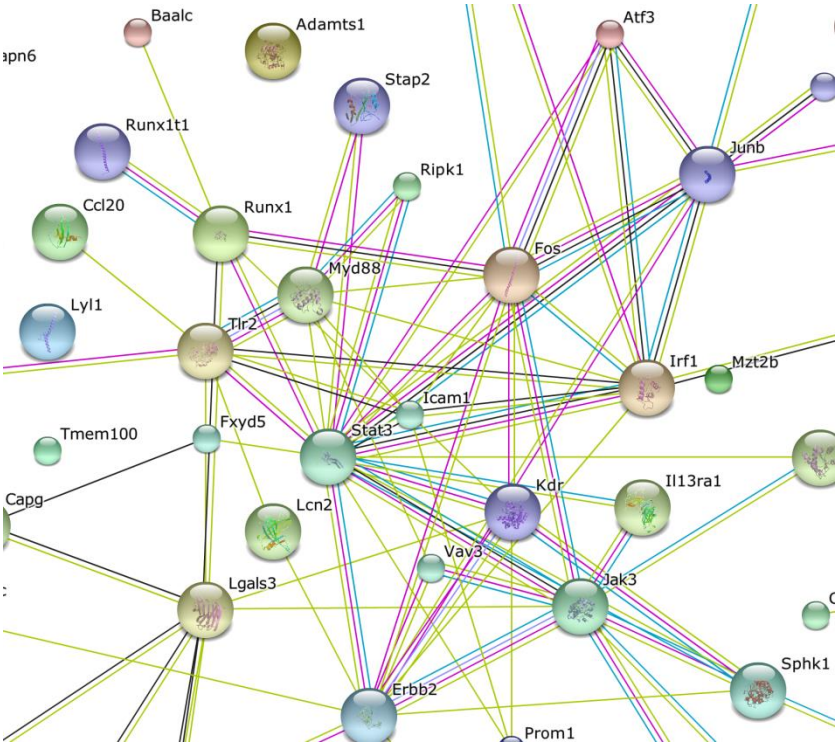

Figure 6.23: STRING analysis of genes unaltered by EPO and upregulated by EPO+LIF at 20 hours. Centre of Figure 6.22. All transcripts were filtered for EPO and LIF vs EPO with parameters of fold change greater than 1.5 and $p<0.001$. The genes represented here were selected for from hierarchical cluster analysis where clusters that were unaltered by EPO but upregulated by EPO+LIF were identified. The nodes represent the proteins encoded by the genes and the lines between the nodes represent functional interactions between them. Confidence score >0.4 with text mining.

Original in colour

6.3.3 Biological functionality of Tlr2

Tlr2 was chosen for further analysis into its effects on myelination from the outcome of this microarray analysis. In the microarrays Tlr2 was not induced by EPO, but it was very highly induced by both LIF alone and EPO+LIF treatments, a pattern of induction that was seen at both time points. Furthermore, Myd88, a signalling mechanism downstream of Tlr2, was also present throughout the microarrays, with a similar expression pattern as Tlr2. Myd88 strengthened the hypothesis that Tlr2 and its corresponding signalling mechanisms are implicated in the inhibition by LIF of EPO-induced Mog.

Tlrs are receptors that reside on the surface of cells and provide a crucial component of the innate immune system. They have the ability to recognise pattern-associated molecular patterns (PAMPs) that reside on the surface of a variety of pathogens, with the same PAMPs being present on many different species. The PAMPs vary very little between species thus allowing Tlrs to recognise a wide range of infectious agents and induce the innate immune response as well as activating the creation of an adaptive immune response (Medzhitov 2000).

In addition to recognising foreign PAMPs, Tlrs have the ability to recognise endogenous danger signals called danger-associated recognition molecules. The majority of these molecules are a product of the immune system, but in the CNS they are known to be released upon disease and infection after cell death and necrosis and the remodelling and regeneration of tissue (Piccinini 2010). Microglia, neurons, astrocytes, and oligodendrocytes of the CNS all express Tlrs. Oligodendrocytes express Tlrs 2 and 3, while Tlr2 is also present on astrocytes and microglia (Kielian 2006, Bsibsi 2012). Generally, the final effect of Tlr stimulation in the CNS is facilitation of innate immune activation, but the exact role of the Tlrs that are expressed in oligodendrocytes is unknown but they may be involved in regulating inflammation, gliosis, and demyelination (Kigerl 2007). A link between Tlr2 and EAE has been determined, although from studies using knockout models it seems that it is Myd88 that is responsible essential for the action of Tlrs (Prinz 2006).

In order to determine a biological functionality of Tlr2 the cells were stimulated with Pam3, an agonist of Tlr2 (Jin 2007). It was hypothesised that Tlr2 stimulation would inhibit EPO-induced Mog as it was upregulated by treatment with LIF and with EPO+LIF. CG4 cells were plated at a density of $4x10^4$ cells/well and differentiated after 24 hours incubation. Simultaneous to differentiation the cells were treated with EPO, LIF, and Pam3 before incubation for 3 days. The experiment was stopped using QIAzol and RT and qPCR were performed to measure Mog expression.

As expected from the results of previous work, LIF inhibited EPO-induced Mog (Fig 6.24). Interestingly, Pam3 also inhibited when added with EPO but without LIF, suggesting that the CG4 cells expressed basal levels of Tlr2 without stimulation by LIF. However, when EPO, LIF, and Pam3 were all added simultaneously Pam3 increased the inhibition shown by LIF to the point where there was no difference between the expression of Mog by the EPO+LIF+Pam3 group and the control group (P=0.09). The experiment was repeated and the same results obtained. These results showed that, as the microarrays suggested, LIF increased Tlr2 expression as stimulation of Tlr2 increased the inhibition seen. Furthermore, the inhibition of EPO-induced Mog by Pam3 alone showed that a basal level of Tlr2 was significant enough to cause Mog inhibition. While several investigations have shown that oligodendrocytes express Tlrs (Bsibsi 2002, Kigerl 2007, Sloane 2010), there is no clarification about the effect of that they have on oligodendrocytes. For example, Bsibsi (2012) found that Tlr2 stimulation promoted oligodendrocyte survival, differentiation, and myelination, a direct contradiction to what has been found in this work in both the gene expression microarrays and follow-up experiments on the effect of Tlr2 on Mog induction (Bsibsi 2012). This contradictory evidence is potentially explained by Wu *et al* (2013) who found that Tlr2 is important for both the demyelination after nerve injury and the subsequent remyelination (Wu 2013).

The work on Tlr2 had shown that Tlr2 has a functional effect on myelination. Tlr2 is the only Tlr that showed a significant upregulation in the gene expression microarrays, but the TLR2 protein must heterodimerise with either TLR1 or TLR6 to create a functional receptor. But, neither of these Tlrs are present on oligodendrocytes, which only express Tlrs 2 and 3 (Bsibsi 2012). The Tlrs must form a heterodimer with one-another before binding to their ligand to induce the required

signalling pathways. Oligodendrocytes only express Tlrs 2 and 3, while Tlr2 must bind with Tlr1 or 6 to form its heterodimer. This presents a paradox as Tlr2 must be associating with something. The responsiveness of oligodendrocytes to Tlr stimulation could be evidence that Tlr2 can form a homodimer, an interaction that has been previously hypothesised but not proven (Oiu 2013). Extensive follow-up experimental investigation would be needed to confirm that a Tlr2 protein homodimer is being formed, or to show that indeed Tlrs 1 or 6 are present on the surface of oligodendrocytes.

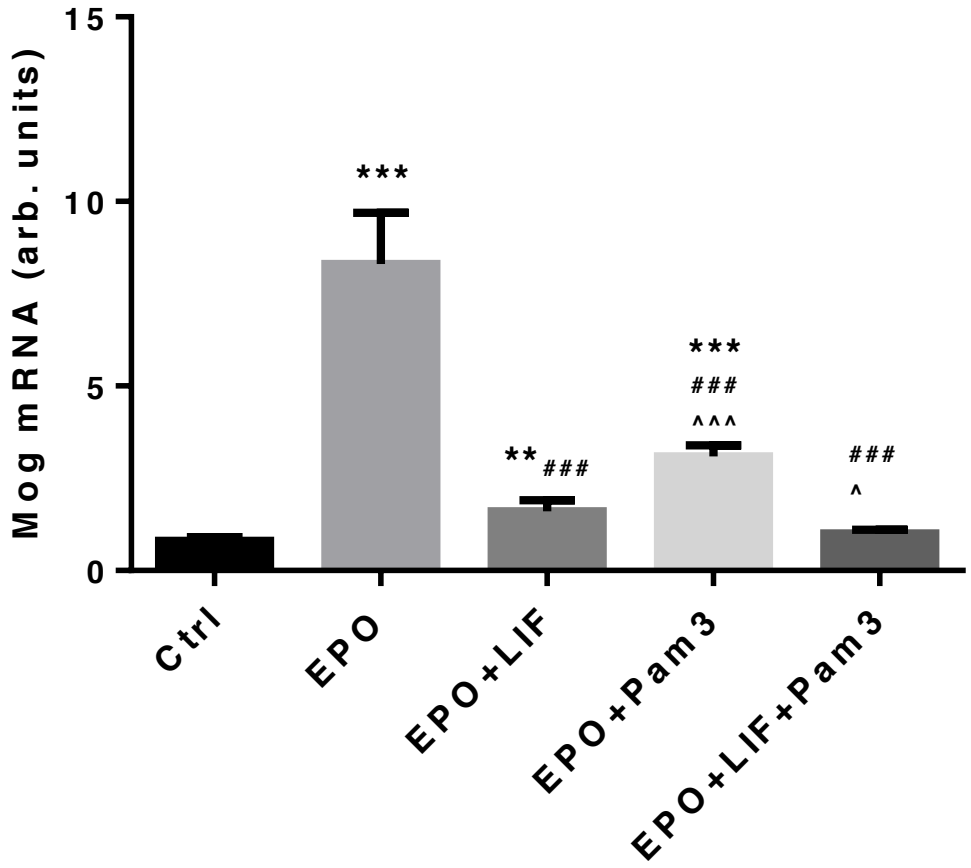

Figure 6.24: Pam3 treatment increased the inhibitory effect of LIF on EPO-induced Mog expression. CG4 cells were plated at a density of 40,000/well and differentiated for three days after treatment with the indicated cytokine. Mog mRNA was measured by qPCR and results are expressed as arbitrary units versus the control. Data represented here are the mean ± SD of quadruplicate samples. ** P<0.01, ***P<0.001 vs ctrl & ##P<0.01, ###P<0.001 vs EPO alone, & ^P<0.05, ^^^P<0.001 vs EPO+LIF.

			P value		
Sample	**Mog Mean**	**SD**	**vs Ctrl**	**vs EPO**	**vs EPO+LIF**
Ctrl	0.8	0.1			
EPO	8.3	1.4	3.37E-05		
EPO+LIF	1.6	0.3	0.0012	6.94E-05	
EPO+Pam3	3.1	0.3	1.14E-05	0.0003	0.0004
EPO+LIF+Pam3	1.0	0.1	0.0902	0.0003	0.0121

6.3.4 Biological functionality of Lipocalin 2

Lcn2 is a protein involved in a range of cellular processes such as cell survival (Kehrer 2010), migration (Yang 2009) and differentiation (Bolignano 2008) and is linked to innate immunity by preventing iron metabolism that is essential of bacterial propagation (Goetz 2002, Yang 2002). Lcn2 has been linked to diseases and injuries of the nervous system. Lcn2 gene expression was found upregulated at the onset of EAE, with expression continuing throughout the course of disease, primarily being expressed in astrocytes and monocytes (Berard 2012). Furthermore, $Lcn^{-/-}$ mice suffered from ameliorated symptoms of EAE (Nam 2014). These experimental findings have also been replicated in human experiments; Lcn2 protein levels were increased in the cerebrospinal fluid of MS patients (Berard 2012) and the gene expression of Lcn2 in the cerebrospinal fluid coincided with active phases of the disease (Marques *et al.* 2012). Lcn2 expression was the most highly upregulated in patients with progressive MS, the final and most severe stage of the disease, over those with relapsing-remitting MS (Al Nimer *et al.* 2016). Furthermore, Lcn2 expression was increased after subarachnoid haemorrhage and $Lcn^{-/-}$ mice were less susceptible to white matter damage following such an injury (Egashira 2014). In the brain, Lcn2 binds to a receptor called the brain type organic cation transporter (24p3R) (Devireddy 2005).

Upon investigating the literature, there seemed to be strong links between Lcn2 and demyelinating diseases, yet its relationship to oligodendrocytes has not been investigated (Berard 2012, Al Nimer *et al.* 2016). Therefore it was thought that it could be a novel molecule to investigate further. The validation was successful (Fig 6.21) so it was decided to treat the CG4 cells with recombinant human Lcn2 to see if it has a functional effect on their myelinating capacity. Both the microarrays and the validation correlated increased Lcn2 with decreased Mog, i.e. it was treatment with LIF and EPO+LIF that caused the most Lcn2 induction, suggesting that it had a causative role in myelin inhibition.

CG4 cells were plated at a density of $4x10^4$ cells/well and differentiated after overnight incubation. EPO and Lcn2 were added at the point of differentiation. Lcn2 has a molecular weight of 25kDa (Flower 1996) so it is roughly comparable in

molecular weight to EPO and LIF, however the expression of 24p3R, the receptor for Lcn2, on these cells is unknown. Therefore, similar concentrations as those used for EPO and LIF were a good starting point, but a range of concentrations of Lcn2 were used (1, 10 and 50ng/ml). The experiment was stopped after 3 days and Mog was measured by qPCR to see if the presence of Lcn2 had inhibited Mog expression.

There was no inhibition of EPO-induced Mog by any of the attempted concentrations of Lcn2 (Fig 6.25). All the treatments induced a significant increase of Mog expression, but the addition of Lcn2 had no significantly different effect than the treatment with EPO alone ($P>0.05$). There was no apparent effect of toxicity of Lcn2 on these cells, and circulating Lcn2 is around 80ng/ml in healthy people, with its expression being highly influenced by the presence of disease; circulating concentrations can reach 800ng/ml (Wheeler 2008). Therefore, one final high concentration of Lcn2 was used to determine if it had any impact at all on these cells.

The experiment was run as before but with just one concentration of 300ng/ml Lcn2. Again, the addition of Lcn2 showed no effect (Fig 6.26). EPO alone increased Mog expression, as expected, but the addition of Lcn2 had no effect on EPO-induced Mog ($P=0.97$). These two experiments led to the conclusion that Lcn2 has no direct effect on oligodendrocytes at the concentrations investigated and it did not cause inhibition of myelination alone as LIF can. This may mean that Lcn2 is involved in the inhibition of myelin gene expression, but it is not sufficient to cause the inhibition alone.

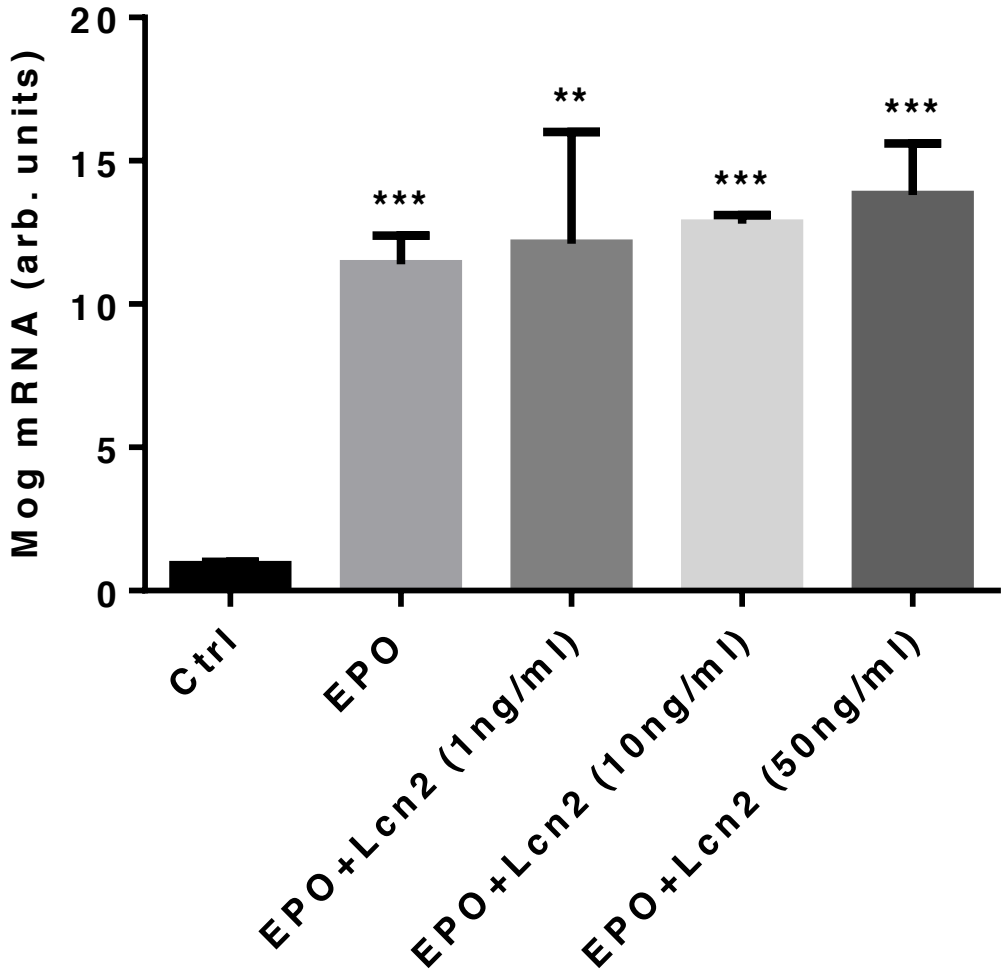

Figure 6.25: Lcn2 treatment did not inhibit EPO-induced Mog expression. CG4 cells were plated at a density of 40,000/well and differentiated for three days after treatment with either EPO alone, or with the addition of Lcn2 at various concentrations. Mog mRNA was measured by qPCR and results are expressed as arbitrary units versus the control. Data represented here are the mean ± SD of quadruplicate samples. ** P<0.01, ***P<0.001 vs the control.

			P value	
Samples	**Mog mean**	**SD**	**vs ctrl**	**vs EPO**
Ctrl	0.9	0.1		
EPO	11.4	1.0	7.48E-07	
EPO+Lcn2 (1ng/ml)	12.1	3.9	0.0012	0.7528
EPO+lcn2 (10ng/ml)	12.8	0.3	1.39E-08	0.0748
EPO+Lcn2 (50ng/ml)	13.8	1.8	6.77E-06	0.0615

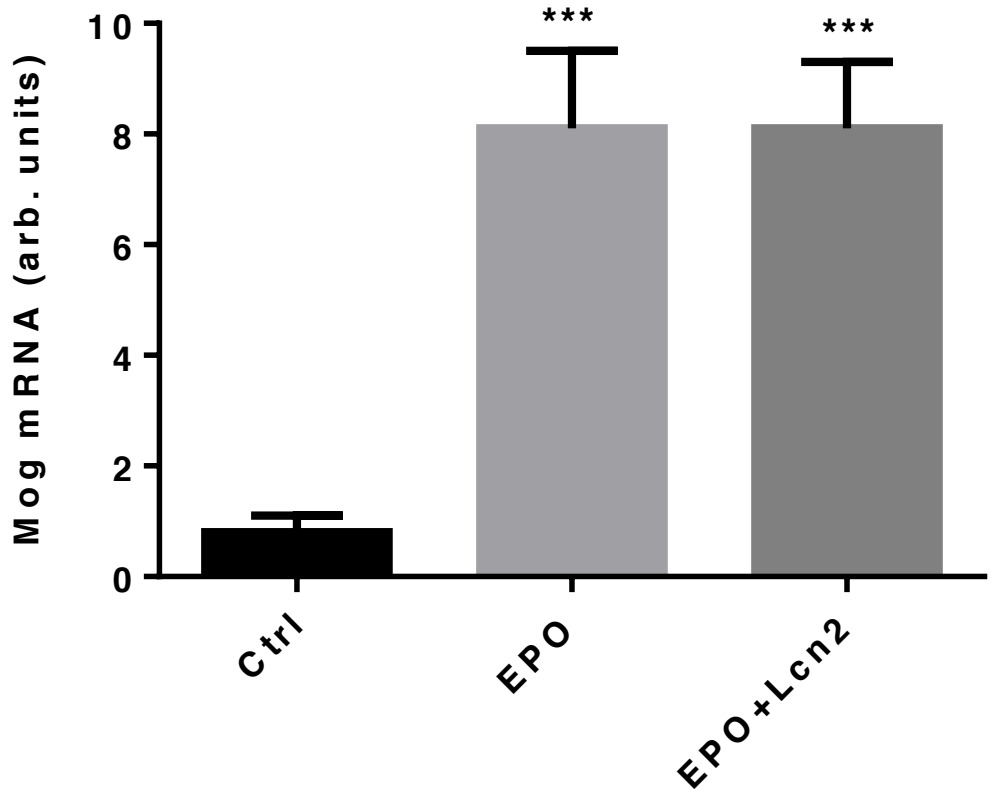

Figure 6.26: High-concentration Lcn2 treatment did not inhibit EPO-induced Mog expression. CG4 cells were plated at a density of 40,000/well and differentiated for three days after treatment with either EPO alone or with the addition of Lcn2 at 300ng/ml. Mog mRNA was measured by qPCR and results are expressed as arbitrary units versus the control. Data represented here are the mean ± SD of quadruplicate samples. ***P<0.001 vs the control.

			P value	
Samples	**Mog mean**	**SD**	**vs ctrl**	**vs EPO**
Ctrl	0.8	0.3		
EPO	8.1	1.4	5.82E-05	
EPO+Lcn2	8.1	1.2	1.90E-05	0.9747

6.4 Conclusions

- Hierarchical clustering was used to identify genes that may inhibit EPO-induced Mog at both 1 hour and 20 hours
- Validation of microarrays by qPCR was carried out to confirm the results seen
- Tlr2 and Lcn2 were identified from the microarrays and a biological functionality in CG4 cells of Tlr2 was confirmed.

The purpose of the gene expression microarray analysis was to determine the effect that LIF had on gene expression in CG4 oligodendrocyte precursor cells. The genes expressed after treatment with LIF alone and when EPO+LIF were added simultaneously were investigated, and comparing these expression profiles to those expressed by EPO treatment alone.

Several methods were used to identify genes that may be important in the inhibition of EPO-induced Mog expression. Initially the most highly regulated genes between EPO versus the control and EPO+LIF versus EPO were found by ordering for fold change. A few genes of interest were identified here, and these will be crucial as they were highly regulated between the groups.

The genes were finally sorted for significance between EPO+LIF and EPO alone, without the original EPO versus the control filter. At 20 hours the p value was reduced to less than or equal to 0.001 because of the large number of genes present. The cluster analyses from the sorted genes elucidated many genes that may have a causative association with the inhibition of EPO-induced Mog expression. Specifically, genes that were unaltered by EPO but upregulated by EPO+LIF and those upregulated by EPO and downregulated by EPO+LIF were investigated further. These patterns of expression help to answer the question of what caused LIF to have an inhibitory effect on EPO-induced Mog.

STRING analysis was used on the selected clusters to help identify genes that had not previously been identified and this pointed to more genes that should be considered.

There were more genes of interest at 20 hours than at 1 hour because more late-induced genes were present. The 20 hour analysis may have been more interesting overall but the genes at 1 hour were important because they show what was initiated first and what then leads on to the later expression.

Several of the genes of interest from the microarrays were validated by qPCR to confirm that the expression detected in the microarrays correlated with qPCR analysis on these samples. The majority of the validations were successful, but a couple that did not correlate highlighted the importance of checking any value from the gene expression microarrays before taking investigations into the specified gene any further.

Socs3 was identified in the microarray analysis at 1 hour. Socs3 is a negative feedback regulator of the JAK-STAT signalling pathway that has been investigated extensively in previous experimental work presented in this thesis (Chapter 4). It was induced significantly by LIF, but not by EPO, and its expression remained elevated when EPO and LIF were both present. This pattern of expression was seen both in the microarray analysis and qPCR analysis on CG4 cells. It is believed that the induction of Socs3 by LIF inhibited EPO-induced Mog expression.

Tlr2 appeared consistently throughout the microarrays and analysis of the literature suggested that it negatively regulated myelination. Its expression was significantly upregulated by the presence of LIF at both time points. Furthermore, Myd88, a signalling molecule that is downstream of Tlr2 was also present consistently throughout the analysis. For these reasons it was decided to test the biological functionality of Tlr2 by stimulating the cells with Pam3, a Tlr2 agonist. Treatment thus increased the inhibitory effect seen by LIF on EPO-induced Mog, suggesting that LIF upregulated Tlr2 and stimulation of this lead to an increase in inhibition.

The results from the gene expression microarrays elucidated new pathways that may be involved in the inhibition of myelination, such as Tlr2 which is novel data as it has been implicated in neuroinflammation and demyelination, but not an inability to produce myelin.

So far the work in the current thesis has gone a long way towards investigating the interaction between EPO and LIF and how LIF had an inhibitory effect on the signalling induced by EPO, including looking at known induction pathways by both cytokines and using gene expression microarrays to elucidate the genetic mechanisms behind the inhibition. The next chapter will look at applying this knowledge to wound healing models, as it is believed that the application of tissue protective cytokines to wounds could accelerate healing and decrease the prevalence of chronic wounds.

Chapter 7. *In vitro* wound healing assay

7.1 Introduction

Wound healing is a complex process that aims to reinstate the strength and integrity of the skin, the body's first defence against invading pathogens. Chronic wounds can develop through a number of mechanisms including a prolonged inflammatory response. Chronic wounds that do not heal cause considerable pain, disability, and possible amputation.

The wound healing process consists of four overlapping stages, each of which prepares the wound for the following stage (Shaw 2009) (Section 1.2.2.1). The first stage of wound healing is haemostasis, the primary aim of which is to prevent exsanguination. Pro-inflammatory cytokines released at this stage include TGF-β, PDGF, FGF, and epidermal growth factor (Werner 2003). Further blood loss is prevented by the formation of a clot from the transformation of fibrin from fibrinogen and the activation of thrombin and platelets (Mosesson 2005).

The next phase is the inflammatory phase which is characterised by the progressive infiltration of neutrophils, macrophages, and lymphocytes and aims to establish an immune barrier against invading microorganisms (Hart 2002). Initially neutrophils destroy debris and bacteria in the wound, but this action is carried out by macrophages later on that also provide various growth factors that are important in controlling inflammation (Velnar 2009). Immune cells that are already present in the tissue become activated in the inflammatory period, which then release a variety of cytokines and chemokines. Inflammation is crucial and will continue as long as debris and bacteria are present, but a prolonged inflammatory response has a negative effect and can lead to a chronic wound.

The third stage, proliferation, follows in which the aim switches from preventing further damage to repair. There is a large amount of cell migration into the wound as well as proliferation of those cells already present that leads to re-epithelialisation

(Ilina and Friedl 2009). Granulation tissue formation is vital in this phase to replace the lost mass of tissue and to aid contraction of the wound (Greaves 2013).

Remodelling is the final stage. It involves the formation of a normal epithelium and of scar tissue below the epithelium and can take up to two years before completion. This last stage is not often orchestrated properly in an attempt to complete healing quickly with priority given to wound closure over aesthetics. In this situation, the type 1 collagen is often laid down by the fibroblasts in excess and in a dense parallel arrangement of the matrix that leads to the development of a scar.

The complex interactions between cytokines, cells and the extracellular matrix are central to wound healing. For example, a lack of PDGF and its receptor have been strongly linked to impaired wound healing; its appearance is delayed in impaired wound healing of aged mice (Ashcroft *et al.* 1997) and human dermal ulcers have significantly lower levels of PDGF than surgically created acute wounds (Pierce *et al.* 1995). Some FGFs are highly upregulated in a wound, for example FGF7 expression increased 100-fold by 24 hours after wounding in humans (Marchese 1995). Blocking FGF2 using a polyclonal antibody led to a reduced cellularity and vascularisation of the granulation tissue (Broadley 1989). VEGFA is also strongly induced by cutaneous injury, with the expression mainly coming from keratinocytes and macrophages, and its receptor is upregulated on the blood vessels of cutaneous tissue (Frank 1995, Lauer *et al.* 2000). Furthermore, reduced expression of VEGFA is associated with defects in wound healing (Lauer *et al.* 2000).

TGF-β is also crucial to wound healing. Wounds sustained by developing embryos heal completely without any evidence of scarring (reviewed in (Larson *et al.* 2010)). The expression of TGF-β isoforms is very different between embryonic and post-natal wounds; embryonic wounds express very high levels of TGF-β3 and very low levels of TGF-β1 whereas adult wounds predominantly express TGF-β1 (Cowin AJ 2001, Ferguson and O'Kane 2004). Suppression of TGF-β1 and/or TGF-β2 resulted in improved adult healing while deletion of TGF-β3 was detrimental (Shah *et al.* 1992, Shah *et al.* 1995). These observations show that the balance of TGF-β

isoforms greatly impacts wound healing and the optimum ratio of TGF-β isoforms is essential for scar forming versus scar-free healing.

It is hypothesised here that EPO could be a tissue-protective cytokine with wound healing capabilities as it is in various other tissues. For example, EPO stimulates platelet aggregation (Malyszko 1995), expression of plasminogen activator-inhibitor (Stasko 2002) and tissue factor (Fuste 2002), plus its anti-inflammatory effects (Brines 2008). There is considerable literature in rat and mouse models to suggest that EPO would have a positive effect in skin wound healing. However, most investigations have been performed using systemic EPO treatment (Elsherbiny 2012, Arslantas 2015) with far fewer successful topical treatments (Hong 2014).

Studying wound healing *in vitro* is difficult because of the multitude of cell types, cytokines, and growth factors that combine in a complex array of interactions in order to close the wound. Replication of this very complex process under laboratory conditions would be a near impossibility.

One simple method used by many laboratories to study wound healing *in vitro* is the scratch assay model. This involves plating cells and growing them until they form a confluent monolayer at which point a scratch or "wound" is made down the centre of the monolayer, removing a section of cells. The cells are then treated with the cytokines or growth factors of interest and the area of the scratch measured immediately and at later time points, thus allowing measurement of the percentage of wound closure (Liang *et al.* 2007).

7.2 sEnd-1 cells

The first cell line that was investigated using the scratch assay model was the mouse skin endothelial cell line known as sEnd-1 cells (Williams *et al.* 1989). Initially, the optimal serum concentration needed to be determined so that the cells remained viable, proliferative and migratory and remained attached to the base of the well. An assessment of the speed of wound closure could then be undertaken. Cells were plated at a density of $2x10^5$ cells/well in 12-well plates and cultured in DMEM containing 10% FCS and 1% pen/strep. It was important that the cells were grown to

confluence so that interactions and signals between cells replicated the intact layer of cells in the endothelium of the skin. Once the cells became confluent, a scratch was made down the centre of each well using a p1000 pipette tip, leaving a wound of about 1.5mm in which there were no cells. At this point a horizontal line was drawn along the underside of the plate as a reference point for the position of the scratch wound ensuring that each time a measurement was taken it recorded in a uniform manner. The medium was removed and the cells were washed twice in serum-free DMEM before the medium was replaced with DMEM with 0, 0.1, 1, or 10% FCS. The scratches were photographed immediately, using the line along the bottom of the plate as a reference point for the image. The area of the scratch was measured using ImageJ. The cells were incubated at 37°C and the scratch was photographed and measured again 24, 48, and 72 hours later (Figure 2.5).

The cells treated with 10% FCS had completely repaired the scratch wound in the monolayer by 24 hours after wounding (Fig 7.1). This meant that this concentration caused wound closure too quickly to accurately measure any differences in treatment used on the cells. The decision had to be made whether to use 1 or 0.1% FCS. Treatment with 0.1% FCS closed the wound at the same rate as 0% FCS and there was not any evidence of unhealthy cells. Therefore, it was decided to use 0.1% serum for future experiments.

Various concentrations of EPO were then used to investigate the effect of this cytokine on the scratch wound healing in sEnd-1 cells. The experiment was conducted in the presence of 0.1% FCS and varying concentrations of EPO were used (0, 0.4, 2, and 10ng/ml). In this preliminary investigation, these concentrations were selected based on previous work in CG4 cells to determine the optimal concentration of EPO. At 24 hours there was no significant difference between any of the EPO concentrations and the control samples (without EPO addition), but at 48 hours both 1ng/ml and 10ng/ml had closed the scratch wound significantly more than the control ($P=0.02$, and 0.01 respectively), with 10ng/ml EPO resulting in complete closure of the scratch wound (Fig 7.2). After investigation of the literature, there are no publications regarding an interaction between sEnd-1 cells and EPO, so this result represents the first evidence that these cells respond to EPO. Furthermore, it suggests that EPO may accelerate wound closure in the endothelium.

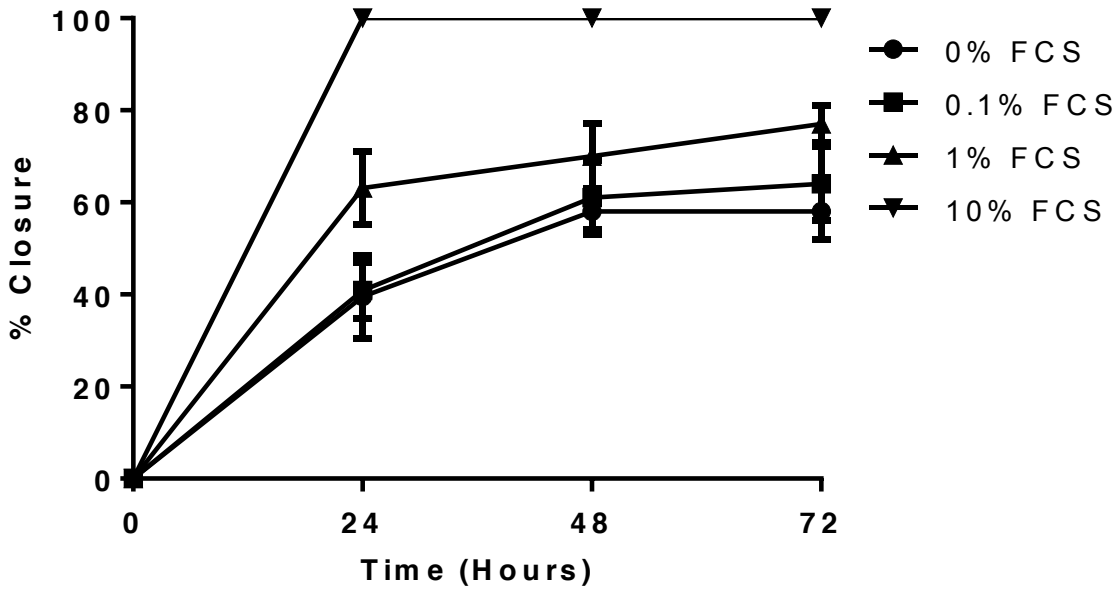

Figure 7.1: Scratch wound closure by sEnd-1 cells treated with varying concentrations of FCS. sEnd-1 cells were plated at a density of $2x10^5$ cells/well in 12-well plates before a 1.5mm scratch was made along the centre of the well containing the confluent cells. The rate at which the wound closed in medium with different percentages of FCS was measured and expressed as percentage closure. 0.1% FCS did not induce significantly more wound closure than the control. 1% FCS resulted in the wound closing more significantly than the control at all time points ($p<0.05$). 10% FCS closed the wound significantly more than the control at all time points ($p<0.001$)

	Time (h)								
	24			48			72		
FCS (%)	Mean closure (%)	SD	P value	Mean closure (%)	SD	P value	Mean closure (%)	SD	P value
0	39.6	0.1		58.1	0.04		57.9	0.06	
0.1	40.8	0.1	0.6539	61.3	0.08	0.5761	64.4	0.08	0.2758
1	63.1	0.1	0.0061	70.5	0.07	0.0349	77.2	0.04	0.0149
10	100	0.1	2.7E-05	100	0	0.0001	100	0	0.0009

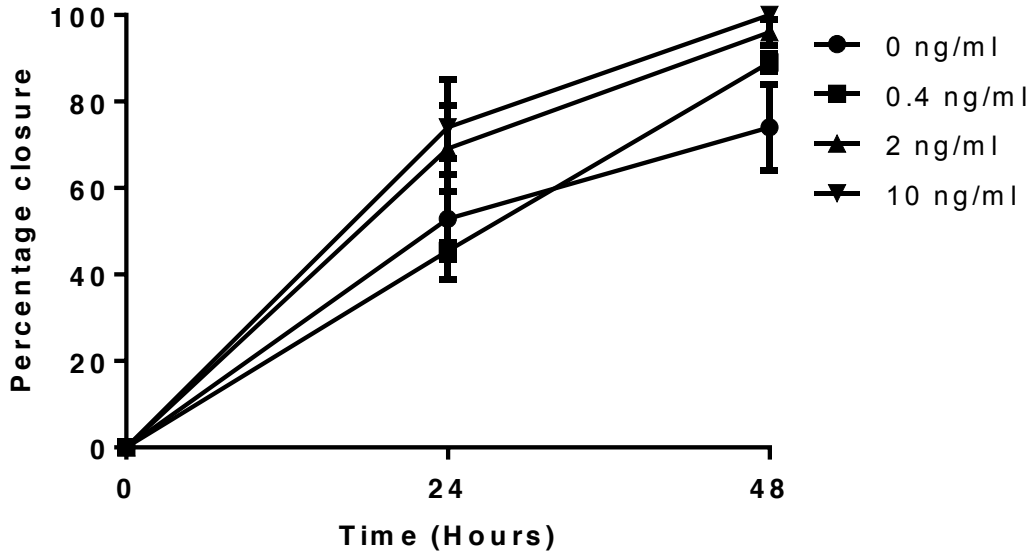

Figure 7.2: EPO concentration response of scratch wound closure by sEnd-1 cells (Experiment 1). sEnd-1 cells were plated at a density of $2x10^5$ cells/well in 12-well plates before a 1.5mm scratch was made along the centre of the well containing confluent cells. The rate at which the wound closed in medium with different concentrations of EPO was measured and expressed as percentage closure. EPO at 2 and 10ng/ml resulted in the scratch wound closing significantly more than the control by 48 hours (p=0.03 and 0.01 respectively).

	Time (h)					
	24			**48**		
EPO (ng/ml)	**Mean closure (%)**	**SD**	**P value**	**Mean closure (%)**	**SD**	**P value**
0	52.9	0.1		73.9	0.1	
0.4	45.5	0.0	0.3978	88.9	0.0	0.0961
2	69.2	0.1	0.1825	95.8	0.0	0.0261
10	74	0.1	0.1523	100	0	0.0139

The experiment in Figure 7.2 demonstrated that EPO influenced sEnd-1 cells to migrate across and close a scratch wound in the cell monolayer. The repeat experiment was performed in exactly the same way as before on cells that were only two passage numbers higher than the original. The cells were treated with 0, 0.2, 2, and 10ng/ml EPO. However, in the repeat experiment, it was observed that with the addition of EPO, at any concentration, there was no effect on the rate of healing, and no significant difference was seen between any samples at either time point (Fig 7.3). This shows significant variability between experimental outcomes. In the second experiment the control scratch wound had closed by 98% in 48 hours, but in the previous experiment the wound had only closed by 74% by the same time point. As the cells were grown to confluence in both experiments and there was no visible difference between them this is unexplained but shows that the experiment produces variable results.

It was decided to compare the effect of LIF treatment on these cells with that of EPO. In an attempt to reduce the variability seen in the previous experiments, 6 replicates were used for each treatment, instead of 3 replicates as used previously. It was also decided to observe the cells at 18 hours post scratch wounding to see if a greater difference was seen at 18 than 24 hours and therefore the effect of the cytokine treatment may be more obvious. The experiment was carried out as before but two concentrations of LIF, 0.2 and 10ng/ml, were used along with EPO at 10ng/ml. This concentration of EPO was used because it had been the concentration that increased scratch wound closure the most in the previous experiment and, despite the variability, 10ng/ml did not seem to be inhibitory compared to the lower concentrations. By 18 hours, both concentrations of LIF resulted in closure of the scratch wound that was significantly quicker than the control (0.2ng/ml $p=0.02$, and 10ng/ml $p=0.01$) (Fig 7.4). In the CG4 OPCs 10ng/ml LIF had an inhibitory effect on myelination (Section 3.2), a negative effect that was not replicated in these sEnd-1 cells as 10ng/ml LIF was the most effective treatment on scratch wound closure here. By 24 hours both concentrations of LIF had again resulted in closure of the scratch wound significantly more than the control (0.2ng/ml $p=0.03$ and 10ng/ml $p=0.003$). There was still no statistical difference between the two concentrations of LIF ($p=0.39$), although 10ng/ml LIF was trending towards closing the scratch wound faster than 0.2ng/ml LIF. As with EPO, there was no information in the literature

about the effect of LIF on these cells, so the positive effect seen represents new knowledge, if replicated.

Even though the first experiment treating these cells with EPO demonstrated that it closed the scratch wound significantly quicker than the control, in two repeat experiments the positive effect of EPO was not replicated. EPO had not closed the wound significantly more than the control treated scratch wound at 18 hours ($p=0.53$), and by 24 hours there was less wound closure than the control, although again this difference was not significant ($p=0.35$).

The conclusions from this experiment as a whole are that LIF speeds up healing time in these cells as a reduced scratch wound area was observed compared to the original after 18 and 24 hours. However, in these experiments EPO did not have a positive effect on scratch wound closure and there is evidence that its presence actually delayed healing in this model with this cell line.

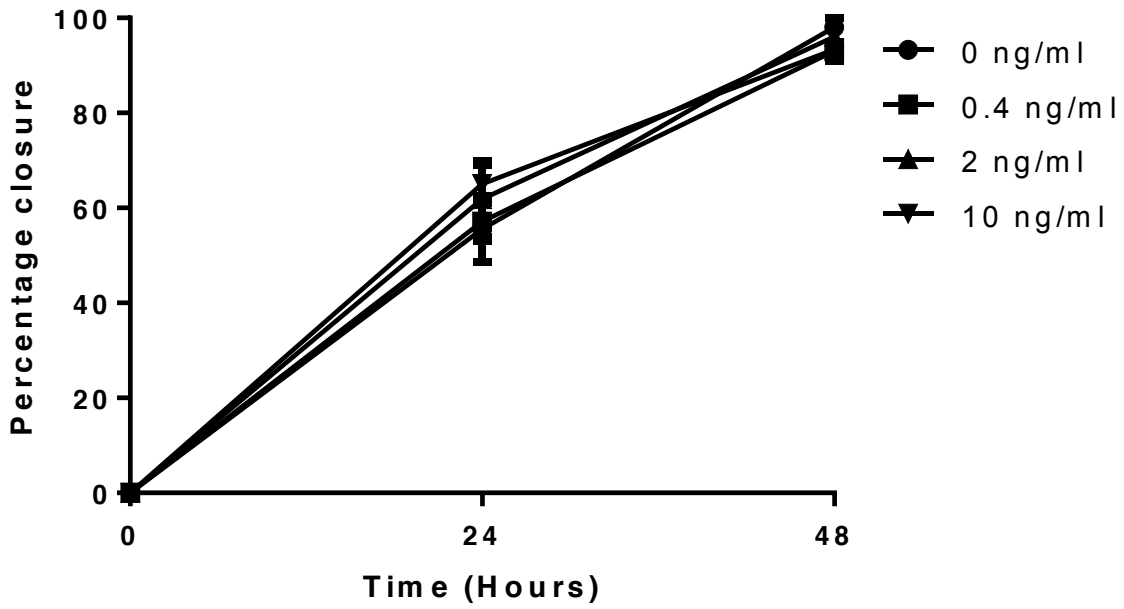

Figure 7.3: EPO concentration response of scratch wound closure by sEnd-1 cells (Experiment 2). sEnd-1 cells were plated at a density of $2x10^5$ cells/well in 12-well plates before a 1.5mm scratch was made along the centre of the cell containing the confluent cells. The rate at which the scratch wound closed in medium with different concentrations of EPO was measured and expressed as percentage closure. No significant difference was seen at any concentration at any time point.

	Time (h)					
	24			**48**		
EPO (ng/ml)	**Mean closure (%)**	**SD**	**P value**	**Mean closure (%)**	**SD**	**P value**
0	55.6	0.07		97.7	0.04	
0.4	57.2	0.04	0.7564	93.1	0.02	0.1188
2	61.9	0.08	0.3684	95.9	0.04	0.6207
10	65.0	0.04	0.1251	93.4	0.01	0.1273

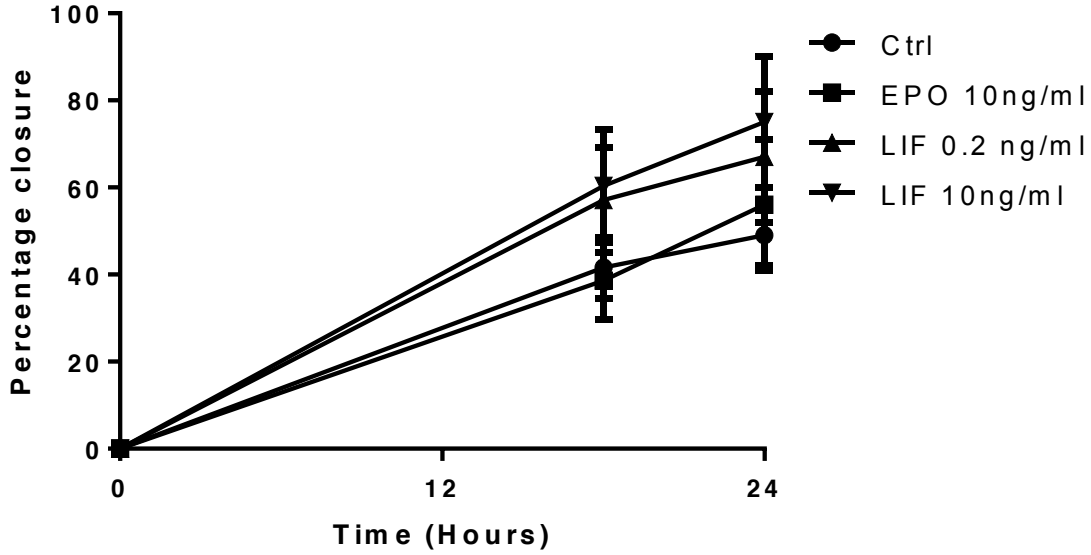

Figure 7.4: Scratch wound closure by sEnd-1 cells treated with EPO or LIF (Experiment 1). sEnd-1 cells were plated at a density of $2x10^5$ cells/well in 12-well plates before a 1.5mm scratch was made along the centre of the well containing the confluent cells. The rate at which the wound closed in medium with either EPO or LIF was measured and expressed as percentage closure. LIF at both concentrations was significantly different from the control at both 18 and 24 hours and there was no significant difference between the concentrations of LIF. EPO induced no significant change in scratch wound closure compared to the control.

	Time (h)					
	18			**24**		
Samples	**Mean closure (%)**	**SD**	**P value**	**Mean closure (%)**	**SD**	**P value**
Ctrl	41.6	0.07		49.3	0.07	
EPO	38.7	0.09	0.5352	55.9	0.15	0.3506
LIF 0.2	57.1	0.12	0.0204	66.9	0.15	0.0275
LIF 10	60.4	0.13	0.0099	74.7	0.15	0.0034

The experiment was repeated to confirm the results. The experimental procedure was carried out exactly as described above and the confluent cells were scratched as before and subjected to the same conditions and the same concentrations of EPO and LIF were used. The experiment showed drastically different results than those seen previously (Fig 7.5). Both cytokines decreased scratch wound healing when compared to the control. In all other previous experiments, the control samples have been noticeably slower to heal than the other treatments, but in this one it is clear that the control samples had healed significantly more than those treated with cytokines.

The results from a 3rd repeat of the experiment are represented in Figure 7.6. Again, this shows different results. At 18 hours LIF 10ng/ml had closed the scratch wound significantly less than the control (P=0.007) but the other two treatments had induced no significant difference to the control. At 24 hours, both 0.2 and 10ng/ml LIF had induced significantly less healing than the control (p= 0.011 and 0.013 respectively), while, with 63% closure compared to 60% by the control, EPO was the only treatment to induce more healing than the control, but this difference was not significant (p=0.72). Again, the results of these two experiments show large variation between experiments and no consensus on the effect of either EPO or LIF treatment on sEnd-1 cells.

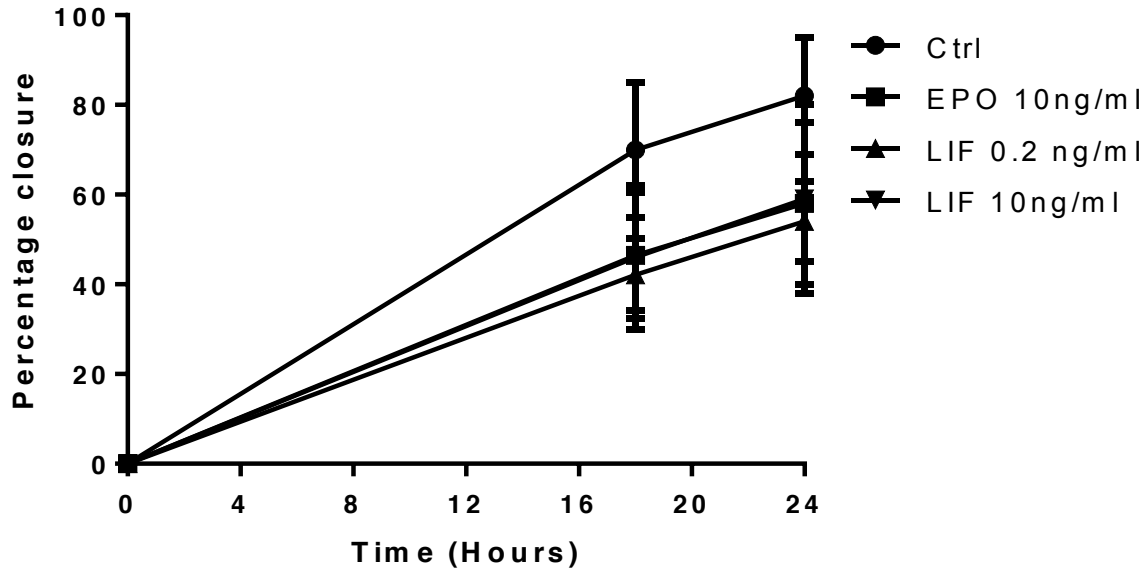

Figure 7.5: Scratch wound closure by sEnd-1 cells treated with EPO or LIF (Experiment 2). sEnd-1 cells were plated at a density of $2x10^5$ cells/well in 12-well plates before a 1.5mm scratch was made along the centre. The rate at which the wound was closing in medium with either EPO or LIF was measured and expressed as percentage closure. All three treatments closed the scratch wound significantly slower than the control at both time points.

	Time (h)					
	18			**24**		
Samples	**Mean closure (%)**	**SD**	**P value**	**Mean closure (%)**	**SD**	**P value**
Ctrl	69.9	0.15		82.4	0.13	
EPO	46.5	0.14	0.0182	57.9	0.18	0.0226
LIF 0.2	42.5	0.08	0.0025	53.9	0.09	0.0015
LIF 10	46.0	0.16	0.0218	58.9	0.21	0.04543

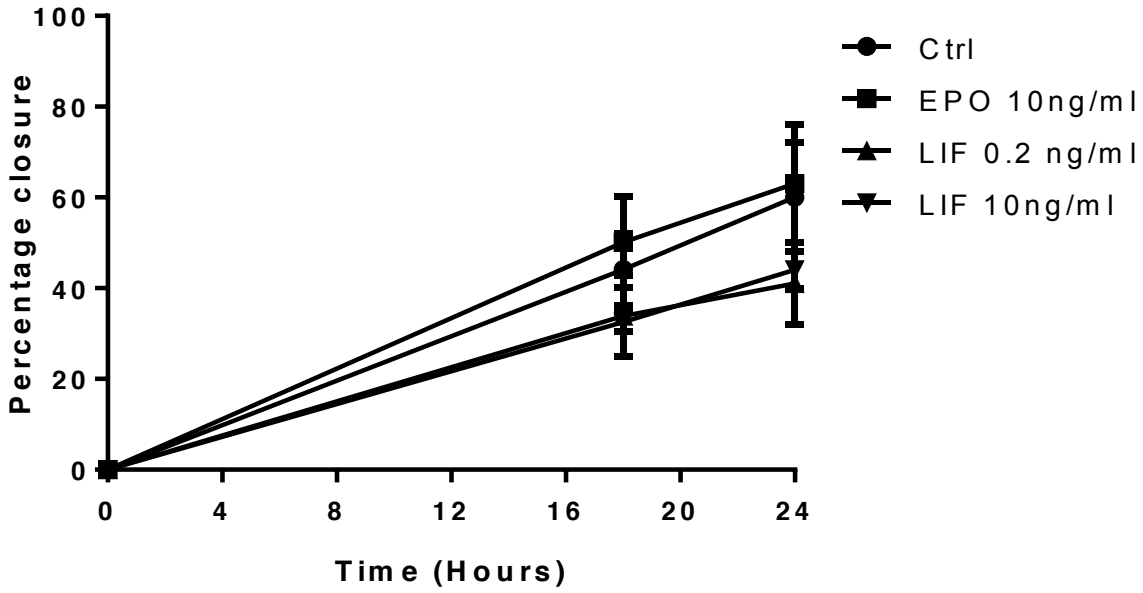

Figure 7.6: Scratch wound closure by sEnd-1 cells treated with EPO or LIF (Experiment 3). sEnd-1 cells were plated at a density of $2x10^5$ cells/well in 12-well plates before a 1.5mm scratch was made along the centre of the well containing the confluent cells. The rate at which the wound closed in medium with either EPO or LIF was measured and expressed as percentage closure. LIF's effect on scratch wound closure at both concentrations was significantly different from the control at both 18 and 24 hours and there was no significant difference between the concentrations of LIF. EPO induced no significant change in scratch wound closure compared to the control.

	Time (h)					
	18			**24**		
Samples	**Mean closure (%)**	**SD**	**P value**	**Mean closure (%)**	**SD**	**P value**
Ctrl	44.2	0.08		59.9	0.12	
EPO	50.1	0.10	0.3013	62.6	0.13	0.7195
LIF 0.2	33.8	0.09	0.0705	41.0	0.09	0.0117
LIF 10	32.5	0.02	0.0079	44.4	0.04	0.0128

The experiment with sEnd-1 cells was repeated for the 4th time because of a lack of continuity between experiments. The only difference between this experiment and the previous ones was that the size of the scratch was measured at 18, 24, 36, and 48 hours to get an accurate idea of progression of the wound closure over a longer period of time. The experiment was set-up in the same way as the previous ones, again using the same concentrations of EPO and LIF. Throughout the experiment EPO closed the wound significantly more than the control, and by the end of the experiment the wounds were 91% closed compared to the initial scratch wound area (Fig 7.7). Neither of the concentrations of LIF induced quicker healing than the control samples. At 0.2ng/ml and at 36 hours, LIF had induced significantly less healing than the control ($p=0.01$). Yet again these results show variation from previous experiments and do not correlate with them in a way that any conclusion about the effect of treatment with either of these cytokines could be reached.

It was decided to measure closure at 6 hours post scratch to determine if the cytokines were having an earlier effect on scratch wound healing that was not detected by 18 hours. As LIF 0.2ng/ml has shown no effect up to this point it was not used. By 6 hours, cells had begun to migrate to close all scratch wounds, with the control samples showing 36.43% closure while EPO and LIF treated samples showed 39.81% and 39.41% respectively, however the difference between the cytokine-treated samples and the control samples was not significant (Fig 7.8). By 24 hours LIF had induced 91% wound closure which was significantly more than the control ($P=0.04$). By 24 hours EPO had not induced significantly more healing than the control ($P=0.42$). From this experiment it can be concluded that the effects of the cytokine treatment are not observed by 6 hours, and that the variability seen among all other previous experiments has not been corroborated.

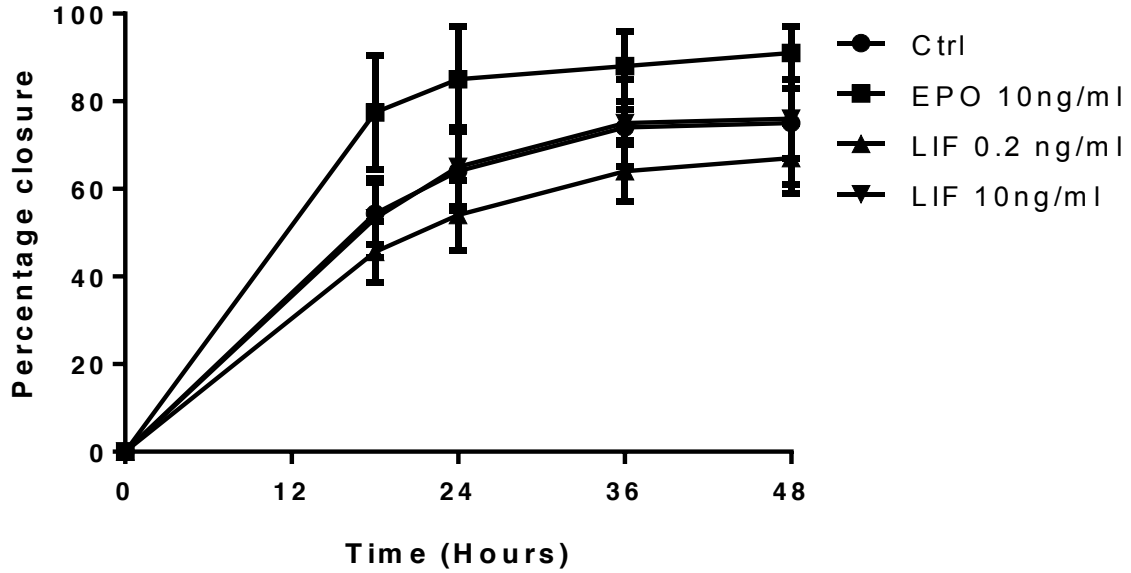

Figure 7.7: Scratch wound closure by sEnd-1 cells treated with EPO or LIF (Experiment 4). sEnd-1 cells were plated at a density of $2x10^5$ cells/well in 12-well plates before a 1.5mm scratch was made along the centre of the well containing the confluent cells. The rate at which the wound closed in medium with either EPO or LIF was measured and expressed as percentage closure. EPO induced significant wound closure compared to the control at all time points ($p<0.01$). LIF at 0.2ng/ml induced significantly less scratch wound closure than the control at 36 hours ($p=0.012$) but not at 48 hours ($p=0.13$). LIF at 2ng/ml did not induce a significantly different wound closure than the control at any time point.

	Time (h)					
	18			**24**		
Samples	**Mean closure (%)**	**SD**	**P value**	**Mean closure (%)**	**SD**	**P value**
Ctrl	54.4	0.07		63.8	0.09	
EPO	77.5	0.13	0.0031	84.6	0.12	0.0068
LIF 0.2	45.6	0.07	0.0585	54.4	0.08	0.0877
LIF 10	53.3	0.09	0.8303	64.5	0.09	0.9017
	Time (h)					
	36			**48**		
Samples	**Mean closure (%)**	**SD**	**P value**	**Mean closure (%)**	**SD**	**P value**
Ctrl	73.9	0.04		74.6	0.08	
EPO	87.6	0.08	0.0046	91.1	0.06	0.0021
LIF 0.2	63.7	0.07	0.0129	67.1	0.08	0.1359
LIF 10	74.8	0.10	0.8405	76.4	0.15	0.8037

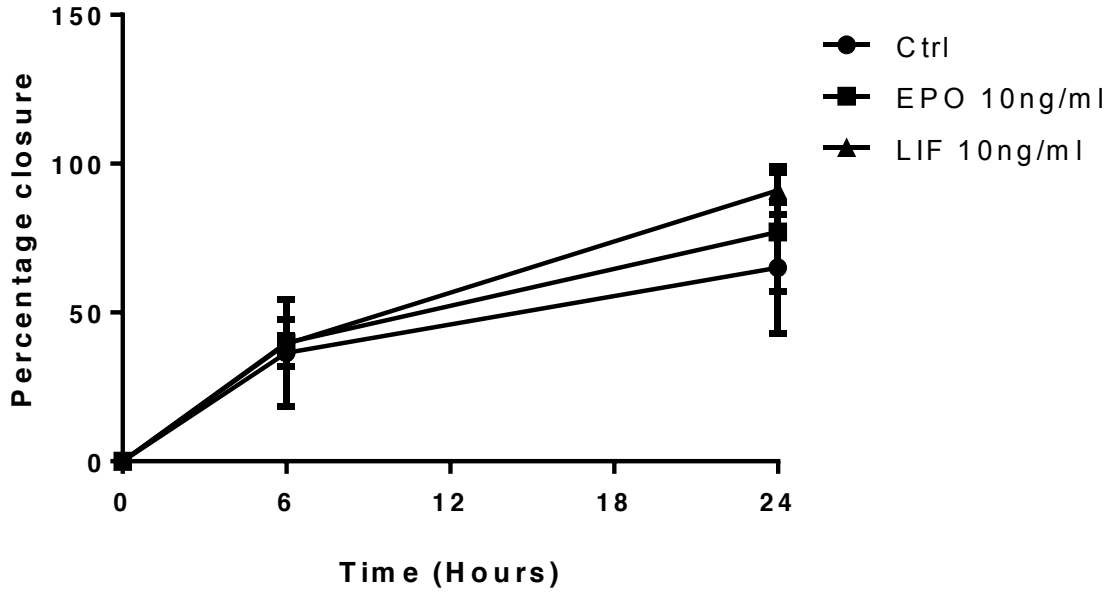

Figure 7.8: Scratch wound closure by sEnd-1 cells treated with EPO or LIF. sEnd-1 cells were plated at a density of $2x10^5$ cells/well in 12-well plates before a 1.5mm scratch was made along the centre of the well containing the confluent cells. The rate at which the wound closed in medium with either EPO or LIF was measured and expressed as percentage closure. A significant difference between cytokine treated and the control scratch wound closure was seen by LIF at 24 hours (p=0.04).

	Time (h)					
	6			**24**		
Samples	**Mean closure (%)**	**SD**	**P value**	**Mean closure (%)**	**SD**	**P value**
Ctrl	36.4	0.18		65.1	0.22	
EPO	39.8	0.08	0.6880	77.2	0.20	0.4181
LIF	39.4	0.03	0.6386	91.1	0.08	0.0420

The final attempt made to elucidate a clear and consistent response from these cells was to carry out the experiment in hypoxia. EPOR is upregulated in hypoxic conditions, in many cell types, in order to make cells more susceptible to EPO (Beleslin-Cokic *et al.* 2004, Emara 2014), therefore reducing the levels of oxygen may make cells more responsive to EPO. It must be noted that in this work "hypoxia" is defined as 5% oxygen, because atmospheric conditions that all other experiments have been conducted in is 21%. However, oxygen tension in the body can range from 14% in the lungs (Miller *et al.* 2010) to less oxygenised organs such as the brain (Dings 1998), eye (Siegfried *et al.* 2010), and bone marrow (Harrison *et al.* 2002) where oxygen tension can range from 0.5 to 7% (Jagannathan 2016). So what I define as hypoxia would not be considered low oxygen *in vivo*. Use of 5% oxygen will induce increased expression of EPOR compared with 21% oxygen which is of benefit to this experimental model. As such, 5% oxygen is used throughout these experiments

The experiment was set up as before, and the wounded cells were treated with 10ng/ml of both EPO and LIF. The difference with this experiment is that the cells were placed into hypoxia once the scratch wound had been made. Placing the cells in hypoxia at the time of wounding is designated "acute hypoxia" for the purposes of these assays. As with previous experiments there was no significant difference in wound healing after treatment with EPO or LIF when compared to the control (Fig 7.9). At 18 hours all three conditions had closed the wound between 40-50% and by 24 hours the results for all three were between 50-60%.

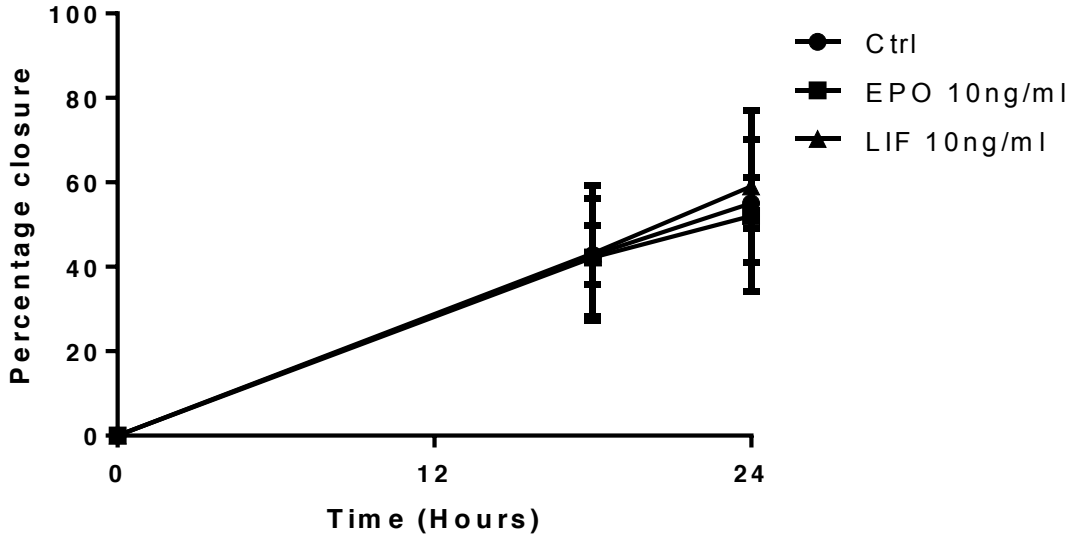

Figure 7.9: Scratch wound closure by sEnd-1 cells in acute hypoxia treated with EPO or LIF. sEnd-1 cells were plated at a density of $2x10^5$ cells/well in 12-well plates before a 1.5mm scratch was made along the centre of the well containing the confluent cells. After wounding the cells were placed into conditions of 5% O_2. The rate at which the wound closed in medium with either EPO or LIF was measured and expressed as percentage closure. No significant difference between healing by the control and cytokine-treated scratch wounds was seen at either time point.

	Time (h)					
	18			**24**		
Samples	**Mean closure (%)**	**SD**	**P value**	**Mean closure (%)**	**SD**	**P value**
Ctrl	42.8	0.07		55.0	0.06	
EPO	42.2	0.14	0.9359	51.9	0.18	0.6925
LIF 10	43.2	0.16	0.9471	58.7	0.18	0.6475

To conclude that hypoxia was not improving the outcome of experiments with sEnd-1 cells the experiment was again repeated but with chronic hypoxia. Cells were placed in hypoxia upon plating, approximately 24 hours before the scratch was made, and this was defined as “chronic hypoxia”. Other than the alterations in oxygen tension the experiment was carried out as before. Again, neither EPO nor LIF induced significantly faster wound healing when compared to the control (Fig 7.10). Both conditions seemed to close the wound slower than the control, but the difference was not significant.

Using the sEnd-1 cell line I could not come to any clear, consistent result. Detachment of the cell monolayer was a consistent problem throughout the experiment, even when the concentration of serum was increased. In an attempt to overcome the problem of detachment, the plates were coated with poly-L-ornithine, a solution that did reduce the amount of detached cells, but it did not completely solve the problem and detachment was still a considerable cause for concern. This problem may have occurred because the cells must be grown to confluence before the scratch can occur so that the cells across the whole plate interact with each other and so that signals progress through the system like they would in the skin. However, after the cells had reached confluence in this model the experiment was still continuing for at least another 24 hours, by which time the level of confluence causes detachment due to a lack of space. The detachment could affect the results because any cells that are detaching from the wound edge would alter the results of the experiment.

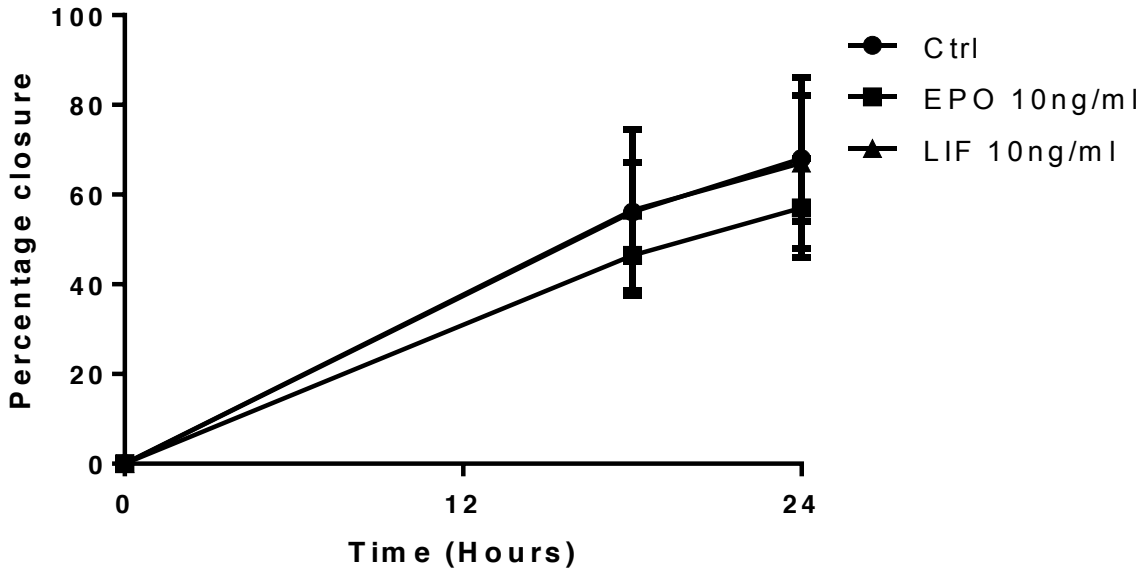

Figure 7.10: Scratch wound closure by sEnd-1 cells in chronic hypoxia treated with EPO or LIF. sEnd-1 cells were plated at a density of $2x10^5$ cells/well in 12-well plates before a 1.5mm scratch was made along the centre of the well containing the confluent cells. After plating the cells were placed into conditions of 5% O_2 The rate at which the wound closed in medium with either EPO or LIF was measured and expressed as percentage closure. No significant difference between healing by the control and cytokine-treated scratch wounds was seen at either time point.

	Time (h)								
	18			**24**			**36**		
Samples	**Mean closure (%)**	**SD**	**P value**	**Mean closure (%)**	**SD**	**P value**	**Mean closure (%)**	**SD**	**P value**
Ctrl	56.1	0.11		68.0	0.14		72.7	0.09	
EPO	46.4	0.09	0.1247	57.2	0.11	0.1667	71.7	0.14	0.8877
LIF	56.5	0.18	0.9597	67.5	0.19	0.9609	66.8	0.16	0.4353

7.3 HaCaT cells

The sEnd-1 cell line provided variable results and no conclusive information on the effect of EPO or LIF on wound healing. Therefore, it was decided to use a different cell line in the hope that the variability was diminished. HaCaT cells are an immortalised human keratinocyte cell line which was the first of its kind to maintain a keratinising phenotype (Boukamp 1988, Seo *et al.* 2012). HaCaT cells have been used for scratch assay investigations before (Walter *et al.* 2010, Pyun *et al.* 2015). Literature searches do not show any evidence that EPO or LIF have been used to stimulate HaCaT cells before. EPOR is present on keratinocyte cell lines (Siebert 2011). Furthermore, increased healing of scratch assays of HaCaT cells was induced through phosphorylation of ERK1/2 (Ranzato *et al.* 2009), which is known to be phosphorylated through EPO signalling (Kuhrt and Wojchowski 2015) (Section 4.4). Conversely, there is no evidence for LIF or LIFR expression in the skin, therefore EPO would be tested first in the model of HaCaT wound healing and, if successful, LIF would then be considered.

The experiment for the HaCaT cells was carried out in exactly the same way as the sEnd-1 cells, except that the Poly-L-ornithine coating was used throughout to optimise the chances that cells detaching would not be a problem. As before, the optimal concentration of FCS was determined in which the cells were viable, proliferative and migratory, but would not heal so quickly that the wound could not be properly measured. The cells were plated at $2x10^5$ cells/well of a 12-well plate based on work by Walter *et al* who plated $10x10^4$ cells/well in 24-well plates (Walter *et al.* 2010). The initial serum-concentrations, as before, were 0, 0.1, 1, and 10% FCS, and the wound size was only measured at 24 hours.

Unlike the serum concentration-response performed on sEnd-1 cells, both 1 and 10% FCS demonstrated significantly faster wound closure in HaCaT cells than the control ($p=0.0002$ and 0.0000004 respectively), with 10% serum exhibiting 97% closure while the control had not yet reached 50% closure (Fig 7.11). Serum at 0.1% had also induced significantly more closure of the scratch wound in HaCaT cells than the control ($p=0.03$) but this time it was only 58.2% compared to 47.7% by the control.

One and ten percent serum closed the wound too quickly to be viable conditions for the scratch assay; therefore 0.1% serum was used for the scratch assay experiments.

HaCaT cells were treated with 1 and 10ng/ml concentrations of EPO and grown in DMEM supplemented with 0.1% serum. The initial experiment carried out demonstrated that in 0.1% serum cells were detaching and the conditions for the experiment were sub optimal. Therefore the experiment was repeated with 1% serum. Neither concentration of EPO showed significantly more wound closure than the control. It appeared that 10ng/ml EPO inhibited scratch wound closure compared to the control throughout the experiment, although there was not a significant difference between the treatments. The increase in scratch wound closure of the lower, but not the higher concentration of EPO suggests that increasing concentrations of EPO between 1 and 10ng/ml decreases cell migration and scratch wound closure in HaCaT cells.

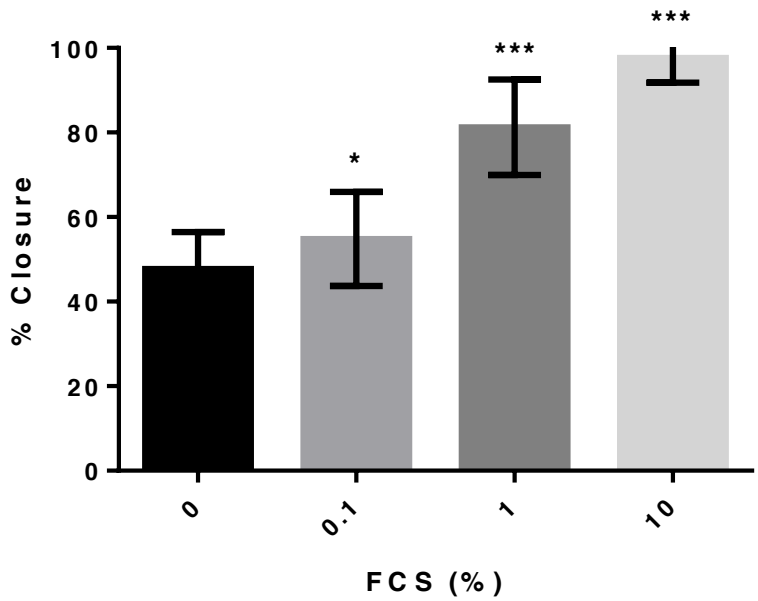

Figure 7.11: Scratch wound closure by HaCaT cells treated with varying concentrations of FCS. HaCaT cells were plated at a density of $2x10^5$ cells/well in 12-well plates before a 1.5mm scratch was made along the centre of the well containing the confluent cells. The rate at which the scratch wound closed in medium with varying concentrations of serum was measured and expressed as percentage closure. *P<0.05, ***P<0.001 versus 0% FCS.

FCS (%)	Mean closure (%)	SD	P value
0	47.7	0.09	
0.1	58.2	0.05	0.0271
1	81.2	0.11	0.0001
10	97.6	0.06	3.78E-07

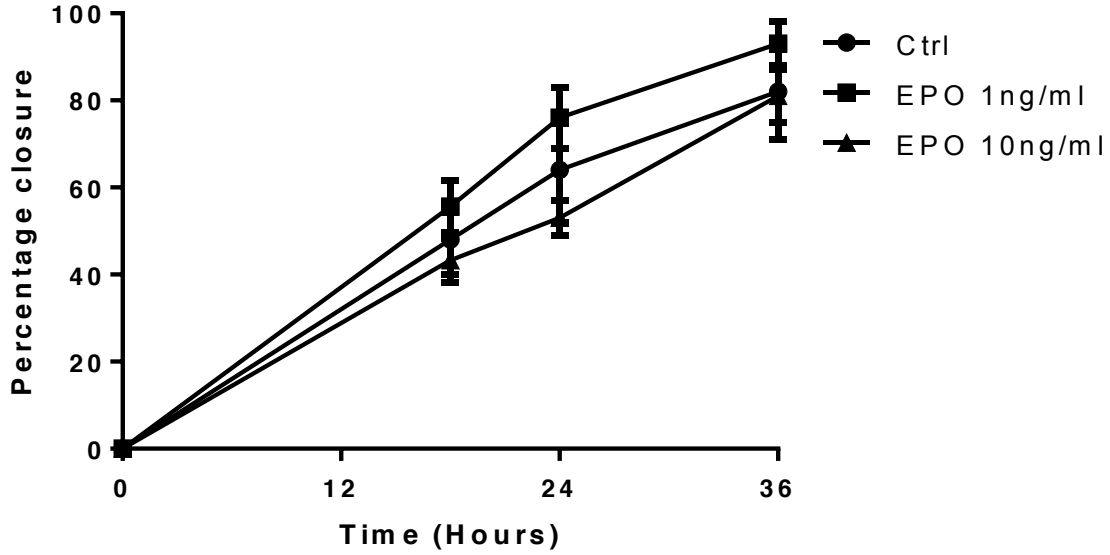

Figure 7.12: Scratch wound closure by HaCaT cells treated with EPO (Experiment 1). HaCaT cells were plated at a density of $2x10^5$ cells/well in 12-well plates before a 1.5mm scratch was made along the centre of the well containing the confluent cells. The rate at which the scratch wound closed in medium with two different concentrations of EPO was measured and expressed as percentage closure. Treatment of the cells with EPO at 10ng/ml (at 36 hours) was the only data point that was significantly different from the control (P=0.004).

	Time (h)								
	18			**24**			**36**		
EPO (ng/ml)	**Mean closure (%)**	**SD**	**P value**	**Mean closure (%)**	**SD**	**P value**	**Mean closure (%)**	**SD**	**P value**
0	48.1	0.08		64.5	0.12		82.5	0.11	
1	55.6	0.06	0.0933	75.9	0.07	0.0811	93.0	0.05	0.0574
10	43.3	0.05	0.2510	53.4	0.04	0.0656	80.9	0.06	0.7761

The experiment was repeated exactly as before, again in 1% serum. At 18 hours both concentrations of EPO resulted in cell migration that closed the wound significantly more than the control (Fig 7.13). However, a large amount of variation was observed in the control samples. At 24 hours, the closure of the scratch wound by the controls ranges from 37.33% to 91.33%, with the mean at 71.25%. This is an immense range of 54% so it is questionable whether or not the results seen can be relied upon. The marked variability in these results mean that this experiment again is not reliable and the results do not provide conclusive evidence for an effect of EPO.

The experiment was attempted again, carried out with exactly the same protocol as before (Fig 7.14). However, in this experiment treatment with EPO produced no significant difference in scratch wound healing than the control. The variability between samples was very low as evidenced by the small error bars on the graph. Again, this experiment can lead to no conclusion about the effect of EPO on wound healing in these cells.

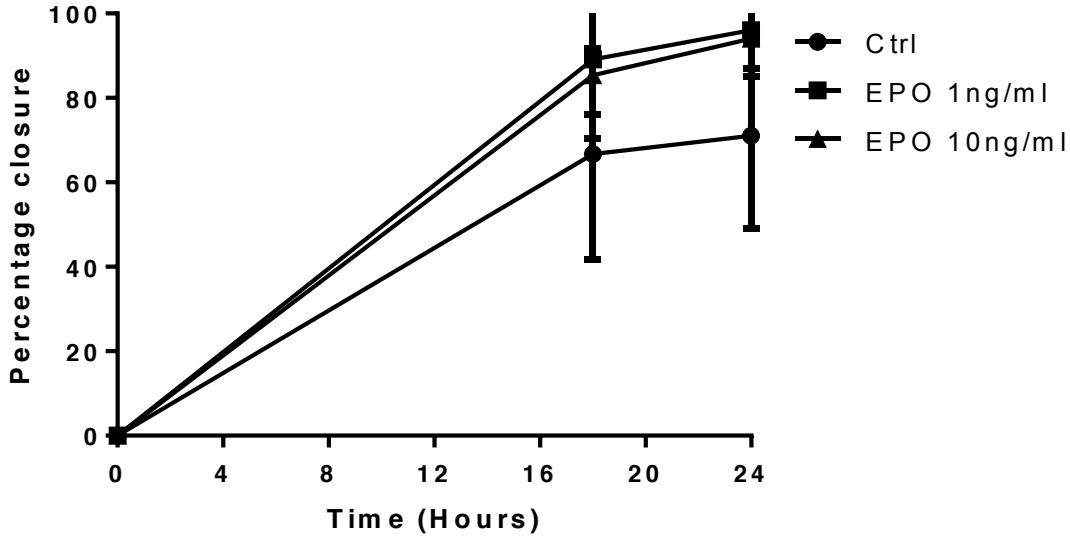

Figure 7.13: Scratch wound closure by HaCaT cells treated with EPO (Experiment 2). HaCaT cells were plated at a density of $2x10^5$ cells/well in 12-well plates before a 1.5mm scratch was made along the centre of the well containing the confluent cells. The rate at which the wound was closing in medium with EPO was measured and expressed as percentage closure. No significant difference between scratch wound closure between the control and EPO-treated wounds was seen at either time point.

	Time (h)					
	18			**24**		
EPO (ng/ml)	**Mean closure (%)**	**SD**	**P value**	**Mean closure (%)**	**SD**	**P value**
0	66.7	0.25		71.3	0.22	
1	89.2	0.13	0.0875	95.7	0.09	0.0509
10	85.4	0.15	0.1630	94.0	0.09	0.0744

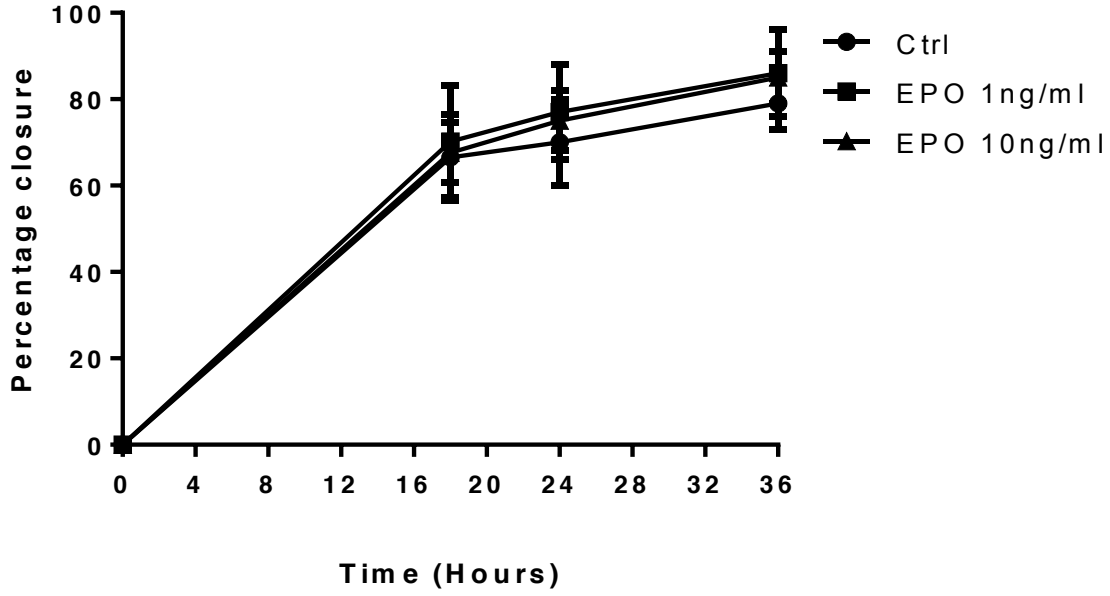

Figure 7.14: Scratch wound closure by HaCaT cells treated with EPO (Experiment 3). HaCaT cells were plated at a density of $2x10^5$ cells/well in 12-well plates before a 1.5mm scratch was made along the centre of the well containing the confluent cells. The rate at which the wound closed in medium with EPO was measured and expressed as percentage closure. No significant difference between healing by the control and EPO-treated scratch wounds was seen at either time point.

	Time (h)								
	18			24			36		
EPO (ng/ml)	**Mean closure (%)**	**SD**	**P value**	**Mean closure (%)**	**SD**	**P value**	**Mean closure (%)**	**SD**	**P value**
0	66.6	0.10		70.3	0.10		79.2	0.06	
1	70.2	0.13	0.6291	77.3	0.11	0.3107	85.9	0.10	0.2236
10	67.6	0.07	0.8472	75.5	0.07	0.3352	85.2	0.06	0.1211

It was hypothesised that the variability in results being obtained from the experiments could again be due to cell detachment. It was proposed that the reduction of serum within the media from 10% to 1% had a detrimental effect on cell adhesion. To overcome this, cells were initially cultured in DMEM containing 10% FCS, but upon plating the cells for the experiment the serum concentration was reduced to 5% before a step-wise further reduction leading down to 1% upon scratch wounding the confluent monolayer. Furthermore, a very high concentration of EPO was used at 100ng/ml with the hypothesis that the concentrations so far had not been sufficient to stimulate EPOR effectively. Less cellular detachment was observed under these conditions, but again there was no significant difference between any concentration of EPO and the control cells (Fig 7.15). The highest concentration of EPO resulted in 79.82% closure of the original scratch wound but the control conditions also resulted in 74.15% closure, so the enhanced positive effect of EPO on scratch wound closure was not significantly different from that of the control.

The results of all these experiments did not lead to any conclusive results. Some experiments showed that EPO had a positive effect on closure of a cell monolayer scratch wound, while other experiments showed no effects at all. The variability in some experiments and the tendency for cell detachment led to the conclusion that EPO does not have any effect in these cells. Therefore, it was decided not to look at the effect of LIF as there was no evidence in the literature of LIFR on keratinocytes and as the model was not working properly it seemed futile to attempt it.

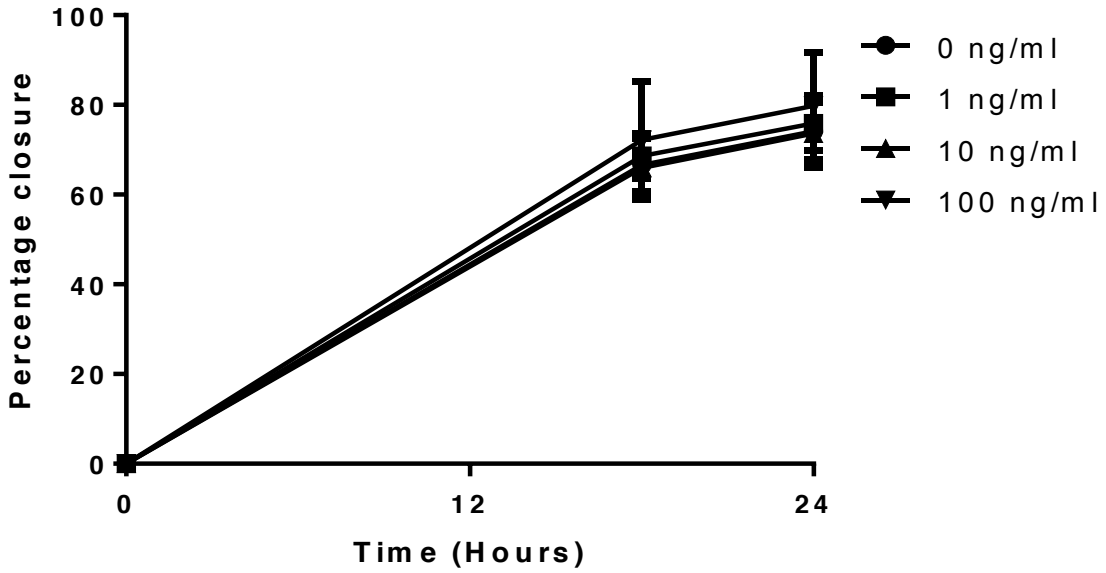

Figure 7.15: Scratch wound closure by HaCaT cells treated with EPO. HaCaT cells were plated at a density of $2x10^5$ cells/well in 12-well plates before a 1.5mm scratch was made along the centre of the well containing the confluent cells. Serum was gradually reduced from 10% FCS during culture to 5% upon plating then 1% when the experiment begun. The rate at which the wound closed in medium with EPO was measured and expressed as percentage closure. No significant difference between healing by the control and EPO-treated wounds was seen at either time point.

	Time (h)					
	18			**24**		
EPO (ng/ml)	**Mean closure (%)**	**SD**	**P value**	**Mean closure (%)**	**SD**	**P value**
0	66.6	0.06		74.15	0.08	
1	68.6	0.05	0.5226	75.84	0.06	0.6796
10	65.9	0.07	0.8554	73.61	0.07	0.9043
100	72.2	0.13	0.3485	79.82	0.12	0.3480

7.4 Conclusion

Previous experimental work in this project has focussed on the effect of treatment with EPO and LIF on the myelinating capacity of CG4 OPCs, thus providing evidence of their potential therapeutic effects on demyelinating diseases, such as MS. Wound healing is a complex process that is easily inhibited or delayed, resulting in the formation of a chronic wound. Both EPO and LIF had some positive effect on myelination by CG4 cells, although to varying intensities, and it was hypothesised that the information gleaned from the previous work could be translated to a wound healing model as cytokines with tissue-protective properties could aid in the correct progression through the four stages of wound healing.

The use of scratch assays to measure the effect that EPO and LIF have on wound healing did not yield any reproducible results. sEnd-1 cells were the first cell line attempted using this model. Initial experiments seemed to suggest that EPO had a positive effect on cell migration and scratch wound closure as those cells treated with EPO closed the scratch wound in the cell monolayer more quickly than the untreated cells. However, this result was not replicated in subsequent experiments. The scratch assay was then performed in hypoxia, both acute and chronic, in an attempt to upregulate EPOR to a greater extent than the expression observed under atmospheric oxygen conditions. However, no change in scratch wound closure was seen between any of the treatments in these experiments. Furthermore, the effect of LIF on these cells was unclear. In some experiments LIF increased scratch wound closure at both 0.2 and 10ng/ml, but in other experiments no difference in wound area was seen when compared to the control. Additionally, there was even evidence in some experiments that LIF could inhibit scratch wound healing.

HaCaT cells were then used in the scratch assay model to see if more reproducible data could be obtained. As HaCaT cells are a human cell line they also offered a closer representation to how the cytokines could affect wound healing in humans. However, again, the results were not reproducible and very different results were observed between experiments.

The main reason to be offered for the lack of reproducibility was cell detachment which occurred in these experiments because the cells were grown to confluence before the wound was created. Attempts were made to limit cell detachment by coating the plates with poly-L-ornithine and by slowly reducing the serum concentration of the medium and while these methods did reduce the amount of detached cells, there was no improvement in the outcome of the experiments.

Unfortunately, the attempt to use EPO and LIF in wound healing models elucidated no reproducible increase in wound healing. A more reliable model in which cell detachment could be properly limited could provide a better method through which to study wound healing. Maybe the best way to achieve this would be a skin cell line that doesn't rely on serum supplementation. Furthermore, the scratch assay only involves one cell monolayer, which does not reflect the complexity of a skin wound, in which several layers and cell types interact with each other and a variety of cytokines and growth factors to close the wound. Perhaps the only effective way to investigate wound healing is *in vivo*, as it is a very complicated process to try to emulate in the lab.

Chapter 8. Conclusions

The discovery that EPOR is expressed on cells other than erythrocyte precursors (Anagnostou *et al.* 1990) prompted investigation into how extensively EPO can influence cellular processes around the body. EPOR is expressed within the brain and EPO can cross the BBB, allowing EPO to have extensive neuroprotective and neuroreparative functions (Masuda *et al.* 1993, Brines *et al.* 2000). EPO's effects are beneficial in preclinical models of EAE (Agnello 2002, Li 2004) and cerebral ischaemia (Villa 2003) demonstrating its potential therapeutic benefit. EPO increases oligodendrogenesis *in vivo* and the expression of myelinating genes by oligodendrocytes *in vitro* (Cervellini *et al.* 2013a, Gonzalez *et al.* 2013).

LIF is a pleiotropic cytokine with a broad spectrum of activities. LIF has been studied as a neuroprotective molecule as it is expressed by astrocytes and neurons and LIFR is expressed by neurons in the CNS (Aloisi 1994, Cheng and Patterson 1997, Scott 2000, Stankoff 2002, Joly *et al.* 2008). LIF was identified as a cytokine that may share the tissue protective properties of EPO (Mengozzi 2014).

The work presented in this thesis aimed to determine the effects of EPO and LIF on myelination by CG4 oligodendrocyte precursor cells and therefore develop a better understanding of the cellular mechanisms related to these effects. As in several cases OPCs are abundant in MS plaques (Wolswijk 1998, Chang 2000), it is believed that it is not a lack of OPCs that cause failure in remyelination, rather an inability of these cells to myelinate (Chari 2002). Therefore, tissue protective cytokines could be a viable solution to stimulate an increase in the myelin produced by oligodendrocytes and consequently increase remyelination.

8.1 LIF does not have the same positive myelinating effects as EPO

The first aim of the experimental work presented in this thesis was to demonstrate the promyelinating effects of LIF on CG4 oligodendrocyte precursor cells. LIF is important for the long-term survival of oligodendrocytes (Barres 1993), has a promyelinating effect (Stankoff 2002), and is beneficial in models of EAE (Butzkueven 2002, 2006). However, some studies offer conflicting results; Marriott

et al (2008) found that LIF limited demyelination in a mouse model of cuprizone-induced demyelination but exogenous LIF treatment offered no benefit to remyelination (Marriott 2008), and Ishibashi *et al* (2006) provided evidence of a bell-shaped concentration response curve *in vitro* with concentrations above 5ng/ml LIF being inhibitory (Ishibashi *et al.* 2006). LIF did increase myelination by CG4 cells, but to a lesser extent than EPO. This provides the first conclusion of this work: LIF increased the expression of Mog by CG4 cells, but the expression of Mog was higher after EPO treatment when compared to LIF treatment. However, it should be considered that these cells were engineered to overexpress EPOR. The model mimics the upregulation of EPOR that occurs in these cells upon injury *in vivo* (Kato *et al.* 2011) and the cells responded to LIF without artificial increase in LIFR or GP130. Therefore, it can still be concluded that the cells do not respond as well to LIF as they do to EPO.

Furthermore, LIF induced a bell-shaped concentration response curve, with higher concentrations inducing no increase in Mog expression in CG4 cells over that of the control. This was the first demonstrated evidence of an inhibitory effect of LIF on myelin gene expression, as it had the capacity to increase myelination at low concentrations, but not at higher ones.

8.2 LIF inhibited EPO-induced Mog expression

The effects of LIF and EPO in combination were measured. I hypothesised that when added simultaneously the two cytokines would have a synergistic effect, or that LIF would not affect Mog expression in any way. However, the results were unexpected as LIF inhibited EPO-induced Mog, even when added at 0.2ng/ml which alone increased Mog expression. This result was replicated several times and showed that there was an inhibitory mechanism that was induced by LIF, but not EPO. Furthermore, potentially this same mechanism could have been the cause of the bell-shaped concentration response curve produced by the addition of LIF to the cell culture conditions; at high concentrations, above 0.2ng/ml, it triggers a feedback mechanism.

LIF also inhibited EPO-induced Mbp expression. Like Mog, Mbp is a myelin gene whose expression is typically seen earlier in OPC differentiation than that of Mog. I decided to study Mog because it is induced late and would be a full representation of the later effects of cytokine treatment on these cells. Mog expression correlates directly with myelin deposition, making it a good marker for myelination in these cells (Solly 1996). However, it was important to also measure the effects on another myelin gene so that it could be concluded that the effect is not unique to Mog. Mbp was increased by EPO, but not by 10ng/ml LIF. Additionally, EPO-induced Mbp was inhibited when the cells were simultaneously treated with both EPO and LIF. As the inhibitory effect of LIF on the expression of Mbp reflected the effect that LIF had on Mog expression it can be concluded with more confidence that LIF inhibited overall myelination in these cells, not just one myelin gene. Previous research into the effect of LIF in the CNS showed that it induces myelination in the CNS (Joly *et al.* 2008, Deverman 2012, Rowe 2014), so this is novel evidence that myelin genes expression is inhibited by LIF in this specific model.

OSM and CNTF were also used in this model as literature indicated that they may also be neuroprotective (Wallace 1999, Butzkueven 2002, Pasquin 2015). These are two cytokines from the same cytokine family as LIF, the IL-6/GP130 family. They both signal through the same receptors as LIF, LIFR and GP130, although CNTF has an additional β-chain receptor termed the CNTFR. In this model, the effect of OSM consistently reflected the effect of LIF on Mog expression. However, throughout these experiments CNTF did produce the same effects of LIF and OSM. The effect of OSM was almost identical to that of LIF, but CNTF consistently had a reduced effect; it induced less Mog expression after treatment with a low concentration and, unlike LIF and OSM, CNTF did not completely inhibit EPO-induced Mog after a high concentration treatment. CNTF is the only cytokine of these three that uses a third receptor, the CNTFR, in addition to the LIFR/GP130 complex. I could hypothesise that this discrepancy was due to a lack, or low expression, of the CNTFR.

8.3 Socs3 expression negatively correlated with Mog induction

I therefore decided to identify the mechanisms that inhibit EPO-induced Mog expression. The JAK/STAT/Socs pathway is an important pathway in IL-6 cytokine signalling. LIF induces conformational changes in JAK2 which allow the binding and phosphorylation of STAT3. These phosphorylated transcription factors dimerise and translocate to the nucleus where they regulate gene expression, including inducing the expression of Socs3. In turn, Socs3 binds to JAK2, preventing further phosphorylation of STAT3 and so inducing an inhibitory feedback mechanism (Babon 2014).

While Socs proteins negatively regulated EPO signalling in one previously published study (Jegalian 2002), this work was in erythrocytes. Any interaction between Socs3 and EPO in models of neuroprotection had not been investigated before this work was published.

As expected, LIF induced Socs3 expression. This expression increased as the concentration of LIF increased, potentially explaining why higher concentrations of LIF (10ng/ml) had an inhibitory effect on Mog expression. Phosphorylation of STAT3 was measured and pSTAT3 levels remained elevated after exposure to a low concentration of LIF (0.2ng/ml) but at a high concentration (10ng/ml) they were inhibited after 20 minutes, again suggesting that at the higher concentration of LIF Socs3 was induced and, therefore, caused the inhibition of pSTAT3. This inhibition was not seen at the low LIF concentration (0.2ng/ml) suggesting that at this concentration not enough Socs3 was induced to cause an inhibition of the signalling pathways induced by LIF. Therefore, this might explain why stimulation with a low concentration of LIF increased Mog expression in the CG4 cells, but a high concentration of LIF did not.

The expression of Socs3 was measured after treatment with EPO alone and in combination with LIF. EPO induced reduced expression of Socs3, not comparable to LIF. The level of Socs3 expression was increased when EPO and LIF were added simultaneously. Therefore, another conclusion of this work is that Socs3 expression negatively correlates with Mog expression. In conditions where Mog was increased (low concentration of LIF and EPO treatment alone) Socs3 expression was low, and

alternatively conditions where Mog expression was inhibited (high concentration of LIF and simultaneous EPO and LIF treatment) Socs3 expression was significantly increased. Furthermore, a known inducer of Socs3, PMA, also inhibited EPO-induced Mog expression. Previous results obtained *in vivo* in LIF-knockout mice suggested a link between LIF-induced Socs3 and protection from demyelination (Emery 2006). However, such a close relationship between the expression of Socs3 and of Mog, and therefore the remyelinating capacity of oligodendrocytes is a novel finding.

8.4 Igf1, CD36 and other genes were important in differentiation and myelination of CG4 cells

Microarray analysis was used to study the effect that differentiation and treatment with EPO had on CG4 cell gene expression. Filtering strategies and hierarchical cluster analysis were utilised to visualise changes in gene expression. Initially, differentiated and undifferentiated samples were compared. From filtering for only those transcripts whose expression changed specifically between these groups a variety of genes were identified such as Hes5, which is downstream of the Notch pathway. This pathway is a negative regulator of myelination so the downregulation of Hes5 is evidence of the importance of the pathway in OPC maturation (Morrison *et al.* 2000, Woodhoo 2007). Ccl20 was also identified, which is increased in situations of neurodegeneration (Das *et al.* 2011, Leonardo 2012). Upon differentiation in these cells Ccl20 is downregulated, supporting the hypothesis that its expression has a negative effect on CG4 cells.

The genes whose expression was significantly different between differentiated and undifferentiated samples was analysed by hierarchical cluster analysis and the resulting heat map image demonstrated that the expression of the large majority of genes was the same, either up- or downregulated, across both the early and late time points.

The genes altered between the EPO-treated samples and the control (differentiated) samples were also considered. H19 was the most highly up-regulated gene across both time points. It is a non-coding RNA that is linked closely to development

(Gabory *et al.* 2010) so its high upregulation in EPO-treated samples demonstrated the pro-developmental effect that EPO has on these cells. Furthermore, Pmp2, a myelin gene, was consistently upregulated by EPO-treated samples at both time points, providing further evidence for the pro-myelinating effect of EPO.

CD36 expression was highly upregulated by EPO treatment at 20 hours, a gene known to be important in cellular differentiation (Christiaens *et al.* 2012). CD36 is a scavenger receptor that binds an array of small biomolecules, including fatty acids (Love-Gregory and Abumrad 2011), a function that suggests it may be important in myelin production (Jay and Hamilton 2016). One paper suggested that deletion of CD36 inhibited peripheral remyelination (Eto *et al.* 2003), but conflicting results showed that $CD36^{-/-}$ mice demonstrated better recovery from spinal cord injury than their wild type littermates (Myers *et al.* 2014). However, CD36 expression has not previously been identified in oligodendrocytes.

Igf1 was identified in the microarrays as one of the most highly upregulated genes in cells treated with EPO versus the control. It is an important neuronal growth factor (Xiang *et al.* 2011) and EPO treatment increased peripheral myelination and Igf1 expression in a model of mouse sciatic nerve injury (Wang *et al.* 2015). EPO and Igf1 have synergistic protective effects in the CNS (Kang *et al.* 2010, Utada *et al.* 2015) and Igf1 has the ability to stimulate EPO production (Kim *et al.* 2008), so the evidence provided by the microarrays that EPO induces Igf1 expression further exemplifies the relationship between these two proteins. Furthermore, the expression of protective molecules, such as Igf1, by EPO treatment provides a further mechanism through which EPO is protective in the CNS.

The difference between the gene expression profiles of samples treated with EPO at the two time points was analysed. When the transcripts were filtered for significance between the EPO-treated and the control group at both time points only 12 transcripts remained. Furthermore, heat map images generated through hierarchical cluster analysis showed very little similarity between the two time points. These observations led to the conclusion that the early gene expression changes induced by EPO were not sustained throughout the experiment and the early-induced genes did not influence the 20 hour time point. Perhaps these genes are just important for the initiation of myelination, but not for sustaining it.

8.5 Tlr2 stimulation inhibited EPO-induced Mog

The genes expressed by the samples treated with EPO and LIF simultaneously were compared their expression to the samples treated with EPO alone. From the hierarchical cluster analysis several clusters were selected that showed a difference between gene expression in EPO and LIF treated groups and those treated with EPO alone. A variety of genes were identified and several were validated by qPCR. Socs3 expression was significantly different between EPO and LIF groups and EPO alone at 1 hour, again highlighting the importance of this signalling protein in the inhibition of EPO-induced myelination.

Two genes identified through comparisons between EPO+LIF-treated groups and EPO treatment alone were Lcn2 and Tlr2, which were both upregulated by the samples treated with EPO+LIF. Analysis of Lcn2 and Tlr2 was performed to identify if the expression changes seen in the microarrays indicated biological functionality in CG4 cells. I hypothesised that Lcn2 treatment would inhibit EPO-induced Mog but treating the cells simultaneously with Lcn2 and EPO had no effect on EPO-induced Mog, even when a very high concentration of Lcn2 was used.

However, Tlr2 was identified as another mechanism through which myelination may be regulated. This receptor was significantly upregulated in conditions where Mog expression is reduced, i.e. LIF alone and EPO and LIF simultaneously. However, stimulating the CG4 cells with EPO and Pam3, a Tlr2 agonist, simultaneously also caused a reduction in Mog expression, suggesting that Tlr2 is also expressed on CG4 cells without LIF stimulation and again showing that it has the capacity to reduce Mog expression. Though, treatment with EPO, LIF and Pam3 completely abolished Mog expression indicating that a combination of stimulants can work together to prevent myelination. This highlights the complicated nature of myelination and the variety of factors that need to be taken into consideration when developing treatments to enhance remyelination. Nevertheless, it can be concluded that Tlr2 is functional at the transcriptional level in these cells and its stimulation has an inhibitory effect on EPO-induced Mog gene expression. The signalling cascade induced by Tlr2 is known but which parts of this pathway are important for myelination is not well understood. Figure 8.1 shows an example of Tlr2 signalling, which results in the upregulation of transcription factors NF-κB and AP-1.

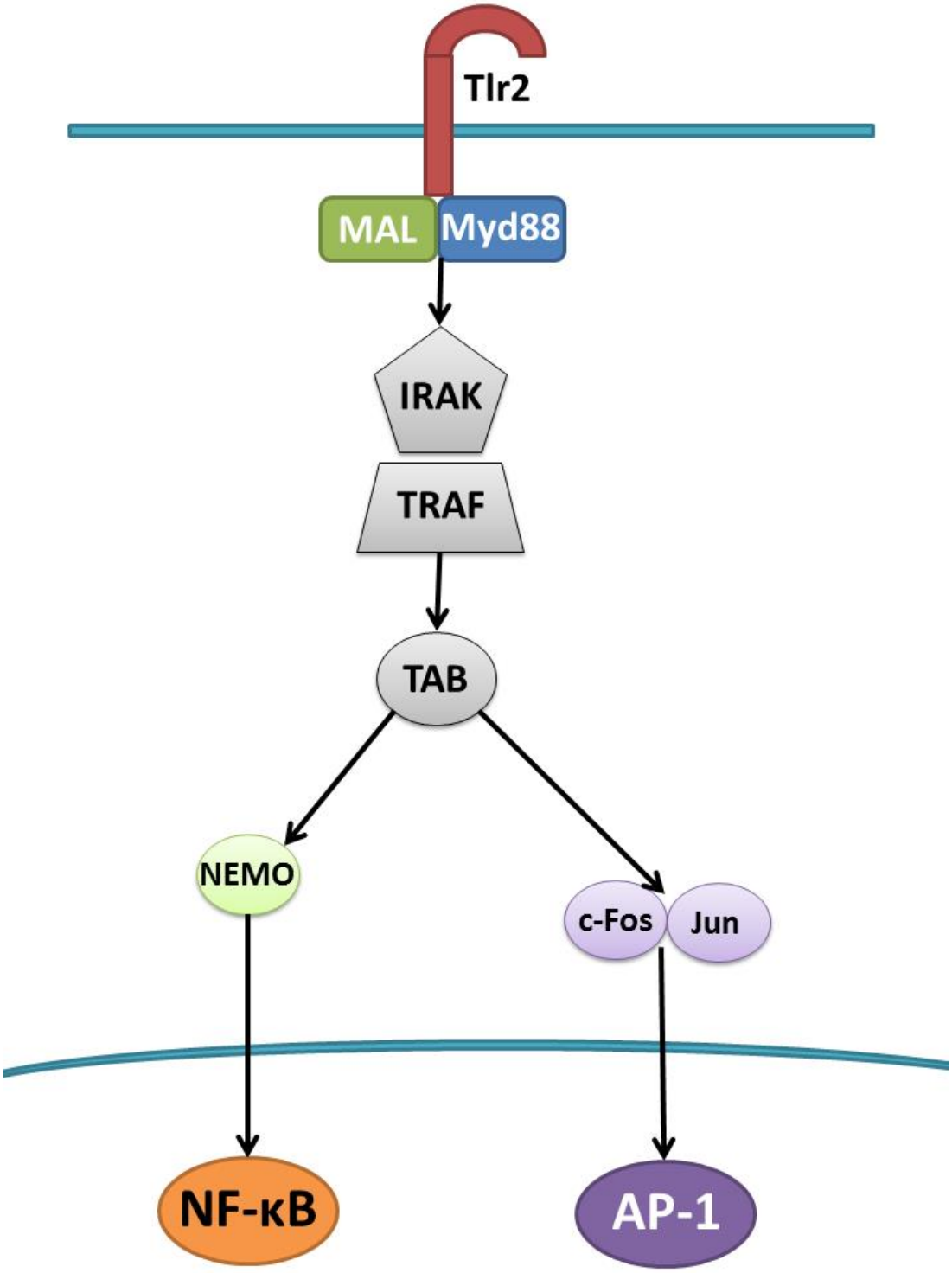

Figure 8.1: The signalling pathways induced by Tlr2. Upon binding of a Tlr2 ligand, adaptor proteins Myd88 and Myd88-adaptor-like protein (MAL) propagate the signal. Signalling cascades then occur, resulting in activation of transcription factors NF-κB and AP-1. Both of these have an effect on myelination or oligodendrocytes death (Hilliard *et al.* 2001, Dobretsova *et al.* 2004). The signalling pathway represented here is simplified as it is not known which sequence of events leads to inhibition of myelination by Tlr2. Adapted from (O'Neill *et al.* 2013)

8.6 Concluding remarks

The data presented in my thesis are the first to demonstrate that LIF has a negative effect on EPO-induced myelin gene expression. Figure 8.2 is a representation of the genes and proteins investigated in this thesis and how they influence myelination. There is ongoing research into the benefit of EPO in treatment of demyelinating diseases (Brines *et al.* 2000, Agnello 2002, Li 2004). However, LIF is upregulated in the injured nervous system (Dowsing 2001, Soilu-Hanninen 2010) so its presence needs to be considered when using EPO treatment to increase myelination.

The signalling protein Socs3 showed strong negative correlation with Mog and induction of Socs3 with PMA also inhibited EPO-induced Mog. It was not known previously that Socs3 correlated with Mog so closely or that it has the potential to inhibit the effects induced by EPO. Clinically, if Socs3 could be inhibited it would increase the promyelinating capacity of EPO and therefore increase the efficacy of EPO treatments.

Gene expression microarrays were used to further identify genes that could influence myelination by oligodendrocytes. Tlr2 was identified in the microarrays and upon further investigation demonstrated biological functionality. Again, inhibition of Tlr2, or suppression of its ligands, in the CNS could have be beneficial to myelination.

The effect of these cytokines in preclinical models should be further investigated. While many models of MS exist, EAE is the most frequently used as its pathology is well understood, the genome of the mice is fully characterised and knockout models can be utilised (Robinson *et al.* 2014). EPO and LIF have both been used in models of EAE (Li 2004, Butzkueven 2006, Savino 2006, Linker 2008, Mengozzi *et al.* 2008), but they have not been used in combination. Also, the effect of endogenous LIF on EPO has not been considered before now. LIF inhibited EPO *in vitro* so it could have inhibitory effects on an EPO treatment. LIF knockout-mice survive into adulthood, so it would be interesting to see if the promyelinating effect of EPO was increased in LIF knockout mice. Socs3 knockout mice would theoretically also demonstrate an increased benefit to EPO treatment. However, Socs3 knockout mice do not survive beyond embryonic day 13 due to placental defects (Roberts 2001).

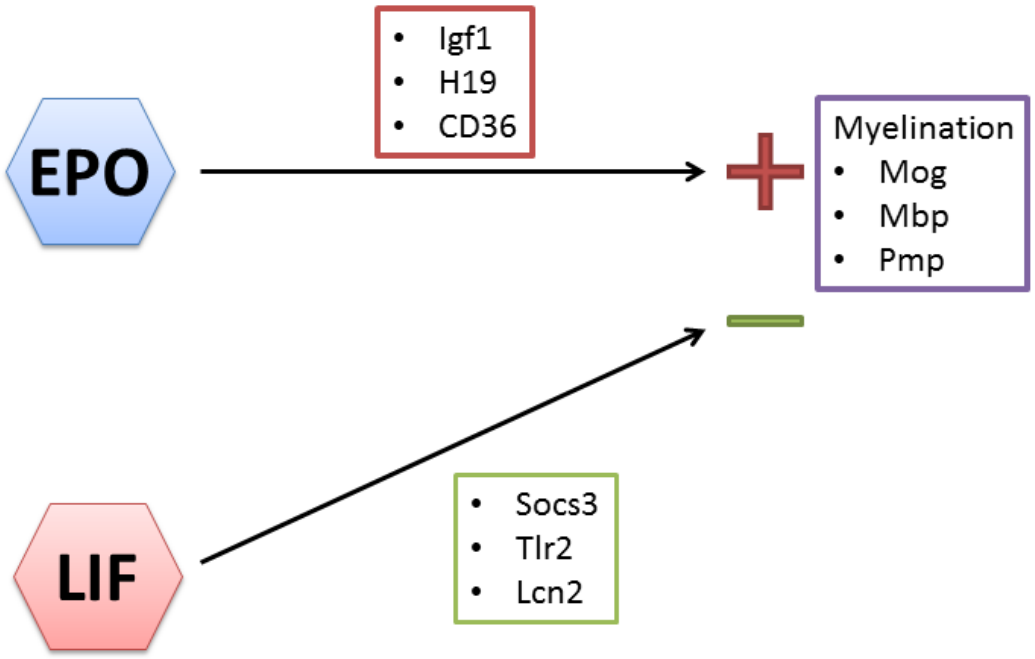

Figure 8.2: Regulation of myelination by EPO and LIF in oligodendrocytes. EPO increases myelination while LIF at a high concentration inhibits it. This figure shows the myelin genes measured and the mechanisms induced by EPO and LIF to regulate myelination.

Demyelination has serious consequences in the CNS and a failure to remyelinate has a considerable detrimental effect on the patient. Remyelination is possible, as evidenced by relapsing-remitting MS in which recurrent attacks of demyelination occur which are followed by repair and complete restoration of function. However, as the disease progresses repair becomes less efficient so strategies to increase remyelination in patients reaching the late stages of disease are required. EPO has potent neuroprotective effects and can aid in increasing myelination, but my thesis demonstrates that the interactions of LIF, and other IL-6 cytokines, need to be considered. Full understanding of the signalling mechanisms that result in inhibition of the promyelinating effects of EPO would help in the identification of strategies to increase the effect of EPO and prevent inhibition by other cytokines. My findings can be therapeutically beneficial because targets that regulate myelination were identified. A full understanding of the regulation of myelination and, importantly, the mechanisms that inhibit myelin production, would allow therapeutics that stimulate only promyelinating factors to be developed.

EPO should be considered a useful promyelinating molecule, but the presence of proteins such as Socs3 that inhibit EPO's promyelinating effects should be properly considered. Furthermore, EPO could be useful in other regenerative strategies. The regeneration of cells, tissues, and organs relies on the promotion of proliferation and protection from apoptosis, and EPO can be used for both of these purposes. Furthermore, its angiogenic effects would be invaluable to promoting regeneration, as angiogenesis is one of the few regenerative processes that higher animals are still capable of. The mechanisms regulating EPO as identified in this project should again be considered in these applications in order to increase EPO's regenerative benefits.

Chapter 9. References

Åberg, N.D., Stanne, T.M., Jood, K., Schiöler, L., Blomstrand, C., Andreasson, U., Blennow, K., Zetterberg, H., Isgaard, J., Jern, C., Svensson, J., 2016. Serum erythropoietin and outcome after ischaemic stroke: A prospective study. BMJ Open 6 (2), e009827.

Agnello, B., Villa, Mennini, Cerami, Brines, Ghezzi, 2002. Erythropoietin exerts an anti-inflammatory effect on the CNS in a model of experimental autoimmune encephalomyelitis. Brain Research 952 (1), 128-134.

Akita, S., Daian, T., Ishihara, H., Fujii, T., Akino, K., 2004. Leukemia inhibitory factor-transfected embryonic fibroblasts and vascular endothelial growth factor successfully improve the skin substitute wound healing by increasing angiogenesis and matrix production. Journal of Dermatological Science 36 (1), 11-23.

Al Nimer, F., Elliott, C., Bergman, J., Khademi, M., Dring, A.M., Aeinehband, S., Bergenheim, T., Romme Christensen, J., Sellebjerg, F., Svenningsson, A., Linington, C., Olsson, T., Piehl, F., 2016. Lipocalin-2 is increased in progressive multiple sclerosis and inhibits remyelination. Neurology Neuroimmunology & Neuroinflammation 3 (1), e191.

Albrengues, J., Bourget, I., Pons, C., Butet, V., Hofman, P., Tartare-Deckert, S., Feral, Chloe c., Meneguzzi, G., Gaggioli, C., 2014. LIF mediates proinvasive activation of stromal fibroblasts in cancer. Cell Reports 7 (5), 1664-1678.

Aloisi, F., Rosa, S., Testa, U., Bonsi, P., Russo, G., Peschle, C., Levi, G., 1994. Regulation of leukemia inhibitory factor synthesis in cultured human astrocytes. The Journal of Immunology 152 (10), 5022-5081.

Alonzi, T., Middleton, G., Wyatt, S., Buchman, V., Betz, U., Muller, W., Musiana, P., Poli, V., Davies, A., 2001. Role of STAT3 and PI3-kinase/AKT in mediating the survival actions of cytokines on sensory neurons. Molecular and Cellular Neuroscience 18 (3), 270-282.

Alper, G., 2012. Acute disseminated encephalomyelitis. Journal of Child Neurology 27 (11), 1408-1425.

Altun, V., Hakvoort, T., Van Zuijlen, P., Van Der Kwast, T., Prens, E., 2001. Nerve outgrowth and neuropeptide expression during the remodeling of human burn wound scars. A 7-month follow-up study of 22 patients. Burns 27 (7), 717-722.

Anagnostou, A., Lee, E., Kessimian, N., Levinson, R., Steiner, M., 1990. Erythropoietin has a mitogenic and positive chemotactic effect on endothelial cells. PNAS 87, 5978-5982.

Anagnostou, A., Liu, Z., Steiner, M., Chin, K., Lee, E., Kessimian, N., Noguchi, C., 1994. Erythropoietin receptor mRNA expression in human endothelial cells. PNAS 91, 3974-3978.

Anand, P., Parrett, A., Martin, J., Zeman, S., Foley, P., Swash, M., Leigh, P., Cedarbaum, J., Lindsay, R., Williams-Chestnut, R., 1995. Regional changes of ciliary neurotrophic factor and nerve growth factor levels in post mortem spinal cord and cerebral cortex from patients with motor disease. Nature Medicine 1 (2), 168-172.

Anderson, S., Miskimins, R., 1994. Involvement of protein kinase c in CAMP regulation of myelin basic protein gene expression. Journal of Neuroscience Research 37 (5), 604-611.

Andreeva, N., Nyamaa, A., Haupt, H., Gross, J., Mazurek, B., 2006. Recombinant human erythropoiesis prevents ischemia-induced apoptosis and necrosis in explant cultures of the rat organ of corti. Neuroscience Letters 396 (2), 86-90.

Annenkov, A., Rigby, A., Amor, S., Zhou, D., Yousaf, N., Hemmer, B., Chernajovsky, Y., 2011. A chimeric receptor of the insulin-like growth factor receptor type 1 (IGF1R) and a single chain antibody specific to myelin oligodendrocyte glycoprotein activates the IGF1R signalling cascade in CG4 oligodendrocyte progenitors. Biochimica et Biophysica Acta (BBA) - Molecular Cell Research 1813 (8), 1428-1437.

Aparicio, E., Mathieu, P., Pereira Luppi, M., Almeira Gubiani, M.F., Adamo, A.M., 2013. The notch signaling pathway: Its role in focal CNS demyelination and apotransferrin-induced remyelination. Journal of Neurochemistry 127 (6), 819-836.

Arcasoy, M.O., Jiang, X., 2005. Co-operative signalling mechanisms required for erythroid precursor expansion in response to erythropoietin and stem cell factor. British Journal of Haematology 130 (1), 121-129.

Archambault, A., Sim, J., Mccandless, E., Klein, R., Russell, J., 2006. Region-specific regulation of inflammation and pathogenesis in experimental autoimmune encephalomyelitis. Journal of Neuroimmunology 181 (1-2), 122-132.

Argaw, A., Zhang, Y., Snyder, B., Zhao, M., Kopp, N., Lee, S., Raine, C., Brosnan, C., John, G., 2006. IL-1beta regulates blood-brain barrier permeability via reactivation of the hypoxia-angiogenesis program. Journal of Immunology 177 (8), 5574-5584.

Arroyo, M., Castilla, M., Gonzalez, P., F, Tan, D., Riesco, A., Casado, S., Caramelo, C., 1998. Role of vascular endothelial growth factor on erythropoietin-related endothelial cell proliferation. Journal of the American Society of Nephrology 9 (11), 1998-2004.

Arslantas, M., Arslantas, R., Tozan, E., 2015. Effects of systemic erythropoietin on ischemic wound healing in rats. Ostomy Wound Management 61 (3), 28-33.

Ashcroft, G.S., Horan, M.A., Ferguson, M.W.J., 1997. The effects of ageing on wound healing: Immunolocalisation of growth factors and their receptors in a murine incisional model. Journal of Anatomy 190 (3), 351-365.

Assanah, M., Bruce, J., Suzuki, S., Chen, A., Goldman, J., Canoll, P., 2009. PDGF stimulates the massive expansion of glial progenitors in the neonatal forebrain. Glia 57 (16), 1835-1847.

Babon, J., Varghese, L., Nicola, N., 2014. Inhibition of IL-6 family cytokines by Socs3. Seminars in Immunology 26, 13-19.

Bader, A., Lorenz, K., Richter, A., Scheffler, K., Kern, L., Ebert, S., Giri, S., Behrens, M., Dornseifer, U., Macchiarini, P., Machens, H., 2011. Interactive role of trauma cytokines and erythropoietin and their theraputic potential for acute and chronic wounds. Rejuvenation Research 14 (1), 57-66.

Badylak, S.F., Russell, A.J., Santin, M., 2009. Introduction: history of regenerative medicine. In: Santin, M. ed. Strategies in regenerative medicine: Integrating biology with materials design. Springer New York, New York, NY, pp. 1-13.

Bao, H., Jacobs-Helber, S., Lawson, A., Penta, K., Wickrema, A., Sawyer, S., 1999. Protein kinase b (c-AKT), phosphatidylinositol 3-kinase, and STAT5 are activated by erythropoietin (EPO) in hcd57 erythroid cells but are constitutively active in an EPO-independent, apoptosis-resistant subclone (hcd57-srei cells). Blood 93 (11), 3757-3773.

Barnett, M., Prineas, J., 2004. Relapsing and remitting multiple sclerosis: pathology of the newly forming lesion. Annals of Neurology 55 (4), 458-468.

Barres, B., Schmid, R., Sendnter, M., Raff, Mc., 1993. Multiple extracellular signals are required for long-term oligodendrocyte survival. Development 118 (1), 283-295.

Barrientos, S., Brem, H., Stojadinovic, O., Tomic-Canic, M., 2014. Clinical application of growth factors and cytokines in wound healing. Wound Repair and Regeneration 22, 569-578.

Barrientos, S., Stojadinovic, O., Golinko, M., Brem, H., Tomic-Canic, M., 2008. Growth factors and cytokines in wound healing. Wound Repair and Regeneration 16 (5), 585-601.

Bartels, C., Späte, K., Krampe, H., Ehrenreich, H., 2008. Recombinant human erythropoietin: Novel strategies for neuroprotective/neuro-regenerative treatment of multiple sclerosis. Therapeutic Advances in Neurological Disorders 1 (3), 193-206.

Bartsch, U., 2003. Neural cams and their role in the development and organization of myelin sheaths. Frontiers in Biosciences 8, d477-d490.

Bartsch, U., Kirchhoff, F., Schachner, M., 1989. Immunohistological localization of the adhesion molecules l1, N-CAM, and MAG in the developing adult optic nerve of mice. The Journal of Comparative Neurology 284 (3), 451-462.

Basak, S., Desai, D., Rho, E., Ramos, R., Maurel, P., Kim, H., 2015. E-cadherin enhances neuregulin signaling and promotes Schwann cell myelination. Glia 63 (9), 1522-1536.

Baumann, H., Wong, G., 1989. Hepatocyte-stimulating factor III shares structural and functional identity with leukemia inhibitory factor. Journal of Immunology 143 (4), 1163-1167.

Baumann, N., Pham-Dinh, D., 2001. Biology of oligodendrocyte and myelin in the mammalian central nervous system. Physiological Reviews 81 (2), 871-927.

Beck, K., Powell-Braxton, L., Widmer, H., Valverde, J., Hefti, F., 1995. Igf1 gene disruption results in reduced brain size, CNS hypomyelination, and loss of hippocampal granule and striatal parvalbumin-containing neurons. Neuron 14 (4), 717-730.

Beleslin-Cokic, B.B, Cokic, V.P, Yu, X, Weksler, B.B, Schechter, A.N., Noguchi, C.T, 2004. Erythropoietin and hypoxia stimulate erythropoietin receptor and nitric oxide production by endothelial cells. Blood 104 (7), 2073-2080.

Beltran, W., Zhang, Q., Kijas, J., Gu, D., Rohrer, H., Jordan, J., Aquirre, G., 2003. Cloning, mapping, and retinal expression of the canine ciliary neurotrophic factor receptor alpha (CNTFRα). Investigative Opthalmology & Visual Science 44 (8), 3642-3649.

Berard, J., Zarruk, J., Arbour, N., Prat, A., Yong, V., Jacques, F., Akira, S., David, S., 2012. Lipocalin 2 is a novel immune mediator of experimental autoimmune encephalomyelitis pathogenesis and is modulated in multiple sclerosis. Glia 60 (7), 1145-1159.

Bergamin, E., Wu, J., Hubbard, S., 2006. Structural basis for phosphotyrosine recognition by suppressor of cytokine signaling-3. Structure 14 (8), 1285-1292.

Bichenkov, E., Ellingson, J., 1999. Temporal quantitative expression of the myelin-associated lipids, ethanolamine plasmalogen, galactocerebroside, and sulfatide, in the differentiating cg-4 glial cell line. Neurochemical research 24 (12), 1549-1556.

Bienvenu, A., Ferrandiz, J., Kaiser, K., Latour, C., Picot, S., 2008. Atresunate-erythropoietin combination for murine cerebral malaria treatment. Acta tropica 106 (2), 104-108.

Bienvenu, A., Picot, S., 2013. Cerebral malaria: Protection by erythropoietin. Methods in molecular biology 982, 315-324.

Bitsch, A., Kuhlmann, T., Da Costa, C., Bunkowski, S., Polak, T., Bruck, W., 2000. Tumour necrosis factor alpha mrna expression in early multiple sclerosis lesions: Correlation with demyelinating activity and oligodendrocyte pathology. Glia 29 (4), 366-375.

Bloch, J., Bachoud-Levi, A., Deglon, N., Lefaucher, J., Winkel, L., Palfi, S., Nguyen, J., Bourdet, C., Gaura, V., Remy, P., Brugieres, P., Boisse, M., Baudic, S., Cesaro, P., Hantraye, P., Aebischer, P., Peschanski, M., 2004. Neurotprotective gene therapy for huntington's disease, using polymer-

encapsulated cells engineered to secrete human ciliary neurotrophic factor: Results of a phase 1 study. Human Gene Therapy 15 (10), 968-975.

Boateng, J., Matthews, K., Stevens, H., Eccleston, H., 2007. Wound healing dressings and drug delivery systems: A review. Journal of Pharmaceutical Sciences 97 (8), 2892-2923.

Boeuf, H., Merienne, K., Jacquot, S., Duval, D., Zeniou, M., Hauss, C., Reinhardt, B., Huss-Garcia, Y., Dierich, A., Frank, D., Hanauer, A., Kedinger, C., 2001. The ribosomal s6 kinases, camp-responsive element-binding, and stat3 proteins are regulated by different leukemia inhibitory factor signaling pathways in mouse embryonic stem cells. The Journal of Biological Chemistry 276 (49), 46204-45211.

Boggs, J., 2006. Myelin basic protein: A multifunctional protein. Cellular and Molecular Life Sciences 63 (17), 1945-1961.

Bohlius, J., Schmidlin, K., Brilliant, C., Schwarzer, G., Trelle, S., Seidenfeld, J., Zwahlen, M., Clarke, M., Weingart, O., Kluge, S., Piper, M., Napoli, M., Rades, D., Steensma, D., Djubegovic, B., Fey, M., Ray-Coguard, I., Moebus, V., Thomas, G., Untch, M., Schumacher, M., Egger, M., Engert, A., 2009. Erythropoietin or darbepoetin for patients with cancer -- meta-analysis based on individual patient data. Cochrane Database Systematic Review Jul 8 (3).

Bohr, S., Patel, S.J., Shen, K., Vitalo, A.G., Brines, M., Cerami, A., Berthiaume, F., Yarmush, M.L., 2013. Alternative erythropoietin-mediated signaling prevents secondary microvascular thrombosis and inflammation within cutaneous burns. PNAS 110 (9), 3513-3518.

Bolignano, D., Donato, V., Coppolino, G., Campo, S., Buemi, A., Lacquaniti, A., Buemi, M., 2008. Neutrophil gelatinase-associated lipocalin (NGAL) as a marker of kidney damage. American Journal of Kidney Diseases: The Official Journal of the National Kidney Foundation 52 (3), 595-605.

Boraschi, D., Rambaldi, A., Sica, A., Ghiara, P., Colotta, F., Wang, J., De Rossi, M., Zoia, C., Remuzzi, G., Bussolino, F., 1991. Endothelial cells express the interleukin-1 receptor type I. Blood 78 (5), 1262-1267.

Boukamp, P., Petrussevska, R., Breitkreutz, D., Hornung, J., Markham, A., Fusenig, N., 1988. Normal keratinization in a spontaneously immortalized aneuploid human keratinocyte cell line. Journal of Cell Biology 106 (3), 761-771.

Boulton, A., 2004. Pressure and the diabetic foot: Clinical science and offloading techniques. The American Journal of Surgery 187, 17S-24S.

Boulton, A., Vileikyte, L., Ragnarson-Tennvall, G., Apelqvist, J., 2005. The global burden of diabetic foot disease. The Lancet 366, 1719-1724.

Boyd, A., Zhang, H., Williams, A., 2013. Insufficient OPC migration into demyelinated lesions is a cause of poor remyelination in MS and mouse models. Acta Neuropathologica 125 (6), 841-859.

Bradford, M., 1976. A rapid and sensitive method for the quantitation of microgram quantities of protein utilizing the principle of protein-dye binding. Analytical Biochemistry 72, 248-254.

Brines, M., Cerami, A., 2008. Erythropoietin-mediated tissue-protection: Reducing collateral damage from the primary injury response. Journal of International Medicine 264, 405-432.

Brines, M., Cerami, A., 2012. The receptor that tames the innate immune response. Molecular Medicine 18, 486-496.

Brines, M., Dunne, A.N., Van Velzen, M., Proto, P.L., Ostenson, C.-G., Kirk, R.I., Petropoulos, I.N., Javed, S., Malik, R.A., Cerami, A., Dahan, A., 2014. Ara290, a nonerythropoietic peptide engineered from erythropoietin, improves metabolic control and neuropathic symptoms in patients with type 2 diabetes. Molecular Medicine 20 (1), 658-666.

Brines, M., Ghezzi, P., Keenan, S., Agnello, D., Lanerolle, N., Cerami, C., Itri, L., Cerami, A., 2000. Erythropoietin crosses the blood-brain barrier to protect against experimental brain injury. PNAS 97 (19), 10526-10531.

Brines, M., Grasso, G., Fiordaliso, F., Sfacteria, A., Ghezzi, P., Fratelli, M., Latini, R., Xie, Q., Smart, J., Su-Rick, C., Pobre, E., Diaz, D., Gomez, D., Hand, C., Coleman, T., Cerami, A., 2004. Erythropoietin mediates tissue protection through an erythropoietin and common b-subunit heteroreceptor. PNAS 101 (41), 14907-14912.

Brines, M., Patel, N., Villa, P., Brines, C., Mennini, T., De Paola, M., Erbayraktar, Z., Erbayraktar, S., Sepodes, B., Thiemermann, C., Ghezzi, P., Yamin, M., Hand, C., Xie, Q.-W., Coleman, T., Cerami, A., 2008. Nonerythropoietic, tissue-protective peptides derived from the tertiary structure of erythropoietin. PNAS Scientists 105 (31), 10925-10930.

Brinkmann, B., Agarwal, A., Sereda, M., Garratt, A., Muller, T., Wende, H., Stassart, R., Nawaz, S., Humml, C., Velanac, V., Radyushkin, K., Goebbels, S., Fischer, T., Franklin, R., Lai, C., Ehrenreich, H., Birchmeier, C., Schwab, M., Nave, K., 2008. Neuregulin-1/Erbb signaling serves distinct functions in myelination of the peripheral and central nervous system. Neuron 59 (4), 581-595.

Broadley, K., Aquino, A., Woodward, S., Buckley-Sturrock, A., Sato, Y., Rifkin, D., Davidson, J., 1989. Monospecific antibodies implicate basic fibroblast growth factor in normal wound repair. Laboratory investigation 61 (5), 571-575.

Bruce, A., Hoggatt, I., Rose, T., 1992. Oncostatin M is a differentiation factor for myeloid leukemia cells. Journal of Immunology 149 (4), 1271-1275.

Bsibsi, M., Nomden, A., Van Noort, J., Baron, W., 2012. Toll-like receptors 2 and 3 agonists differentially affect oligodendrocyte survival, differentiation, and

myelin membrane formation. Journal of neuroscience research 90 (2), 388-398.

Bsibsi, M., Ravid, R., Gveric, D., Van Noort, J., 2002. Broad expression of toll-like receptors in the human central nervous system. Journal of Neuropathology and Experimental Neurology 61 (11), 1013-1021.

Buckley, G., Metcalfe, A.D., Ferguson, M.W.J., 2011. Peripheral nerve regeneration in the mrl/mpj ear wound model. Journal of Anatomy 218 (2), 163-172.

Buckley, G., Wong, J., Metcalfe, A., Ferguson, M., 2012. Denervation affects regenerative responses in MRL/MpJ and repair in c57bl/6 ear wounds. Journal of Anatomy 220 (1), 3-12.

Buemi, M., Galeano, M., Sturiale, A., Ientile, R., Crisafulli, C., Parisi, A., Catania, M., Calapai, G., Impala, P., Aloisi, C., Squadrito, F., Altavilla, D., Bitto, A., Tuccari, G., Frisina, N., 2004. Recombinant human erythropoietin stimulates angiogenesis and healing of ischemic skin wounds. Shock 22 (2), 169-173.

Buemi, M., Lacquaniti, A., Maricchiolo, G., Bolignano, D., Campo, S., Cernaro, V., Sturiale, A., Grasso, G., Buemi, A., Allegra, A., Donato, V., Genovese, L., 2009. Regenerative medicine: Does erythropoietin have a role? Current Pharmaceutical Design 15 (17), 2026-2036.

Buemi, M., Vaccaro, M., Sturiale, A., Galeano, M., Sansotta, C., Cavallari, V., Floccari, F., D'amico, D., Torre, V., Calapai, G., Frisina, N., Guarneri, F., Vermiglio, G., 2002. Recombinant human erythropoietin influences revasularization and healing in a rat model of random ischaemic flaps. Acta Dermato-Venereologica 82 (6), 411-417.

Burdon, T., Stracey, C., Chambers, I., Nichols, J., Smith, A., 1999. Suppression of SHP-2 and ERK signalling promotes self-renewal of mouse embryonic stem cells. Developmental Biology 210 (1), 30-43.

Burnette, W., 1981. "Western blotting": Electrophoretic transfer of proteins from sodium dodecyl sulfate - polyacrylamide gels to unmodified nitrocellulose and radiographic detection with antibody and radioiodinated protein a. Analytical Biochemistry 112 (2), 195-203.

Butzkueven, H., Emery, B., Cipriani, T., Marriott, M., Kilpatrick, T., 2006. Endogenous leukemia inhibitory factor production limits autoimmune demyelination and oligodendrocyte loss. Glia 53 (7), 696-703.

Butzkueven, H., Zhang, J., Soilu-Hanninen, M., Hochrein, H., Chionh, F., Shipham, K., Emery, B., Turnley, A., Petratos, S., Ernst, M., Bartlett, P., Kilpatrick, T., 2002. LIF receptor signaling limits immune-mediated demyelination by enhancing oligodendrocyte survival. Nature Medicine 8 (6), 613-619.

Byts, N., Samoylenko, A., Fasshauer, T., Ivanisevic, M., Hennighausen, L., Ehrenreich, H., Siren, A., 2008. Essential tole for STAT5 in the neurotrophic but not in the neuroprotective effect of erythropoietin. Cell Death and Differentiation 15 (4), 783-792.

Campana, W., Misasi, R., O'brien, J., 1998. Identification of a neurotrophic sequence in erythropoietin. International Journal of Molecular Medicine 1 (1), 235-276.

Carbajal, K., Miranda, J., Tsukamoto, M., Lane, T., 2011. Cxcr4 signaling regulates remyelination by endogenous oligodendrocyte progenitor cells in a viral model of demyelination. Glia 59 (12), 1813-1821.

Carmeliet, P., 2003. Angiogenesis in health and disease. Nat Med 9 (6), 653-660.

Carson, M., Behringer, R., Brinster, R., Mcmorris, F., 1993. Insulin-like growth factor 1 increases brain growth and central nervous system myelination in transgenic mice. Neuron 10 (4), 729-740.

Carson, M., Doose, J., Melchior, B., Schmid, C., Ploix, C., 2006. CNS immune priviledge: Hiding in plain sight. Immunological Reviews 213, 48-65.

Carvalho, G., Lefaucheur, C., Cherbonnier, C., Metivier, D., Chapel, A., Pallardy, M., Bourgeade, M., Charpentier, B., Hirsch, F., Kroemer, G., 2005. Chemosensitization by erythropoietin through inhibition of the NF-κB rescue pathway. Oncogene 24 (5), 737-745.

Casals-Pascual, C., Idro, R., Gicheru, N., Gwer, S., Kitsao, B., Gitau, E., Mwakesi, R., Roberts, D.J., Newton, C.R.J.C., 2008. High levels of erythropoietin are associated with protection against neurological sequelae in African children with cerebral malaria. PNAS 105 (7), 2634-2639.

Casals-Pascual, C., Idro, R., Picot, S., Roberts, D.J., Newton, C.R.J.C., 2009. Can erythropoietin be used to prevent brain damage in cerebral malaria? Trends in Parasitology 25 (1), 30-36.

Cervellini, I., Annenkov, A., Brenton, T., Chernajovsky, Y., Ghezzi, P., Mengozzi, M., 2013a. Erythropoietin (EPO) increases myelin gene expression in CG4 oligodendrocyte cells through the classical EPO receptor. Molecular Medicine (19), 223-229.

Cervellini, I., Ghezzi, P., Mengozzi, M., 2013b. Therapeutic efficacy of erythropoietin in experimental autoimmune encephalomyelitis in mice, a model of multiple sclerosis. In: Ghezzi, P., Cerami, A. eds. Tissue-protective cytokines: Methods and protocols. Humana Press, Totowa, NJ, pp. 163-173.

Chan, J., Watkins, T., Cosgaya, J., Zhang, C., Chen, L., Reichardt, L., Shooter, E., Barres, B., 2004. NGF controls axonal receptivity to myelination by Schwann calls or oligodendrocytes. Neuron 43 (2), 183-191.

Chandrasekhar, S., Harvey, A.K., 1996. Modulation of PDGF mediated osteoblast chemotaxis by leukemia inhibitory factor (LIF). Journal of Cellular Physiology 169 (3), 481-490.

Chang, A., Nishiyama, A., Peterson, J., Prineas, J., Trapp, B., 2000. NG2-positive oligodendrocyte progenitor cells in adult human brain and multiple sclerosis lesions. Journal of Neuroscience 20 (17), 6404-6412.

Chang, A., Tourtellotte., W., Rudick, R., Trapp, B., 2002. Premyelinating oligodendrocytes in chronic lesions of multiple sclerosis. New England Journal of Medicine 346 (3), 165-73.

Chari, D., Blakemore, W., 2002. Efficient recolonisation of progenitor-depleted areas of he CNS by adult oligodendrocyte progenitor cells. Glia 37 (4), 307-313.

Charles, P., Hernandez, M., Stankoff, B., Aigrot, M., Colin, C., Rougon, G., Zalc, B., Lubetzki, C., 2000. Negative regulation of central nervous system myelination by polysialylated-neural cell adhesion molecule. Proceedings of the National Academy of Sciences of the USA 97 (13), 7585-7590.

Chatterjee, P., 2005. Pleiotropic renal actions of erythropoietin. Lancet 365 (9474), 1890-1892.

Chen, L., Tredget, E.E., Wu, P.Y.G., Wu, Y., 2008. Paracrine factors of mesenchymal stem cells recruit macrophages and endothelial lineage cells and enhance wound healing. PLoS One 3 (4), e1886.

Chen, S., Benveniste, E., 2004. Oncostatin M: A pleiotropic cytokine in the central nervous system. Cytokine and Growth Factor Reviews 15 (5), 379-391.

Chen, Y., Balasubramaniyan, V., Peng, J., Hurlock, E., Tallquist, M., Li, J., Lu, Q., 2007. Isolation and culture of rat and mouse oligodendrocyte precursor cells. Nature Protocols 2 (5), 1044-1051.

Cheng, J.-G., Patterson, P.H., 1997. LIF is an autocrine factor for sympathetic neurons. Molecular and Cellular Neuroscience 9 (5–6), 372-380.

Cherepkova, M., Sineva, G., Pospelov, V., 2016. Leukemia inhibitory factor (LIF) withdrawal activates mtor signaling pathway in mouse embryonic stem cells through the Mek/Erk/Tsc2 pathway. Cell Death and Disease 7 (e2050).

Chesnokova, V., Medled, S., 2000. Leukemia inhibitory factor mediates the hypothalamic pituitary adrenal axis response to inflammation. Endocrinology 141 (11), 4032-4040.

Choi, D., Schroer, S., Lu, S., Wang, L., Wu, X., Liu, Y., Zhang, Y., Gaisano, H., Wagner, K., Wu, H., Retnakaran, R., Woo, M., 2010. Erythropoietin protects against diabetes through direct effects on pancreatic beta cells. Journal of Experimental Medicine 207 (13), 2831-2842.

Chollangi, S., Mather, T., Rodgers, K., Ash, J., 2012. A unique loop structure in oncostatin M determines binding affinity toward oncostatin M receptor and leukemia inhibitory factpr receptor. Journal of Biological Chemistry 287 (39), 32848-32859.

Chong, Z., Kang, J., Maiese, K., 2002. Erythropoietin is a novel vascular protectant through activation of Akt1 and mitochondrial modulation of cysteine proteases. Circulation 106 (23), 2973-2979.

Chong, Z.Z., Maiese, K., 2007. Erythropoietin involves the phosphatidylinositol 3-kinase pathway, 14-3-3 protein and Foxo3a nuclear trafficking to preserve endothelial cell integrity. British Journal of Pharmacology 150 (7), 839-850.

Christiaens, V., Van Hul, M., Lijnen, H.R., Scroyen, I., 2012. Cd36 promotes adipocyte differentiation and adipogenesis. Biochimica et Biophysica Acta (BBA) - General Subjects 1820 (7), 949-956.

Clatterbuck, R., Price, D., Koliatsos, V., 1993. Ciliary neurotrophic factor prevents retrograde neuronal death in the adult central nervous system. Proceedings of the National Academy of Scientists 90 (6), 2222-2226.

Compston, A., 1998. Mcalpine's multiple sclerosis, Churchill Livingstone, London, UK.

Compston, A., Coles, A., 2008. Multiple sclerosis. The Lancet 372 (9648), 1502-1517.

Cowin, H.T., Brosnsn P., Ferguson M., 2001. Expression of TGFβ and its receptors in murine fetal and adult dermal wounds. European Journal of Dermatology 11 (5), 424-431.

Crawford, A., Chambers, C., Franklin, R., 2013. Remyelination: The true regeneration of the central nervous system. Journal of Comparative Pathology 149 (2-3), 242-254.

Cruz-Orengo, L., Daniels, B.P., Dorsey, D., Basak, S.A., Grajales-Reyes, J., Xe, G., Mccandless, E.E., Piccio, L., Schmidt, R.E., Cross, A.H., Crosby, S.D., Klein, R.S., 2014. Enhanced sphingosine-1-phosphate receptor 2 expression underlies female CNS autoimmunity susceptibility. The Journal of Clinical Investigation 124 (6), 2571-2584.

Dallner, C., Woods, A., Deller, T., Kirsch, M., Hofmann, H., 2002. CNTF and CNTF receptor alpha are constitutively expressed by astrocytes in the mouse brain. Glia 37 (4), 374-378.

Das, M., Leonardo, C.C., Rangooni, S., Pennypacker, K.R., Mohapatra, S., Mohapatra, S.S., 2011. Lateral fluid percussion injury of the brain induces Ccl20 inflammatory chemokine expression in rats. Journal of Neuroinflammation 8, 148-148.

David, S., Kroner, A., 2011. Repertoire of microglial and macrophage response after spinal cord injury. Nature Reviews: Neuroscience 12 (7), 388-399.

Davis, S., Aldrich, T., Stahl, N., Pan, L., Taga, T., Kishimoto, T., Ip, N., Tancopoulos, G., 1993. LIFR beta and gp130 as heterodimerizing signal transducers of the tripartite CNTF receptor. Science 260 (5115), 1805-1808.

De Monasterio-Schrader, P., Jahn, O., Tenzer, S., Wichert, S., Patzig, J., Werner, H., 2012. Systematic approaches to central nervous system myelin. Cellular and Molecular Life Sciences 69 (17), 2879-2894.

Decker, L., Desmarquet-Trin-Dinh, C., Taillebourg, E., Ghislain, J., Vallat, J., Charnay, P., 2006. Peripheral myelin maintenance is a dynamic process requiring constant Krox20 expression. Journal of Neuroscience 26 (38), 9771-9779.

Deguine, J., Barton, G., 2014. Myd88: A central player in innate immune signaling. F1000prime reports 4 (6).

Demetz, G., Laux, M., Scherhag, A., Hoekstra, T., Suttorp, M.M., Dekker, F., Roest, M., Marcus-Kalish, M., Mittelman, M., Ott, I., 2014. The influence of erythropoietin on platelet activation, thrombin generation and fvii/active fvii in patients with AMI. Thrombosis Journal 12 (1), 1-7.

Depping, R., Kawakami, K., Ocker, H., Wagner, J., Heringlake, M., Noetzold, A., Sievers, H., Wagner, K., 2005. Expression of the erythropoietin receptor in human heart. The Journal of Thoracic and Cardiovascular Surgery 130 (3), 877.e1-877.e4.

Desmoulière, A., Redard, M., Darby, I., Gabbiani, G., 1995. Apoptosis mediates the decrease in cellularity during the transition between granulation tissue and scar. The American Journal of Pathology 146 (1), 56-66.

Deverman, B., Patterson, P., 2012. Exogenous leukemia inhibitory factor stimulates oligodendrocyte progenitor cell proliferation and enhances hippocampal remyelination. Journal of Neuroscience 32 (6), 2100-2109.

Devireddy, L., Gazin, C., Zhu, X., Green, M., 2005. A cell-surface receptor for lipocalin 24p3 selectively mediates apoptosis and iron uptake. Cell 123 (7), 1293-1305.

Digicaylioglu, M., Bichet, S., Marti, H., Wenger, R., Rivas, L., Bauer, C., Gassmann, M., 1995. Localization of specific erythropoietin binding sites in defined areas of the mouse brain. PNAS 92 (9), 3717-3720.

Digicaylioglu, M., Lipton, S., 2001. Erythropoietin-mediated neuroprotection involves cross-talk between JAK2 and NF-κB signalling cascades. Nature 412 (6847), 641-647.

Ding, T., Song, H., Wang, X., Khatua, A., Paria, B., 2008. Leukemia inhibitory factor ligand-receptor signaling is important for uterine receptivity and implantation in golden hamsters (*mesocricetus auratus)*. Reproduction 135 (1), 41-53.

Dings, J., Meixensberger, J., Jager, A., Roosen, K., 1998. Clinical experience with 118 brain tissue oxygen partial pressure catheter probes. Neurosurgery 43 (5), 1082-1095.

Dobretsova, A., Kokorina, N.A., Wight, P.A., 2004. Potentiation of myelin proteolipid protein (Plp) gene expression is mediated through AP-1-like binding sites. Journal of Neurochemistry 90 (6), 1500-1510.

Dowsing, B., Romeo, R., Morrison, W., 2001. Expression of leukemia inhibitory factor in human nerve following injury. Journal of Neurotrauma 18 (11), 1279-1287.

Dugas, J., Ibrahim, A., Barres, B., 2012. The T3-induced gene Klf9 regulates oligodendrocyte differentiation and myelin regeneration. Molecular and Cellular Neuroscience 50, 45-57.

Duval, D., Reinhardt, B., Kedinger, C., Boeuf, H., 2000. Role or suppressors of cytokine signaling (Socs) in leukemia inhibitory factor (LIF) -dependent embryonic stem cell survival. . The FASEB journal 14, 1577-1584.

Dzietko, M., Felderhoff-Mueser, U., Sifringer, M., Krutz, B., Bittigau, P., Thor, F., Heumann, R., Bührer, C., Ikonomidou, C., Hansen, H.H., 2004. Erythropoietin protects the developing brain against n-methyl-d-aspartate receptor antagonist neurotoxicity. Neurobiology of Disease 15 (2), 177-187.

Ebert, B., Franklin Bunn, H., 1999. Regulation of the erythropoietin gene. Blood 94 (6), 1864-1877.

Egashira, Y., Hua, Y., Keep, R., Xi, G., 2014. Acute white matter injury after experimental subarachnoid hemorrhage: Potential role of lipocalin 2. Stroke 45 (7), 2141-2143.

Egrie, J., Browne, J., 2001. Development and characterization of novel erythropoiesis stimulating protein (NESP). Nephrology, Dialysis, Transplantation 16 (Suppl 3), 3-13.

Ehrenreich, H., Hasselblatt, M., Dembowski, C., Cepek, L., Lewczuk, P., Stiefel, M., Rustenbeck, H., Breite, N., Jacob, S., Knerlich, F., Bohn, M., Poser, W., Ruther, E., Kochen, M., Gefeller, O., Gleiter, C., Wessel, T., De Ryck, M., Itri, L., Prange, H., Cerami, A., Brines, M., Siren, A., 2002. Erythropoietin therapy for acute stroke is both safe and beneficial. Molecular Medicine 8 (8), 495-505.

Ehrenreich, H., Weissenborn, K., Prange, H., Schneider, D., Weimar, C., Wartenberg, K., Schellinger, P., Bohn, M., Becker, H., Wegrzyn, M., Jahnig, P., Herrmann, M., Knauth, M., Bahr, M., Heide, W., Wagner, A., Schwab, S., Reichmann, H., Schwendemann, G., Dengler, R., Kastrup, A., Bartels, C., EPO Stroke Trial Group, 2009. Recombinant human erythropoietin in the treatment of acute ischemic stroke. Stroke 40 (12), e647-656.

Ehrenreich, H.B.C., Sargin. D., Stawicki. S., Krampe. H., 2008. Recombinant human erythropoietin in the treatment of human brain disease: Focus on cognition. Journal of Renal Nutrition 18 (1), 146-153.

Eid, T., Brines, M.L., Cerami, A., Spencer, D.D., Kim, J.H., Schweitzer, J.S., Ottersen, O.P., De Lanerolle, N.C., 2004. Increased expression of erythropoietin receptor on blood vessels in the human epileptogenic hippocampus with sclerosis. Journal of Neuropathology & Experimental Neurology 63 (1), 73-83.

Elbashir, S., Harborth, J., Lendeckel, W., Yalcin, A., Weber, K., Tuschl, 2001. Duplexes of 21-nucleotide RNAs mediate RNA interference in cultures mammalian cells. Letters to Nature 411, 494-498.

Eller, K., Schroll, A., Banas, M., Kirsch, A., Huber, J., Nairz, M., Skvortsov, S., Weiss, G., Rosenkranz, A., Theurl, I., 2013. Lipocalin-2 expressed in innate immune cells is an endogenous inhibitor of inflammation in murine nephrotoxic serum nephritis. PLoS One 8 (7), e67693.

Elsherbiny, A., Hogger, D., Borozadi, M., Schmidt, C., Plock, J., Largo, R., Lindenblatt, N., Giovanoli, P., Contaldo, C., 2012. EPO reverses defective wound repair in hypercholesterolaemic mice by increasing functional angiogenesis. Journal of Plastic, Reconstructive & Aesthetic surgery: JPRAS 65 (11), 1559-1568.

Emara, M., Turner, A., Allalunis-Turner, J., 2014. Hypoxia differentially upregulates the expression of embryonic, fetal and adult hemoglobin in human glioblastoma cells. International Journal of Oncology 44 (3), 950-958.

Emerich, D., Lindner, M., Winn, S., Chen, E., Frydel, B., Kordower, J., 1996. Implants of encapsulated human cntf-producing fibroblasts prevent behavioral deficits and striatal degeneration in a rodent model of Huntington's disease. Journal of Neuroscience 16 (16), 5168-5181.

Emery, B., Cate, H., Marriott, M., Merson, T., Binder, M., Snell, C., Soo, P., Murray, S., Croker, B., Zhang, J., Alexander, W., Cooper, H., Butzkueven, H., Kilpatrick,T., 2006. Suppressor of cytokine signalling 3 limits protection of leukemia inhibitory factor receptor signalling against central demyelination. PNAS 103 (20), 7859-7864.

Erbayraktar, S., Grasso, G., Sfacteria, A., Xie, Q., Coleman, T., Kreilgaard, M., Torup, L., Sager, T., Erbayraktar, Z., Gokmen, N., Yilmaz, O., Ghezzi, P., Villa, P., Fratelli, M., Casagrande, S., Leist, M., Helboe, L., Gerwein, J., Christensen, S., Geist, M., Pedersen, L., Cerami-Hand, C., Wuerth, J., Cerami, A., Brines, M., 2003. Asialoerythropoietin is a nonerythropoietic cytokine with broad neuroprotective activity *in vivo*. PNAS 100 (11), 6741-6746.

Erbayraktar, Z., Erbayraktar, S., Yilmaz, O., Cerami, A., Coleman, T., Brines, M., 2009. Nonerythropoietic tissue protective compounds are highly effective facilitators of wound healing. Molecular Medicine 15 (7-8), 235-241.

Ernsberger, U., Sendtner, M., Rohrer, H., 1989. Proliferation and differentiation of embryonic chick sympathetic neurons: Effects of ciliary neurotrophic factor. Neuron 2 (3), 1275-1284.

Ernst, M., Jenkins, B., 2004. Acquiring signalling specificity from the cytokine receptor GP130. Trends in Genetics 20 (1), 23-32.

Erta, M., Quintana, A., Hidalgo, J., 2012. Interleukin-6, a major cytokine in the central nervous system. International Journal of Biological Sciences 8 (9), 1254-1266.

Eto, M., Yoshikawa, H., Fujimura, H., Naba, I., Sumi-Akamaru, H., Takayasu, S., Itabe, H., Sakoda, S., 2003. The role of CD36 in peripheral nerve remyelination after crush injury. European Journal of Neuroscience 17 (12), 2659-2666.

Fairchild, D., Conrad, K., 1999. Expression of the erythropoietin receptor by trophoblast cells in the human placenta. Biology of Reproduction 60, 861-870.

Fancy, S., Baranzini, S., Zhao, C., Yuk, D., Irvine, K., Kaing, S., Sanai, N., Franklin, R., Rowitch., D 2009. Dysregulation of the Wnt pathway inhibits timely myelination and remyelination in the mammalian Cns. Genes and development 23 (13), 1571-1585.

Faroni, A., Mobasseri, S.A., Kingham, P.J., Reid, A.J., 2015. Peripheral nerve regeneration: Experimental strategies and future perspectives. Advanced Drug Delivery Reviews 82–83, 160-167.

Fatouros, M., Dalekos, G.N., Mylonakis, E., Vekinis, G., Kappas, A.M., 1999. Alterations in body weight, breaking strength, and wound healing in wistar rats treated pre- and postoperatively with erythropoietin or granulocyte macrophage–colony stimulating factor: Evidence of a previously unknown anabolic effect of erythropoietin? Journal of Laboratory and Clinical Medicine 133 (3), 253-259.

Fenjves, E., Ochoa, M., Cabrera, O., Mendez, A., Kenyon, N., Inverardi, L., Ricordi, C., 2003. Human, nonhuman primate, and rat pancreatic islets express erythropoietin receptors. Transplantation 75 (8), 1356-1360.

Ferguson, M.W.J., O'kane, S., 2004. Scar–free healing: From embryonic mechanisms to adult therapeutic intervention. Philosophical Transactions of the Royal Society B: Biological Sciences 359 (1445), 839-850.

Fire, A., Xu, S., Montgomery, M., Kostas, S., Driver, S., Mello, C., 1998. Potent and specific genetic interference by double-stranded RNA in caenorhabditis elegans. Nature 391 (6669), 806-811.

Fisher, J.W., Koury, S., Ducey, T., Mendel, S., 1996. Erythropoietin production by interstitial cells of hypoxic monkey kidneys. British Journal of Haematology (95), 27-32.

Flores, A., Narayanan, S., Morse, E., Shick, H., Yin, X., Kidd, G., Avila, R., Kirschner, D., Macklin, W., 2008. Constitutively active Akt induces enhanced myelination in the CNS. The Journal of Neuroscience 28 (28), 7174-7183.

Flower, D., 1996. The lipocalin protein family: Structure and function. The Biochemical Journal 318 (1), 1-14.

Frank, S., Hubner, G., Breier, G., Longaker, M., Greenhalgh, D., Werner, S., 1995. Regulation of vascular endothelial growth factor expression in cultured keratinocytes. Implications for normal and impaired wound healing. Journal of Biological Chemistry 270 (21), 12607-12613.

Franklin, R., 2002. Why does remyelination fail in multiple sclerosis? Nature Reviews Neuroscience 3 (9), 705-714.

Franklin, R., Ffrench-Constant, C., 2008. Remyelination in the CNS: From biology to therapy. Nature Reviews Neuroscience 9 (11), 839-855.

Franklin, R.J.M., Bayley, S.A., Milner, R., Ffrench-Constant, C., Blakemore, W.F., 1995. Differentiation of the O-2a progenitor cell line CG-4 into oligodendrocytes and astrocytes following transplantation into glia-deficient areas of CNS white matter. Glia 13 (1), 39-44.

Fu, P., Jing, X., Arcasoy, M., 2009. Constitutively active erythropoietin receptor expression in breast cancer cells promotes cellular proliferation and migration through a MAP-kinase dependent pathway. Biochemical and Biophysical Research Communications 379 (3), 696-701.

Fuhrmann, S., Grabosch, K., Kirsch, M., Hofmann, H., 2003. Distribution of the CNTF receptor alpha protein in the central nervous system of the chick embryo. The Journal of Comparative Neurology 461 (1), 111-122.

Fuller, M., Dechant, A., Rothstein, B., Caprariello, A., Wang, R., Hall, A., Miller, R., 2007. Bone morphogenic proteins promote gliosis in demyelinating spinal cord lesions. Annals of Neurology 62 (3), 288-300.

Fuste, B., Serradell, M., Escolar, G., Cases, A., Mazzara, R., Castillo, R., Ordinas, A., Diaz-Ricart, M., 2002. Erythropoietin triggers a signaling pathway in endothelial cells and increases the thrombogenicity of their extracellular matrices in vitro. Thrombosis and Haemostasis 88 (4), 541-702.

Gabory, A., Jammes, H., Dandolo, L., 2010. The H19 locus: Role of an imprinted non-coding RNA in growth and development. BioEssays 32 (6), 473-480.

Gaesser, J., Fyffe-Maricich, S., 2016. Intrecellular signaling pathway regulation of myelination and remyelination in the CNS. Experimental Neurology.

Galkowska, H., Wojewodzka, U., Olszewski, W., 2006. Chemokines, cytokine, and growth factors in keratinocytes and dermal endothelial cells in the margin of chronic diabetic foot ulcers. Wound Repair and Regeneration 14 (5), 558-565.

Gearing, D., Thut, C., Vandenbos, T., Gimpel, S., Delaney, P., King, J., Price, V., Cosman, D., Beckmann, M., 1991. Leukemia inhibitory factor receptor is structurally related to the IL-6 sigal transducer, GP130. The EMBO Journal 10 (10), 2839-2848.

Geleano, M., Altavilla, D., Cucinotta, D., Russo, G., Calo, M., Bitto, A., Marini, H., Marini, R., Elena, A., Seminara, P., Minutoli, L., Torre, V., Squadrito, 2004.

Recombinant human erythropoietin stimulates angiogenesis and wound healing in the genetically diabetic mouse. Diabetes 53, 2509-2517.

Ghezzi, P., 2004. Erythropoietin as an antiapoptotic, tissue-protective cytokine. Cell Death and Differentiation 11, S37-S44.

Gibran, N., Jang, Y., Isik, F., Greenhalgh, D., Muffley, L., Underwood, R., Usui, M., Larsen, J., Smith, D., Bunnett, N., Ansel, J., Olerud, J., 2002. Diminished neuropeptide levels contribute to the impaired cutaneous healing response associated with diabetes mellitus. Journal of Surgical Research 108 (1), 122-128.

Gielen, E., Baron, W., Vandeven, M., Steels, P., Hoekstra, D., Ameloot, M., 2006. Rafts in oligodendrocytes: Evidence and structure-function relationship. Glia 54 (6), 499-512.

Glaiano, R., Tepper, O., Pelo, C., Bhatt, K., Callaghan, M., Bastidas, N., Bunting, S., Steinmetz, H., Gurtner, G., 2004. Topical vascular endothelial growth factor accelerates diabetic wound healing through increased angiogenesis and by mobilizing and recruiting bone marrow-derived cells. The American Journal of Pathology 164 (6), 1935-1947.

Goddard, D., Berry, M., Butt, A., 1999. In vivo actions of fibroblast growth factor-2 and insulin-like growth factor-1 on oligodendrocyte development and myelination in the central nervous system. Journal of Neuroscience Research 57 (1), 74-85.

Goebbels, S., Oltrogge, J., Kemper, R., Heilmann, I., Bormuth, I., Wolfer, S., Wichert, S., Mobius, W., Liu, X., Lappe-Siefke, C., Rossner, M., Groszer, M., Suter, U., Frahm, J., Boretius, S., Nave, K., 2010. Elevated phosphatidylinositol 3,4,5-trisphosphate in glia triggers cell-autonomous membrane wrapping and meylination. The Journal of Neuroscience 30 (26), 8953-8964.

Goetz, D., Holmes, M., Borregaard, N., Bluhm, M., Raymond, K., Strong, R., 2002. The neutrophil lipocalin NGAL is a bacteriostatic agent that interferes with siderophore-mediated iron acquisition. Molecular Cell 10 (5), 1033-1043.

Gonsalvez, D., Ferner, A.H., Peckham, H., Murray, S.S., Xiao, J., 2015. The roles of extracellular related-kinases 1 and 2 signaling in CNS myelination. Neuropharmacology.

Gonzalez, F., Larpthaveesarp, A., Mcquillen, P., Derugin, N., Wendland, M., Spadafora, R., Ferriero, D., 2013. Erythropoietin increases neurogenesis and oligodendrogliosis of svz precursor cells after neonatal stroke. Stroke 44 (3), 753-758.

Gonzalez, F.F., Larpthaveesarp, A., Mcquillen, P., Derugin, N., Wendland, M., Spadafora, R., Ferriero, D.M., 2013. Erythropoietin increases neurogenesis and oligodendrogliosis of svz precursor cells after neonatal stroke. Stroke; a Journal of Cerebral Circulation 44 (3), 753-758.

Gopalakrishnan, B., Wolff, J., 2009. SiRNA and DNA transfer to cultured cells. Methods in Molecular Biology 480, 31-52.

Gouin, F., Coulliaud, S., Cottrel, M., Godard, A., Passuti, N., Heymann, D., 1999. Presence of leukaemia inhibitory factor (LIF) and LIF-receptor chain (GP130) in osteoclast-like cells cultured from human giant cell tumour of bone. Ultrastructural Distribution. Cytokine 11 (4), 282-289.

Gould, R.M., Oakley, T., Goldstone, J.V., Dugas, J.C., Brady, S.T., Gow, A., 2008. Myelin sheaths are formed with proteins that originated in vertebrate lineages. Neuron Glia Biology 4 (02), 137-152.

Greaves, N., Ashcroft, K., Baguneid, M., Bayat, Ardeshir, 2013. Current understanding of molecular and cellular mechanisms in fibroplasia and angiogenesis during acute wound healing. Journal of Dermatological Science 72, 206-217.

Guardiola-Diaz, H.M., Ishii, A., Bansal, R., 2012. Erk1/2 MAPK and Mtor signaling sequentially regulates progression through distinct stages of oligodendrocyte differentiation. Glia 60 (3), 476-486.

Gunawardana, D., Basser, R., Davis, I., Cebon, J., Mitchell, P., Underhill, C., Kilpatrick, T., Reardon, K., Crump, D., Ng, S., Nation, R., Begley, G., 2003. A phase I study of recombinant human leukemia inhibitory factor in patients with advanced cancer. Clinical Cancer Research 9, 2056-2065.

Günter, C.I., Bader, A., Dornseifer, U., Egert, S., Dunda, S., Grieb, G., Wolter, T., Pallua, N., Von Wild, T., Siemers, F., Mailänder, P., Thamm, O., Ernert, C., Steen, M., Sievers, R., Reichert, B., Rahmanian-Schwarz, A., Schaller, H., Hartmann, B., Otte, M., Kehl, V., Ohmann, C., Jelkmann, W., Machens, H.-G., 2013. A multi-center study on the regenerative effects of erythropoietin in burn and scalding injuries: Study protocol for a randomized controlled trial. Trials 14, 124-124.

Guo, S., Li, Z., Gong, J., Xiang, M., Zhang, P., Zhao, G., Li, M., Zheng, A., Zhu, X., Lei, H., Minoru, T., Li, H., 2015. Oncostatin M confers neuroprotection against ischemic stroke. Journal of Neuroscience 35 (34), 12047-12062.

Gupta, R., Rowshan, K., Chao, T., Mozaffar, T., Steward, O., 2004. Chronic nerve compression induces local demyelination and remyelination in a rat model of carpal tunnel syndrome. Experimental Neurology 187 (2), 500-508.

Hagemeyer, N., Boretius, S., Ott, C., Von Streitberg, A., Welpinghus, H., Sperling, S., Frahm, J., Simons, M., Ghezzi, P., Ehrenreich, H., 2012. Erythropoietin attenuates neurological and histological consequences of toxic demyelination in mice. Molecular Medicine 18 (1), 628-635.

Hamed, S., Ullmann, Y., Masoud, M., Hellou, E., Khamaysi, Z., Teot, L., 2010. Topical erythropoietin promotes wound repair in diabetic rats. Journal of Investigative Dermatology 130, 287-294.

Hao, W., Tashiro, S., Hasegawa, T., Sato, Y., Kobayashi, T., Tando, T., Katsuyama, E., Fuji, A., Watanabe, R., Morita, M., Miyamoto, K., Morioka, H., Nakamura, M., Matsumoto, M., Amizuka, N., Toyama, Y., Miyamoto, T., 2015. Hyperglycemia promotes Schwann cell de-differentiation and de-myelination via sorbitol accumulation and IGF1 protein down-regulation. Journal of biological chemistry 290 (28), 17106-17115.

Hardee, M., Cao, Y., Fu, P., Jiang, X., Zhao, Y., Rabbani, Z., Vujaskovic, Z., Dewhirst, M., Arcasoy, M., 2007. Erythropoietin blockade inhibits the induction of tumor angiogenesis and progression. PLoS One 2 (6), e549.

Haroon, Z.A., Amin, K., Jiang, X., Arcasoy, M.O., 2003. A novel role for erythropoietin during fibrin-induced wound-healing response. The American Journal of Pathology 163 (3), 993-1000.

Harrison, J.S., Rameshwar, P., Chang, V., Bandari, P., 2002. Oxygen saturation in the bone marrow of healthy volunteers. Blood 99 (1), 394-394.

Hart, J., 2002. Inflammation. 1: Its role in the healing of acute wounds. Journal of Wound Care 11 (6), 205-209.

Hayakawa, K., Seo, J., Pham, L., Miyamoto, N., Som, A., Guo, S., Kim, K., Lo, E., Arai, K., 2012. Cerebral endothelial derived vascular endothelial growth factor promotes the migration but not the proliferation of oligodendrocyte precursor cells in vitro. Neuroscience Letters 513 (1), 42-46.

Heeschen, C., Aicher, A., Lehmann, R., Fichtlscherer, S., Vasa, M., Urbich, C., Mildner-Rihm, C., Martin, H., Zeiher, A., Dimmeler, S., 2003. Erythropoietin is a potent physiologic stimulus for endothelial progenitor cell mobilization. Blood 102 (4), 1340-1346.

Heinrich, P., Behrmann, I., Haan, S., Hermanns, H., Muller-Newen, G., Schaper, F., 2003. Principles of interleukin (IL)-6-type cytokine signalling and its regulation. Journal of Biochemistry 374, 1-20.

Hempel, C., Hyttel, P, Staalso, T, Nyengaard, J, Kurtzhals, J, 2012. Erythropoietin treatment alleviates ultrastructural myelin changes induced by murine cerebral malaria. Malaria Journal 11 (216).

Hilliard, B.A., Mason, N., Liu, T.S., Liou, H., Hunter, C., Chen, Y.H., 2001. The REL/NF-κB family of transcription factors plays pivotal roles in the development of experimental autoimmune encephalomyelitis. Faseb Journal 15 (5), A1067-A1067.

Hilton, D., Nicola, N., Metcalf, D., 1991. Distribution of receptors for leukemia inhibitory factor on murine hemopoietic and hepatic cells. Journal of Cellular Physiology 146 (2), 207-215.

Hinds, M., Maurer, T., Zhang, J., Nicola, N., Norton, R., 1998. Solution structure of leukemia inhibitory factor. The Journal of Biological Chemistry 273 (22), 13738-13745.

Hinks, G., Franklin, R., 1999. Distinctive patterns of PDGFa, FGF2, IGF1, and TGFβ1 gene experssion during remyelination of experimentally-induced spinal cord demyelination. Molecular and Cellular Neuroscience 14 (2), 153-168.

Hirashima, M., 2009. Regulation of endothelial cell differentiation and arterial specification be VEGF and Notch signaling. Anatomical Science International 84 (3), 95-101.

Hiscott, J., 2011. Cytokines. Current Opinion in Immunology 23 (5), 561-563.

Hofman, F., Hinton, D., Johnson, K., Merrill, J., 1989. Tumor necrosis factor identified in multiple sclerosis brain. The Journal of Experimental Medicine 170 (2), 607-612.

Hong, J., Park, S., 2014. The combined effect of recombinant human epidermal growth factor and erythropoietin on full-thickness wound healing in diabetic rat model. International Wound Journal 11 (4), 373-378.

Hortner, M., Nielsch, U., Mayr, L., Heinrich, P., Haan, S., 2002. A new high affinity binding site for suppressor of cytokine signaling-3 on the erythropoieitn receptor. European Journal of Biochemistry 269, 2516-2526.

Hou, J., Wang, S., Shang, Y.C., Chong, Z.Z., Maiese, K., 2011. Erythropoietin employs cell longevity pathways of sirt1 to foster endothelial vascular integrity during oxidant stress. Current Neurovascular Research 8 (3), 220-235.

Hu, Q., Ang, B., Karsak, M., Hu, W., Cui, X., Duka, T., Takeda, Y., Chia, W., Sankar, N., Ng, Y., Ling, E., Maciag, T., Small, D., Trifonova, R., Kopan, R., Okano, H., Nakafuku, M., Chiba, S., Hirai, H., Aster, J., Schachner, M., Pallen, C., Watanabe, K., Xiao, Z., 2003. F3/contactin acts as a functional ligand for notch during oligodendrocyte maturation. Cell 115 (2), 163-175.

Huang, J., Jarjour, A., Nait Oumesmar, B., Kerninon, C., Williams, A., Krezel, W., Kagechika, H., Bauer, J., Zhao, C., Baron-Van Ecercooren, A., Chambon, P., Ffrench-Constant, C., Franklin, R., 2011. Retinoid x receptor gamma signaling accelerates CNS remyelination. Nature Neuroscience 14 (1), 45-53.

Ibrahim, A., Scher, N., Williams, G., Sridhara, R., Li, N., Chen, G., Leighton, J., Booth, B., Gobburu, J., Rahman, A., Hsieh, Y., Wood, R., Vause, D., Pazdur, R., 2003. Approval summary for zoledronic acid for treatment of multiple myelome and cancer bone metastases. Clinical Cancer Research 9 (7), 2394-2399.

Ichikawa, Y., 1969. Differentiation of a cell line of myeloid leukemia. Journal of Cellular Physiology 74 (3), 223-234.

Ichikawa, Y., 1970. Further studies on the differentiation of a cell line of myeloid leukemia. Journal of Cellular Physiology 76 (2), 175-184.

Ilina, O., Friedl, P., 2009. Mechanisms of collective cell migration at a glance. Journal of Cell Science 122 (18), 3203-3208.

Ip, N., Yancopoulos, G., 1992. Ciliary neurotrophic factor and its receptor complex. Progress in Growth Factor Research 4 (2), 139-155.

Ishibashi, T., Dakin, K., Stevens, B., Lee, P., Kozlov, S., Stewart, C., Fields, D., 2006. Astrocytes promote myelination in response to electrical impulses. Neuron 49, 823-832.

Ishii, A., Furusho, M., Bansal, R., 2013. Sustained activation of ERK1/2 MAPK in oligodendrocytes and Schwann cells enhances myelin growth and stimulates oligodendrocyte progenitor expansion. The Journal of Neuroscience 33 (1), 175-186.

Ishii, A., Fyffe-Maricich, S., Furusho, M., Miller, R., Bansal, R., 2012. ERK1/ERK2 MAPK signaling is required to increase myelin thickness independent of oligodendrocyte differentiation and initiation of myelination. Journal of Neuroscience 32 (26), 8855-8864.

Jacobs, K., Shoemaker, C., Rudersdorf, R., Neill, S., Kaufman, R., Mufson, A., Seehra, J., Jones, S., Hewick, R., 1985. Isolation and characterization of genomic and cDNS clones of human erythropoietin. Nature 313 (6005), 806-810.

Jagannathan, L., Cuddapah, S., Costa, M., 2016. Oxidative stress under ambient and physiological oxygen tension in tissue culture. Current Pharmacology Reports 2 (2), 64-72.

James, S.E., Booth, S., Gilbert, P., Jones, I., Shevchenko, R., 2009. Clinical approaches to skin regeneration. In: Santin, M. ed. Strategies in regenerative medicine: Integrating biology with materials design. Springer New York, New York, NY, pp. 1-33.

Janssens, K., Maheshwari, A., Van Den Haute, C., Baekelandt, V., Stinissen, P., Hendriks, J., Slaets, H., Hellings, N., 2015. Oncostatin M protects against demyelination by inducing a protective microglial phenotype. Glia 63 (10), 1729-1737.

Jasper, M., Care, A., Sullivan, B., Ingman, W., Aplin, J., Robertson, S., 2011. Macrophage-derived LIF and IL1b regulate alpha(1,2)fucosyltransferase 2 (fut2) expression in mouse unterine epithelial cells during early pregnancy. Biology of Reproduction 84 (1), 179-188.

Jay, A.G., Hamilton, J.A., 2016. The enigmatic membrane fatty acid transporter CD36: New insights into fatty acid binding and their effects on uptake of oxidized LDL. Prostaglandins, Leukotrienes and Essential Fatty Acids (PLEFA).

Jeffery, N., Blakemore, W., 1997. Locomotor deficits induced by experimental spinal cord demyelination are abolished by spontaneous remyelination. Brain 120 (1), 27-37.

Jegalian, A., Wu, H., 2002. Differential roles of Socs family members in EPOR signal transduction. Journal of Interferon & Cytokine research 22 (8), 853-860.

Jelkmann, W., 2005. Effects of erythropoietin on brain function. Current Pharmaceutical Biotechnology 6 (1), 65-79.

Jessen, K., Mirsky, R., 2005. The origin and development of glial cells in peripheral nerves. Nature Reviews: Neuroscience 6, 671-682.

Jin, M., Kim, S., Heo, J., Lee, M., Kim, H., Paik, S., Lee, H., Lee, J., 2007. Crystal structure of the TLR1-TLR2 heterodimer induced by binding of a tri-acylated lipopeptide. Cell 130 (6), 1071-1082.

John, G., Shankar, S., Shafit-Zagardo, B., Massimi, A., Lee, S., Raine, C., Brosnan, C., 2002. Multiple sclerosis: Re-expression of a developmental pathway that restricts oligodendrocyte maturation. Nature Medicine 8 (10), 1115-1121.

Joly, S., Lange, C., Thiersch, M., Samardzija, M., Grimm, C., 2008. Leukemia inhibitory factor extends the lifespan of injured photoreceptors in vivo. The Journal of Neuroscience 28 (51), 13765-13774.

Joseph A. Nielsen, P., Hudson, L., Nielsen, J., Pierre Lau, Hudson., L., 2010. The Genetics of Oligodendrocytes. The biology of oligodendrocytes Cambridge University Press.

Jubinsky, P., Krijanovski, O., Nathan, D., Tavernier, J., Sieff, C., 1997. The beta chain of the interleukin-3 receptor functionally associates with the erythropoietin receptor. Blood 90 (5), 1867-1873.

Juul, S., Mcpherson, R., Farrell, F., Jolliffe, L., Ness, D., Gleason, C., 2004. Erythropoietin concentrations in cerebrospinal fluid of nonhuman primates and fetal sheep following high-dose recombinant erythropoietin. Neonatology 85 (2), 138-144.

Juul, S., Anderson, D., Li, Y., Christensen, R., 1998. Erythropoietin and erythropoietin receptor in the developing human central nervous system. Pediatr Res 43 (1), 40-49.

Juul, S., Stallings, S., Christensen, R., 1999. Erythropoietin in the cerebrospinal fluid of neonates who sustained CNS injury. Pediatr Res 46 (5), 543-543.

Kaiser, K., Texier, A., Ferrandiz, J., Buguez, A., Meiller, A., Latour, C., Peyron, F., Cespuglio, R., Picot, S., 2006. Recombinant human erythropoietin prevents the death of mice during cerebral malaria. The Journal of Infectious Diseases 193 (7), 987-995.

Kang, Y.-J., Digicaylioglu, M., Russo, R., Kaul, M., Achim, C., Fletcher, L., Masliah, E., Lipton, S., 2010. Erythropoietin plus insulin-like growth factor-1 protects against neuronal damage in a murine model of human immunodeficiency virus-associated neurocognitive disorders. Annals of Neurology 68 (3), 342-352.

Kapitsinou, P., Liu, Q., Unger, T., Rha, J., Davidoff, O., Keith, B., Epstein, J., Moores, S., Erickson-Miller, C., Haase, W., 2010. Hepatic HIF-2 regulates erythropoietic responses to hypoxia in renal anemia. Blood 116 (16), 3039-3048.

Kato, S., Amano, H., Y, Eshima, K., Aoyama, N., Tamaki, H., Sakagami, H., Satoh, Y., Izumi, T., Majima, M., 2010. Effect of erythropoietin on angiogenesis with the increased adhesion of platelets to the microvessels in the hind-limb ischemia model in mice. Journal of Pharmacological Sciences 112 (2), 167-175.

Kato, S., Aoyama, M., Kakita, H., Hida, H., Kato, I., Ito, T., Goto, T., Hussein, M., Sawamoto, K., Togari, H., Asai, K., 2011. Endogenous erythropoietin from astrocyte protects the oligodendrocyte precursor cell against hypoxic and reoxygenation injury. Journal of Neuroscience Research 89 (10), 1566-1574.

Keast, D., Fraser, C., 2004. Treatment of chronic skin ulcers in individuals with anemia of chronic disease using recombinant human erythropoietin (EPO): A review of four cases. Ostomy Wound Management 50 (10), 64-70.

Kehrer, J., 2010. Lipocalin-2: Pro- or anti-apoptotic? Cell Biology and Toxicology 26 (2), 83-89.

Kielian, T., 2006. Toll-like receptors in central nervous system glial inflammation and homeostasis. Journal of Neuroscience Research 83 (5), 711-730.

Kigerl, K., Lai, W., Rivest, S., Hart, R., Satoskar, A., Popovich, P., 2007. Toll-like receptor (TLR)-2 and TLR-4 regulate inflammation, gliosis, and myelin sparing after spinal cord injury. Journal of Neurochemistry 102 (1), 37-50.

Kilic, E., Kilic, U., Soliz, J., Bassetti, C., Gassmann, M., Hermann, D., 2005. Brain-derived erythropoietin protects from focal cerebral ischemia by dual activation of ERK-1/-2 and AKT pathways. FASEB J 19 (14), 2026-2028.

Kim, I., Kim, C., Yim, Y., Ahn, Y., 2008. Autocrine function of erythropoietin in IGF-1-induced erythropoietin biosynthesis. NeuroReport 19 (17), 1699-1703.

Kirkeby, A., Torup, L., Bochsen, L., Kjalke, M., Abel, K., Theilgaard-Monch, K, Johansson, P, Bjorn, S., Gerwien, J., Leist, M., 2008. High-dose erythropoietin alters platelet reactivity and bleeding time in rodents in contrast to the neuroprotective variant carbamyl-erythropoietin (cEPO). Thrombosis and Haemostasis 99 (4), 720-720.

Knabe, W., Knerlich, F., Washausen, S., Kietzmann, T., Sirén, A., Brunnett, G., Kuhn, H., Ehrenreich, H., 2004. Expression patterns of erythropoietin and its receptor in the developing midbrain. Anatomy and Embryology 207 (6), 503-512.

Knapp, P., Bartlett, W., Skoff, R., 1987. Culutred oligodendrocytes mimic in vivo phenotypic characteristics: Cell shape, expression of myelin-specific antigens, and membrane prodeuction. Developmental Biology 120 (2), 356-365.

Konishi, Y., Chui, D., Hirose, H., Kunishita, T., Tabira, T., 1993. Trophic effect of erythropoietin and other hematopoietic factors on central cholinergic neurons in vitro and in vivo. Brain Research 609 (1-2), 29-35.

Koopman, P., Cotton, G., 1984. A factor produced by feeder cells which inhibits embryonal carcinoma cell differentiation. Experimental Cell Research 154, 233-242.

Koury, S., Bondurant, M., Koury, M., Semenza, G., 1991. Localization of cells producing erythropoietin in murine liver by in situ hybridization. Blood 77 (11), 2497-2503.

Koury, S., Bondurant, Mc, Koury, Mj, 1988. Localization of erythropoietin synthesizing cells in murine kidneys by in situ hybridization. Blood 71 (2), 524-527.

Krebs, D., Hilton, D., 2000. Socs: Physiological suppressors of cytokine signaling. Journal of Cell Science 113 (16), 2813-2819.

Kuffler, 2015. Platelet-rich plasma promotes axon regeneration, wound healing, and pain reduction: Fact or fiction. Molecular Neurobiology 52, 990-1014.

Kuhl, N., De Keyser, J., De Vries, H., Hoekstra, D., 2002. Insulin-like growth factor binding proteins-1 and -2 differentially inhibit rat oligodendrocyte precursor cell survival and differentiation in vitro. Journal of Neuroscience Research 69 (2), 207-216.

Kuhrt, D., Wojchowski, D., 2015. Emerging EPO and EPO receptor regulators and signal transducers. Blood 125 (23), 3536-3541.

Kumar, A., Brockes, J., 2012. Nerve dependence in tissue, organ, and appendage regeneration. Trends in Neurosciences 35 (11), 691-699.

Kurek, J., Bennett, T., Bower, J., Muldoon, C., Austin, L., 1998. Leukaemia inhibitory factor (LIF) production in a mouse model of spinal trauma. Neuroscience Letters 12 (249), 1-4.

La Ferla, K., Reimann, C., Jelkmann, W., Hellwig-Burgel, T., 2002. Inhibition of erythropoietin gene expression signaling involved the transcription factors GATA-2 and NF-κB. The FASEB journal 16 (13), 1811-1813.

Ladiwala, U., Lachance, C., Simoneau, S., Bhakar, A., Barker, P., Antel, J., 1998. P75 neurotrophin receptor expression on adult human oligodendrocytes: Signaling without cell death response to NGF. Journal of Neuroscience 18 (4), 1297-1304.

Larson, B., Longaker, M., Lorenz, H., 2010. Scarless fetal wound healing: A basic science review. Plastic and Reconstructive Surgery 126 (4), 1172-1180.

Lauer, G., Sollberg, S., Cole, M., Krieg, T., Eming, S., Flamme, I., Stürzebecher, J., Mann, K., 2000. Expression and proteolysis of vascular endothelial growth

factor is increased in chronic wounds. Journal of Investigative Dermatology 115 (1), 12-18.

Lee, X., Shao, Z., Sheng, G., Pepinsky, B., Mi, S., 2014. Lingo-1 regulated oligodendrocyte differentiation by inhibiting Erbb2 translocation and activation in lipid rafts. Molecular and Cellular Neurosciences 60, 36-42.

Leist, M., Ghezzi, P., Grasso, G., Bianchi, R., Villa, P., Fratelli, M., Savino, C., Bianchi, M., Nielsen, J., Gerwien, J., Kallunki, P., Larsen, A., Helboe, L., Christensen, S., Pedersen, L., Nielsen, M., Torup, L., Sager, T., Sfacteria, A., Erbayraktar, Z., Gokmen, N., Yilmaz, O., Cerami-Hand, C., Xie, Q., Coleman, T., Cerami, A., Brines, M., 2004. Derivatives of erythropoietin that are tissue protective but not erythropoietic. Science 305, 239-242.

Leonardo, C., Musso, J., Rowe, D., Collier, L., Mohapatra, S., Pennypacker, K., 2012. Ccl20 is associated with neurodegeneration following experimental traumatic brain injury and promotes cellular toxicity in vitro. Translational Stroke Research 3 (3), 357-363.

Li, W., Maeda, Y., Yuan, R., Elkabes, S., Cook, S., Dowling, P., 2004. Beneficial effect of erythropoietin on experimental allergic encephalomyelitis. Annals of Neurology 56 (6), 767-777.

Liang, C., Park, A., Guan, J., 2007. In vitro scratch assay: A convenient and inexpensive method for analysis of cell migration in vitro. Nat. Protocols 2 (2), 329-333.

Liang, C., Park, A., Guan, J., 2007. *In vitro* scratch assay: A convenient and inexpensive method for analysis of cell migration *in vitro*. Nature Protocols 2 (2), 329-333.

Liebetanz, D., Merkler, D., 2006. Effects of commissural de- and remyelination on motor skill behaviour in the cuprizone mouse model of multiple sclerosis. Experimental Neurology 202 (1), 217-224.

Lin, F., Lin, C., Browne, J., Smalling, R., Egrie, J., Chen, K., Fox, G., Martin, F., Stabinsky, Z., Badrawi, S., Lai, P., Goldwasser, E., 1985. Cloning and expression of the human erythropoietin gene. Proceedings of the National Academy of Scientists USA 82 (22), 7580-7584.

Lin, S., Fan, L., Pang, Y., Rhodes, P., Mitchell, H., Cai, Z., 2005. Igf-1 protects oligodendrocyte progenitor cells and improves neurological functions following cerebral hypoxia–ischemia in the neonatal rat. Brain Research 1063 (1), 15-26.

Lin, Z., Kondo, T., Ishida, Y., Takayasu, T., Mukaida, N., 2003. Essential involvement of IL-6 in the skin wound-healing process as evidenced by delayed wound healing in IL-6 deficient mice. Journal of Leukocyte Biology 73 (6), 713-721.

Lindholm, D., Eriksson, O., Makela, J., Belluardo, N., Korhonen, L., 2012. PGC-1α: A master gene that is hard to master. Cellular and Molecular Life Sciences 69, 2465-2468.

Linker, R., Kruse, N., Israel, S., Wei, T., Seubert, S., Hombach, A., Holtmann, B., Luhder, F., Ransohoff, R., Sendtner, M., Gold, R., 2008. Leukemia inhibitory factor deficiency modulates the immune response and limits autoimmune demyelination: A new role for neutotrophic cytokine in neuroinflammation. Journal of Immunology 180 (4).

Livak, K., Schmittgen, T., 2001. Analysis of relative gene expression data using real-time quantitative PCR and the 2(-delta delta c(t)) method. Methods 25 (4), 402-408.

Lotz, M., Moats, T., Villiger, P., 1992. Leukemia inhibitory factor is expressed in cartilage and synovium and can contribute to the pathogenesis of arthritis. Journal of Clinical Investigation 90 (3), 888-896.

Love-Gregory, L., Abumrad, N., 2011. CD36 genetics and the metabolic complications of obesity. Current Opinion in Clinical Nutrition & Metabolic Care 14 (6), 527-534.

Love, S., 2006. Demyelinating diseases. Journal of Clinical Pathology 59, 1151-1159.

Lucchinetti, C., Bruck, W., Parisi, J., Scheithauer, B., Rodriguez, M., Lassmann, H., 1999. A quantitative analysis of oligodendrocytes in multiple sclerosis lesions. Brain 122 (12), 2279-2295.

Lucchinetti, C., Bruck, W., Parisi, J., Scheithauer, B., Rodriguez, M., Lassmann, H., 2000. Heterogeneity of multiple sclerosis lesions: Implications for the pathogenesis of demyelination. Annals of Neurology 47 (6), 707-717.

Mackenzie, I., Marant, S., Bloomfield, G., Macdonald, T., O'riordan, J., 2013. Incidence and prevalence of multiple sclerosis in the UK 1990-2012: A descriptive study in the general practice research database. Journal of Neurology, Neurosurgery and Psychiatry 85 (1), 76-84.

Malyszko, J., Malayszko, J., Borawski, J., Rydzewski, A., Kalinowski, M., Azzadin, A., Mysliwiec, M., Buczko, W., 1995. A study of platelet functions, some hemostatic and fibrinolytic parameters in relation to serotonin in hemodialyzed patients under erythropoietin therapy. Thrombosis Research 77 (2), 133-143.

Marchese, C., Chedid, M., Dirsch, O., Csaky, K., Santanelli, F., Latini, C., Larochelle, W., Torrisi, M., Aaronson, S., 1995. Modulation of keratinocyte growth factor and its receptor in reepithelializing human skin. The Journal of Experimental Medicine 182 (5), 1369-1376.

Marine, J.-C., Mckay, C., Wang, D., Topham, D., Parganas, E., Nakajima, H., Pendeville, H., Yasukawa, H., Sasaki, A., Yoshimura, A., Ihle, J., 1999.

Socs3 is essential in the regulation of fetal liver erythropoiesis. Cell 98 (5), 617-627.

Marques, F., Mesquita, S., Sousa, J., Coppola, G., Gao, F., Geschwind, D., Columba-Cabezas, S., Aloisi, F., Degna, M., Cerqueira, J., Sousa, N., Correia-Neves, M., Palha, J., 2012. Lipocalin 2 is present in the EAE brain and is modulated by natalizumab. Frontiers in Cellular Neuroscience 6 (33).

Marriott, M., Emery, B., Cate, H., Binder, M., Kemper, D., Wu, Q., Kolbe, S., Gordon, I., Wang, H., Egan, G., Murray, S., Butzkueven, H., Kilpatrick, T., 2008. Leukemia inhibitory factor signalling modulated both central nervous system demyelination and myelin repair. Glia 56 (6), 686-698.

Marshall, J., Gauldie, J., Nielsen, L., Bienenstock, J., 1993. Leukemia inhibitory factor production by rat mast cells. European Journal of Immunology 23 (9), 2116-2120.

Martens, H., Malgrange, B., Robert, F., Charlet, C., De Groote, D., Heymann, D., Godard, A., Soulillou, J.P., Moonen, G., Geenen, V., 1996. Cytokine production by human thymic epithelial cells: Control by the immune recognition of the neurohypophysial self-antigen. Regulatory Peptides 67 (1), 39-45.

Martin, M. (2013). Physiology of wound healing. Wound Healing and Skin Integrity. M. Flanagan, Wiley-Blackwell**:** 33-51.

Martini, R., Groh, J., Bartsch, 2010. Comparative biology of Schwann cells and oligodendrocytes. The biology of oligodendrocytes Cambridge University Press.

Mashayekhi, F., Hadiyan, S., Salehi, Z., 2015. Administration of leukemia inhibitory factor increases opalin and myelin oligodendrocyte glycoprotein expression in the cerebral cortex in a curpizone-induced model of demyelination. Folia Neuropathologica 53 (2), 147-152.

Masuda, S., Nagao, M., Takahata, K., Konishi, Y., Gallayas, F., Tabira, T., Sasaki, R., 1993. Functional erythropoiein receptor of the cells with neural characteristics. The Journal of Biological Chemistry 268 (15), 11208-11216.

Matranga, C., Tomari, Y., Shin, C., Bartel, D., Zamore, P., 2005. Passenger-strand cleavage facilitates assembly of siRNA into AGO2-containing RNAi enzyme complexes. Cell 123 (4).

Matsushita, K., Itoh, S., Ikeda, S., Yamamoto, Y., Yamauchi, Y., Hayashi, M., 2014. LIF/STAT3/Socs3 signalling pathway in murine bone marrow stromal cells suppresses osteoblast differentiation. Journal of Cellular Biochemistry 115 (1262-1268).

Mcclure, M., Threlkeld, S., Fitch, R., 2007. Auditory processing and learning/memory following erythropoietin administration in neonatally hypoxic-ischemic injured rats. Brain Research 1132 (1), 203-209.

Mcmorris, F., Dubois-Dalcq, M., 1988. Insulin-like growth factor 1 promotes cell proliferation and oligodendroglial commitment in rat glial progenitor cells developing in vitro. Journal of Neuroscience Research 21 (2-4), 199-209.

Mcmurtry, I., Davidson, A., Reeves, J., Grover, R., 1975. Inhibition of hypoxic pulmonary vasoconstriction by calcium antagonists in isolated rat lungs. Circulation Research 38 (2), 99-104.

Mcnulty, S., Crouch, M., Smart, D., Rumsby, M., 2001. Differentiation of bipolar CG-4 line oligodendrocytes is associated with regulation of CREB, MAP kinase and PKC signalling pathways. Neuroscience Research 41 (3), 217-226.

Mctigue, D., Tripathi, R., 2008. The life, death, and replacement of oligodendrocytes in the adult CNS. Journal of Neurochemistry 107 (1), 1-19.

Medana, I., Mai, N., Day, N., Hien, T., Bethell, D., Phu, N., Farrar, J., White, N., Turner, G., 2001. Cellular stress and injury responses in the brains of adult vietnamese patients with fatal plasmodium falciparum malaria. Neuropathology and Applied Neurobiology 27 (6), 421-433.

Medzhitov, R., Janeway, C, 2000. Innate immune recognition: Mechanisms and pathways. Immunological Reviews 173, 89-97.

Mela, A., Goldman, J., 2013. Cd82 blocks cmet activation and overcomes hepatocyte growth factor effects on oligodendrocyte precursor differentiation. Journal of Neuroscience 33 (18), 7952-7960.

Meloche, S., Vella, F., Voisin, L., Ang, S., Saba-El-Leil, M., 2004. Erk2 signaling and early embryo stem cell self-renewal. Cell Cycle 3 (3), 241-243.

Mengozzi, M., Cervellini, I., Bigini, P., Martone, S., Biondi, A., Pedotti, R., Gallo, B., Barbera, S., Mennini, T., Boraso, M., Marinovich, M., Petit, E., Bernaudin, M., Bianchi, R., Viviani, B., Ghezzi, P., 2008. Endogenous erythropoietin as part of the cytokine network in the pathogenesis of experimental autoimmune encephalomyelitis. Molecular Medicine 14 (11-12), 682-688.

Mengozzi, M., Cervellini, I., Villa, P., Erbayraktar, Z., Gokmen, N., Yilmaz, O., Erbayraktar, S., Manohasandra, M., Van Hummelen, P., Vandenabeele, P., Chernajovsky, Y., Annenkov, A., Ghezzi, P., 2012. Erythropoieitn-induced changed in brain gene expression reveal induction of synaptic plasticity genes in experimental stroke. PNAS 109 (24), 9617-9622.

Mengozzi, M., Ermilov, P., Annenkov, A., Ghezzi, P., Pearl, F., 2014. Definition of a family of tissue-protective cytokines using functional cluster analysis: A proof-of-concept study. Frontiers in Immunology 5 (115).

Metcalf, D., Nicola. N., 1992. Actions of leukaemia inhibitory factor on megakaryocyte and platelet formation. Ciba Foundation Symposium 167, 174-182.

Metcalfe, A., Ferguson, M., 2007. Tissue engineering of replacement skin: The crossroads of biomaterials, wound healing, embryonic development, stem cells and regeneration. Journal of the Royal Society Interface 4 (14), 413-437.

Mi, H., Haeberle, H., Barres, B., 2001. Induction of astrocyte differentiation by endothelial cells. The Journal of Neuroscience 21 (5), 1538-1547.

Mi, S., Miller, R., Lee, X., Scott, M., Shulag-Morskaya, S., Shao, Z., Chang, J., Thill, G., Levesque, M., Zhang, M., Hession, C., Sah, D., Trapp, B., He, Z., Jung, V., Mccoy, J., Pepinsky, R., 2005. Lingo-1 negatively regulates myelination by oligodendrocytes. Nature Neuroscience 8 (6), 745-751.

Miller, G., Mugler, J., Altes, T., Cai, J., Mata, J., De Lange, E., Tobias, W., Cates, G., Brookeman, J., 2010. A short-breath-hold technique for lung po2 mapping with 3he MRI. Magnetic Resonance in Medicine 63 (1), 127-136.

Miller, R., 2002. Regulation of oligodendrocyte development in the vertebrate CNS. Progress in Neurobiology 67 (6), 451-467.

Miller, R., Petajan, J., Bryan, W., Armon, C., Barohn, R., Goodpasture, J., Hoagland, R., Parry, G., Ross, M., Stromatt, S., 1996. A placebo-controlled trial of recombinant human ciliary neurotrophic (rhCNTF) factor in amyotrophic lateral sclerosis. RhCNTF ALS study group. Annals of Neurology 39 (2), 256-260.

Miranda-Hernandez, S., Gerlach, N., Fletcher, J., Biros, E., Mack, M., Korner, H., Baxter, A., 2011. Role for MYD88, TLR2 and TLR9 but not TLR1, TLR4, or TLR6 in experimental autoimmune encephalomyelitis. Journal of Immunology 187 (2), 791-804.

Miro, V., Boyd, A., Zhao, J., Yuen, T., Ruckh, J., Shadrach, J., Wijngaarden, P., Wagers, A., Williams, A., Franklin, R., Ffrench-Constant, C., 2013. M2 microglia/macrophages drive oligodendrocyte differentiation during CNS remyelination. Nature Neuroscience 16 (9), 1211-1218.

Mirsky, R., Winter, J., Abney, E., Pruss, R., Gavrilovic, J., Raff, M., 1980. Myelin-specific proteins and glycolipids in rat Schwann cells and oligodendrocytes in culture. Journal of Cell Biology 84 (3).

Mitchell, T., John, S., 2005. Signal transducer and activator of transcription (STAT) signalling and T-cell lymphomas. Immunology 114 (3), 301-312.

Miyake, T., Kung, C., Goldwasser, E., 1977. Purification of human erythropoietin. The Journal of Biological Chemistry 252 (15), 5558-5564.

Moidunny, S., Dias, R., Wesseling, E., Sekino, Y., Boddeke, H., Sebastiao, A., Biber, K., 2010. Interleukin-6-type cytokines in neuroprotection and neuromodulation: Oncostatin M, but not leukemia inhibitory factor, requires neuronal adenosine a1 receptor function. Journal of Neurochemistry 114 (6), 1667-1677.

Moreau, J., Donaldson, D., Bennett, F., Witek-Giannotti, J., Clark, S., Wong, G., 1988. Leukaemia inhibitory factor is identical to the myeloid growth factor human interleukin for da cells. Nature 336 (15), 690-692.

Morel, D., Taupin, J., Potier, M., Deminière, C., Potaux, L., Gualde, N., Moreau, J., 2000. Renal synthesis of leukaemia inhibitory factor (LIF), under normal and inflammatory conditions. Cytokine 12 (3), 265-271.

Mori, M., Yamaguchi, K., Abe, K., 1989. Purification of a lipoprotein lipase-inhibiting protein produced by a melanoma cell line associated with cancer cachexia. Biochemical and Biophysical Research Communications 160 (3), 1085-1092.

Morrison, S., Perez, S., Qiao, Z., Verdi, J., Hicks, C., Weinmaster, G., Anderson, D., 2000. Transient notch activation initiates an irreversible switch from neurogenesis to gliogenesis by neural crest stem cells. Cell 101 (5), 499-510.

Mosesson, M., 2005. Fibrinogen and fibrin structure and functions. Journal of Thrombosis and Haemostasis 3, 1894-1904.

Munzel, E., Williams, A., 2013 Promoting remyelination in multiple sclerosis - recent advances. Drugs 73 (18), 2017-2029.

Myers, S., Andres, K., Hagg, T., Whittemore, S., 2014. Cd36 deletion improves recovery from spinal cord injury. Experimental Neurology 256, 25-38.

Nairz, M., Schroll, A., Moschen, A., Sonnweber, T., Theurl, M., Theurl, I., Taub, N., Jamnig, C., Neurauter, D., Huber, L., Tilg, H., Moser, P., Weiss, G., 2011. Erythropoietin contrastingly affects bacterial infection and experimental colitis by inhibiting nuclear factor-κb-inducible immune pathways. Immunity 34 (1), 61-74.

Naka, T., Narazaki, M., Hirata, M., Matsumoto, T., Minamoto, S., Aono, A., Nishimoto, N., Kajita, T., Taga, T., Yoshizaki, K., Akira, S., Kishimoto, T., 1997. Structure and function of a new STAT-induced stat inhibitor. Nature 387, 924-929.

Nakahara, J., Tan-Takeuchi, K., Seiwa, C., Yagi, T., Aiso, S., Kawamura, K., Asou, H., 2001. Myelin basic protein is necessary for the regulation of myelin-associated glycoprotein expression in mouse oligodendroglia. Neuroscience Letters 298 (3), 163-166.

Nam, Y., Kim, J., Seo, M., Kim, J., Jin, M., Jeon, S., Seo, J., Lee, W., Bing, S., Jee, Y., Lee, W., Park, D., Kook, H., Suk, K., 2014. Lipocalin-2 protein deficiency ameliorates experimental autoimmune encephalomyelitis: The pathogenic role of lipocalin-2 in the central nervous system and peripheral lymphoid tissues. The Journal of Biological Chemistry 289 (24), 16773-16789.

Ni, H., Ding, N., Harper, M., Yang, Z., 2002. Expression of leukemia inhibitory factor receptor and GP130 in mouse uterus during early pregnancy. Molecular reproduction and development 63, 143-150.

Nicholson, S., De Souza, D., Fabri, L., Corbin, J., Willson, T., Zhang, J., Silva, A., Asimakis, M., Farley, A., Nash, A., Metcalf, D., Hilton, D., Nicola, N., Baca, M., 2000. Suppressor of cytokine signalling-3 preferentially binds to the SHP-2-binding site on the shared cytokine receptor subunit GP130. PNAS 97 (12), 6493-6498.

Nicola, N., Babon, J., 2015. Leukemia inhibitory factor (LIF). Cytokine & Growth Factor Reviews 26 (5), 533-544.

Nielsen, J., Maric, D., Lau, P., Barker, J., Hudson, L., 2006. Identification of a novel oligodendrocyte cell adhesion protein using gene expression profiling. Journal of Neuroscience 26 (39), 9881-9891.

Niwa, H., Burdon, T., Chambers, I., Smith, A., 1998. Self-renewal of pluripotent embryonic stem cells is mediated via activation of STAT3. Genes and development 12 (13), 2048-2060.

Nolan, T., Hands, R., Bustin, S., 2006. Quantification of mRNA using real-time rt-PCR. Nature Protocols 1 (3), 1559-1582.

O'callaghan, J., Sriram, K., Miller, D., 2008. Defining "neuroinflammation". Annals of the New York Academy of Sciences 1139, 318-330.

O'neill, L., Golenbock, D., Bowie, A.G., 2013. The history of toll-like receptors - redefining innate immunity. Nat Rev Immunol 13 (6), 453-460.

Ogunshola, O., Stewart, W., Mihalcik, V., Solli, T., Madri, J., Ment, L., 2000. Neuronal VEGF expression correlates with angiogenesis in postnatal developing rat brain. Developmental Brain Research 119 (1), 139-153.

Ohnuki, M., Takahashi, K., 2015. Present and future challenges of induced pluripotent stem cells. Philosophical Transactions of the Royal Society of London B: Biological Sciences 370 (1680).

Ohya, W., Funakoshi, H., Kurosawa, T., Nakamura, T., 2007. Hepatocyte growth factor (HGF) promotes oligodendrocyte progenitor cell proliferation and inhibits its differentiation during postnatal development in the rat. Brain Research 1147, 51-65.

Oiu, Y., Ding, Y., Zou, L., Tan, Z., Liu, T., Fu, X., Xu, W., 2013. Divergent roles of amino acid residues inside and outside the bb loop affect human toll-like receptor (TLR)2/2, TLR2/1 and TLR2/6 responsiveness. PLoS One 8 (4), e61508.

Oliveira, N., Rosa, P., Borges, L., Dias, E., Oliveira, F., Cassio, I., 2014. Treatment of diabetic foot complications with hyperbaric oxygen therapy: A retrospective experience. Foot and Ankle Surgery 20, 140-143.

Omari, K., John, G., Lango, R., Raine, C., 2006. Role for Cxcr2 and Cxcl1 on glia in multiple sclerosis. Glia 53 (1), 24-31.

Ott, C., Martens, H., Hassouna, I., Oliveira, B., Erck, C., Zafeiriou, M., Peteri, U., Hesse, D., Gerhart, S., Altas, B., Kolbow, T., Stadler, H., Kawabe, H., Zimmermann, W., Nave, K., Schulz-Schaeffer, W., Jahn, O., Ehrenreich, H., 2015. Widespread expression of erythropoietin receptor in brain and its induction by injury. Molecular Medicine 21 (1), 803-815.

Ozturk, M., Ustek, D., Akbas, F., Kosem, M., Abaci, N., Alagol, F., Ozturk, G., Kotan, C., 2007. The presence of erythropoietin receptor in parathyroid cells. Journal of Endocrinological Investigation 30 (11), RC35-RC37.

Paglia, D., Kondo, S., Ng, K., Sauder, D., Mckenzie, R., 1996. Leukaemia inhibitory factor is expressed by normal human keratinocytes in vitro and in vivo. British Journal of Dermatology 134 (5), 817-823.

Pang, Y., Zheng, B., Fan, L., Rhodes, P., Cai, Z., 2007. Igf-1 protects oligodendrocyte progenitors against TNFα-induced damage by activation of PI3k/Akt and interruption of the mitochondrial apoptotic pathway. Glia 55 (11), 1099-1107.

Park, S., Solomon, D., Vartanian, T., 2001. Growth factor control of CNS myelination. Developmental Neuroscience 23, 327-337.

Parsa, C., Matsumoto, A., Kim, J., Riel, R., Pascal, L., Walton, G., Thompson, R., Petrofski, J., Annex, B., Stamler, J., Koch, W., 2003. A novel protective effect of erythropoietin in the infarcted heart. Journal of Clinical Investigation 112 (7), 999-1007.

Pasquin, S., Sharma, M., Gauchat, J., 2015. Ciliary neurotrophic factor (CNTF): New facets of an old molecule for treating neurodegenerative and metabolic syndrome pathologies. Cytokine & Growth Factor Reviews 26 (5), 507-515.

Patrikios, P., Stadelmann, C., Kutzelnigg, A., Rauschka, H., Schmidbauer, M., Laursen, H., Sorensen, P., Bruck, W., Luccinetti, C., Lassmann, H., 2006. Remyelination is extensive in a subset of multiple sclerosis patients. Brain 129 (12), 3165-3172.

Penn, J., Grobbelaar, A., Rolfe, K., 2012. The role of the TGF-β family in wound healing, burns and scarring: A review. International Journal of Burns and Trauma 2 (1), 18-28.

Peters, B., Voineskos, A., Szeszko, P., Lett, T., Derosse, P., Guha, S., Karlsgodt, K., Ikuta, T., Felsky, D., John, M., Rotenberg, D., Kennedy, J., Lencz, T., Malhotra, A., 2014. Brain white matter development is associated with a human-specific haplotype increasing the synthesis of long chain fatty acids. Journal of Neuroscience 34 (18), 6367-6376.

Pfeiffer, S., Warrington, A., Bansal, R., 1993. The oligodendrocyte and its many cellular processes. Trends in Cell Biology 3 (6), 191-197.

Piccinini, A., Midwood, K., 2010. Dampening inflammation by modulating TLR signalling. Mediators Inflamm. 672395

Picot, S., Bienvenu, A., Konate, S., Sissoko, S., Barry, A., Diarra, E., Bamba, K., Djimdé, A., Doumbo, O., 2009. Safety of epoietin beta-quinine drug combination in children with cerebral malaria in mali. Malaria Journal 8, 169.

Pierce, G., Tarpley, J., Yanagihara, D., Mustoe, T., Fox, G., Thomason, A., 1992. Platelet-derived growth factor (bb homodimer), transforming growth-factor beta 1, and basic fibroblast growth factor in dermal wound healing. Neovessel and matrix formation and cessation of repair. American Journal of Pathology 140 (6), 1375-1388.

Pierce, G., Tarpley, J., Tseng, J., Bready, J., Chang, D., Kenney, W., Rudolph, R., Robson, M., Vande Berg, J., Reid, P., 1995. Detection of platelet-derived growth factor (PDGF)-aa in actively healing human wounds treated with recombinant PDGF-bb and absence of PDGF in chronic nonhealing wounds. Journal of Clinical Investigation 96 (3), 1336-1350.

Plateel, M., Teissier, E., Chcchelli, R., 1997. Hypoxia dramatically increases the nonspecific transport of blood-borne proteins to the brain. Journal of Neurochemistry 68, 874-7.

Prineas, J., Kwon, E., Cho, E., Sharer, L., 1984. Continual breakdown and regeneration of myelin in progressive multiple sclerosis plaquesa. Annals of the New York Academy of Sciences 436 (1), 11-32.

Prinz, M., Garbe, F., Schmidt, H., Mildner, A., Gutcher, I., Wolter, K., Piesche, M., Schroers, R., Weiss, E., Kirschning, C., Rochford, C., Bruck, W., Becher, B., 2006. Innate immunity mediated by TLR9 modulates pathogenicity in an animal model of multiple sclerosis. Journal of Clinical Investigation 116 (2), 456-464.

Profyris, C., Tziotzios, C., Do Vale, I., 2012. Cutaneous scarring: Pathophysiology, molecular mechanisms, and scar reduction therapeutics. Journal of the American Academy of Dermatology 66 (1), 1-10.

Pyun, D., Choi, H., Yoon, H., Thambi, T., Lee, D., 2015. Polyurethane foam containing rhEGF as a dressing material for healing diabetic wounds: Synthesis, characterization, in vitro and in vivo studies. Colloids and Surfaces B: Biointerfaces 135, 699-706.

Quadros, M., Peruzzi, F., Kari, C., Rodeck, U., 2004. Complex regulation of signal transducers and activators of transcription 3 activation in normal and malignant keratinocytes. Cancer Research 64 (11), 3934-3939.

Quinn, J., Wells, G., 1998. An assessment of clinical wound evaluation scales. Academic Emergency Medicine 5 (6), 583-586.

Ranzato, E., Patrone, M., Pedrazzi, M., Burlando, B., 2009. Hmgb1 promotes scratch wound closure of HaCaT keratinocytes via ERK1/2 activation. Molecular and Cellular Biochemistry 332 (1), 199-205.

Readhead, C., Takasashi, N., Shine, H., Saavedra, R., Sidman, R., Hood, L., 1990. Role of myelin basic protein in the formation of central nervous system myelin. Annals of the New York Academy of Sciences 605 (1), 280-285.

Rieckmann, P., Albrecht, M., Kitze, B., Weber, T., Tumani, H., Broocks, A., Luer, W., Helwig, A., Poser, S., 1995. Tumor necrosis factor-alpha messenger RNA expression in patients with relapsing-remitting multiple sclerosis is associated with disease activity. Annals of Neurology 37 (1), 82-88.

Rittchen, S., Boyd, A., Burns, A., Park, J., Fahmy, T., Metcalfe, S., Williams, A., 2015. Myelin repair in vivo is increased by targeting oligodendrocyte precursor cells with nanoparicles encapsulating leukaemia inhibitory factor (LIF). Biomaterials 56, 78-85.

Rizzo, J., Brouwers, M., Hurley, P., Seidenfeld, J., Arcasoy, M., Spivak, J., Bennett, C., Bohlius, J., Evanchuk, D., Goode, M., Jakubowski, A., Regan, D., Somerfield, M., 2010. American society of hematology/american society of clinical oncology clinical practice guideline update on the use of epoetin and darbepoetin in adult patients with cancer. Blood 116 (20), 4045-4059.

Roberts, A., Robb, L., Rakar, S., Hartley, L., Cluse, L., Nicola, N., Metcalfe, D., Hilton, D., Alexander, W., 2001. Plavental defects and embryonic lethality in mice lacking suppressor of cytokine signaling 3. PNAS 98 (16), 9324-9329.

Robinson, A., Harp, C., Noronha, A., Miller, S., 2014. The experimental autoimmune encephalomyelitis (EAE) model of MS: Utility for understanding disease pathophysiology and treatment. Handbook of Clinical Neurology 122, 173-189.

Robinson, R., Grey, L., Staunton, D., Vankelecom, H., Vernalls, A., Moreau, J., Stuart, D., Heath, J., Jones, E., 1994. The crystal structure and biological function of leukemia inhibitory factor: Implications for receptor binding. Cell 77, 1101-1116.

Rovaris, M., Confavreux, C., Furlan, R., Kappos, L., Comi, G., Filippi, M., 2006. Secondary progressive multiple sclerosis: Current knowledge and future challenges. The Lancet: Neurology 5 (4), 343-354.

Rowe, D., Collier, L., Seifert, H., Chapman, C., Leonardo, C., Willing, A., Pennypacker, K., 2014. Leukemia inhibitor factor promotes functional recovery and oligodendrocyte survival in rat models of focal ischemia. The European Journal of Neuroscience 40 (7), 3111-3119.

Ruprecht, K., Kuhlmann, T., Seif, F., Hummel, V., Bruck, W., Rieckmann, P., 2001. Effects of oncostatin M on human cerebral endothelial cells and expression in inflammatory brain lesions. Journal of Neuropathology and Experimental Neurology 60 (11), 1087-1098.

Sabo, J., Aumann, T., Merlo, D., Kilpatrick, T., Cate, H., 2011. Remyelination is altered by bone morphogenic protein signaling in demyelinated lesions. The Journal of Neuroscience 31 (12), 4504-4510.

Saiki, R., Gelfand, D., Stoffel, S., Scharf, S., Hiquchi, R., Horn, G., Mullis, K., Erlich, H., 1988. Primer-directed enzymatic amplification of DNA with a thermostable DNA polymerase. Science 239 (4836), 487-491.

Salehi, Z., Hadiyan, S., Navidi, R., 2013. Ciliary neurotrophic factor role in myelin oligodendrocyte glycoprotein expression in cuprizone-induced multiple sclerosis mice. Cellular and Molecular Neurobiology 33 (4), 531-535.

Sanders, R., Mason, D., Foy, C., Huggett, J., 2014. Considerations for accurate gene expression measurement by reverse transcription quantitative PCR when analysing clinical samples. Analytical and Bioanalytical Chemistry 406 (26), 6471-6483.

Sano, S., Itami, S., Takeda, K., Tarutani, M., Yamaguchi, Y., Miura, H., Yoshikawa, K., Akira, S., Takeda, J., 1999. Keratinocyte-specific ablation of STAT3 exhibits impaired skin remodeling, but does not affect skin morphogenesis. The EMBO Journal 18 (17), 4657-4668.

Sargin, D., Friedrichs, H., El-Kordi, A., Ehrenreich, H., 2010. Erythropoietin as neuroprotective and neurodegenerative treatment strategy: Comprehensive overview of 12 years of preclinical and clinical research. Best practice & research. Clinical Anaesthesiology 24 (4), 573-594.

Sarrazy, V., Billet, F., Micallef, L., Coulomb, B., Desmouliere, A., 2011. Mechanisms of pathological scarring: Role of myofibroblasts and current developments. Wound Repair and Regeneration 19 (Suppl. 1), s10-15.

Sasaki, A., Yasukawa, H., Shouda, T., Kitamura, T., Dikic, I., Yoshimura, A., 2000. Cis3/Socs3 suppresses erythropoietin (EPO) signaling by binding the EPO receptor and JAK2. Journal of Biological Chemistry 275 (38), 29338-29347.

Savino, C., Pedotti, R., Baggi, F., Ubiali, F., Gallo, B., Nava, S., Bigini, P., Barbera, S., Fumagalli, E., Mennini, T., Vezzani, A., Rizzi, M., Coleman, T., Cerami, A., Brines, M., Ghezzi, P., Bianchi, R., 2006. Delayed administration of erythropoietin and its non-erythropoietic derivatives ameliorates chronic murine autoimmune encephalomyelitis. Journal of Neuroimmunology 172 (1-2), 27-37.

Scheller, E., Hankenson, K., Reuben, J., Krebsbach, P., 2011. Zoledronic acid inhibits macrophage Socs3 expression and enhances cytokine production. Journal of Cellular Biochemistry 112 (11), 3364-3372.

Schena, M., Shalon, D., Davis, R., Brown, P., 1995. Quantitative monitoring of gene expression patterns with a complementary DNA microarray. Science 270 (5235), 467-470.

Scherer, S., Vogelbacker, H., Kamholz, J., 1992. Axons modulate the expression of proteolipid protein in the CNS. Journal of Neuroscience Research 32 (2), 138-148.

Schmitz, J., Weissenbach, M., Haan, S., Heinrich, P., Schaper, F., 2000. Socs3 exerts it inhibitory function on interleukin-6 signal transduction through the SHP2 recruitment site of GP130. The Journal of Biological Chemistry 275 (17), 12848-12856.

Schneider-Maunoury, S., Topilko, P., Seitanidou, T., Levi, G., Cohen-Tannoudji, M., Pournin, S., Babinet, C., Charnay, P., 1993. Disruption of Krox-20 results in alteration of rhombomeres 3 and 5 in the developing hindbrain. Cell 75 (6), 1199-1214.

Scolding, N., Frith, S., Linington, C., Morgan, B., Campbell, A., Compston, D., 1989. Myelin-oligodendrocyte glycoprotein (Mog) is a surface marker of oligodendrocyte maturation. Journal of Neuroimmunology 22 (3), 169-176.

Scott, R., Gurusinghe, A., Rudovsky, A., Kozlakivsky, V., Murray, S., Satoh, M., Cheema, S., 2000. Expression of leukemia inhibitory factor receptor mRNA in sensory dorsal root ganglion and spinal motor neurons of the neonatal rate. Neuroscience letters 295, 49-53.

Semenza, G., Dureza, R., Traystman, M., Gearhart, J., Antonarakis, S., 1990. Human erythropoietin gene expression in transgenic mice: Multiple transcription initiation sites and *cis*-acting regulatory elements. Molecular and Cellular Biology 10 (3), 930-938.

Seo, M., Kang, T., Lee, C., Lee, A., Noh, M., 2012. HaCaT keratinocytes and primary epidermal keratinocytes have different transcriptional profiles of cornified envelope-associated genes to T helper cell cytokines. Biomolecules & Therapeutics 20 (2), 171-176.

Shah, M., Foreman, D., Ferguson, M., 1995. Neutralisation of TGF-beta 1 and TGF-beta 2 or exogenous addition of TGF-beta 3 to cutaneous rat wounds reduces scarring. Journal of Cell Science 108 (3), 985-1002.

Shah, M., Foreman, D., Ferguson, M., 1992. Originally published as volume 1, issue 8787. Control of scarring in adult wounds by neutralising antibody to transforming growth factor β. The Lancet 339 (8787), 213-214.

Shaw, J., Sicree, R., Zimmet, P., 2009. Global estimates of the prevalence of diabetes for 2010 and 2030. Diabetes Research and clinical Practice 87, 4-14.

Shen, J., Wu, Y., Xu, J., Zhang, J., Sinclair, S., Yanoff, M., Xu, G., Li, W., Xu, G., 2010. Erk- and Akt-dependent neuroprotection by erythropoietin (EPO) against glyoxal-ages via modulation of Bcl-xl, bax, and bad. Investigative Ophthalmology & Visual Science 51 (1), 35-46.

Shen, M., Skoda, R., Cardiff, R., Campos-Torres, J., Leder, P., Ornitz, D., 1994. Expression of LIF in transgenic mice results in altered thymic epithelium and apparent interconversion of thymic and lymph node morphologies. The EMBO Journal 13 (6), 1375-1385.

Shinar, Y., Mcmorris, F., 1995. Developing oligodendroglia express mRNA for insulin-like growth factor-1, a regulator of oligodendrocyte development. Journal of Neuroscience Research 42 (4), 516-527.

Siebert, N., Xu, W., Grambow, E., Zechner, D., Vollmar, B., 2011. Erythropoietin imporves skin wound healing and activates the TGF-β signaling pathway. Laboratory Investigation 91, 1753-1765.

Siegfried, C., Shui, Y., Holekamp, N., Bai, F., Beebe, D., 2010. Oxygen distribution in the human eye: Relevance to the etiology of open-angle glaucoma after vitrectomy. Investigative Ophthalmology & Visual Science 51 (11), 5731-5738.

Siren, A., Knerlich, F., Poser, W., Gleiter, C., Bruck, W., Ehrenreich, H., 2001. Erythropoietin and erythropoietin receptor in human ischemic/hypoxic brain. Acta Neuropathologica 101 (3), 271-276.

Sloane, J., Batt, C., Ma, Y., Harris, Z., Trapp, B., Vartanian, T., 2010. Hyaluronan blocks oligodendrocyte progenitor maturation and remyelination through TLR2. PNAS 107 (25), 11555-11560.

Smith, A., Heath, J., Donaldson, D., Wong, G., Moreau, J., Stahl, M., Rogers, D., 1988. Inhibition of pluripotent embryonic stem cell differentiation by purified polypeptides. Nature 336, 688-690.

Smith, K., Blakemore, W., Mcdonald, 1979. Central remyelination restores conduction. Nature 280 (5721), 345-354.

Smith, K., Blakemore, W., Mcdonald, W., 1979. Central remyelination restores secure conduction. Nature 280 (5721), 395-396.

Snyder, B., Waldman, B., 2009. Venous thromboembolism prophylaxis and wound healing in patients undergoing major orthopedic surgery. Advances in Skin and Wound Healing 22 (7), 311-5.

Socolovsky, M., Nam, H., Fleming, M., Haase, V., Brugnara, C., Lodish, H., 2001. Ineffective erythropoiesis in stat5a$^{-/-}$5b$^{-/-}$ mice due to decreased survival of early erythroblasts. Blood 98 (12), 3261-3273.

Sohn, J., Natale, J., Chew, L., Belachew, S., Cheng, Y., Aguirre, A., Lytle, J., Nait-Oumesmar, B., Kerninon, C., Kanai-Azuma, M., Kanai, Y., Gallo, V., 2006. Identification of SOX17 as a transcription factor that regulates oligodendrocyte development. Journal of Neuroscience 26 (38), 9722-9735.

Soilu-Hanninen, M., Broberg, E., Roytta, M., Mattila, P., Rinne, J., Hukkanen, V., 2010. Expression of LIF and LIF receptor beta in alzheimer's and parkinson's diseases. Acta Neurologica Scandinavica 121 (1), 44-50.

Solly, S., Daubas, P., Monge, M., Dautigny, A., Zalc, B., 1997. Functional analysis of the mouse myelin/oligodendrocyte glycoprotein gene promoter in the oligodendroglial CG4 cell line. Journal of Neurochemistry 68 (4), 1705-1711.

Solly, S., Monge, T., Demerens, C., Lubetzki, C., Gardinier, M., Matthieu, J., Zalc, B., 1996. Myelin/oligodendrocyte glycoprotein (Mog) expression is associated with myelin deposition. Glia 18, 39-48.

Sorg, H., Krueger, C., Schulz, T., Menger, M., Schmitz, F., Vollmar, B., 2009. Effects of erythropoietin in skin wound healing are dose related. The FASEB journal 23 (9), 3049-3058.

Spivak, J., 2005. The anaemia of cancer: Death by a thousand cuts. Nature Reviews: Cancer 5, 543-555.

Stahl, N., Boulton, T., Farruggella, T., Ip, N., Davis, S., Witthuhn, B., Quelle, F., Silvennoinen, O., Barbieri, G., Pellegrini, S., Ihle, J., Yancopoulos, G., 1994. Association and activation of JAK/TYK kinases by CNTF-LIF-OSM-IL-6 beta-receptor components. Science 263, 92-95.

Stankoff, B., Aigrot, M., Noel, F., Wattilliaux, A., Zalc, B., Lubetzki, C., 2002. Ciliary neurotrophic factor (CNTF) enhances myelin formation: A novel role for CNTF and CNTF-related molecules. Journal of Neuroscience 22 (21), 9221-9227.

Starr, R., Willson, T., Viney, E., Murray, L., Rayner, J., Jenkins, B., Gonda, T., Alexander, W., Metcalf, D., Nicola, N., Hilton, D., 1997. A family of cytokine-inducible inhibitors of signalling. Nature 387, 917-921.

Stasko, J., Drouet, L., Soria, C., Mazoyer, E., Caen, J., Kubisz, P., 2002. Erythropoietin and granulocyte colony-stimulating factor increase plasminogen activator inhibitor-1 release in huvec culture. Thrombosis Research 105 (2), 161-164.

Steinman, M., 1996. Multiple sclerosis: A coordinated immunological attack against myelin in the central nervous system. Cell 85 (3), 299-302.

Stewart, C., Kaspar, P., Brunet, L., Bhatt, H., Gadi, I., Kontgen, F., Abbondanzo, S., 1992. Blastocyst implantation depends on maternal expression of leukaemia inhibitory factor. Nature 359 (6390), 76-79.

Stockli, K., Lillien, L., Naher-Noe, M., Breitfeld, G., Hughes, R., Raff, M., Thoenen, H., Sendtner, M., 1991. Regional distribution, developmental changes, and cellular localization of CNTF-mRNA and protein in the rat brain. The Journal of Cell Biology 115 (2), 447-459.

Stohlawetz, P., Dzirlo, L., Hergovich, N., Lackner, E., Menisk, C., Eichler, H., Kabrna, E., Geissler, K., Jilma, B., 2000. Effects of erythropoietin on platelet reactivity and thrombopoiesis in humans. Blood 95 (9), 2983-2989.

Strunk, T., Hartel, C., Temming, P., Matzke, N., Zimmer, J., Schultz, C., 2008. Erythropoietin inhibits cytokine production of neonatal and adult leukocytes. Acta Paediatrica 97 (1), 16-20.

Sturn, A., Quackenbush, J., Trajanoski, Z., 2000. Genesis: Cluster analysis of microarray data. Bioinformatics 18 (1), 207-208.

Su, K., Shyue, S., Kou, Y., Ching, L., Chiang, A., Yu, Y., Chen, C., Pan, C., Lee, T., 2011. Beta common receptor integrates the erythropoietin signaling in activation of endothelial nitric oxide synthase. Journal of Cellular Physiology 226 (12), 3330-3339.

Sussman, C., Vartanian, T., Miller, R., 2005. Tre Erbb4 neuregulin receptor mediates suppression of oligodendrocyte maturation. The Journal of Neuroscience 25 (24), 5757-5762.

Suvannavejh, G., Lee, H., Padilla, J., Dal Canto, M., Barrett, T., Miller, S., 2000. Divergent roles for p55 and p75 tumor necrosis factor receptors in the pathogenesis of Mog935-55-induced experimental autoimmune encephalomyelitis. Cellular Immunology 205 (1), 24-33.

Suzuki, S., Tanaka, K., Nogawa, S., Ito, D., Dembo, T., Kosakai, A., Fukuuchi, Y., 2000. Immunohistochemical detection of leukemia inhibitory factor after focal cerebral ischemia in rats. Journal of Cerebral Blood Flow and Metabolism 20 (4), 661-668.

Suzuki, S., Yamashita, T, Tanaka, K, Hattori, H, Sawamoto, K, Okano, H, Suzuki, N, 2005. Activation of cytokine signaling through leukemia inhibitory factor receptor (lifr)/gp130 attenuates ischemic brain injury in rats. Journal of Cerebral Blood Flow and Metabolism 25 (6), 685-693.

Suzuma, K., Takagi, H., Otani, A., Honda, Y., 1998. Hypoxia and vascular endothelial growth factor stimulate angiogenic integrin expression in bovine microvascular endothelial cells. Investigative Opthalmology & Visual Science 39 (6), 1028-1035.

Sweet, T., Del Valle, L., Khalili, K., 2002. Molecular biology and immunoregulation of human neurotropic jc virus in CNS. Journal of Cellular Physiology 191 (3), 249-256.

Szepietowski, J., Walker, C., Mckenna, D., Hunter, J., Mckenzie, R., 2001. Leukaemia inhibitory factor and interleukin-8 expression in nonmelanoma skin cancers. Clinical and Experimental Dermatology 26 (1), 72-78.

Szklarczyk, D., Franceschini, A., Wyder, S., Forslund, K., Heller, D., Huerta-Cepas, J., Simonovic, M., Roth, A., Santos, A., Tsafou, K., Kuhn, M., Bork, P., Jensen, L., Von Mering, C., 2015. String v10: Protein-protein interaction networks, integrated over the tree of life. Nucleic Acids Research 43 (Database issue), D447-452.

Takahashi, K., Yamanaka, S., 2006. Induction of pluripotent stem cells from mouse embryonic and adult fibroblast cultures by defined factors. Cell 126 (4), 663-676.

Tanaka, M., Miyajima, A., 2003. Oncostatin m, a multifunctional cytokine. Reviews of Physiology, Biochemistry and Pharmacology 149, 39-52.

Terstegen, L., Gatsios, P., Bode, J., Schaper, F., Heinrich, P., Graeve, L., 2000. The inhibition of interleukine-6-dependent STAT activation by mitogen-activated

protein kinases depends on tyrosine 759 in the cytoplasmic tail of glycoprotein 130. The Journal of Biological Chemistry 275 (25), 18810-18817.

Tomida, M., Yamamoto-Yamagucki, Y., Hozumi, M., 1984. Purification of a factor inducing differentiation of mouse myeloid leukemic m1 cells from conditioned medium of mouse fibroblast L929 cells. The Journal of Biological Chemistry 259 (17), 10978-10982.

Tontsch, U., Archer, D., Dubois-Dalcq, M., Duncan, I., 1994. Transplantation of an oligodendrocyte cell line leading to extensive myelination. PNAS 91 (24), 11616-11620.

Topilko, P., Schneider-Maunoury, S., Levi, G., Baron-Van, Evercooren, A., Chennoufi, A., Seitanidou, T., Babinet, C., Charnay, P., 1994. Krox-20 controls myelination in the peripheral nervouse system. Nature 371 (6500), 796-799.

Torup, 2007. Neuroprotection with or without erythropoiesis; sometimes less is more. British Journal of Pharmacology 151 (8), 1141-1142.

Towbin, H., Staehelin, T., Gordon, J., 1979. Electrophoretic transfer of proteins from polyacrylamide gels to nitrocellulose sheets: Procedure and some applications. PNAS 76 (9), 4350-4354.

Traka, M., Podojil, J., Mccarthy, D., Miller, S., Popko, B., 2016. Oligodendrocyte death results in immune-mediated CNS demyelination. Nature Neuroscience 19 (1), 65-76.

Tsai, H., Frost, E., To, V., Robinson, S., Ffrench-Constant, C., Geertman, R., Ransohoff, R., Miller, R., 2002. The chemokine receptor Cxcr2 controls positioning of oligodendrocyte precursors in developing spinal cord by arresting their migration. Cell 110, 373-383.

Tsai, T., Lu, C., Wallace, C., Chang, W., Chen, S., Huang, C., Tsai, N., Lan, M., Sung, P., Liu, C., Yip, H., 2015. Erythropoietin improves long-term neurological outcome in acute ischemic stroke patients: A randomized, prospective, placebo-controlled clinical trial. Critical Care 19 (1), 49.

Utada, K., Ishida, K., Tohyama, S., Urushima, Y., Mizukami, Y., Yamashita, A., Uchida, M., Matsumoto, M., 2015. The combination of insulin-like growth factor 1 and erythropoietin protects against ischemic spinal cord injury in rabbits. Journal of Anesthesia 29 (5), 741-748.

Vanderlocht, J., Hellings, N., Hendricks, J., Vandenabeele, F., Moreels, M., Buntinx, M., Hoekstra, D., Antel, J., Stinissen, P., 2006. Leukemia inhibitory factor is produced by myelin-reactive T cells from multiple sclerosis patients and protects against tumor necrosis factor-alpha-induced oligodendrocyte apoptosis. Journal of Neuroscience Research 83 (5), 763-774.

Velnar, T., Bailey, T., Smrkolj, V., 2009. The wound healing process: An overview of the cellular and molecular mechanisms. The Journal of International Medical Research 37 (5), 1528-1542.

Villa, P., Bigini, P., Mennini, T., Agnello, D., Laragione, T., Cagnotto, A., Viviani, B., Marinovich, M., Cerami, A., Coleman, T., Brines, M., Ghezzi, P., 2003. Erythropoietin selectively attenuates cytokine production and inflammation in cerebral ischemia by targeting neuronal apoptosis. Journal of Experimental Medicine 198 (6), 971-975.

Vollgraf, U., Wegner, M., Richter-Landsberg, C., 1999. Activation of AP-1 and nuclear factor-κb transcription factors is involved in hydrogen peroxide-induced apoptotic cell death of oligodendrocytes. Journal of Neurochemistry 73 (6), 2501-2509.

Wallace, P., Macmaster, J., Rouleau, K., Brown, T., Loy, J., Donaldson, K., Wahl, A., 1999. Regulation of inflammatory responses by oncostatin M. Journal of Immunology 162 (9), 5547-5555.

Walter, M., Wright, K., Fuller, H., Macneil, S., Johnson, W., 2010. Mesenchymal stem cell-conditioned medium accelerates skin wound healing: An in vitro study of fibroblast and keratinocyte scratch assays. Experimental Cell Research 316 (7), 1271-1281.

Wang, L., Zhang, Z., Wang, Y., Zhang, R., Chopp, M., 2004. Treatment of stroke with erythropoietin enhances neurogenesis and angiogenesis and improves neurological function in rats. Stroke 2004 (35), 1732-1737.

Wang, M., Doucette, J., Nazarali, A., 2011. Conditional tet-regulated over-expression of Hoxa2 in CG4 cells increases their proliferation and delays their differentiation into oligodendrocyte-like cells expressing myelin basic protein. Cellular and Molecular Neurobiology 31 (6), 875-886.

Wang, S., Sdrulla, A., Disibio, G., Bush, G., Nofziger, D., Hicks, C., Weinmaster, G., Barres, B., 1998. Notch receptor activation inhibits oligodendrocytes differentiation. Neuron 21 (1), 63-75.

Wang, W., Li, D., Li, Q., Wang, L., Bai, G., Yang, T., Li, Q., Zhu, Z., Sun, H., 2015. Erythropoietin promotes peripheral nerve regeneration in rats by upregulating expression of insulin-like growth factor-1. Archives of Medical Science: AMS 11 (2), 433-437.

Warner, L., Mancias, P., Butler, I., Mcdonald, C., Keppen, L., Koob, G., Lupski, J., 1998. Mutations in the early growth response 2 (Egr2) gene are associated with hereditary myelinopathies. Nature Genetics 18 (4), 382-384.

Waubant, E., 2006. Biomarkers indicative of blood-brain barrier disruption in multiple sclerosis. Disease Markers 22 (4), 235-244.

Wei, X., Li, Y., Sun, X., Zhu, X., Feng, Y., Liu, J., Jiang, Y., Shang, H., Cui, L., Cao, Y., 2014. Erythropoietin protects against murine cerebral malaria

through actions on host cellular immunity. Infection and Immunity 82 (1), 165-173.

Weiss, G., Goodnough, L., 2005. Anemia of chronic disease. New England Journal of Medicine 352 (10), 1011-1023.

Weiss, T., Samson, A., Niego, B., Daniel, P., Medcalf, R., 2006. Oncostatin M is a neuroprotective cytokine that inhibits excitotoxic injury *in vitro* and *in vivo*. FASEB J 20 (13), 2369-2371.

Wen, R., Tao, W., Yiwen, L., Sieving, P., 2012. CNTF and retina. Progress in Retinal and Eye Research 31 (2), 136-151.

Werner, S., Grose, R., 2003. Regulation of wound healing by growth factors and cytokines. Physiological Reviews 83 (3), 835-870.

Westenfelder, C., Baranowski, R., 2000. Erythropoietin stimulates proliferation of human renal carcinoma cells. Kidney International 58 (2), 647-657.

Westenfelder, C., Biddle, D., Baranowski, R., 1999. Human, rat, and mouse kidney cells express functional erythropoietin receptors. Kidney International 55 (3), 808-820.

Wheeler, D., Devarajan, P., Ma, Q., Harmon, K., Monaco, M., Cvijanovich, N., Wong, H., 2008. Serum neutrophil gelatinase-associated lipocalin (NGAL) as a marker of acute kidney injury in critically ill children with septic shock. Critical Care Medicine 36 (4), 1297-1303.

Whiting, D., Guariguata, L., Weil, C., Shaw, J., 2011. Idf diabetes atlas: Global estimates of the prevalence of diabetes for 2011 and 2030. Diabetes Research and Clinica Practice 94 (3), 311-321.

Wiesener, M., Jurgensen, J., Rosenberger, C., Scholze, C., Horstrup, J., Warnecke, C., Mandriota, S., Bechmann, I., Frei, U., Pugh, C., Ratcliffe, P., Bachmann, S., Maxwell, P., Eckardt, K., 2003. Widespread hypoxia-inducible expression of HIF-2α in distince cell populations of different organs. FASEB J 17 (2), 271-273.

Williams, A., Piaton, G., Lubetzki, C., 2007. Astrocytes - friends or foes in multiple sclerosis. Glia 55 (13), 1300-1312.

Williams, R., Hilton, D., Pease, S., Willson, T., Stewart, C., Gearing, D., Wagner, E., Metcalf, D., Nicola, N., Gough, N., 1988. Myeloid leukemia inhibitory factor maintains the developmental potential of embryonic stem cells. Nature 336, 684-7.

Williams, R., Risau, W., Zerwes, H., Drexler, H., Aguzzi, A., Wagner, E., 1989. Endothelioma cells expressing the polyoma middle T oncogene induce hemangiomas by host cell recruitment. Cell 57 (6), 1053-1063.

Winearls, C., Oliver, D., Paippard, M., Reid, C., Downing, M., Cotes, M., 1986. Effect of human erythropoietin derived from recombinant DNA on the

anaemia of patients maintained by chronic haemodialysis. The Lancet 1986 (2), 1175-8.

Witthuhn, B., Quelle, F., Silvennoinen, O., Yi, T., Tang, B., Miura, O., Ihle, J., 1993. JAK2 associates with the erythropoietin receptor and is tyrosine phosphorylated and activated following stimulation with erythropoietin. Cell 74, 227-236.

Wolf, R., Gilmore, L., Friese, P., Downs, T., Burstein, S., Dale, G., 1997. Erythropoietin potentiates thrombus development in a canine arterio-venous shunt model. Thrombosis and Haemostasis 77 (5), 1020-1024.

Wolswijk, G., 1998. Chronic stage multiple sclerosis lesions contain a relatively quiescent population of oligodendrocyte precursor cells. The Journal of Neuroscience 18 (2), 601-609.

Wolswijk, G., Noble, M., 1989. Identification of an adult-specific glial progenitor cell. Development 105 (2), 387-400.

Woodhoo, A., Duran, M., Mirsky, R., Jessen, K., 2007. Regulation of the immature phenotype by Notch signalling. Neuron Glia Biology 3 (S13).

Wu, H., Liu, X., Jaenisch, R., Lodish, H., 1995. Generation of committed erythroid BFU-E and CFU-E progenitors does not require erythropoietin or the erythropoietin receptor. Cell 83, 59-67.

Wu, S., Rau, C., Lu, T., Wu, C., Wu, Y., Tzeng, S., Chen, Y., Hseih, C., 2013. Knockout of TLR4 and TLR2 impair the nerve regeneration by delayed demyelination but not remyeliantion. Journal of Biomedical Science 20 (62), 1-7.

Xiang, Y., Ding, N., Xing, Z., Zhang, W., Liu, H., Li, Z., 2011. Insulin-like growth factor-1 regulates neurite outgrowth and neuronal migration from organotypic cultured dorsal root ganglion. International Journal of Neuroscience 121 (2), 101-106.

Xu, G., Kang, D., Zhang, C., Lou, H., Sun, C., Yang, Q., Lu, L., X, G., Zhang, J., Wang, F., 2015. Erythropoietin protects retinal cells in diabetic rats through upregulatinf ZNT8 via activating ERK pathway and inhibiting HIF-1α expression. Biochemistry and Molecular Biology 56 (13), 8166-8178.

Xu, Y., Kershaw, N., Luo, C., Soo, P., Pocock, M., Czabotar, P., Hilton, D., Nicola, N., Garrett, T., Zhang, J., 2010. Crystal structure of the entire ectodomain of GP130: Insights into the molecular assembly of the tall cytokine receptor complexes. The Journal of Biological Chemistry 285 (28), 21214-21218.

Yang, J., Bielenberg, D., Rodig, S., Doiron, R., Clifton, M., Kung, A., Strong, R., Zurakowski, D., Moses, M., 2009. Lipocalin 2 promotes breast cancer progression. PNAS 106 (10), 3913-3918.

Yang, J., Goetz, D., Li, J., Wang, W., Mori, K., Setlik, D., Du, T., Erdjument-Bromage, H., Tempst, P., Strong, R., Barasch, J., 2002. An iron delivery pathway mediated by a lipocalin. Molecular Cell 10 (5), 1045-1056.

Yarden, Y., Sliwkowski, M., 2001. Untangling the Erbb signalling network. Nature Reviews Molecular Cell Biology 2 (2), 127-137.

Yeo, Y., Martínez Gómez, J., Croxford, J., Gasser, S., Ling, E., Schwarz, H., 2012. Cd137 ligand activated microglia induces oligodendrocyte apoptosis via reactive oxygen species. Journal of Neuroinflammation 9, 173-173.

Yoshino, J., Monkawa, T., Tsuji, M., Hayashi, M., Saruta, T., 2003. Leukemia inhibitory factor is involved in tubular regeneration after experimental acute renal failure. Journal of the American Society of Nephrology 14 (12), 3090-3101.

Zanjani, E., Poster, J., Burlington, H., Mann, Li., Wasserman, L., 1977. Liver as the primary site of erythropoietin formation in the fetus. Journal of Laboratory and Clinical Medicine 89 (3), 640-644.

Zenker, J., Stettner, M., Ruskamo, S., Domènech-Estévez, E., Baloui, H., Médard, J.-J., Verheijen, M., Brouwers, J., Kursula, P., Kieseier, B., Chrast, R., 2014. A role of peripheral myelin protein 2 in lipid homeostasis of myelinating Schwann cells. Glia 62 (9), 1502-1512.

Zhang, J., Li, Y, Cui, Y, Chen, J, Lu, M, Elias, S, Chopp, M, 2005. Erythropoietin treatment improves neurological functional recovery in EAE mice. Brain Research 1034 (1-2), 34-39.

Zhang, X., Hamada, J., Nishimoto, A., Takahashi, Y., Murai, T., Tada, M., Moriuchi, T., 2007. Hoxc6 and Hoxc11 increase transcription of s100β gene in BRDU-induced in vitro differentiation of GOTO neuroblastoma cells into Schwannian cells. Journal of Cellular and Molecular Medicine 11 (2), 299-306.

Zhu, B., Ishida, Y., Robinson, G., Pacher-Zavisin, M., Yoshimura, A., Murphy, P., Hennighausen, L., 2008. Socs3 negatively regulates the GP130–STAT3 pathway in mouse skin wound healing. Journal of Investigative Dermatology 128 (7), 1821-1829.

Zorick, T.S., Syroid, D.E., Arroyo, E., Scherer, S.S., Lemke, G., 1996. The transcription factors SCIP and KROX-20 mark distinct stages and cell fates in Schwann cell differentiation. Molecular and Cellular Neuroscience 8 (2–3), 129-145.

Zou, Y.R., Zhang, J., Wang, J., Peng, L., Li, G.S., Wang, L., 2016. Erythropoietin receptor activation protects the kidney from ischemia/reperfusion-induced apoptosis by activating ERK/P53 signal pathway. Transplantation Proceedings 48 (1), 217-221.

Appendix I

LIF (ng/ml)	Mog Ct	Mean Mog	Hprt1 Ct	Mean Hprt1	Mog-Hprt1	Mog fold induction	Mog mean	sd	P value
0	31.86	31.4	23.81	24.0	7.35	1.00	0.8	0.3	
1A	30.91		24.27						
1B	30.26	30.2	22.88	23.0	7.19	1.11			
1B	30.14		23.14						
1C	31.63	31.7	24.21	24.0	7.70	0.78			
1C	31.67		23.69						
1D	32.23	32.4	23.94	23.7	8.67	0.40			
1D	32.49		23.45						
0.004	30.42	30.7	23.8	24.1	6.59	1.69	1.8	0.5	0.0184
2A	30.94		24.39						
2B	31.45	31.1	23.99	23.9	7.20	1.11			
2B	30.81		23.87						
2C	30.35	30.5	24.3	24.3	6.18	2.24			
2C	30.59		24.28						
2D	30.87	30.9	24.71	24.5	6.37	1.97			
2D	30.94		24.36						
0.2	28.75	28.9	22.89	22.8	6.08	2.41	2.9	0.4	0.0001
3A	29.06		22.77						
3B	30.3	30.1	24.47	24.5	5.64	3.27			
3B	29.94		24.5						
3C	30.29	30.4	24.76	24.7	5.77	2.98			
3C	30.59		24.58						
3D	30.14	30.0	24.42	24.3	5.73	3.06			
3D	29.84		24.1						
2	31.41	31.5	24.8	24.9	6.62	1.65	1.6	0.2	0.0071
4A	31.6		24.97						
4B	31.5	31.6	24.65	24.7	6.94	1.32			
4B	31.68		24.65						
4C	31.1	31.2	24.38	24.5	6.74	1.53			
4C	31.34		24.59						
4D	31.32	31.6	25.12	25.1	6.47	1.83			
4D	31.87		25.13						
10	30.52	30.3	23.14	23.2	7.17	1.13	1.2	0.4	0.2163
5A	30.15		23.19						
5B	31.75	31.8	23.91	23.9	7.89	0.69			
5B	31.78		23.85						
5C	31.61	32.0	24.94	25.0	7.05	1.23			
5C	32.44		25.02						
5D	31.1	31.3	24.71	24.7	6.67	1.60			
5D	31.53		24.59						

Table A1: Raw data related to Figure 3.1 showing Ct values obtained by qPCR on CG4 cells treated with a range of doses of LIF. P values throughout are expressed vs control, unless otherwise stated

Cytokie (ng/ml)	Mog Ct	Mean Mog	Hprt1 Ct	Mean Hprt1	Mog-Hprt1	Mog fold induction	Mog mean	SD	P Value
0L, 0E	33.89	33.69	25.38	25.31	8.38	1.00	0.9	0.2	
1A	33.49		25.25						
1B	33.1	33.03	24.52	24.64	8.39	0.99			
1B	32.96		24.76						
1C	33.09	33.20	24.78	24.75	8.45	0.95			
1C	33.3		24.71						
1D	32.6	32.90	23.96	23.97	8.93	0.68			
1D	33.19		23.97						
0L, 10E	30.32	30.66	25.28	25.3	5.36	8.11	7.7	1.4	0.0001
3A	30.99		25.32						
3B	30.31	30.31	25.13	24.94	5.37	8.03			
3B	30.3		24.74						
3C	29.79	29.98	24.59	24.74	5.24	8.82			
3C	30.16		24.89						
3D	30.29	30.33	24.68	24.47	5.87	5.70			
3D	30.37		24.25						
0.2L, 0E	33.17	33.23	28.43	24.58	8.65	0.83	1.7	0.8	0.0873
2A	33.29		24.58						
2B	31.83	32.41	24.26	24.46	7.95	1.34			
2B	32.98		24.65						
2C	32.21	32.34	25.31	25.32	7.02	2.58			
2C	32.47		25.33						
2D	32.23	32.42	25	25.12	7.3	2.11			
2D	32.6		25.23						
0.2L, 10E	31.3	31.13	24.51	24.59	6.54	4.23	3.9	0.9	0.0327
7A	30.95		24.66						
7B	32.08	31.81	24.74	24.68	7.13	2.81			
7B	31.53		24.61						
7D	31.59	31.59	25.38	25.14	6.45	4.50			
7D	31.59		24.9						

Table A2: Raw data related to Figure 3.2A showing Ct values obtained by qPCR on CG4 cells treated with doses of LIF at 0.2ng/ml and/or EPO 10ng/ml.

Cytokine (ng/ml)	Mog Ct	Mean Mog	Hprt1 Ct	Mean Hprt1	Mog-Hprt1	Mog fold induction	Mog mean	SD	P Value
0	32.86	32.95	24.24	24.33	8.62	1.00	1.5	0.9	
1A	33.03		24.41						
1B	31.39	31.62	23.78	24.34	7.29	2.52			
1B	31.85		24.89						
1D	32.98	32.49	23.90	23.90	8.59	1.02			
1D	31.99		No Ct						
0L, 10E	28.63	28.78	24.66	24.62	4.17	21.93	20.6	5.2	0.0016
6A	28.93		24.57						
6B	29.27	29.28	24.66	24.66	4.62	16.00			
6B	29.29		24.66						
6C	29.53	29.53	25.07	25.00	4.53	17.03			
6C	29.53		24.93						
6D	27.96	28.22	24.56	24.37	3.85	27.28			
6D	28.47		24.17						
10L, 0E	32.10	31.91	24.65	24.63	7.29	2.52	1.6	0.8	0.8975
5B	31.72		24.60						
5C	32.66	32.75	24.65	24.50	8.25	1.29			
5C	32.84		24.35						
5D	33.40	33.02	24.36	24.42	8.60	1.01			
5D	32.63		24.47						
10L, 10E	31.30	31.13	24.51	24.59	6.54	4.23	3.9	0.9	0.0327
7A	30.95		24.66						
7B	32.08	31.81	24.74	24.68	7.13	2.81			
7B	31.53		24.61						
7D	31.59	31.59	25.38	25.14	6.45	4.50			
7D	31.59		24.90						

Table A3: Raw data related to Figure 3.2B showing Ct values obtained by qPCR on CG4 cells treated with doses of LIF at 10ng/ml and/or EPO 10ng/ml.

Cytokine (ng/ml)	Mbp Ct	Mean Mbp	Hprt 1 Ct	Mean Hprt1	Mbp-Hprt1	Mbp fold induction	Mbp mean	SD	P Value
Ctrl	21.45	21.90	24.09	24.19	-2.29	1.00	1.3	0.4	
1A	22.34		24.28						
1B	21.95	21.98	24.65	24.60	-2.62	1.25			
1B	22.01		24.54						
1C	21.66	21.83	24.67	24.89	-3.06	1.71			
1C	21.99		25.10						
0L, 10E	19.91	19.93	24.28	24.52	-4.60	4.94	5.7	1.1	0.0013
3A	19.94		24.76						
3B	19.98	20.10	25.07	25.14	-5.04	6.73			
3B	20.22		25.21						
3C	19.49	19.73	24.90	24.74	-5.01	6.57			
3C	19.97		24.57						
3D	20.12	20.33	24.80	24.81	-4.49	4.58			
3D	20.53		24.82						
10L, 0E	21.26	21.69	25.46	25.28	-3.59	2.46	1.9	0.9	0.3383
2A	22.12		25.10						
2B	21.35	21.67	25.34	25.43	-3.77	2.78			
2B	21.98		25.52						
2C	21.91	22.01	24.79	24.98	-2.97	1.60			
2C	22.11		25.16						
2D	22.02	22.46	24.14	24.42	-1.96	0.80			
2D	22.89		24.69						
10L, 10E	21.85	21.86	25.34	25.18	-3.32	2.04	1.4	0.6	0.7971
4A	21.87		25.02						
4B	22.30	22.52	24.75	24.77	-2.25	0.97			
4B	22.73		24.78						
4C	22.39	22.52	25.44	25.14	-2.62	1.26			
4C	22.65		24.84						

Table A4: Raw data related to Figure 3.3 showing Ct values obtained by qPCR on CG4 cells treated with doses of LIF at 10ng/ml and/or EPO 10ng/ml.

									P value	
Cytokine (ng/ml)	**Mog Ct**	**Mean Mog**	**Hprt 1 Ct**	**Mean Hprt1**	**Mog-Hprt1**	**Mog fold induction**	**Mog mean**	**sd**	**vs Ctrl**	**vs EPO**
Ctrl	32.52	32.73	24.39	24.42	8.32	1.00	1.4	0.3		
1A	32.94		24.44							
1B	32.40	32.51	25.10	24.93	7.58	1.67				
1B	32.61		24.76							
1C	32.75	32.73	24.65	24.81	7.93	1.31				
1C	32.71		24.96							
1D	32.41	32.59	24.93	24.94	7.66	1.58				
1D	32.77		24.94							
EPO	29.94	29.66	25.30	25.18	4.49	14.22	17.8	4.7	0.0004	
4A	29.38		25.05							
4B	28.99	29.11	24.97	24.99	4.12	18.32				
4B	29.23		25.01							
4C	29.93	29.80	25.28	25.32	4.48	14.32				
4C	29.66		25.36							
4D	29.25	29.32	25.78	25.60	3.72	24.25				
4D	29.38		25.42							
OSM	33.90	33.46	25.98	25.89	7.57	1.68	1.4	0.2	0.8745	
2A	33.01		25.79							
2B	33.66	33.79	25.66	25.86	7.93	1.31				
2B	33.91		26.05							
2C	33.70	33.60	26.01	25.81	7.79	1.44				
2C	33.49		25.60							
2D	33.78	33.98	25.98	25.99	7.99	1.26				
2D	34.17		26.00							
CNTF	33.03	33.23	25.74	25.81	7.43	1.85	1.9	0.2	0.0543	
3A	33.43		25.87							
3B	32.54	32.93	25.63	25.69	7.24	2.11				
3B	33.31		25.75							
3C	33.29	33.31	25.69	25.60	7.71	1.52				
3C	33.33		25.51							
3D	32.88	33.20	25.74	25.84	7.36	1.94				
3D	33.51		25.93							
EPO+ OSM	33.93	33.70	26.53	26.25	7.45	1.83	1.6	0.3	0.3001	0.0022
5B	33.46		25.97							
5C	34.18	33.84	26.49	26.33	7.52	1.74				
5C	33.50		26.16							
5D	34.16	34.14	26.14	26.26	7.88	1.35				
5D	34.12		26.38							
EPO+ CNTF	32.92	32.49	25.91	26.05	6.44	3.68	3.5	1.1	0.0117	0.0011
6A	32.05		26.19							
6B	31.77	32.00	25.96	25.97	6.03	4.89				
6B	32.22		25.98							
6C	34.06	33.90	26.68	26.69	7.21	2.16				
6C	33.73		26.70							
6D	32.74	32.67	26.15	26.04	6.63	3.22				
6D	32.59		25.92							

Table A5: Raw data related to Figure 3.4 showing Ct values obtained by qPCR on CG4 cells treated with doses of OSM or CNTF at 10ng/ml and/or EPO 10ng/ml.

Samples	Mog Ct	Mean Mog	Hprt1 Ct	Mean Hprt1	Mog-Hprt1	Mog fold induction	Mog mean	sd	P value
Ctrl	30.62	30.6	23.85	24.0	6.57	1.00	1.1	0.3	
1A	30.55		24.18						
1B	29.52	29.8	23.85	23.8	6.01	1.47			
1B	30.09		23.74						
1C	31.36	31.6	24.88	24.7	6.87	0.82			
1C	31.83		24.58						
1D	31.32	31.4	24.71	24.7	6.69	0.92			
1D	31.45		24.69						
LIF	29.82	29.8	24.91	24.8	5.06	2.86	2.3	0.6	0.0101
2A	29.8		24.6						
2B	30.57	30.8	24.94	25.1	5.69	1.85			
2B	30.93		25.19						
2C	30.12	30.3	24.42	24.5	5.81	1.70			
2C	30.54		24.63						
2D	29.31	29.5	24.68	24.4	5.11	2.76			
2D	29.7		24.12						
OSM	28.63	28.5	23.31	23.4	5.07	2.84	3.0	0.6	0.0016
3A	28.34		23.53						
3B	28.97	29.1	24.03	24.5	4.61	3.90			
3B	29.14		24.87						
3C	29.96	29.9	24.87	24.6	5.28	2.45			
3C	29.79		24.32						
3D	29.26	29.4	24.48	24.3	5.14	2.70			
3D	29.57		24.08						
CNTF	31.27	31.1	24.84	24.8	6.32	1.19	1.3	0.2	0.1874
4A	30.96		24.76						
4B	31.21	31.3	24.92	25.1	6.19	1.31			
4B	31.4		25.32						
4C	31.4	31.5	24.94	25.1	6.36	1.16			
4C	31.56		25.3						
4D	30.91	31.1	25.22	25.2	5.85	1.65			
4D	31.22		25.22						

Table A6: Raw data related to Figure 3.5 showing Ct values obtained by qPCR on CG4 cells treated with doses of LIF OSM or CNTF at 0.2ng/ml.

									P value	
Cytokine (10ng/ml)	**Mog Ct**	**Mean Mog**	**Hprt1 Ct**	**Mean Hprt1**	**Mog-Hprt1**	**Mog fold induction**	**Mog mean**	**sd**	**vs Ctrl**	**vs EPO**
Ctrl	32.49	32.65	24.09	24.19	8.46	1.00	1.1	0.1		
1A	32.80		24.28							
1B	32.94	33.00	24.65	24.60	8.41	1.04				
1B	33.06		24.54							
1C	33.29	33.16	24.67	24.89	8.28	1.14				
1C	33.03		25.10							
EPO	29.65	29.52	24.28	24.52	5.00	11.00	12.0	2.8	0.0012	
3A	29.39		24.76							
3B	29.73	29.73	25.07	25.14	4.59	14.62				
3B	29.73		25.21							
3C	29.43	29.42	24.90	24.74	4.68	13.74				
3C	29.40		24.57							
3D	30.19	30.18	24.80	24.81	5.37	8.51				
3D	30.17		24.82							
LIF	32.92	32.84	25.46	25.28	7.56	1.87	1.3	0.4	0.3122	
2A	32.76		25.10							
2B	33.24	33.31	25.34	25.43	7.88	1.50				
2B	33.37		25.52							
2C	32.84	33.25	24.79	24.98	8.28	1.14				
2C	33.66		25.16							
2D	32.77	33.06	24.14	24.42	8.64	0.88				
2D	33.34		24.69							
EPO+LIF	33.63	33.32	25.34	25.18	8.14	1.25	1.4	0.4	0.2420	0.0003
4A	33.01		25.02							
4B	32.98	33.10	24.75	24.77	8.33	1.09				
4B	33.22		24.78							
4C	33.36	33.35	25.44	25.14	8.21	1.19				
4C	33.33		24.84							
4D	33.33	33.16	25.70	25.67	7.49	1.96				
4D	32.99		25.64							
EPO+24h LIF	32.01	32.26	26.60	25.58	6.69	3.42	3.1	1.1	0.0221	0.0010
5A	32.51		24.55							
5B	32.17	32.23	25.13	25.26	6.97	2.82				
5B	32.28		25.39							
5C	32.84	32.71	25.15	25.12	7.59	1.83				
5C	32.58		25.09							
5D	31.86	31.90	25.54	25.55	6.35	4.33				
5D	31.93		25.56							
EPO+48h LIF	30.43	30.53	25.04	25.08	5.45	8.06	8.6	1.8	0.0009	0.0888
6A	30.63		25.12							
6B	30.94	30.68	24.77	24.88	5.80	6.32				
6B	30.41		24.98							
6C	30.38	30.25	25.26	25.08	5.17	9.78				
6C	30.12		24.90							
6D	29.91	29.97	24.80	24.88	5.10	10.30				
6D	30.03		24.95							

Table A7: Raw data related to Figure 4.1 showing Ct values obtained by qPCR on CG4 cells treated with LIF and EPO at 10ng/ml.

Cytokine (10ng/ml)	Egr2	Mean Egr2	Hprt1	Mean Hprt1	Egr2-Hprt1	Egr2 fold induction	Egr2 mean	SD	P Value
Ctrl	31.49	31.62	24.87	24.89	6.74	1.00	0.8	0.1	
1A	31.75		24.90						
1B	31.76	31.62	24.96	24.67	6.96	0.86			
1B	31.48		24.37						
1C	31.80	31.85	24.59	24.55	7.30	0.68			
1C	31.89		24.50						
1D	31.69	31.70	25.11	24.71	7.00	0.84			
1D	31.71		24.30						
EPO	24.46	24.59	24.74	24.94	-0.34	135.30	104.7	21.1	0.00006
3A	24.72		25.13						
3B	24.81	24.76	24.53	24.56	0.19	93.05			
3B	24.70		24.59						
3C	24.76	24.68	24.80	24.42	0.27	88.65			
3C	24.60		24.03						
3D	24.71	24.67	24.80	24.61	0.07	101.83			
3D	24.63		24.41						
LIF	29.50	29.52	24.69	24.82	4.70	4.10	4.4	0.6	0.00002
2A	29.53		24.94						
2B	29.34	29.40	24.59	24.59	4.81	3.81			
2B	29.45		24.59						
2C	29.45	29.22	24.66	24.83	4.39	5.10			
2C	28.98		25.00						
2D	29.01	28.84	24.43	24.35	4.49	4.74			
2D	28.67		24.27						
LIF + EPO	24.49	24.40	25.23	25.23	-0.84	190.02	113.7	57.5	0.00774
4A	24.30		25.23						
4B	24.19	24.37	24.82	24.58	-0.21	123.21			
4B	24.54		24.33						
4C	24.32	24.56	23.54	23.70	0.86	58.69			
4C	24.79		23.85						
4D	24.23	24.15	23.67	23.79	0.36	82.71			
4D	24.07		23.90						

Table A8: Raw data related to Figure 4.2 showing Egr2 Ct values obtained by qPCR on CG4 cells treated with LIF and EPO at 10ng/ml.

LIF (10ng/ml)	Socs3 Ct	Mean Socs3	Hprt1 Ct	Mean Hprt1	Socs3-Hprt1	Socs3 fold induction	Mog mean	SD	P Value
Ctrl	23.77	23.89	25.47	25.32	-1.43	1	0.9	0.2	
2A	24.01		25.17						
2B	23.87	23.93	24.67	24.76	-0.83	0.66			
2B	23.99		24.84						
2C	23.86	23.88	25.1	25.19	-1.32	0.92			
2C	23.89		25.28						
2D	23.27	23.24	24.65	24.73	-1.50	1.05			
2D	23.2		24.81						
30mins	20.54	20.4	24.8	24.86	-4.46	8.17	9.2	1.0	3.34E-06
1A	20.26		24.92						
1B	20.11	20.15	24.59	24.68	-4.53	8.54			
1B	20.19		24.76						
1C	19.85	19.93	24.71	24.73	-4.81	10.37			
1C	20		24.75						
1D	20.29	20.19	24.83	24.87	-4.68	9.51			
1D	20.08		24.9						
1hr	21.42	21.35	24.68	24.78	-3.43	4.00	3.7	0.6	6.88E-05
3A	21.28		24.88						
3B	21.52	21.51	24.93	24.65	-3.14	3.27			
3B	21.49		24.36						
3C	21.3	21.26	24.86	24.81	-3.55	4.33			
3C	21.22		24.75						
3D	21.42	21.56	24.56	24.68	-3.12	3.22			
3D	21.7		24.79						
4hrs	22.24	22.13	24.77	24.92	-2.79	2.57	2.4	0.3	0.0002
4A	22.01		25.06						
4B	22.41	22.50	25.41	25.42	-2.92	2.81			
4B	22.58		25.42						
4C	22.69	22.73	25.2	25.22	-2.49	2.08			
4C	22.77		25.24						
4D	22.01	22.26	24.85	24.82	-2.57	2.20			
4D	22.5		24.79						
24hrs	22.33	22.39	25.3	25.23	-2.84	2.66	2.7	0.2	5.99E-06
6A	22.45		25.16						
6B	22.11	22.22	25.1	25.17	-2.96	2.88			
6B	22.32		25.24						
6C	22.22	22.32	25.27	25.25	-2.93	2.82			
6C	22.42		25.22						
6D	22.82	23.25	26.18	26	-2.75	2.50			
6D	23.68		25.82						

Table A9: Raw data related to Figure 4.4 showing Socs3 Ct values obtained by qPCR on CG4 cells treated with LIF at 10ng/ml added at different time points.

LIF (ng/ml)	Socs3	Mean Socs3	Hprt1	Mean Hprt1	Socs3 - Hprt1	Socs3 fold induction	Socs3 mean	SD	P Value
0	22.6	22.6	23.99	24.4	-1.79	1.00	0.9	0.2	
1A	22.69		24.87						
1B	22.52	22.6	23.92	24.1	-1.52	0.83			
1B	22.63		24.27						
1C	22.84	22.7	24.53	24.6	-1.92	1.10			
1C	22.51		24.66						
1D	22.95	23.1	24.13	24.3	-1.15	0.64			
1D	23.29		24.4						
0.004	22.95	23.0	24.71	24.6	-1.60	0.88	0.7	0.2	0.2066
2A	23.02		24.45						
2B	23.05	23.1	24.57	24.5	-1.46	0.80			
2B	23.1		24.49						
2C	23.96	23.4	23.73	23.7	-0.27	0.35			
2C	22.88		23.66						
2D	22.65	22.6	23.95	23.9	-1.24	0.68			
2D	22.61		23.78						
0.2	21.71	21.7	23.86	24.2	-2.53	1.67	1.4	0.2	0.0108
3A	21.69		24.59						
3B	22.28	22.2	24.03	24.2	-2.07	1.21			
3B	22.08		24.46						
3C	22.62	22.3	24.34	24.4	-2.15	1.28			
3C	21.98		24.55						
3D	22.17	22.3	24.63	24.7	-2.42	1.55			
3D	22.4		24.78						
2	21.86	21.8	25.19	24.8	-2.93	2.20	3.1	0.9	0.0039
4A	21.79		24.31						
4B	20.83	21.0	24.23	24.3	-3.34	2.93			
4B	21.16		24.43						
4C	21.59	21.6	24.84	24.9	-3.26	2.77			
4C	21.69		24.95						
4D	20.58	20.8	24.45	24.7	-3.93	4.41			
4D	20.96		24.94						
10	20.84	20.8	24.63	24.6	-3.74	3.88	4.4	0.4	0.00007
5A	20.83		24.52						
5B	21.09	21.3	24.91	25.1	-3.86	4.21			
5B	21.44		25.34						
5C	20.99	20.9	25.11	24.9	-4.00	4.64			
5C	20.86		24.74						
5D	20.98	21.0	25.04	25.1	-4.07	4.87			
5D	21.1		25.18						

Table A10: Raw data related to Figure 4.5 showing Socs3 Ct values obtained by qPCR on CG4 cells treated with LIF at various doses.

									P Value	
Sample (ng/ml)	**Socs3 Ct**	**Mean Socs3**	**Hprt 1 Ct**	**Mean Hprt1**	**Socs3 - Hprt1**	**Socs3 FC**	**Socs 3 mean**	**SD**	**vs ctrl**	**vs EPO**
Ctrl	22.88	22.94	24.60	24.46	-1.52	1.00	0.9	0.1		
1A	23.00		24.31							
1B	23.17	23.05	24.45	24.42	-1.38	0.91				
1B	22.92		24.39							
1C	23.50	23.56	24.79	24.59	-1.03	0.71				
1C	23.61		24.38							
1D	23.53	23.62	25.03	24.86	-1.25	0.83				
1D	23.70		24.69							
EPO	21.77	21.74	24.78	24.71	-2.97	2.74	2.6	0.4	0.0003	
3A	21.70		24.63							
3B	21.54	21.65	24.00	24.28	-2.63	2.17				
3B	21.76		24.56							
3C	21.70	21.52	24.01	24.20	-2.68	2.23				
3C	21.34		24.38							
3D	21.26	21.51	24.53	24.65	-3.14	3.08				
3D	21.75		24.76							
LIF	20.28	20.21	24.16	24.10	-3.89	5.19	5.4	0.6	4.56E-06	0.0002
2A	20.14		24.04							
2B	20.00	20.27	24.52	24.40	-4.14	6.15				
2B	20.53		24.28							
2C	21.34	21.20	24.82	24.97	-3.78	4.79				
2C	21.05		25.12							
2D	20.30	20.36	24.15	24.31	-3.95	5.39				
2D	20.42		24.46							
EPO+ LIF	20.39	20.49	25.09	25.06	-4.57	8.31	7.9	0.5	1.72E-07	3.74E-06
4A	20.59		25.03							
4B	19.72	19.81	24.21	24.25	-4.45	7.62				
4B	19.89		24.29							
4C	20.24	20.25	25.11	24.84	-4.59	8.43				
4C	20.26		24.57							
4D	20.67	20.61	25.00	25.01	-4.40	7.39				
4D	20.55		25.02							

Table A11: Raw data related to Figure 4.6 showing Socs3 Ct values obtained by qPCR on CG4 cells treated with LIF and EPO at 10ng/ml.

Cytokine (10ng/ml)	Mog Ct	Mean Mog	Hprt1	Mean Hprt1	Mog-Hprt1	Mog fold induction	Mog mean	SD	P Value
Ctrl	25.26	25.3	25.98	26.3	-1.05	1.00	0.7	0.3	
1A	25.26		26.63						
1B	24.26	25.0	25.54	25.9	-0.86	0.88			
1B	25.78		26.22						
1C	25.46	25.9	25.52	25.5	0.40	0.37			
1C	26.32		25.47						
1D	25.82	25.7	24.87	25.6	0.06	0.46			
1D	25.56		26.39						
LIF	21.79	21.7	26.24	25.8	-4.03	7.92	7.2	1.0	0.00002
2A	21.67		25.28						
2B	23.45	23.0	26.87	27.0	-4.02	7.84			
2B	22.47		27.08						
2C	20.5	20.7	24.39	24.6	-3.90	7.24			
2C	20.89		24.8						
2D	21.09	21.3	24.43	24.9	-3.56	5.72			
2D	21.6		25.38						
OSM	21.16	21.3	25.89	25.5	-4.16	8.66	7.1	1.5	0.0002
3A	21.51		25.1						
3B	22.45	21.5	25.07	25.0	-3.54	5.64			
3B	20.48		24.94						
3C	21.43	21.7	25.34	25.3	-3.65	6.06			
3C	21.92		25.3						
3D	20.71	20.8	24.75	24.8	-4.09	8.22			
3D	20.81		24.94						
CNTF	21.27	21.2	24.74	24.7	-3.52	5.56	4.6	1.5	0.0021
4A	21.18		24.75						
4B	21.39	21.4	24.74	25.0	-3.59	5.84			
4B	21.34		25.17						
4C	23.77	23.2	25.73	25.6	-2.45	2.64			
4C	22.63		25.56						
4D	22.51	22.4	25.47	25.5	-3.11	4.17			
4D	22.27		25.52						

Table A12: Raw data related to Figure 4.8 showing Socs3 Ct values obtained by qPCR on CG4 cells treated with LIF, OSM and CNTF at 10ng/ml.

									P Value	
Samples	**Socs3 Ct**	**Mean Socs3**	**Hprt1**	**Mean Hprt1**	**Socs3-Hprt1**	**Socs3 FC**	**Socs3 mean**	**SD**	**vs Ctrl**	**vs LIF**
Ctrl	23.61	23.9	24.31	24.3	-0.45	1.00	1.1	0.1		
1A	24.14		24.33							
1B	24.11	24.0	24.52	24.7	-0.68	1.18				
1B	23.87		24.83							
1C	23.53	23.9	24.43	24.7	-0.74	1.23				
1C	24.36		24.94							
LIF	22.36	22.2	24.86	24.7	-2.54	4.26	4.0	0.4	0.0003	
2A	21.98		24.55							
2B	22.15	22.2	24.86	24.7	-2.53	4.23				
2B	22.24		24.58							
2C	21.78	22.1	24.41	24.4	-2.26	3.51				
2C	22.47		24.35							
siRNA1	21.34	21.8	24.14	24.3	-2.55	4.30	4.8	0.6	0.0006	0.1331
3A	22.2		24.5							
3B	21.31	21.5	24.57	24.4	-2.91	5.52				
3B	21.62		24.18							
3C	21.77	21.7	24.32	24.4	-2.66	4.64				
3C	21.7		24.47							
siRNA2	21.79	21.8	24.74	25.1	-3.28	7.14	6.4	0.7	0.0002	0.0068
4A	21.88		25.49							
4B	21.68	21.7	24.68	24.7	-2.97	5.74				
4B	21.72		24.65							
4C	21.98	21.9	25.02	25.1	-3.13	6.41				
4C	21.91		25.12							
siRNA1+2	21.48	21.8	24.49	24.6	-2.83	5.22	5.5	0.4	0.00004	0.0097
5A	22.02		24.67							
5B	21.49	21.3	24.24	24.4	-3.02	5.94				
5B	21.18		24.46							
5C	22.36	22.3	25.14	25.2	-2.88	5.39				
5C	22.32		25.29							

Table A13: Raw data related to Figure 4.9 showing Socs3 Ct values obtained by qPCR on CG4 cells treated with LIF and Socs3 siRNAs for 24 hours

									P value	
Samples	**Socs 3 Ct**	**Mean Socs3**	**Hprt 1**	**Mean Hprt1**	**Socs3 - Hprt1**	**Socs3 FC**	**Socs 3 mean**	**SD**	**vs Ctrl**	**Vs LIF**
Ctrl	23.67	23.8	24.17	25.1	-1.28	1.00	1.0	0.0		
6A	23.93		25.99							
6B	24.14	24.1	25.44	25.4	-1.26	0.99				
6B	24.11		25.33							
6C	23.83	24.0	25.39	25.3	-1.30	1.01				
6C	24.1		25.14							
LIF	21.33	21.4	24.77	24.7	-3.32	4.11	4.5	0.7	0.0012	
7A	21.38		24.58							
7B	21.09	21.1	24.98	24.8	-3.71	5.37				
7B	21.13		24.65							
7C	21.16	21.2	24.41	24.5	-3.30	4.06				
7C	21.17		24.52							
siRNA1	20.5	20.5	24.25	24.2	-3.65	5.17	6.2	0.9	0.0006	0.0665
8A	20.56		24.11							
8B	20.72	20.6	24.39	24.6	-4.01	6.63				
8B	20.38		24.73							
8C	21.01	21.0	25.11	25.0	-4.07	6.89				
8C	20.92		24.95							
siRNA2	21.25	21.2	24.29	24.5	-3.31	4.07	4.2	0.2	0.00001	0.5235
9A	21.23		24.8							
9B	20.65	20.8	24.27	24.3	-3.43	4.44				
9B	20.99		24.23							
9C	20.87	20.7	23.8	24.0	-3.32	4.10				
9C	20.59		24.29							
siRNA1+2	20.49	20.5	24.27	23.9	-3.38	4.27	4.1	0.4	0.0002	0.4324
10A	20.56		23.53							
10B	20.56	20.5	23.99	23.6	-3.14	3.63				
10B	20.39		23.24							
10C	20.21	20.2	23.64	23.6	-3.41	4.36				
10C	20.27		23.65							

Table A14: Raw data related to Figure 4.9 showing Socs3 Ct values obtained by qPCR on CG4 cells treated with LIF and Socs3 siRNAs for 48 hours

									p value	
Samples	**Mog Ct**	**Mean Mog**	**Hprt 1 Ct**	**Mean Hprt1**	**Mog-Hprt1**	**Mog FC**	**Mog mean**	**sd**	**vs Ctrl**	**vs EPO**
Ctrl	32.39	32.53	24.65	24.72	7.81	0.84	1.1	0.2		
1A	32.67		24.79							
1B	32.07	32.19	24.60	24.64	7.55	1.00				
1B	32.30		24.67							
1C	31.75	31.55	24.24	24.18	7.38	1.13				
1C	31.35		24.11							
1D	31.90	32.23	25.06	25.11	7.12	1.35				
1D	32.56		25.16							
EPO	28.30	28.28	25.32	25.12	3.16	21.04	19.0	2.4	5.5E-06	
2A	28.25		24.92							
2B	28.55	28.60	25.39	25.10	3.50	16.62				
2B	28.64		24.81							
2C	28.50	28.53	25.34	25.08	3.45	17.21				
2C	28.55		24.82							
2D	27.48	27.48	24.25	24.32	3.16	20.97				
2D	27.48		24.39							
EPO+LIF	33.83	34.47	27.26	27.43	7.04	1.42	1.3	0.1	0.2035	5.75E-0.6
3A	35.11		27.60							
3B	33.90	33.75	26.45	26.54	7.21	1.27				
3B	33.59		26.62							
3C	33.22	33.42	26.21	26.17	7.25	1.23				
3C	33.61		26.12							
3D	34.07	34.15	26.67	26.75	7.40	1.11				
3D	34.22		26.82							
EPO+LIF +Socs3 si	34.61	35.24	27.81	27.72	7.52	1.02	1.5	0.3	0.0816	6.41E-06
4A	35.87		27.63							
4B	34.41	34.14	27.24	27.27	6.87	1.61				
4B	33.86		27.30							
4C	34.08	33.78	27.01	26.86	6.92	1.55				
4C	33.47		26.70							
4D	34.01	33.95	27.13	27.15	6.80	1.69				
4D	33.88		27.17							
EPO+LIF +Ctrl si	33.83	34.37	26.43	26.51	7.87	0.80	0.6	0.1	0.0299	4.74E-05
5A	34.91		26.58							
5B	34.46	35.00	26.59	26.68	8.32	0.59				
5B	35.54		26.77							
5D	37.46	35.98	27.61	27.51	8.47	0.53				
5D	34.50		27.41							

Table A15: Raw data related to Figure 4.10 showing Mog Ct values obtained by qPCR on CG4 cells treated with EPO, LIF and Socs3 siRNA.

ZA (µM/ml)	Socs3 Ct	Mean Socs3	Hprt 1 Ct	Mean Hprt1	Socs3 - Hprt1	Socs3 fold induction	Socs3 mean	SD	P Value
0	19.98	20.23	23.78	23.93	-3.70	1.00	0.9	0.1	
1A	20.48		24.07						
1B	20.17	20.10	23.71	23.61	-3.51	0.88			
1B	20.03		23.51						
1C	19.82	19.86	23.38	23.5	-3.64	0.96			
1C	19.9		23.61						
0.1	19.92	19.97	23.23	23.19	-3.22	0.72	0.9	0.2	0.6451
2A	20.01		23.15						
2B	19.73	19.81	23.63	23.52	-3.72	1.01			
2B	19.88		23.41						
2C	20.47	20.47	24.23	24.1	-3.64	0.96			
2C	20.46		23.97						
1	19.55	19.64	22.63	22.9	-3.26	0.74	0.9	0.1	0.4141
3A	19.73		23.17						
3B	20.55	20.50	24.17	24.1	-3.60	0.94			
3B	20.45		24.03						
3C	19.78	19.83	23.54	23.45	-3.63	0.95			
3C	19.87		23.36						
10	20.1	20.09	23.55	23.23	-3.15	0.68	0.9	0.2	0.6448
4A	20.07		22.91						
4B	19.61	19.66	23.56	23.31	-3.65	0.97			
4B	19.71		23.06						
4C	20.3	20.35	23.83	24.07	-3.73	1.02			
4C	20.39		24.31						

Table A16: Raw data related to Figure 4.11 showing Socs3 Ct values obtained by qPCR on CG4 cells treated with ZA at various doses

									P value	
Samples	**Mog Ct**	**Mean Mog**	**Hprt 1 Ct**	**Mean Hprt 1**	**Mog-Hprt 1**	**Mog FC**	**Mog mean**	**SD**	**vs Ctrl**	**vs EPO**
Ctrl	32.28	31.76	23.65	24.37	7.39	1.00	0.7	0.2		
1A	31.23		25.09							
1B	33.27	32.25	24.45	24.16	8.09	0.61				
1B	31.23		23.87							
1C	31.42	31.26	23.51	23.18	8.08	0.62				
1C	31.09		22.85							
1D	31.69	31.30	23.60	23.32	7.98	0.66				
1D	30.90		23.03							
EPO	29.53	29.93	24.68	25.14	4.79	6.04	7.9	2.1	0.0005	
2A	30.33		25.60							
2B	29.55	29.55	26.37	25.60	3.96	10.78				
2B	29.55		24.82							
2C	28.54	28.83	24.13	24.46	4.37	8.08				
2C	29.11		24.78							
2D	28.87	28.62	24.14	24.00	4.62	6.80				
2D	28.36		23.85							
EPO+LIF	32.63	32.40	25.30	25.51	6.89	1.41	1.3	0.3	0.0210	0.0007
3A	32.16		25.72							
3B	32.35	31.93	25.12	25.18	6.75	1.55				
3B	31.51		25.24							
3C	32.25	32.52	25.21	25.29	7.24	1.11				
3C	32.79		25.36							
3D	33.25	33.39	25.20	25.90	7.50	0.93				
3D	33.53		26.59							
EPO+LIF +ZA 1	32.73	32.95	25.80	26.01	6.95	1.36	1.5	0.3	0.0038	0.0035
4B	33.17		26.21							
4C	32.99	32.72	25.49	25.61	7.12	1.21				
4C	32.45		25.72							
4D	32.26	32.45	25.86	25.95	6.50	1.85				
4D	32.64		26.04							
EPO+LIF +ZA 10	32.39	32.47	26.34	25.87	6.61	1.72	1.3	0.3	0.0132	0.0008
5A	32.55		25.39							
5B	33.44	33.29	26.15	25.98	7.31	1.06				
5B	33.13		25.81							
5C	32.87	33.39	25.95	26.19	7.20	1.14				
5C	33.90		26.42							
5D	33.71	33.91	27.08	27.07	6.84	1.46				
5D	34.10		27.06							

Table A17: Raw data related to Figure 4.12 showing Mog Ct values obtained by qPCR on CG4 cells treated with EPO, LIF and ZA at various doses.

									P Value	
Samples	**Mog Ct**	**Mean Mog**	**Hprt 1 Ct**	**Mean Hprt 1**	**Mog-Hprt 1**	**Mog FC**	**Mog mean**	**SD**	**vs Ctrl**	**vs EPO**
Ctrl	32.45	32.75	24.40	24.34	8.41	1.00	0.9	0.1		
1A	33.05		24.28							
1B	32.82	33.24	24.75	24.69	8.55	0.91				
1B	33.65		24.63							
1C	32.90	32.87	24.23	24.36	8.52	0.93				
1C	32.84		24.48							
1D	32.96	33.27	24.56	24.68	8.59	0.88				
1D	33.58		24.80							
Ctrl+ZA	33.75	33.93	24.70	24.66	9.27	0.55	0.8	0.2	0.1909	
2A	34.11		24.62							
2B	33.41	33.18	24.50	24.57	8.61	0.87				
2B	32.94		24.64							
2C	33.60	33.29	24.84	24.91	8.38	1.02				
2C	32.97		24.98							
2D	33.99	33.59	24.41	24.39	9.20	0.58				
2D	33.18		24.36							
EPO	29.90	29.85	24.85	24.78	5.07	10.13	8.2	2.2	0.0005	
3A	29.80		24.71							
3B	30.48	30.29	24.63	24.65	5.65	6.80				
3B	30.10		24.66							
3C	30.87	30.87	24.76	25.02	5.86	5.88				
3C	30.87		25.27							
3D	29.93	29.79	24.85	24.68	5.11	9.88				
3D	29.64		24.51							
EPO+ZA	31.58	31.42	25.40	25.30	6.12	4.89	5.1	0.8	0.0001	0.0693
4A	31.25		25.19							
4B	30.96	31.12	24.74	24.84	6.28	4.39				
4B	31.27		24.94							
4C	29.93	30.59	24.79	24.77	5.83	6.00				
4C	31.25		24.74							

Table A18: Raw data related to Figure 4.13 showing Mog Ct values obtained by qPCR on CG4 cells treated with EPO and ZA at various doses

									P value	
Samples	**Socs3 Ct**	**Mean Socs3**	**Hprt 1**	**Mean Hprt1**	**Socs3 - Hprt1**	**Socs3 FC**	**Socs3 mean**	**SD**	**vs ctrl**	**vs EPO**
Ctrl	23.78	23.78	24.17	24.31	-0.52	1.00	1.1	0.3		
1A	23.49		24.44							
1B	23.66	23.66	24.41	24.51	-0.85	1.25				
1B	23.67		24.60							
1C	23.78	23.78	24.88	24.82	-1.04	1.43				
1C	24.02		24.76							
1D	23.89	23.89	24.37	24.13	-0.23	0.82				
1D	23.55		23.88							
EPO	22.96	22.96	26.05	25.69	-2.73	4.61	2.9	1.2	0.0327	
2A	22.98		25.33							
2B	23.13	23.13	25.33	25.06	-1.93	2.64				
2B	23.36		24.78							
2C	22.68	22.68	24.74	24.53	-1.85	2.50				
2C	22.87		24.31							
2D	22.81	22.81	23.99	24.12	-1.31	1.72				
2D	22.63		24.24							
PMA	22.72	22.72	23.94	24.26	-1.54	2.02	1.8	0.5	0.0525	0.1582
3A	22.60		24.58							
3B	23.05	23.05	24.08	24.30	-1.25	1.65				
3B	22.70		24.51							
3C	22.70	22.70	24.65	24.45	-1.75	2.33				
3C	22.90		24.24							
3D	23.66	23.66	24.23	24.44	-0.78	1.19				
3D	23.27		24.65							
EPO+ PMA	20.57	20.57	23.88	24.33	-3.76	9.38	8.7	0.5	2.033 E-07	0.0001
4A	20.63		24.77							
4B	20.87	20.87	24.58	24.43	-3.56	8.17				
4B	21.30		24.27							
4C	20.59	20.59	24.02	24.22	-3.63	8.57				
4C	20.71		24.41							
4D	20.77	20.77	24.72	24.40	-3.63	8.57				
4D	20.63		24.07							

Table A19: Raw data related to Figure 4.14 showing Socs Ct values obtained by qPCR on CG4 cells treated with EPO and/or PMA.

									P value	
Samples	**Mog Ct**	**Mean Mog**	**Hprt 1**	**Mean Hprt 1**	**Mog-Hprt 1**	**Mog FC**	**Mog mean**	**SD**	**vs Ctrl**	**vs EPO**
Ctrl	31.46	31.4	23.66	23.7	7.71	1.00	3.0	0.1		
1A	31.31		23.69							
1B	31.58	31.7	23.7	24.0	7.72	0.99				
1B	31.87		24.31							
1D	32.19	32.0	24.01	24.0	8.01	0.81				
1D	31.88		24.03							
EPO	28.73	28.7	24.26	24.2	4.49	9.35	10.1	1.9	0.0011	
2A	28.59		24.09							
2C	28.29	28.2	23.99	24.1	4.10	12.21				
2C	28.19		24.29							
2D	28.42	28.5	23.82	23.9	4.59	8.69				
2D	28.55		23.97							
PMA	30.86	31.4	24.34	24.2	7.16	1.47	1.4	0.3	0.0539	
3A	31.85		24.06							
3B	31.23	31.2	23.94	23.9	7.33	1.31				
3B	31.23		23.87							
3C	30.55	30.7	23.66	23.7	6.93	1.72				
3C	30.77		23.8							
3D	31.44	31.6	23.92	23.9	7.67	1.03				
3D	31.71		23.9							
EPO+ PMA	29.59	29.7	24.29	24.2	5.46	4.77	4.8	0.3	2.3226 E-06	0.0021
4A	29.77		24.16							
4B	29.71	29.6	24.11	24.2	5.44	4.84				
4B	29.55		24.28							
4C	29.89	29.7	24.22	24.3	5.39	5.01				
4C	29.57		24.47							
4D	30.01	30.2	24.76	24.6	5.57	4.41				
4D	30.35		24.46							

Table A20: Raw data related to Figure 4.15 showing Mog Ct values obtained by qPCR on CG4 cells treated with EPO and/or PMA.

									P value	
Samples	**Egr2 Ct**	**Mean Egr2**	**Hprt 1 Ct**	**Mean Hprt1**	**Egr2-Hprt1**	**Egr2 FC**	**Egr2 mean**	**SD**	**vs ctrl**	**vs EPO**
Ctrl	33.24	33.25	24.25	24.35	8.90	1.00	1.0	0.2		
1A	33.26		24.45							
1B	33.42	33.19	24.51	24.53	8.66	1.19				
1B	32.95		24.55							
1C	33.67	33.65	24.65	24.65	9.00	0.94				
1C	33.62		24.65							
1D	34.43	33.81	24.36	24.36	9.46	0.68				
1D	33.19		24.35							
EPO	30.84	30.91	24.28	24.15	6.76	4.41	5.7	1.3	0.0006	
2A	30.97		24.01							
2B	30.44	30.67	24.23	24.34	6.34	5.92				
2B	30.90		24.44							
2C	30.38	30.42	24.23	24.31	6.11	6.92				
2C	30.45		24.38							
LIF	32.74	32.35	24.59	24.45	7.91	1.99	2.7	0.7	0.0030	0.0086
4A	31.96		24.30							
4B	31.54	31.76	24.35	24.43	7.34	2.96				
4B	31.98		24.50							
4C	32.13	31.92	24.15	24.19	7.73	2.25				
4C	31.70		24.22							
4D	31.74	31.84	24.80	24.75	7.09	3.51				
4D	31.93		24.69							
LIF and EPO	29.87	29.96	24.59	24.59	5.37	11.59	11.9	1.1	1.4881 E-06	0.0011
5A	30.04		24.59							
5B	29.90	29.91	24.77	24.78	5.14	13.59				
5B	29.92		24.78							
5C	29.74	29.71	24.41	24.30	5.41	11.24				
5C	29.68		24.19							
5D	29.81	29.89	24.56	24.47	5.42	11.16				
5D	29.97		24.38							

Table A21: Raw data related to Figure 5.1 showing Egr2 Ct values obtained by qPCR on CG4 cells treated with EPO and/or LIF.

									P value	
Samples	**Socs3 Ct**	**Mean Socs3**	**Hprt1**	**Mean Hprt1**	**Socs3-Hprt1**	**Socs3 FC**	**Socs3 mean**	**SD**	**vs ctrl**	**vs EPO**
Ctrl	24.99	25.09	24.25	24.35	0.74	1.00	1.0	0.1		
1A	25.19		24.45							
1B	25.15	25.11	24.51	24.53	0.57	1.12				
1B	25.06		24.55							
1C	25.48	25.49	24.65	24.65	0.84	0.94				
1C	25.49		24.65							
1D	25.35	25.22	24.36	24.36	0.86	0.92				
1D	25.09		24.35							
EPO	24.36	24.53	24.28	24.15	0.38	1.28	1.3	0.2	0.0487	
2A	24.69		24.01							
2B	25.07	24.95	24.23	24.34	0.61	1.09				
2B	24.83		24.44							
2C	24.25	24.44	24.23	24.31	0.13	1.52				
2C	24.63		24.38							
LIF	22.45	22.39	24.59	24.45	-2.06	6.96	6.1	0.8	1.3101 E-05	0.0002
4A	22.32		24.30							
4B	22.53	22.69	24.35	24.43	-1.74	5.56				
4B	22.85		24.50							
4C	22.74	22.51	24.15	24.19	-1.68	5.35				
4C	22.27		24.22							
4D	22.70	22.76	24.80	24.75	-1.99	6.61				
4D	22.82		24.69							
LIF and EPO	22.80	22.79	24.59	24.59	-1.80	5.82	6.3	1.2	0.0001	0.0010
5A	22.78		24.59							
5B	22.41	22.51	24.77	24.78	-2.27	8.03				
5B	22.61		24.78							
5C	22.49	22.49	24.41	24.30	-1.81	5.86				
5C	22.49		24.19							
5D	22.81	22.80	24.56	24.47	-1.67	5.31				
5D	22.79		24.38							

Table A22: Raw data related to Figure 5.1 showing Socs3 Ct values obtained by qPCR on CG4 cells treated with EPO and/or LIF.

									P value	
Samples	**CD36 Ct**	**Mean CD36**	**Hprt 1 Ct**	**Mean Hprt1**	**CD36-HPRT1**	**Log 2 FC**	**CD36 FC**	**sd**	**vs ctrl**	**vs EPO**
Ctrl	38	38	23.16	23.44	14.56	-0.14	-0.1	0.1		
6A	38		23.72							
6B	38	38	23.63	23.575	14.43	0				
6B	38		23.52							
6C	38	38	23.57	23.52	14.49	-0.06				
6C	38		23.46							
6D	38	38	23.19	23.31	14.69	-0.27				
6D	38		23.43							
EPO 10	26.85	27.03	23.86	23.7	3.33	11.10	11.0	0.2	7.06E-11	
7A	27.21		23.54							
7B	26.84	27.03	23.58	23.77	3.26	11.17				
7B	27.22		23.96							
7C	26.88	26.96	23.39	23.64	3.32	11.11				
7C	27.03		23.88							
7D	26.83	26.82	23.05	23.14	3.69	10.74				
7D	26.81		23.22							
LIF 10	38	38	23.84	23.81	14.20	0.23	0.2	0.2	0.0189	1.52E-10
9A	38		23.77							
9B	37.41	37.71	23.64	23.64	14.07	0.36				
9B	38		23.64							
9C	38	38	23.66	23.56	14.44	-0.02				
9C	38		23.46							
9D	38	38	23.67	23.77	14.23	0.20				
9D	38		23.87							
EPO10 LIF10	28.9	28.82	23.72	23.81	5.01	9.42	9.6	0.3	0.0001	
10A	28.73		23.89							
10B	28.39	28.52	23.81	23.96	4.56	9.87				
10B	28.64		24.1							
10C	28.53	28.50	23.76	23.77	4.73	9.7				
10C	28.46		23.78							
10D	28.64	28.78	23.71	23.61	5.17	9.26				
10D	28.92		23.51							

Table A23: Raw data related to Figure 5.5 showing CD36 Ct values obtained by qPCR on CG4 cells treated with EPO and/or LIF.

									P value	
Samples	**Igf1 Ct**	**Mean Igf1**	**Hprt 1**	**Mean Hprt 1**	**Igf1-Hprt 1**	**Log_2 FC**	**Igf1 FC**	**SD**	**vs ctrl**	**vs EPO**
Ctrl	38.36	37.22	23.16	23.44	13.78	-0.61	-0.7	0.8		
6A	36.08		23.72							
6B	36.75	36.75	23.63	23.58	13.18	0.00				
6B	No Ct		23.52							
6C	38.10	38.21	23.57	23.52	14.70	-1.52				
6C	38.44		23.46							
6D	38.10	38.10	23.19	23.31	14.79	-1.62				
6D	No Ct		23.43							
EPO	31.95	31.85	23.86	23.70	8.15	5.03	4.7	0.6	0.0001	
7A	31.75		23.54							
7B	31.82	31.82	23.58	23.77	8.05	5.13				
7B	31.82		23.96							
7C	31.89	32.15	23.39	23.64	8.51	4.66				
7C	32.41		23.88							
7D	32.41	32.51	23.05	23.14	9.38	3.80				
7D	32.62		23.22							
LIF 10	36.22	35.91	23.84	23.81	12.10	1.07	-0.1	0.8	0.3663	9.14E-05
9A	35.60		23.77							
9B	37.63	37.02	23.64	23.64	13.38	-0.21				
9B	36.72		23.64							
9C	38.19	37.63	23.66	23.56	14.07	-0.90				
9C	36.52		23.46							
9D	37.91	37.30	23.67	23.77	13.53	-0.36				
9D	36.70		23.87							
EPO+ LIF	32.50	32.75	23.72	23.81	8.94	4.24	4.0	0.3	8.87E-05	0.1067
10A	32.99		23.89							
10B	32.75	32.82	23.81	23.96	8.86	4.32				
10B	32.88		24.10							
10C	33.06	33.19	23.76	23.77	9.42	3.75				
10C	33.33		23.78							
10D	33.09	33.05	23.71	23.61	9.44	3.74				
10D	33.01		23.51							

Table A24: Raw data related to Figure 5.7 showing Igf1 Ct values obtained by qPCR on CG4 cells treated with EPO and/or LIF.

									P value	
	Fos	**Mean Fos**	**Hprt1**	**Mean Hprt1**	**Fos-Hprt1**	**Log FC**	**Log FC**	**Log St Dev**	**vs Ctrl**	**vs EPO**
Ctrl	26.58	26.75	23.46	23.48	3.27	-0.45	-0.2	0.2		
1a	26.92		23.5							
1b	26.12	26.2	23.4	23.37	2.83	0				
1b	26.27		23.34							
1c	26.39	26.39	23.34	23.32	3.07	-0.25				
1c	26.13		23.3							
1d	26.48	26.45	23.44	23.47	2.98	-0.16				
1d	26.42		23.5							
EPO	25.02	25.02	23.44	23.425	1.595	1.23	1.4	0.3	0.0002	
2a	24.03		23.41							
2b	No Ct	25.35	23.56	23.545	1.805	1.02				
2b	25.35		23.53							
2c	25.01	24.91	23.43	23.43	1.475	1.35				
2c	24.8		23.43							
2d	24.57	24.46	23.39	23.455	1.005	1.82				
2d	24.35		23.52							
LIF 10	21.78	21.85	23.35	23.365	-1.52	4.35	4.5	0.2	1.78E-08	2.61E-06
4a	21.91		23.38							
4b	22.12	21.91	23.61	23.77	-1.86	4.69				
4b	21.7		23.93							
4c	21.84	21.81	23.5	23.58	-1.77	4.60				
4c	21.78		23.66							
4d	22.24	21.99	23.7	23.605	-1.62	4.45				
4d	21.73		23.51							
EPO +LIF	21.78	21.76	23.46	23.56	-1.8	4.63	4.4	0.3	2.74E-07	1.31E-05
5a	21.74		23.66							
5b	22.06	22.08	23.2	23.145	-1.07	3.90				
5b	22.09		23.09							
5c	21.53	21.66	23.23	23.25	-1.60	4.42				
5c	21.78		23.27							
5d	21.92	21.86	23.47	23.49	-1.63	4.45				
5d	21.8		23.5							

Table A25: Raw data related to Figure 6.2 showing Fos Ct values obtained by qPCR on CG4 cells treated with EPO and/or LIF.

									P value	
	JunB	**Mean JunB**	**Hprt1**	**Mean Hprt1**	**JunB-Hprt1**	**Log FC**	**Log FC mean**	**Log SD**	**vs Ctrl**	**vs EPO**
Ctrl	28.44	28.33	23.46	23.48	4.85	0.13	0.0	0.2		
1a	28.22		23.50							
1b	28.11	28.35	23.40	23.37	4.98	0.00				
1b	28.58		23.34							
1c	28.54	28.58	23.34	23.32	5.26	-0.28				
1c	28.61		23.30							
1d	28.31	28.16	23.44	23.47	4.69	0.29				
1d	28.00		23.50							
EPO	27.07	27.37	23.44	23.43	3.94	1.04	0.8	0.2	0.0024	
2a	27.66		23.41							
2b	27.79	27.82	23.56	23.55	4.28	0.70				
2b	27.85		23.53							
2c	27.88	27.80	23.43	23.43	4.37	0.61				
2c	27.71		23.43							
2d	27.54	27.60	23.39	23.46	4.15	0.83				
2d	27.66		23.52							
LIF 10	24.64	24.49	23.35	23.37	1.13	3.85	4.1	0.3	5.08E-07	9.56E-07
4a	24.34		23.38							
4b	24.44	24.29	23.61	23.77	0.52	4.46				
4b	24.13		23.93							
4c	24.27	24.43	23.50	23.58	0.85	4.13				
4c	24.59		23.66							
4d	24.71	24.64	23.70	23.61	1.04	3.94				
4d	24.57		23.51							
EPO+ LIF	24.36	24.55	23.46	23.56	0.99	3.99	3.8	0.3	1.01E-06	2.22E-06
5a	24.74		23.66							
5b	24.64	24.75	23.20	23.15	1.60	3.38				
5b	24.85		23.09							
5c	24.55	24.39	23.23	23.25	1.14	3.84				
5c	24.22		23.27							
5d	24.18	24.48	23.47	23.49	0.99	3.99				
5d	24.77		23.50							

Table A26: Raw data related to Figure 6.3 showing JunB Ct values obtained by qPCR on CG4 cells treated with EPO and/or LIF.

									P value	
Samples	**Socs3**	**Mean Socs3**	**Hprt1**	**Mean Hprt1**	**Socs3-Hprt1**	**Log FC**	**Log FC Mean**	**Log SD**	**vs Ctrl**	**vs EPO**
Ctrl	23.52	23.51	23.46	23.48	0.03	0.03	-0.2	0.2		
1A	23.49		23.5							
1B	23.17	23.43	23.4	23.37	0.06	0				
1B	23.68		23.34							
1C	23.66	23.77	23.34	23.32	0.45	-0.39				
1C	23.87		23.3							
1D	23.78	23.79	23.44	23.47	0.32	-0.26				
1D	23.79		23.5							
EPO	23.58	23.68	23.44	23.43	0.26	-0.2	0.2	0.3	0.079	
2A	23.78		23.41							
2B	23.24	23.37	23.56	23.55	-0.18	0.24				
2B	23.49		23.53							
2C	22.95	23.01	23.43	23.43	-0.42	0.48				
2C	23.07		23.43							
2D	22.99	23.08	23.39	23.46	-0.38	0.44				
2D	23.16		23.52							
LIF 10	20.82	20.86	23.35	23.37	-2.51	2.57	2.5	0.2	2.06E-06	2.17E-05
4A	20.89		23.38							
4B	21.6	21.61	23.61	23.77	-2.16	2.22				
4B	21.62		23.93							
4C	21.13	21.26	23.5	23.58	-2.36	2.38				
4C	21.38		23.66							
4D	20.84	20.96	23.7	23.61	-2.65	2.71				
4D	21.07		23.51							
EPO+ LIF	21.28	21.42	23.46	23.56	-2.14	2.20	1.9	0.3	3.47E-05	0.0003
5A	21.56		23.66							
5B	21.21	21.31	23.2	23.15	-1.84	1.89				
5B	21.41		23.09							
5C	21.16	21.16	23.23	23.25	-2.09	2.15				
5C	21.16		23.27							
5D	22.05	22.05	23.47	23.49	-1.44	1.49				
5D	22.05		23.5							

Table A27: Raw data related to Figure 6.6 showing Socs3 Ct values obtained by qPCR on CG4 cells treated with EPO and/or LIF.

									P value	
Samples	**Tnfrsf1a**	**Mean Tnfrsf1a**	**Hprt1**	**Mean Hprt1**	**Tnfrsf1a-Hprt1**	**Log FC**	**Log FC mean**	**SD**	**vs Ctrl**	**vs EPO**
Ctrl	23.91	24.01	23.46	23.48	0.53	0.08	0.4	0.4		
1A	24.10		23.50							
1B	23.59	23.81	23.40	23.37	0.44	0.51				
1B	24.03		23.34							
1C	23.30	23.34	23.34	23.32	0.02	0.07				
1C	23.37		23.30							
1D	23.70	23.93	23.44	23.47	0.45	0.90				
1D	24.15		23.50							
EPO	23.19	23.06	23.44	23.43	-0.37	0.60	0.4	0.3	0.9387	
2A	22.92		23.41							
2B	22.91	23.48	23.56	23.55	-0.07	0.10				
2B	24.04		23.53							
2C	23.70	23.86	23.43	23.43	0.43	0.22				
2C	24.02		23.43							
2D	23.45	23.76	23.39	23.46	0.31	0.58				
2D	24.07		23.52							
LIF 10	22.48	23.00	23.35	23.37	-0.37	1.24	1.3	0.3	0.0106	0.0035
4A	23.51		23.38							
4B	23.29	23.06	23.61	23.77	-0.72	1.79				
4B	22.82		23.93							
4C	21.97	22.32	23.50	23.58	-1.26	1.09				
4C	22.67		23.66							
4D	22.87	23.05	23.70	23.61	-0.56	1.16				
4D	23.22		23.51							
EPO+ LIF	22.47	22.93	23.46	23.56	-0.63	1.11	1.0	0.3	0.0501	0.0215
5A	23.39		23.66							
5B	22.51	22.57	23.20	23.15	-0.58	1.21				
5B	22.62		23.09							
5C	22.58	22.57	23.23	23.25	-0.68	1.28				
5C	22.56		23.27							
5D	22.35	22.73	23.47	23.49	-0.75	0.53				
5D	23.11		23.50							

Table A28: Raw data related to Figure 6.9 showing Tnfrsf1a Ct values obtained by qPCR on CG4 cells treated with EPO and/or LIF.

									P value	
Samples	**Inhba**	**Mean Inhba**	**Hprt1**	**Mean Hprt1**	**Inhba - Hprt1**	**Log FC**	**Log FC Mean**	**SD**	**vs Ctrl**	**vs EPO**
Ctrl	36.08	35.75	23.46	23.48	12.27	-0.51	-0.7	0.8		
1A	35.42		23.50							
1B	35.45	35.13	23.40	23.37	11.76	0.00				
1B	34.81		23.34							
1C	No Ct	36.94	23.34	23.32	13.62	-1.86				
1C	36.94		23.30							
1D	35.26	35.51	23.44	23.47	12.04	-0.27				
1D	35.75		23.50							
EPO	38.13	36.57	23.44	23.43	13.14	-1.38	-0.6	0.6	0.8771	
2A	35.00		23.41							
2B	No Ct	35.96	23.56	23.55	12.42	-0.65				
2B	35.96		23.53							
2C	34.52	35.06	23.43	23.43	11.63	0.13				
2C	35.59		23.43							
2D	34.25	35.63	23.39	23.46	12.17	-0.41				
2D	37.00		23.52							
LIF 10	33.07	32.90	23.35	23.37	9.54	2.23	1.9	0.3	0.0011	0.0004
4A	32.73		23.38							
4B	33.36	33.61	23.61	23.77	9.84	1.92				
4B	33.86		23.93							
4C	33.68	33.78	23.50	23.58	10.20	1.57				
4C	33.87		23.66							
4D	33.81	33.51	23.70	23.61	9.90	1.86				
4D	33.20		23.51							
EPO+ LIF	33.41	32.91	23.46	23.56	9.35	2.41	1.3	0.8	0.0158	0.0117
5A	32.41		23.66							
5B	34.24	34.47	23.20	23.15	11.33	0.44				
5B	34.70		23.09							
5C	33.84	33.53	23.23	23.25	10.28	1.49				
5C	33.21		23.27							
5D	34.59	34.33	23.47	23.49	10.85	0.92				
5D	34.07		23.50							

Table A29: Raw data related to Figure 6.11 showing Inhba Ct values obtained by qPCR on CG4 cells treated with EPO and/or LIF.

									P value	
Samples	**Mag**	**Mean Mag**	**Hprt1**	**Mean Hprt1**	**Mag-Hprt1**	**Log FC**	**Mean Log FC**	**SD**	**vs Ctrl**	**vs EPO**
Ctrl	27.98	26.52	23.16	23.44	3.08	-1.20	-0.1	0.8		
6A	25.06		23.72							
6B	25.46	25.46	23.63	23.58	1.88	0.00				
6B	25.45		23.52							
6C	24.71	24.65	23.57	23.52	1.13	0.75				
6C	24.58		23.46							
6D	25.09	25.09	23.19	23.31	1.78	0.11				
6D	25.08		23.43							
EPO	24.06	23.82	23.86	23.70	0.11	1.77	1.6	0.4	0.0114	
7A	23.57		23.54							
7B	24.04	24.60	23.58	23.77	0.83	1.05				
7B	25.16		23.96							
7C	23.58	23.51	23.39	23.64	-0.13	2.01				
7C	23.43		23.88							
7D	23.48	23.61	23.05	23.14	0.47	1.41				
7D	23.73		23.22							
LIF 10	24.93	25.32	23.84	23.81	1.52	0.36	0.4	0.2	0.2506	0.0024
9A	25.71		23.77							
9B	24.85	24.89	23.64	23.64	1.25	0.63				
9B	24.93		23.64							
9C	25.10	25.17	23.66	23.56	1.61	0.28				
9C	25.23		23.46							
9D	25.00	25.16	23.67	23.77	1.39	0.49				
9D	25.32		23.87							
EPO+LIF	24.93	24.64	23.72	23.81	0.84	1.05	1.2	0.5	0.0328	0.3255
10A	24.35		23.89							
10B	23.77	23.94	23.81	23.96	-0.02	1.90				
10B	24.10		24.10							
10C	24.80	24.87	23.76	23.77	1.10	0.78				
10C	24.94		23.78							
10D	24.22	24.35	23.71	23.61	0.73	1.15				
10D	24.47		23.51							

Table A30: Raw data related to Figure 6.15 showing Mag Ct values obtained by qPCR on CG4 cells treated with EPO and/or LIF.

									P value	
Samples	**Pmp2**	**Mean Pmp2**	**Hprt 1**	**Mean Hprt1**	**Pmp2 - Hprt1**	**Log FC**	**Log FC mean**	**SD**	**vs Ctrl**	**vs EPO**
Ctrl	29.17	29.10	23.16	23.44	5.66	0.08	0.0	0.2		
6A	29.03		23.72							
6B	29.00	29.32	23.63	23.58	5.74	0.00				
6B	29.63		23.52							
6C	29.04	29.14	23.57	23.52	5.62	0.12				
6C	29.23		23.46							
6D	29.28	29.39	23.19	23.31	6.08	-0.33				
6D	29.49		23.43							
EPO	23.63	23.85	23.86	23.70	0.15	5.60	5.2	0.3	1.14E-07	
7A	24.06		23.54							
7B	24.26	24.48	23.58	23.77	0.71	5.03				
7B	24.70		23.96							
7C	24.21	24.28	23.39	23.64	0.64	5.10				
7C	24.34		23.88							
7D	23.94	23.94	23.05	23.14	0.81	4.94				
7D	23.94		23.22							
LIF 10	28.68	28.77	23.84	23.81	4.96	0.78	0.3	0.4	0.1828	1.34E-06
9A	28.85		23.77							
9B	29.92	29.61	23.64	23.64	5.97	-0.23				
9B	29.29		23.64							
9C	28.88	29.00	23.66	23.56	5.44	0.31				
9C	29.11		23.46							
9D	28.84	29.11	23.67	23.77	5.34	0.40				
9D	29.38		23.87							
EPO+ LIF	25.32	25.49	23.72	23.81	1.69	4.06	4.0	0.4	1.36E-06	0.0025
10A	25.66		23.89							
10B	25.05	25.21	23.81	23.96	1.25	4.49				
10B	25.36		24.10							
10C	25.70	25.84	23.76	23.77	2.07	3.68				
10C	25.97		23.78							
10D	25.61	25.60	23.71	23.61	1.99	3.76				
10D	25.58		23.51							

Table A31: Raw data related to Figure 6.16 showing Pmp2 Ct values obtained by qPCR on CG4 cells treated with EPO and/or LIF.

									P value	
Samples	**Pgc1**	**Mean Pgc1**	**Hprt1**	**Mean Hprt1**	**Pgc1-Hprt1**	**Log FC**	**Log FC Mean**	**SD**	**vs Ctrl**	**vs EPO**
Ctrl	30.17	30.35	23.16	23.44	6.91	-0.22	-0.1	0.3		
6a	30.52		23.72							
6b	30.13	30.27	23.63	23.58	6.69	0.00				
6b	30.40		23.52							
6c	29.95	29.99	23.57	23.52	6.47	0.22				
6c	30.02		23.46							
6d	30.66	30.46	23.19	23.31	7.15	-0.46				
6d	30.26		23.43							
EPO	29.29	29.20	23.86	23.70	5.50	1.20	1.1	0.2	0.0007	
7a	29.10		23.54							
7b	29.32	29.33	23.58	23.77	5.56	1.13				
7b	29.34		23.96							
7c	29.08	29.17	23.39	23.64	5.54	1.16				
7c	29.26		23.88							
7d	29.03	29.10	23.05	23.14	5.97	0.72				
7d	29.17		23.22							
LIF 10	30.61	30.71	23.84	23.81	6.91	-0.22	-0.1	0.2	0.8668	0.0001
9a	30.81		23.77							
9b	30.58	30.60	23.64	23.64	6.96	-0.27				
9b	30.62		23.64							
9c	30.32	30.41	23.66	23.56	6.85	-0.16				
9c	30.50		23.46							
9d	30.06	30.39	23.67	23.77	6.61	0.08				
9d	30.71		23.87							
EPO+ LIF	29.83	29.88	23.72	23.81	6.08	0.62	0.6	0.0	0.0021	0.0104
10a	29.93		23.89							
10b	29.94	30.02	23.81	23.96	6.07	0.62				
10b	30.10		24.10							
10c	29.54	29.82	23.76	23.77	6.05	0.64				
10c	30.10		23.78							
10d	29.54	29.61	23.71	23.61	6.00	0.70				
10d	29.67		23.51							

Table A32: Raw data related to Figure 6.17 showing Ppargc1a (also known as Pgc1) Ct values obtained by qPCR on CG4 cells treated with EPO and/or LIF.

									P value	
Samples	**Tlr2**	**Mean Tlr2**	**Hprt1**	**Mean Hprt1**	**Tlr2-Hprt1**	**Log FC**	**Log Fc Mean**	**SD**	**vs Ctrl**	**vs EPO**
Ctrl	33.36	33.03	23.16	23.44	9.59	-0.16	0.2	0.5		
6A	32.69		23.72							
6B	31.95	32.04	23.63	23.58	8.47	0.96				
6B	32.13		23.52							
6C	32.65	32.94	23.57	23.52	9.43	0.00				
6C	33.23		23.46							
6D	32.99	32.90	23.19	23.31	9.58	-0.16				
6D	32.80		23.43							
EPO 10	32.60	32.98	23.86	23.70	9.28	0.15	0.0	0.5	0.7496	
7A	33.35		23.54							
7B	32.68	32.55	23.58	23.77	8.78	0.64				
7B	32.42		23.96							
7C	33.34	33.06	23.39	23.64	9.43	0.00				
7C	32.78		23.88							
7D	33.67	33.23	23.05	23.14	10.09	-0.67				
7D	32.78		23.22							
LIF 10	29.86	29.80	23.84	23.81	5.99	3.43	3.2	0.4	9.28E-05	7.44E-05
9A	29.73		23.77							
9B	30.21	30.45	23.64	23.64	6.81	2.62				
9B	30.68		23.64							
9C	29.80	29.67	23.66	23.56	6.11	3.32				
9C	29.54		23.46							
9D	29.93	29.89	23.67	23.77	6.11	3.31				
9D	29.84		23.87							
EPO+LIF	29.23	29.28	23.72	23.81	5.48	3.95	3.6	0.3	2.92E-05	2.4E-05
10A	29.33		23.89							
10B	30.01	30.05	23.81	23.96	6.10	3.33				
10B	30.09		24.10							
10C	29.94	29.64	23.76	23.77	5.87	3.56				
10C	29.34		23.78							
10D	29.72	29.62	23.71	23.61	6.01	3.42				
10D	29.51		23.51							

Table A33: Raw data related to Figure 6.20 showing Tlr2 Ct values obtained by qPCR on CG4 cells treated with EPO and/or LIF.

									P value	
Samples	**Lcn2**	**Mean Lcn2**	**Hprt1**	**Mean Hprt1**	**Lcn2-Hprt1**	**Log FC**	**Log FC Mean**	**SD**	**vs Ctrl**	**vs EPO**
Ctrl	30.92	30.86	23.16	23.44	7.42	-0.20	0.0	0.1		
6A	30.79		23.72							
6B	30.45	30.80	23.63	23.58	7.22	0.00				
6B	31.14		23.52							
6C	30.86	30.77	23.57	23.52	7.25	-0.03				
6C	30.67		23.46							
6D	31.15	30.50	23.19	23.31	7.19	0.03				
6D	29.85		23.43							
EPO 10	30.17	30.25	23.86	23.70	6.55	0.68	0.5	0.4	0.0546	
7A	30.32		23.54							
7B	29.94	30.10	23.58	23.77	6.33	0.89				
7B	30.26		23.96							
7C	30.58	30.42	23.39	23.64	6.78	0.44				
7C	30.25		23.88							
7D	30.30	30.46	23.05	23.14	7.33	-0.11				
7D	30.62		23.22							
LIF 10	28.04	28.02	23.84	23.81	4.21	3.01	2.5	0.3	7.38E-06	0.0003
9A	27.99		23.77							
9B	28.52	28.56	23.64	23.64	4.92	2.31				
9B	28.59		23.64							
9C	28.11	28.35	23.66	23.56	4.79	2.43				
9C	28.59		23.46							
9D	28.39	28.72	23.67	23.77	4.95	2.28				
9D	29.04		23.87							
EPO+LIF	28.44	28.27	23.72	23.81	4.46	2.76	2.6	0.3	6.3E-06	0.0002
10A	28.09		23.89							
10B	27.83	28.14	23.81	23.96	4.18	3.04				
10B	28.44		24.10							
10C	28.58	28.71	23.76	23.77	4.94	2.29				
10C	28.83		23.78							
10D	28.44	28.45	23.71	23.61	4.84	2.38				
10D	28.46		23.51							

Table A34: Raw data related to Figure 6.21 showing Lcn2 Ct values obtained by qPCR on CG4 cells treated with EPO and/or LIF.

									P value		
Samples	**Mog Ct**	**Mean Mog**	**Hprt 1**	**Mean Hprt1**	**Mog-Hprt 1**	**Mog FC**	**Mog mean**	**SD**	**vs Ctrl**	**vs EPO**	**vs EPO+ LIF**
Ctrl	30.37	30.36	24.52	24.46	5.90	1.00	0.8	0.1			
1A	30.34		24.40								
1B	30.44	30.32	23.96	24.03	6.29	0.76					
1B	30.19		24.10								
1C	30.31	30.20	23.88	23.96	6.24	0.79					
1C	30.08		24.03								
1D	30.12	30.24	24.01	24.04	6.20	0.81					
1D	30.35		24.06								
EPO	27.53	27.42	24.84	24.81	2.61	9.75	8.3	1.4	3.36823 E-05		
2A	27.31		24.78								
2B	27.86	27.95	24.72	24.78	3.18	6.59					
2B	28.04		24.83								
2C	27.72	27.59	24.64	24.70	2.89	8.03					
2C	27.46		24.76								
2D	27.40	27.29	24.57	24.56	2.73	8.97					
2D	27.17		24.54								
EPO+ LIF	30.69	30.87	25.81	25.82	5.05	1.80	1.6	0.3	0.0012	6.9369 E-05	
3A	31.04		25.83								
3B	30.29	30.43	25.28	25.38	5.04	1.80					
3B	30.56		25.48								
3C	31.27	31.09	26.04	25.94	5.16	1.67					
3C	30.91		25.83								
3D	31.11	31.13	25.58	25.57	5.56	1.26					
3D	31.15		25.56								
EPO+ PAM3	28.79	28.72	24.49	24.53	4.19	3.26	3.1	0.3	1.14228 E-05	0.0003	0.0004
4A	28.65		24.57								
4B	29.15	29.21	24.69	24.74	4.47	2.69					
4B	29.27		24.79								
4C	28.80	29.03	24.66	24.72	4.31	3.00					
4C	29.25		24.77								
4D	29.47	29.33	25.26	25.21	4.12	3.42					
4D	29.19		25.16								
EPO+LIF+PAM3	31.30	31.32	25.10	25.27	6.05	0.90	1.0	0.1	0.0902	0.0003	0.0121
5A	31.34		25.44								
5B	31.87	31.80	25.90	25.95	5.86	1.03					
5B	31.73		25.99								
5C	31.07	31.01	25.35	25.28	5.73	1.12					
5C	30.94		25.20								

Table A35: Raw data related to Figure 6.24 showing Mog Ct values obtained by qPCR on CG4 cells treated with EPO, LIF and/or Pam3.

									P value	
Samples	**Mog**	**Mean Mog**	**Hprt1**	**Mean Hprt1**	**Mog-Hprt1**	**Mog FC**	**Mog mean**	**sd**	**vs Ctrl**	**vs EPO**
Ctrl	31.48	31.41	23.91	24.08	7.33	0.91	0.9	0.1		
1A	31.33		24.25							
1B	31.24	31.35	24.19	24.16	7.19	1.00				
1B	31.45		24.12							
1C	31.79	31.73	24.34	24.32	7.42	0.86				
1C	31.67		24.29							
1D	31.91	31.87	24.19	24.17	7.70	0.70				
1D	31.82		24.15							
EPO	28.37	28.23	24.59	24.62	3.61	12.00	11.4	1.0	7.4797 E-07	
2A	28.08		24.65							
2B	28.49	28.64	25.02	25.03	3.62	11.92				
2B	28.79		25.03							
2C	28.16	28.07	24.38	24.45	3.62	11.92				
2C	27.97		24.52							
2D	28.29	28.28	24.53	24.40	3.88	9.95				
2D	28.26		24.27							
EPO+Lcn2 (1ng/ml)	27.56	27.59	24.05	24.20	3.39	13.93	12.1	3.9	0.0012	0.7528
3A	27.61		24.34							
3B	27.73	27.55	24.34	24.41	3.14	16.56				
3B	27.37		24.48							
3C	28.67	28.45	24.67	24.58	3.87	9.99				
3C	28.23		24.49							
3D	29.32	29.01	24.90	24.81	4.20	7.94				
3D	28.69		24.71							
EPO+Lcn2 (10ng/ml)	27.75	27.82	24.28	24.30	3.52	12.77	12.8	0.3	1.3955 E-08	0.0748
4A	27.88		24.32							
4B	27.72	27.71	24.15	24.24	3.47	13.18				
4B	27.70		24.33							
4C	28.06	28.04	24.54	24.49	3.55	12.51				
4C	28.01		24.44							
EPO+Lcn2 (50ng/ml)	28.14	28.18	24.62	24.65	3.53	12.64	13.8	1.8	6.7665 E-06	0.0615
5A	28.22		24.68							
5B	28.02	28.10	24.86	24.89	3.22	15.73				
5B	28.18		24.91							
5C	28.16	28.14	24.67	24.84	3.30	14.83				
5C	28.11		25.00							
5D	28.47	28.66	25.11	25.05	3.61	11.96				
5D	28.84		24.98							

Table A35: Raw data related to Figure 6.25 showing Mog Ct values obtained by qPCR on CG4 cells treated with EPO and/or Lcn2.

									P value	
Samples	**Mog**	**Mean Mog**	**Hprt1**	**Mean Hprt1**	**Mog-Hprt1**	**Mog FC**	**Mog mean**	**sd**	**vs Ctrl**	**vs EPO**
Ctrl	33.71	33.44	24.21	24.33	9.11	0.48	0.8	0.3		
1A	33.17		24.45							
1B	32.11	32.17	23.88	24.11	8.06	1.00				
1B	32.23		24.34							
1C	33.24	33.04	24.72	24.76	8.28	0.86				
1C	32.84		24.80							
1D	32.69	32.90	24.46	24.42	8.49	0.74				
1D	33.11		24.37							
EPO	30.09	30.28	24.90	24.83	5.45	6.11	8.1	1.4	5.8256E-05	
2A	30.47		24.76							
2B	29.91	29.95	24.91	24.91	5.04	8.14				
2B	29.98		24.91							
2C	30.05	30.02	25.29	25.22	4.81	9.55				
2C	29.99		25.14							
2D	30.46	30.44	25.41	25.48	4.96	8.57				
2D	30.41		25.54							
EPO+ Lcn2	30.01	30.15	24.95	25.02	5.13	7.62	8.1	1.2	1.9092E-05	0.9747
3A	30.29		25.09							
3B	29.73	29.73	24.89	24.83	4.90	8.97				
3B	29.72		24.77							
3C	30.08	29.94	25.02	25.06	4.88	9.06				
3C	29.79		25.09							
3D	30.60	30.74	25.34	25.40	5.34	6.59				
3D	30.88		25.46							

Table A36: Raw data related to Figure 6.26 showing Mog Ct values obtained by qPCR on CG4 cells treated with EPO and/or Lcn2.